ABSTRACT

MASS, OLGA. Synthetic Methodology to Address What Makes Chlorophylls Green. (Under the direction of Professor Dr. Jonathan S. Lindsey).

Chlorophylls are the most abundant pigments in nature. Over 10^{11} tons of chlorophylls are produced annually on Earth. The role of this leaf pigment in photosynthesis is to absorb sunlight and funnel the resulting energy to the reaction centers. The combination of the 13^1-oxophorbine skeleton, central metal, and peripheral substituents endows chlorophylls with unique spectral properties.

This work describes new synthetic methodologies to gain access to stable chlorophyll mimics (chlorins and bacteriochlorins). The resulting chlorophyll mimics are used to probe the effects of structural features on spectral and photophysical properties. This study is essential for gaining a deep understanding of the function of these photosynthetic pigments. This knowledge should also enable a more thoughtful and rational design of synthetic chlorophylls for various applications.

The long-wavelength absorption of chlorins derives from a transition that encompasses the 2,3- and 12,13-positions. Chlorophyll *a* bears a 3-vinyl group and a 13-keto group, as well as a full complement of substituents at the other β-pyrrole sites. Herein, a new de novo route was developed to access a set of chlorins carrying two auxochromes at the 3- and 13-positions and lacking any other substituents. Comparative studies of the photophysical and redox properties of 13- versus 12-substituted chlorins, synthesized previously, revealed only very slight differences between the isomeric 12- and 13-substituted chlorins.

Second, the new methodology was utilized in the synthesis of fully unsubstituted 13^1-oxophorbine and phorbine (which lacks an oxo group in the isocyclic ring) macrocycles, core benchmarks against which the properties of all chlorophylls with their diverse substituents can be measured. The spectral properties and electronic structure of the 13^1-oxophorbine closely resemble those of the corresponding analogues of chlorophyll *a*. Accordingly, the fundamental electronic properties of chlorophylls are primarily a consequence of the 13^1-oxophorbine base macrocycle.

Natural photosynthetic pigments bacteriochlorophylls *c*, *d* and *e* undergo self-assembly to create an organized antenna system, the chlorosome. A key challenge in preparing artificial chlorosomes remains the synthesis of the appropriate pigment (chlorin) equipped with a set of functional groups suitable for forming a network of non-covalent interactions, thereby holding the pigments at the proper distance and orientation to assure efficient energy transfer. This work reports the de novo synthesis of three analogues of chlorosomal bacteriochlorophylls; the analogues differ in the aryl substituent at the 10-position. The self-assembly process of the chlorosomal bacteriochlorophyll mimics has been studied in solution. The UV-vis absorption spectra reveal a bathochromic shift of ~1700 cm^{-1} of the Q_y band in a nonpolar solvent, indicating extensive assembly. The synthesis of other mimics, amphipathic chlorins for incorporation into a protein matrix, was inspired by cytochrome *c*, an electron-transport protein in mitochondria.

Synthetic bacteriochlorins are of interest for fundamental studies in photochemistry due to their strong absorption in the near-infrared spectral region and their close similarity with natural bacteriochlorophylls. A de novo route to 5-methoxybacteriochlorins entails self-

condensation of a dihydrodipyrrin–acetal, which in turn is prepared from a 2-(2-nitroethyl)pyrrole species and an α,β-unsaturated ketone–acetal (e.g., 1,1-dimethoxy-4-methylpent-3-en-2-one). Here, a new, scalable route to 1,1-dimethoxy-4-methylpent-3-en-2-one removes a significant previous impediment to the overall route. Second, the new route was employed to gain access to new α,β-unsaturated ketones and corresponding dihydrodipyrrins. A dihydrodipyrrin bearing a 1,3-dioxolan-2-yl moiety afforded the bacteriochlorin (30% yield) containing a 2-hydroxyethoxy substituent at the 5-position. Subsequent bromination proceeded regioselectively at the 15-position to give a *trans*-(5,15)-AB-bacteriochlorin building block. The results taken together afford deeper understanding of the scope and limitations of the de novo route and also advance the capabilities for tailoring synthetic bacteriochlorins.

Synthetic Methodology to Address What Makes Chlorophylls Green

by
Olga Mass

A dissertation submitted to the Graduate Faculty of
North Carolina State University
in partial fulfillment of the
requirements for the degree of
Doctor of Philosophy

Chemistry

Raleigh, North Carolina

2012

APPROVED BY:

_____	_____
Jonathan S. Lindsey Committee Chair	Daniel L. Comins
_____	_____
Reza A. Ghiladi	David A. Shultz

DEDICATION

This work is dedicated to my parents.

BIOGRAPHY

Olga Mass was born in Petropavlovsk-Kamchatsky, USSR. In 1992, her family moved to Moscow. She has two younger brothers, Artur and Ilya. Olga earned a Bachelor of Science degree with honors in Chemical Engineering in 2005 from Lomonosov State Moscow Academy of Fine Chemical Technology. She continued her education in the same university to receive a Master of Science degree with honors in Technology and Biotechnology of Biologically Active Compounds. During that time she was involved in chlorophyll chemistry under the supervision of Professors Andrey F. Mironov and Mikhail A. Grin. In the summer of 2007, Olga began her doctoral studies in chemistry at North Carolina State University where she joined Professor Jonathan S. Lindsey's research group. Her doctoral work was devoted to the most vital pigments, chlorophylls. To date, she has published eight papers in this field including one review.

ACKNOWLEDGMENTS

First, I would like to thank my advisor, Dr. Jonathan S. Lindsey. It was an honor to be his graduate student. He has taught me what high standards in chemistry research are. I strongly appreciate his advice, ideas, time, patience, and feedback that made my graduate school experience fruitful and stimulated my professional growth as a scientist. His genuine passion for science was contagious and inspiring; it will be always a motivation in my future career pursuits.

I would like to thank my committee members: Dr. Daniel L. Comins, Dr. David A. Shultz, and Dr. Reza A. Ghiladi for reviewing my work and helpful suggestions.

I thank all faculty and staff that I worked with at North Carolina State University, Department of Chemistry. Without their assistance, this work would not be successful. In particular, I would like to thank the director of the X-ray structural facility, Dr. Paul Boyle, and the supervisor of the nuclear magnetic resonance facility, Dr. Sabapathy Sankar.

It was a great pleasure to work with all past and present group members. I am especially thankful to Dr. Marcin Ptaszek and Dr. Ana Muresan for their support and friendship during the beginning of my graduate studies. I am grateful to Dr. Masahiko Taniguchi for his indispensable advice in my experimental and presentation work. I thank our group administrator, Ann Norcross, for her geniality, understanding, and wisdom in problem solving.

Professors Dewey Holten, David F. Bocian, and members of their research groups accomplished photophysical studies that greatly complemented this work in their collaboration.

Lastly, there are no words to express how thankful I am to my family for their belief in me.

TABLE OF CONTENTS

LIST OF FIGURES

LIST OF SCHEMES

LIST OF CHARTS

LIST OF TABLES

LIST OF EQUATIONS

CHAPTER I

Introduction. About Chlorophylls

Chlorophylls – the most abundant biological pigments[1] – are vital in photosynthesis due to their unique photophysical properties. In the light-harvesting antenna complexes of photosynthetic organisms, chlorophylls absorb light and funnel the energy to the reaction centers. The macrocycle of chlorophylls is the basis for their characteristic spectral features. According to the macrocycle type, all known chlorophylls belong to one of three groups: porphyrins, chlorins and bacteriochlorins (Chart I.1). A porphyrin is an 18π-electron aromatic tetrapyrrole. Chlorins and bacteriochlorins differ from their parent porphyrins in having one or two pyrrole ring(s) reduced at the *β*-position(s), respectively. The degree of saturation of the tetrapyrrole determines the difference in absorption properties of chlorophylls. Thus, the fully unsaturated tetrapyrrole macrocycle, porphyrin, is present in the c-type chlorophylls of some algae and prokaryotes. Porphyrins strongly absorb in the blue spectral region (B or Soret band), and only moderately in the red region around 620 nm (long-wavelength or Q_y band). The dihydroporphyrin macrocycle, chlorin, is present in chlorophylls *a*, *b*, *d* and *e*, and in bacteriochlorophylls *c*, *d*, and *e* of green bacteria. These chlorin-type chlorophylls have characteristic absorption bands of similar intensity, herewith the Q_y band is significantly stronger and red-shifted compared to the one of the porphyrin. The tetrahydroporphyrin macrocycle, bacteriochlorin, is present in bacteriochlorophylls of purple bacteria that absorb in the near ultraviolet and strongly in the near infrared (Figure I.1).

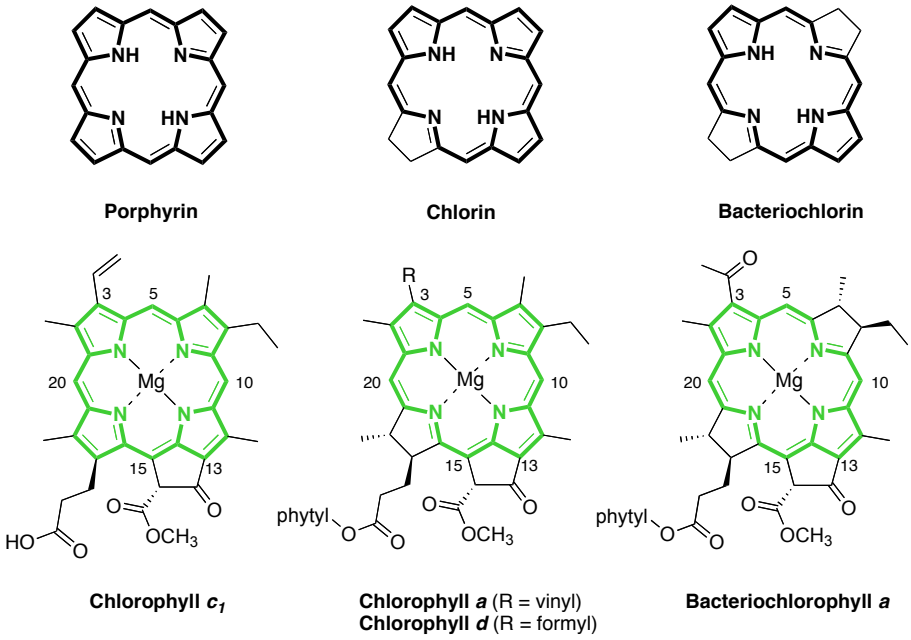

Chart I.1 Three π-systems in natural chlorophylls (top), and representative examples (bottom).

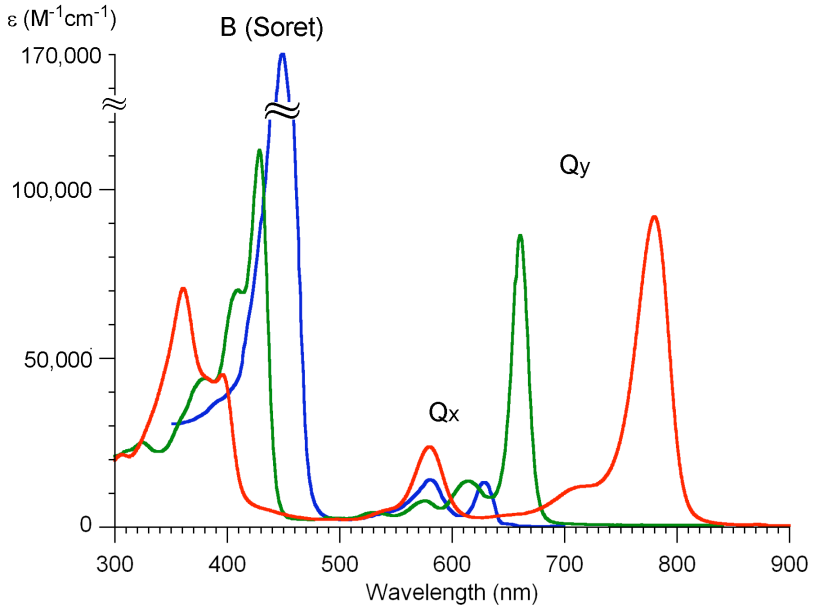

Figure I.1. Representative absorption spectra of a porphyrin [chlorophyll c_1 (blue line)],[2] chlorin [chlorophyll *a* (green line)],[3] and bacteriochlorin [bacteriochlorophyll *a* (red line)].[4]

Porphyrin-type chlorophylls comprise only about 10% of all known chlorophylls,[1] whereas the majority of chlorophylls represent a chlorin-type or a bacteriochlorin-type. Indeed, a c-chlorophyll might be the most ancient photosynthetic pigment and it is the precursor to most chlorophylls,[5] yet the abundance ratio of chlorophylls suggests that Nature found hydroporphyrins (chlorins and bacteriochlorins) to be superior in performing photosynthetic functions. The photophysical properties of hydroporphyrins make them attractive molecules in a wide range of fundamental and applied studies including artificial photosynthesis. The work described in this manuscript is devoted to hydroporphyrins.

The long-wavelength absorption band (Q_y band) in the chlorin and bacteriochlorin absorption spectra originates from a transition from the electronic ground state (S_0) to the lowest excited singlet state (S_1). The Q_x band (profound in the bacteriochlorin spectrum) corresponds to the transition from the electronic ground state (S_0) to the second excited singlet state (S_2), and the Soret (B_x and B_y) bands corresponds to even higher excited states.

A bare chlorin macrocycle turns to be insufficient to mimic the absorption properties of natural chlorins. Thus, the reduction of a fully unsubstituted porphyrin to the corresponding chlorin leads to significant intensification of the Q_y band, but actually does not cause the redshift characteristic for natural chlorins. The resulting benchmark magnesium chlorin (Chart I.2) lacking any peripheral substituents exhibits a Q_y band at 610 nm (ε_{Qy} = 56,000 $M^{-1}cm^{-1}$),[6] whereas chlorophyll *a* absorbs at 661 nm (ε_{Qy} = 78,200 $M^{-1}cm^{-1}$).[7]

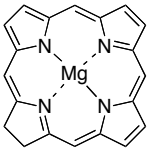

Chart I.2. A benchmark magnesium chlorin.

So, if not a macrocycle and a central metal, what structural constituents contribute to the intense green color of chlorophylls and their absorption in the far-red region? Natural chlorophylls carry a full complement of substituents around the macrocycle periphery, but only a few of the substituents are believed to provide necessary functionality in natural systems, and others may have a secondary role. Most natural chlorophylls contain auxochromic groups at the 3-, 7-, and 13-positions, and alkyl groups at the 2-,8-, and 12-positions. Studies on naturally derived chlorins showed that the auxochromes at the 3- and 13- positions are the most essential in determining the spectral properties of chlorophylls.[8] Changing even one of those substituents can significantly alter the spectral properties of a chromophore. Thus, chlorophyll *a* and chlorophyll *d* (Chart I.1) vary only in the nature of the substituent at the 3-position, but this slight change results in a profound difference in spectral properties (Figure I.2).

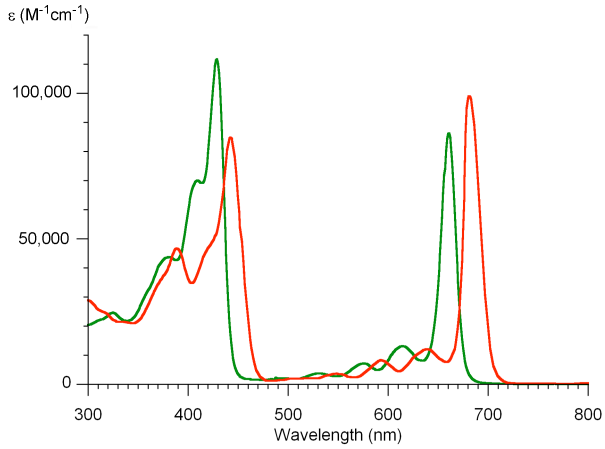

Figure I.2. Absorption spectra of chlorophyll *a* (green line)[3] and chlorophyll *d* (red line) in diethyl ether at room temperature.[9]

The understanding of the influence of substituents would be greatly enriched with the study of reconstitution of a chlorophyll molecule starting from a simple unsubstituted chlorin and progressing by adding one, two, or more groups to the desired locations. Such a study is aimed to find a minimum structural requirement for a synthetic chlorin to closely resemble natural chlorophylls. Moreover, the understanding of the correlation between structure and property provides a necessary rationale in the design of chromophores for a particular application. The current handicap for this exploration is a limited number of means to obtain such a systematic progression of chlorins (or bacteriochlorins). Four distinct approaches to prepare hydroporphyrins can be highlighted: (1) derivatization of naturally occurring chlorophylls (semisynthesis);[10] (2) hydrogenation of or addition to synthetic porphyrins/chlorins;[11] (3) total synthesis for reproduction of natural chlorophylls (the 46-step total synthesis of chlorin e_6 trimethyl ester, the precursor to the natural chlorophyll *a*, developed by Woodward);[12] and (4) de novo synthesis of chlorophyll analogs. Besides the

instability of both naturally derived hydroporphyrins, and hydroporphyrins obtained by reduction of porphyrins/chlorins, the first three approaches are characterized in general by modest control over substituent patterns around the macrocycle. To overcome the problems associated with the hydroporphyrin synthesis, a long-term goal of Dr. Jonathan Lindsey's research group has been to develop a versatile rational synthetic methodology to stable chlorophyll macrocycles enabling control over the introduction of specific substituents.

A recently developed de novo route to 3,10,13-substituted chlorins allowed a more comprehensive examination of substituent effect on the spectral properties of dihydroporphyrins.[13,14] Here, we continued the work on synthetic methodology to hydroporphyrins with the goal to determining the correlation between the structure and photophysical and spectral properties, in other words, green color, of chlorophyll. First, a new de novo synthesis of two chlorins carrying two auxochromic groups at the 3- and 13-positions (like chlorophylls *a* and *d*) and lacking meso-substituents was developed (Chapter II). The new methodology allowed the synthesis of a progression of chlorophyll benchmarks and, therefore, an attempt to answer to the question "what makes chlorophylls green?" (Chapter III). Further, the methodology to gain access to synthetic chlorins was applied to prepare simple mimics of chlorosomal bacteriochlorophyll self-aggregates carrying only functional groups (Chapter IV). Next, new methodology was developed to a tetrahydroporphyrin, a *trans*-AB-bacteriochlorin building block with a linear alignment of substituents, to gain access to the additional sites of derivatization (Chapter V). All such synthetic hydroporphyrins carry a geminal dimethyl group in each reduced ring to stabilize

the molecules against adventitious dehydrogenation. Altogether, over 20 new hydroporphyrins were prepared and studied in this work.

References

(1) (a) Scheer, H. In *Chlorophylls*; Scheer, H.; Ed.; CRC Press, Boca Raton, FL, USA, 1991, pp 3–30. (b) Scheer, H. In *Chlorophylls and Bacteriochlorophylls*; Grimm, B.; Porra, R. J.; Rüdiger, W.; Scheer, H.; Eds.; Springer: Dordrecht, 2006, pp 2–26.

(2) Jeferey, S. W. Biochimi. Biophys. Acta **1972**, *279*, 15–33.

(3) Strain, H. H.; Thomas, M. R.; Katz, J. J. *Biochim. Biophys. Acta* **1963**, *75*, 306–311.

(4) Connolly, J. S.; Samuel, E. B.; Janzen, A. F. *Photochem. Photobiol.* **1982**, *36*, 565–574.

(5) Larkum, A. W. D. In *Chlorophylls;* Scheer, H.; Ed.; CRC Press, Boca Raton, FL, USA, 1991, pp 367–383.

(6) (a) Eisner, U.; Linstead, R. P. *J. Chem. Soc.* **1955**, 3742–3749. (b) Gouterman, M. In *The Porphyrins*; Dolphin, D., Ed.; Academic Press: New York, 1978; Vol. III, pp 1–165.

(7) Strain, H. H.; Svec, W. A. In *The Chlorophylls*; Vernon, L. P., Seely, G. R., Eds.; Academic Press: New York, 1966, pp 21–66.

(8) (a) Smith, K. M.; Goff, D. A.; Simpson, D. J. *J. Am. Chem. Soc.* **1985**, *107*, 4946–4954. (b) Boldt, N. J.; Donohoe, R. J.; Birge, R. R.; Bocian, D. F. *J. Am. Chem. Soc.* **1987**, *109*, 2284–2298. (c) Abraham, R. J.; Rowan, A. E.; Smith, N. W.; Smith, K. M. *J. Chem. Soc., Perkin Trans. 2* **1993**, 1047–1059. (d) Tamiaki, H.; Miyatake, T.; Tanikaga, R. *Tetrahedron Lett.* **1997**, *38*, 267–270.

(9) Kobayashi, M. In *Chlorophylls and Bacteriochlorophylls*; Grimm, B.; Porra, R. J.; Rüdiger, W.; Scheer, H.; Eds.; Springer: Dordrecht, 2006, pp 79–94.

(10) (a) Smith, K. M. In *Chlorophylls*; Scheer, H., Ed.; CRC Press: Boca Raton, FL, 1991, pp 115−143. (b) Hynninen, P. H. In *Chlorophylls*; Scheer, H., Ed.; CRC Press: Boca Raton, FL, 1991, pp 145−209. (c) Pandey, R. K.; Zheng, G. In *The Porphyrin Handbook*; Kadish, K. M., Smith, K. M., Guilard, R., Eds.; Academic Press: San Diego, CA, 2000; Vol. 6, pp 157−230. (d) Pavlov, V. Y.; Ponomarev, G. V. *Chem. Heterocycl. Compd.* **2004**, *40*, 393−425.

(11) (a) Montforts, F.-P.; Gerlach, B.; Höper, F. *Chem. Rev.* **1994**, *94*, 327−347. (b) Montforts, F.-P.; Glasenapp-Breiling, M. *Prog. Heterocycl. Chem.* **1998**, *10*, 1−24. (c) Vicente, M. G. H. In *The Porphyrin Handbook*; Kadish, K. M., Smith, K. M., Guilard, R., Eds.; Academic Press: San Diego, CA, 2000; Vol. 1, pp 149−199. (d) Jaquinod, L. In *The Porphyrin Handbook*; Kadish, K. M., Smith, K. M., Guilard, R.,

Eds.; Academic Press: San Diego, CA, 2000; Vol. 1, pp 201−237. (e) Montforts, F.-P.; Glasenapp-Breiling, M. *Fortschr. Chem. Org. Naturst*. **2002**, *84*, 1−51.

(12) Woodward, R. B.; Ayer, W. A.; Beaton, J. M.; Bickelhaupt, F.; Bonnett, R.; Buchschacher, P.; Closs, G. L.; Dutler, H.; Hannah, J.; Hauck, F. P.; Ito, S.; Langemann, A.; Legoff, E.; Leimgruber, W.; Lwowski, W.; Sauer, J.; Valenta, Z.; Volz, H. *Tetrahedron* **1990**, *46*, 7599–7659.

(13) Laha, J. K.; Muthiah, C.; Taniguchi, M.; McDowell, B. E.; Ptaszek, M.; Lindsey, J. S. *J. Org. Chem.* **2006**, *71*, 4092–4102.

(14) Kee, H. L.; Kirmaier, C.; Tang, Q.; Diers, J. R.; Muthiah, C.; Taniguchi, M.; Laha, J. K.; Ptaszek, M.; Lindsey, J. S.; Bocian, D. F.; Holten, D. *Photochem. Photobiol*. **2007**, *83*, 1125–1143.

CHAPTER II

Synthesis and Photochemical Properties of 12-Substituted vesus 13-Substituted Chlorins

II.1. Introduction

Understanding the effects of substituents on the spectral properties of chlorophyll molecules is of fundamental importance. Knowledge gained from such studies also enables subtle tuning of the absorption bands of chlorins, which is of interest for application in solar energy conversion[1] as well as diverse biomedical fields such as polychromatic flow cytometry,[2] molecular imaging,[3] and photodynamic therapy.[4] In this regard, synthetic macrocycles that contain the chlorin chromophore and that bear relatively few substituents at designated sites are essential for such studies to pinpoint the effects of specific substituents.

A general route for the de novo synthesis of chlorins is shown in Scheme II.1.[5-7] The synthesis employs the condensation of an Eastern half and a Western half followed by metal-mediated oxidative cyclization. The Western half contains a geminal dimethyl group, a key design feature that stabilizes the hydroporphyrin macrocycle toward oxidation. The de novo route requires far more synthetic effort than semisynthetic methods that begin with chlorophylls;[8-21] however, the de novo route affords greater versatility in the scope and range of substituents that can be introduced, and is well suited to the preparation of sparsely substituted chlorins. The de novo route has been used to construct chlorins bearing a wide variety of substituents and substituent patterns.[5-7,22-35] Among various substituents and patterns, the examination of auxochromes at the 3- and 13-positions is of interest because (i)

the long-wavelength absorption band of chlorophylls originates from a transition that encompasses rings A and C, and (ii) chlorophylls *a* and *b* each contain auxochromes substituted in these rings, namely a 3-vinyl group and a 13-keto group.[32,36-38]

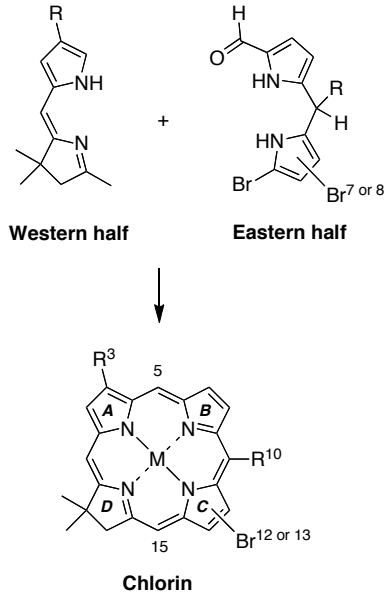

Scheme II.1. De novo synthesis of 12- or 13-substituted chlorins.

To probe the effects of auxochromes on the spectral properties of chlorins, in the past few years we have reported the synthesis of more than twenty chlorins that bear a 10,13-substituent pattern (and often other substituents, particularly a 3-substituent),[26,27,32-35] as well as two target 3,13-substituted chlorins that lack a 10-substituent.[26] Building on the latter chemistry, we recently intended to prepare a 13-substituted chlorin that lacks a 10-substituent en route to the corresponding fully unsubstituted 13^1-oxophorbine. However, this attempt was not successful. X-ray analysis of the putative 13-acetyl-15-bromochlorin (**ZnC-A^{13}Br^{15}**), the key intermediate for installation of the five-membered isocyclic ring (spanning

positions 13 and 15), showed the acetyl group at the 12-position instead (**ZnC-A^{12}Br^{15}**; vide infra). Obviously, intramolecular α-arylation[27] of the 12-acetyl group and the 15-position cannot form the isocyclic ring. Consequently, the two target chlorins **ZnC-E^{3}E^{13}** and **ZnC-E^{3}A^{13}** (and their chlorin precursors **ZnC-Br^{3}Br^{13}** and **ZnC-E^{3}Br^{13}**) reported by us previously as 13-substituted chlorins[26] actually are the isomeric 12-substituted macrocycles **ZnC-E^{3}E^{12}** and **ZnC-E^{3}A^{12}** (and the precursors are **ZnC-Br^{3}Br^{12}** and **ZnC-E^{3}Br^{12}**), respectively (Chart II.1). The structures assigned for all of the 10,13-substituted chlorins are correct.

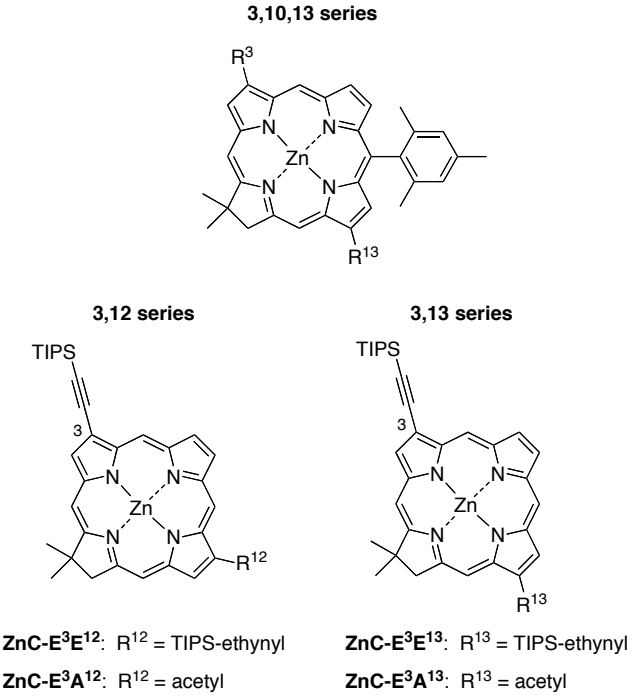

Chart II.1. 3-Substituted chlorins: 3,10,13-, 3,12- and 3,13-pattern.

The synthesis of the fully unsubstituted 13[1]-oxophorbine remains an important objective. Because such synthesis requires the ability to prepare the 13-acetylchlorin (lacking the 10-substituent), and the prior error in assignments is restricted to the 10-unsubstituted (but not 10-substituted) chlorins,[26] we carried out a lengthy study to understand how the regiochemistry of substitution in ring C depends on the nature of the10-substituent. The provision for introduction of substituents in ring C of the chlorin is set at the dipyrromethane stage. The dipyrromethane required for the synthesis of 13-substituted chlorins carries a 1-formyl group and two bromo groups: the electrophilic α-carbon atom bonded with a bromo group serves for condensation with a Western half, and the β-bromo group in turn enables subsequent modifications at the 13-site. Thus, the 12- versus 13-substitution in the chlorins originates from a change in the regiochemistry upon introduction of the bromine atoms in the 1-formyldipyrromethane.

This chapter first describes the bromination of 1-formyldipyrrromethanes (which contain a 5-aryl substituent or no 5-substituent) and characterizes the brominated dipyrromethane products. Note that the 5- (or meso-) position of the dipyrromethane corresponds to the 10-position of the chlorin. This study reveals an unexpected interplay of steric and electronic effects in controlling the regiochemistry of dibromination of 1-formyldipyrromethanes. Next, the chapter describes a rational synthesis of 8,9-dibromo-1-formyldipyrromethane, which provides the critical precursor for the rational synthesis of 3,13-disubstituted chlorins and thereby overcomes the undesired regiochemistry upon dibromination of a 5-unsubstituted 1-formyldipyrromethane. The photophysical and redox properties of the resulting 3,13-disubstituted chlorins are presented and are compared with

that from the previously synthesized 3,12-disubstituted chlorin isomers.[32,36] Taken together, this work provides access to chlorins for fundamental studies of the effects of substituents on the spectral properties of molecules related to the chlorophylls.

A portion of the results presented in this chapter stemmed from a team effort including Marcin Ptaszek and Masahiko Taniguchi; photochemical studies were accomplished by James R. Diers, and Hooi Ling Kee.

II.2. Results and Discussion

II.2.1. Bromination of Dipyrromethanes

Many studies have been reported concerning the bromination of pyrroles,[39] and bromo-substituted dipyrrins (the oxidized counterparts of dipyrromethanes) have longstanding use in classical porphyrin syntheses.[40] On the other hand, the bromination of dipyrromethanes has been less extensively investigated, particularly where nearly all pyrrole positions are open.[41] Introduction of bromine atoms in dipyrromethanes plays an important role in the synthesis of Eastern halves for the preparation of substituted chlorins. The Lindsey group reported previously that bromination of 1-formyldipyrromethanes lacking a 5-substituent (**II-1**) or containing a 5-substituent (**II-2**) with 1 mol equiv of NBS at –78 °C proceeded to the 9-position, affording **II-1-Br**^{9} and **II-2-Br**^{9}, respectively.[26] This result was expected (and confirmed here as shown in Scheme II.2) given the deactivation of the α-formyl-substituted pyrrole ring, and the known course of aromatic electrophilic substitution of 2-alkylpyrroles.[42] On the other hand, we report here that bromination of 1-formyldipyrromethanes with 2 mol equiv of NBS proceeds with a more subtle outcome: the

site of the second bromination depends on the nature of the 5-substituent (R^5 in Scheme II.2). The key results are described below.

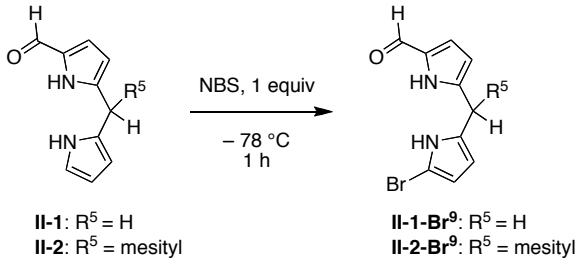

Scheme II.2. Monobromination of 1-formyldipyrromethanes.

The bromination of 1-formyldipyrromethanes[43] **II-1** and **II-2** was carried out with 2 mol equiv of NBS under the same conditions applied previously[26] (2 mol equiv of NBS at –78 through –20 °C). The results are shown in Scheme II.3. The bromination of 5-unsubstituted dipyrromethane **II-1** afforded the isomeric dibromodipyrromethanes **II-1-Br^{8,9}** and **II-1-Br^{7,9}** in the ratio 1:5, as well as trace quantities of the monobrominated dipyrromethane **II-1-Br^{9}** and the unstable tribrominated dipyrromethane **II-1-Br^{3,7,9}**. The ratio of isomers was determined on the basis of ^{1}H NMR spectroscopy of the crude mixture, relying on the noticeable difference in chemical shifts of the pyrrolic protons of the pair of dibromodipyrromethane isomers (**II-1-Br^{8,9}** and **II-1-Br^{7,9}**; Figure II.1). The two isomers were separable upon column chromatography [silica, hexanes/CH_2Cl_2/ethyl acetate (7:2:1)], where dibromodipyrromethane **II-1-Br^{7,9}** was less polar than its isomer **II-1-Br^{8,9}**.

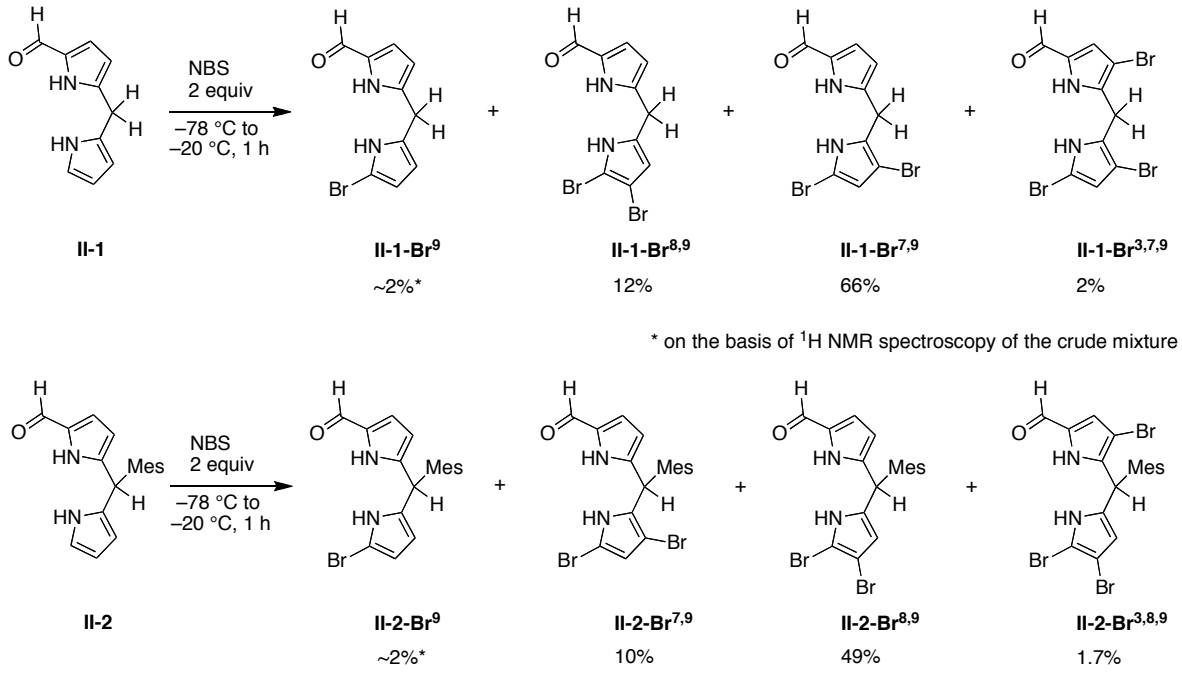

Scheme II.3. Dibromination of 1-formyldipyrromethanes.

This result prompted us to repeat the very bromination of 5-mesityldipyrromethane **II-2** described earlier.[26] Thus, bromination of 5-mesityldipyrromethane **II-2** under the same conditions led to the isomeric dibromodipyrromethanes **II-2-Br^{8,9}** and **II-2-Br^{7,9}** in the ratio 5:1, as well as very small amounts of monobromodipyrromethane **II-2-Br^{9}** and unstable tribromodipyrromethane **II-2-Br^{3,8,9}** (Scheme II.3). 7,9-Dibromodipyrromethane **II-2-Br^{7,9}** was less polar than its isomer, 8,9-dibromopyrromethane **II-2-Br^{8,9}**, and the two dibromodipyrromethanes were readily isolated (although **II-2-Br^{7,9}** and **II-2-Br^{3,8,9}** were isolated in estimated 90% purity). Finally, an analogous bromination study of 1-formyl-5-phenyldipyrromethane resulted in a 5:1 ratio of the 8,9-dibromo versus 7,9-

dibromodipyrromethane product, indicating that the 5-phenyl substituent caused the same regiochemical outcome as the 5-mesityl substituent (Scheme II.4).

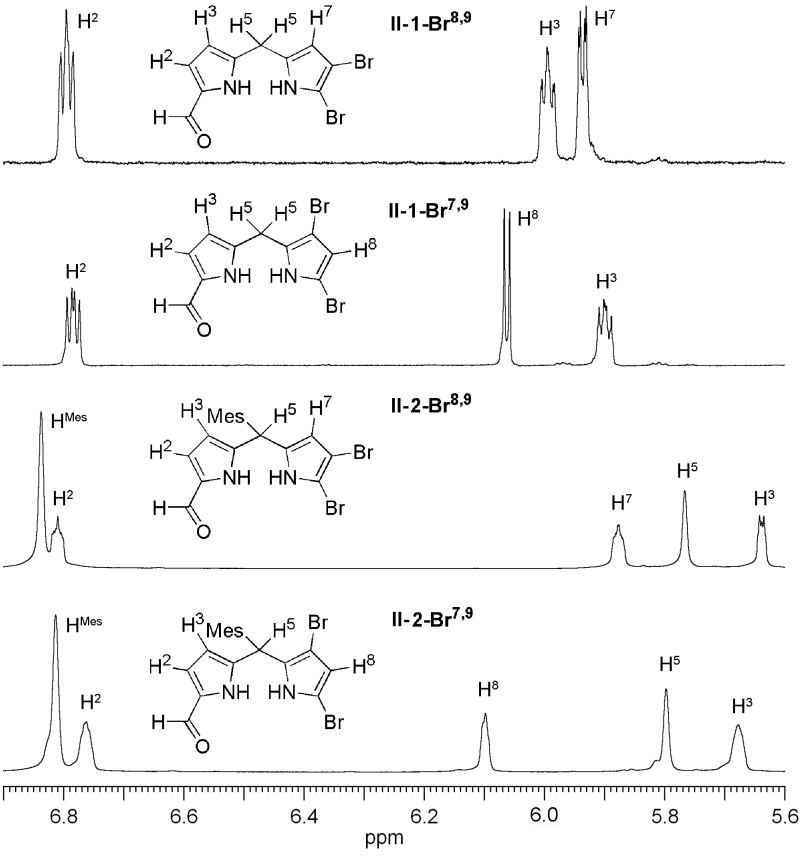

Figure II.1. ^{1}H NMR spectra showing diagnostic features for 7,9- versus 8,9-dibromodipyrromethanes.

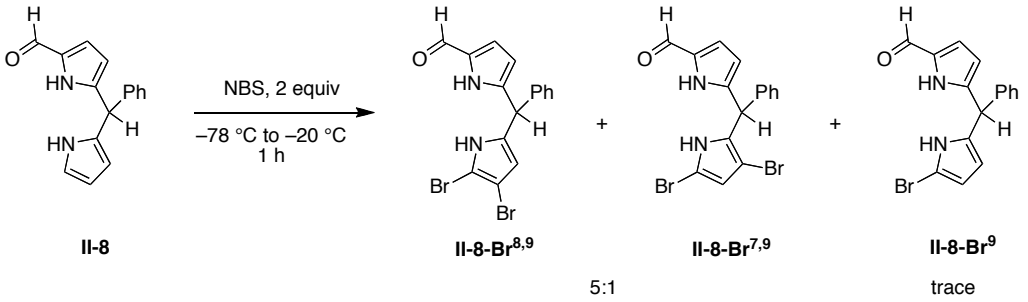

Scheme II.4. Dibromination of 1-formyl-5-phenyldipyrromethane.

This study demonstrates that the regioselectivity of bromination is affected by the steric bulk of the 5-substituent. The first bromination occurs at the 9-position for both **II-1** and **II-2**. In the case of 9-bromo-1-formyldipyrromethane (**II-1-Br**^{9}), both positions C-7 and C-8 are sterically accessible for the second bromination. Position 7 is flanked by the bridging –CH_2– and H^8; position 8 is flanked by the 9-bromo group and H^7. Consequently, the second bromination occurs preferentially at the 7-position (giving **II-1-Br**^{7,9}). On the other hand, the CPK projection of 9-bromodipyrromethanes (analogues of **II-1-Br** lacking the 1-formyl group) shows how the bulky 5-substituent hinders the 7-position (Figure II.2), thereby explaining the major direction of the second bromination in this case to the less sterically shielded 8-position (giving **II-2-Br**^{8,9}).

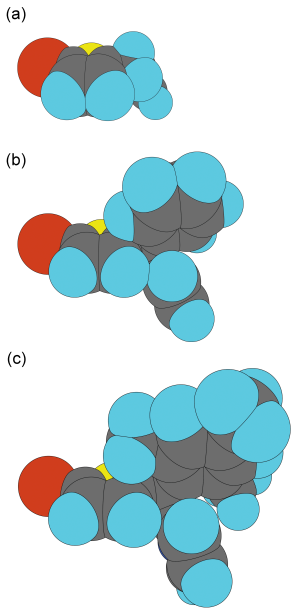

Figure II.2. Optimized structures of 9-bromodipyrromethanes using MM2 (CPK projection). 9-Bromodipyrromethane (a) shows little or no steric differentiation of the 7- and 8-positions toward bromination whereas for 9-bromo-5-phenyldipyrromethane (b) and 9-bromo-5-mesityldipyrromethane (c) the steric effect of the 5-aryl substituent suppresses bromination at the neighboring 7-position.

II. 2.2. Synthesis

A. 12-Acetylchlorin. The 5-unsubstituted 7,9-dibromodipyrromethane **II-1-Br**[7,9] (interpreted previously as an 8,9-dibromodipyrromethane[26]) was synthesized at the preparative level under the same conditions as in the previous work.[26] Full characterization by a number of two-dimensional NMR experiments (HH-COSY, NOESY and TOCSY) confirmed the position of the bromo groups at positions 7 and 9. Dibromodipyrromethane **II-1-Br**[7,9] was condensed with Western half[44] **II-3** in CH_2Cl_2 upon treatment with a solution of $TsOH \cdot H_2O$ in MeOH followed by Zn(II)-mediated oxidative cyclization using 2,2,6,6-tetramethylpiperidine, $Zn(OAc)_2$ and AgOTf open to air.[7,30] Chlorin **FbC-Br**[12] was obtained in 8% yield. Acetylation can be achieved by Pd-mediated coupling using tributyl(1-

ethoxyvinyl)tin[45] followed by acidic hydrolysis. Previously THF was used for such reactions.[26,27,30,32,46] New conditions developed recently for hydroporphyrin acetylation [CH_3CN/DMF (3:2), C. Ruzié and J. S. Lindsey, unpublished data] afford shorter reaction time (2.5 versus 20 h) with comparable if not increased yield. Application of such conditions afforded **FbC-A^{12}** in 78% yield. Chlorin **FbC-A^{12}** was subjected to regioselective bromination (under acidic conditions[35]) at the 15-position to give **FbC-A^{12}Br^{15}** in 40% yield (Scheme II.5). Two-dimensional NMR experiments of both **FbC-Br^{12}** and **FbC-A^{12}Br^{15}**, and X-ray analysis of **FbC-A^{12}Br^{15}** confirmed the structures of each chlorin, and, therefore, the position of bromo groups at positions 7 and 9 in the chlorin precursor, namely dipyrromethane **II-1-Br^{7,9}**.

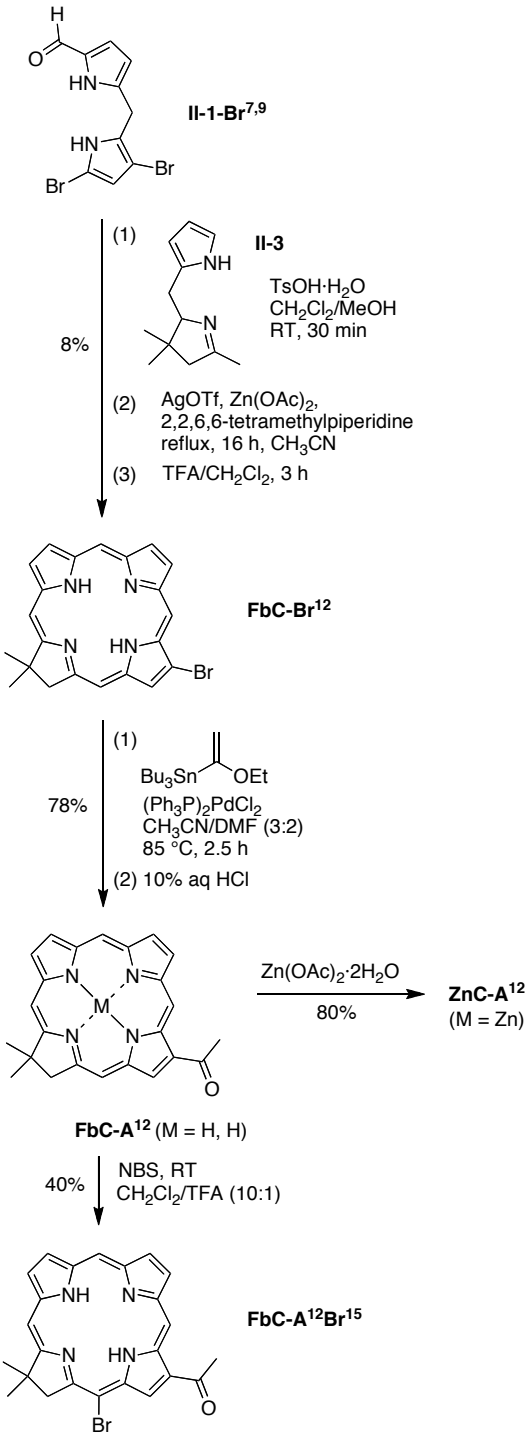

Scheme II.5. Synthesis of 12-acetylchlorin.

B. 8,9-Dibromo-1-formyldipyrromethane. To overcome the undesired regiochemical outcome upon direct dibromination of 1-formyldipyrromethane **II-1**, a stepwise synthesis of 8,9-dibromodipyrromethane **II-1-Br**[8,9] was developed. The stepwise synthesis relies on a sequence of formylation and bromination where each newly introduced substituent provides regioselectivity for the next reaction (Scheme II.6). The synthesis begins with 4-bromopyrrole-2-carboxaldehyde (**II-4**).[26] Reduction of **II-4** with $NaBH_4$ in THF/MeOH (10:1) afforded the corresponding carbinol **II-4-OH**, which was subjected to solventless condensation with pyrrole (20 mol equiv versus **II-4**) in the presence of a mild Lewis acid ($InCl_3$) to give 5-unsubstituted 8-bromodipyrromethane **II-5** in 58% yield. Attempts to purify **II-5** by crystallization were unsuccessful. Purification by column chromatography afforded **II-5** as a colorless oil that was fully characterized, although the oil darkened quickly and decomposed upon long-term storage. Dipyrromethane **II-5** was previously obtained in similar manner but with HCl catalysis, and was not fully characterized.[30] A number of prior stepwise syntheses of sparsely substituted dipyrromethanes have employed a similar approach, often with the use of protective groups.[22,42,47-53]

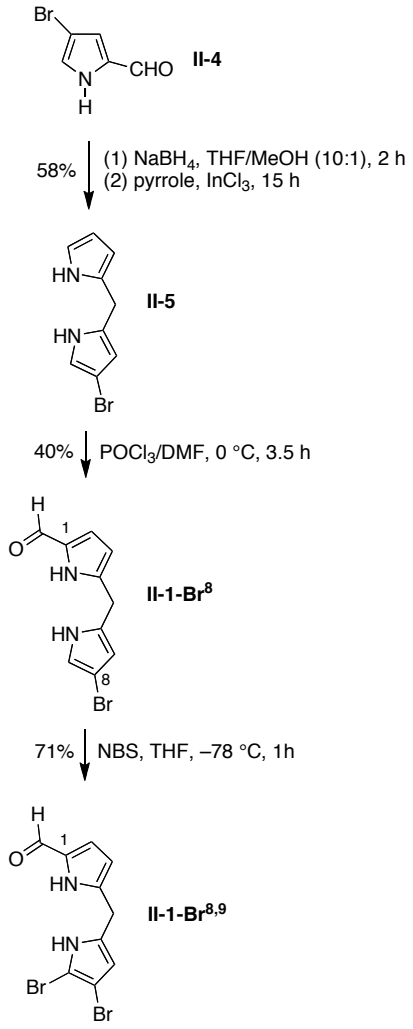

Scheme II.6. New route to 8,9-dibromodipyrromethane.

The standard Vilsmeier-Haack formylation[54] of **II-5** afforded 1-formyl-8-bromodipyrromethane **II-1-Br^{8}** in 40% yield. Protection of the pyrrolic nitrogen atom to direct formylation to the 1-position is not required: the 8-bromo group deactivates the adjacent 9-position, and formylation proceeded regioselectively at the most active site in the dipyrromethane, namely the 1-position. Treatment of **II-1-Br^{8}** with 1 mol equiv of NBS at –78 °C afforded 8,9-dibromodipyrromethane **II-1-Br^{8,9}** as the major product in 71% yield.

Here, the deactivation caused by the 1-formyl group prevents bromination at the 2-position. Dipyrromethane **II-1-Br**[8,9] was crystalline, thus allowing purification without use of column chromatography. The regioselectivity of bromination was established by NMR spectroscopy (HH-COSY and NOESY experiments). Compound **II-1-Br**[8,9] can be stored in the solid form at 4 °C for at least 10 weeks without decomposition.

C. 3,13-Substituted Chlorins. Two 3,13-substituted chlorins bearing auxochromic groups were synthesized using the novel 8,9-dibromodipyrromethane **II-1-Br**[8,9]. Thus, the reaction of Eastern half **II-1-Br**[8,9] with the Western half bearing a bromine substituent (**II-6**)[26] was carried out in the standard way, affording chlorin **ZnC-Br**^{3}**Br**^{13} in 9% yield. Sonogashira coupling with (triisopropylsilyl)acetylene in the presence of $Pd_2(dba)_3$, P(*o*-tol)$_3$ and triethylamine afforded the diethynyl chlorin **ZnC-E**^{3}**E**^{13} in 35% yield (Scheme II.7).

A chlorin bearing a 3-ethynyl and 13-acetyl group was prepared as shown in Scheme II.8. Eastern half **II-1-Br**[8,9] was condensed with ethynyl-substituted Western half **II-7**[26] in CH_2Cl_2 upon treatment with a solution of $TsOH \cdot H_2O$ in MeOH. The yield upon oxidative cyclization under conventional heating did not exceed 2%, whereas microwave irradiation afforded the target chlorin **ZnC-E**^{3}**Br**^{13} in 5% yield. The Pd-mediated acetylation of **ZnC-E**^{3}**Br**^{13} was carried out in four steps including demetalation of zinc in TFA/CH_2Cl_2, acetylation under conditions analogous to those used in preparation of **FbC-A**^{13}, acidic hydrolysis in 10% aqueous HCl and metalation with $Zn(OAc)_2 \cdot 2H_2O$. In this manner, chlorin **ZnC-E**^{3}**A**^{13} was obtained in 59% yield.

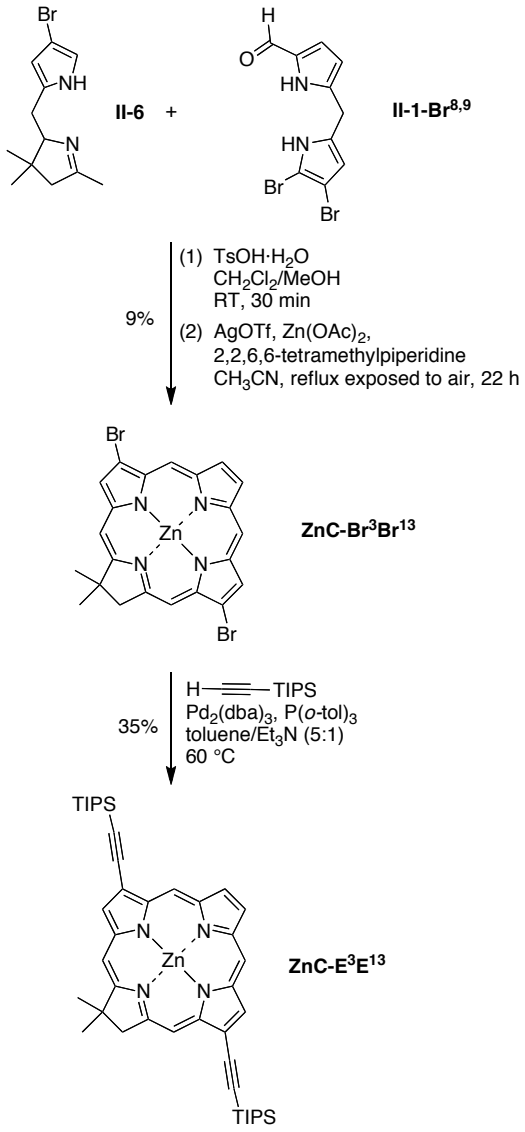

Scheme II.7. Synthesis of 13-ethynylchlorins.

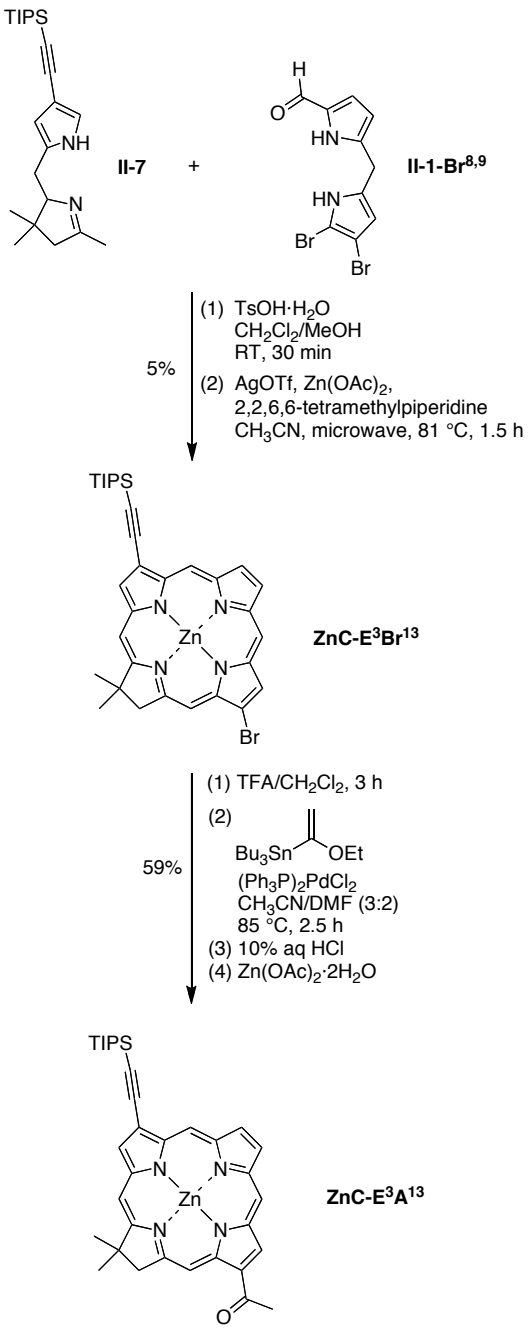

Scheme II.8. Synthesis 13-acetylchlorins.

I.2.3. Chemical Characterization

The chlorins were characterized by ^{1}H NMR spectroscopy (including NOESY), ^{13}C NMR spectroscopy (for 3,13-disubstituted chlorins), matrix-assisted laser desorption mass spectrometry (using a matrix of 1,4-bis(5-phenyloxazol-2-yl)benzene),[55] high-resolution electrospray ionization mass spectrometry, and absorption and fluorescence spectroscopy.[56,57]

X-ray structures of a number of chlorins were obtained to verify the substitution patterns described herein as well as several other patterns described previously (Chart II.2). Chlorin **FbC-A^{12}Br^{15}** was prepared via the 5-unsubstituted dipyrromethane **II-1-Br^{7,9}**; chlorin **ZnC-Br^{3}Br^{13}** was prepared from 5-unsubstituted dipyrromethane **II-1-Br^{8,9}**; the X-ray structure thus confirms the integrity of the substitution pattern for the new synthetic route to 8,9-dibromodipyrromethanes. Additional X-ray structures of two chlorins (**ZnC-M^{10}Br^{13}**, **ZnC-T^{5}M^{10}A^{13}**) and an oxophorbine (**FbOP-T^{5}M^{10}**) confirm the pattern of 10,13-, 5,10,13-, and 5,10,13,15-substituents, respectively. Each of these macrocycles was prepared previously[26,27] via the intermediacy of a 5-mesityldipyrromethane that bears the 8,9-dibromo substitution pattern, thus confirming the integrity of the 8,9-dibromination of the 5-mesityldipyrromethane. Other X-ray structures of chlorins have validated the reported substitution at the 7-position.[30]

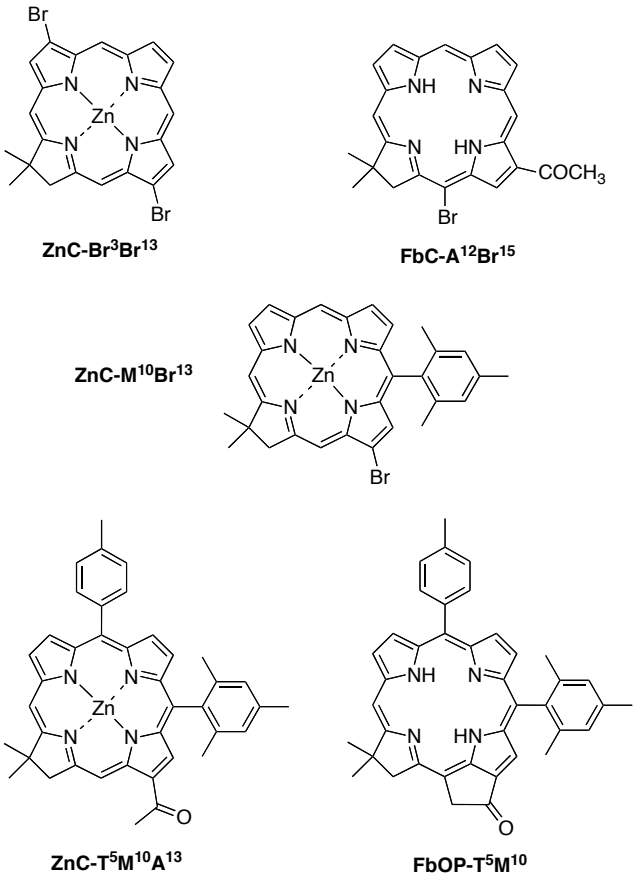

Chart II.2. Chlorins characterized by X-ray analysis.

II.2.4. Spectroscopy

A. Optical Spectra. The electronic ground-state absorption spectra of **ZnC-E^{3}E^{13}** and **ZnC-E^{3}E^{12}** are shown in Figure II.3A, respectively. The longest wavelength absorption feature for each compound is the $Q_y(0,0)$ band and corresponds to the $S_0 \rightarrow S_1$ transition. This band lies at a slightly longer wavelength for **ZnC-E^{3}E^{12}** than **ZnC-E^{3}E^{13}** (645 versus 643 nm). An analogous but slightly larger shift is observed for the near-UV Soret feature, which corresponds to a transition from S_0 to a higher singlet excited state. Both the $Q_y(0,0)$ and Soret maxima for **ZnC-E^{3}A^{12}** are also bathochromically shifted from those for **ZnC-**

E^{3}A^{13} (Figure II.4), and the shifts are 2 to 4 times larger than that found for **ZnC-E^{3}E^{12}** versus **ZnC-E^{3}E^{13}**. These results also show that incorporation of the acetyl group in place of the ethynyl group at either the 12 or 13 position results in a shift of the Q_y and Soret absorption features to longer wavelengths compared to the unsubstituted chlorin (Table II.1), in keeping with the prior studies of synthetic chlorins.[32,36] The ratios of the peak intensities of the Soret and Q_y bands are essentially the same for ethyne or acetyl at the 12 or 13 positions, and the same is true for the integrated intensities of the band contours (Table II.1).

Table II.1. Photophysical properties of zinc chlorins.[a]

Compound[b]	λ_B (nm)	$\lambda_{Qy(0,0)}$ absn (nm)	$\lambda_{Qy(0,0)}$ emis (nm)	$\frac{I_B}{I_{Q_y}}$[c]	$\frac{\Sigma_B}{\Sigma_{Q_y}}$[d]	Φ_f	τ_f (ns)	$(k_f)^{-1}$ (ns)
ZnC[e]	398	602	602	3.4	4.1	0.062	1.7	27
ZnC-E^{3}E^{12}[f]	420	645	646	1.5	2.2	0.18	3.1	17
ZnC-E^{3}E^{13}	416	643	644	1.3	2.2	0.23	3.7	16
ZnC-E^{3}A^{12}[g]	428	655	657	1.2	2.0	0.22	4.1	19
ZnC-E^{3}A^{13}	420	648	650	1.3	2.2	0.24	4.6	19

[a]All samples were measured at room temperature in toluene. [b]For nomenclature, see text and Chart II.1. [c]Ratio of the peak intensities of the B and $Q_y(0,0)$ bands. [d]Ratio of the integrated intensities of the B (B_x plus B_y components) and Q_y absorption manifolds, which includes the (0,0) and (1,0) features. [e]From Ref 32. [f]From Ref 32 wherein the compound was initially assigned as **ZnC-E^{3}E^{13}**. [g]From Ref 32 wherein the compound was initially assigned as **ZnC-E^{3}A^{13}**.

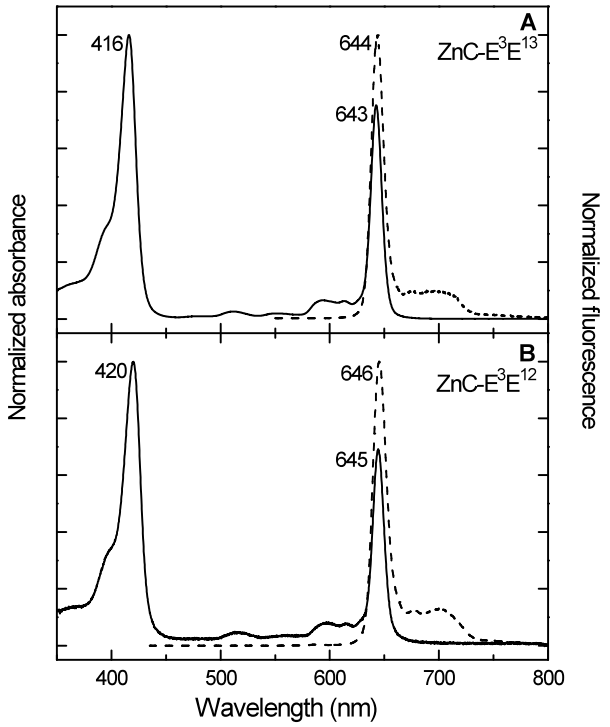

Figure II.3. Absorption and fluorescence spectra of **ZnC-E^{3}E^{13}** (A) and **ZnC-E^{3}E^{12}** (B) in toluene. The peak wavelengths (nm) are indicated.

The $Q_y(0,0)$ $S_1 \rightarrow S_0$ fluorescence feature for each chlorin is shown in Figures II.3 and II.4. For each compound, there is very little Stokes shift from the corresponding absorption maximum. This finding is in accord with prior results on a large series of synthetic chlorins, indicating very little change in structural or electronic characteristics of the chlorin macrocycle following excitation. The average Stokes shift for the two acetyl-substituted chlorins **ZnC-E^{3}A^{13}** and **ZnC-E^{3}A^{12}** (~50 cm^{-1}) is larger than that for the ethynyl-substituted analogs **ZnC-E^{3}E^{13}** and **ZnC-E^{3}E^{12}** (~25 cm^{-1}). This difference may reflect in part rotation of the acetyl group with respect to macrocycle in the excited state;

however, given the small magnitudes of the shifts for both substituents, this effect is not substantial.

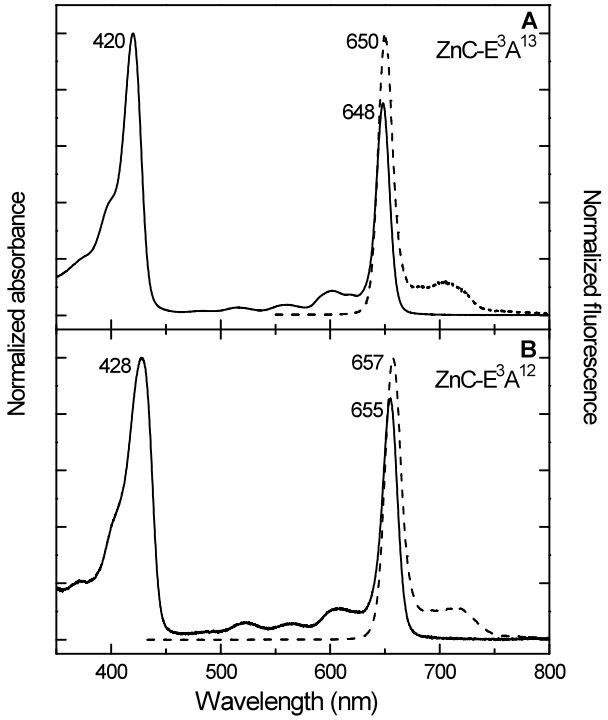

Figure II.4. Absorption and fluorescence spectra of **ZnC-E^{3}A^{13}** (A) and **ZnC-E^{3}A^{12}** (B) in toluene. The peak wavelengths (nm) are indicated.

B. Fluorescence Quantum Yields and Excited-State Lifetimes. The fluorescence quantum yields (Φ_f) and singlet excited-state lifetimes (τ_S) for the four substituted chlorins are given in Table II.1 along with the values for the parent chlorin **ZnC** (lacking any meso or β-pyrrole substituents). The incorporation of an ethynyl substituent at the 13-position of **ZnC-E^{3}E^{13}** versus the 12-position of **ZnC-E^{3}E^{12}** gives modestly larger values for Φ_f (0.23 versus 0.18) and τ_S (3.7 ns versus 3.1 ns). Similar results are obtained for the analogous

acetyl derivatives **ZnC-E^{3}A^{13}** versus **ZnC-E^{3}A^{12}**: Φ_f = 0.24 versus 0.22 and τ_S = 4.6 ns versus 4.1 ns. Insights into the origins of these differences can be seen from the common dependence of both Φ_f and τ_S on the rate constants for $S_1 \rightarrow S_0$ spontaneous fluorescence (k_f), $S_1 \rightarrow S_0$ internal conversion (k_{ic}), and $S_1 \rightarrow T_1$ intersystem crossing (k_{isc}) via Eqs. (II.1) and (II.2).

$$\tau_S = (k_f + k_{ic} + k_{isc})^{-1} \qquad \text{(II.1)}$$

$$\Phi_f = k_f / (k_f + k_{ic} + k_{isc}) \qquad \text{(II.2)}$$

Eq. (II.3) shows how the radiative (fluorescence) rate constant is calculated from the measured values of Φ_f and τ_S (Table II.1)

$$k_f = \Phi_f / \tau_S \qquad \text{(II.3)}$$

The calculated k_f values are essentially the same for **ZnC-E^{3}E^{12}** and **ZnC-E^{3}E^{13}** [(16 ns)$^{-1}$ and (17 ns)$^{-1}$, respectively] and the same is true for **ZnC-E^{3}A^{13}** and **ZnC-E^{3}A^{12}** [both (19 ns)$^{-1}$]. This finding, when factored into Eqs (II.1) and (II.2) indicates that the greater Φ_f and τ_S values that result from placement of either an ethyne or acetyl at the 13- versus 12-position must derive from a decrease in one or both of the nonradiative rate constants (k_{ic}, k_{isc}). The energy-gap law would predict a slightly smaller internal-conversion rate constant for analogous 13- versus 12-substituted chlorins because the former compounds have a slightly greater S_1 excited-state energy (as seen by the $Q_y(0,0)$ absorption and emission wavelengths, Table II.1). Because k_{isc} typically dominates over k_{ic} for chorins,[32] and given that 13- versus 12-substituted chlorins exhibit slightly larger Φ_f and τ_S values, it is likely that

the k_{isc} values are also smaller when an ethyne or acetyl group is placed at the 13-position compared to the 12-position. A possible underlying cause of this effect is that an ethyne or acetyl at the 13-position results in a slightly greater extent of electron delocalization off the macrocycle compared to the same group located at the 12-position.

C. Electrochemistry. The incorporation of two ethyne groups to the parent chlorin **ZnC** causes a significant (~0.1 V) shift of the first oxidation potential to more positives values (Table II.2); furthermore, with the first ethyne at the 3-position, the $\Delta E_{1/2}^{ox}$ value is effectively the same whether the second ethyne group is located at the 12- versus 13-position (+0.40 V versus +0.41 V). Basically the same is true for 3-ethynyl chlorins in which an acetyl group is placed at the 12- or 13-position (+0.42 V or +0.44 V). Turning to the first reduction potentials, the incorporation of two ethynyl groups causes a substantial (~0.25 V) shift to less negative values; furthermore, with the first ethyne at the 3 position, the $\Delta E_{1/2}^{red}$ value is effectively the same whether the second ethyne is located at the 12- or 13-position (−1.49 V or −1.48 V). Again, the same is true for the addition of an acetyl group at the 12- or 13-position of a 3-ethynyl porphyrin (−1.42 V or −1.41 V). Although there are insignificant differences if the second substituent (ethyne or acetyl) is added at the 12- or 13-position, the differences in reduction potentials of the ethynyl-acetyl chlorins (**ZnC-E^{3}A^{12}** or **ZnC-E^{3}A^{13}**) are ~0.07 V less negative than those for the bis-ethynyl chlorins (**ZnC-E^{3}E^{12}** or **ZnC-E^{3}E^{13}**); the corresponding oxidation potentials of the former complexes are only ~0.02 V more positive than those of the former. Thus, the ethynyl-acetyl chlorins are significantly easier to reduce than the bis-ethynyl analogs, but are only marginally harder to oxidize.

Table II.2. Redox properties and orbital energies of zinc chlorins.

Compound	Redox Potential (V)[a]			Orbital Energy (eV)					
	$\Delta E_{1/2}^{ox}$	$\Delta E_{1/2}^{red}$	ΔE_{redox}[b]	HOMO–1	HOMO	LUMO	LUMO+1	ΔE_{MO}[c]	$\Delta E_{0,0}$[d]
ZnC	+0.30[e]	−1.74[e]	2.04	−5.16	−4.79	−2.12	−1.55	2.67	2.06
ZnC-E^{3}E^{12}	+0.40[f]	−1.49[f]	1.89	−5.31	−4.94	−2.43	−1.79	2.51	1.92
ZnC-E^{3}E^{13}	+0.41	−1.48	1.89	−5.32	−4.94	−2.43	−1.75	2.51	1.93
ZnC-E^{3}A^{12}	+0.42[g]	−1.42[g]	1.84	−5.36	−5.02	−2.58	−1.88	2.45	1.89
ZnC-E^{3}A^{13}	+0.44	−1.41	1.85	−5.36	−5.04	−2.57	−1.81	2.47	1.91

[a]Measured in butyronitrile/0.1 M *n*-BuN_4PF_6; potentials versus $FeCp_2/FeCp_2^+$ = +0.19 V. [b]$\Delta E_{redox} = \Delta E_{1/2}^{ox} - \Delta E_{1/2}^{red}$. [c]$\Delta E_{MO} = E_{LUMO} - E_{HOMO}$. [d] $\Delta E_{0,0}$ is the energy of the lowest singlet excited state in toluene from Table II.1. [e]From Ref 36. [f]The oxidation and reduction potentials reported in Ref 36, where the compound was assigned as **ZnC-E^{3}E^{13}**, were +0.40 V and −1.51 V. [g]From Ref 36 wherein the compound was initially assigned as **ZnC-E^{3}A^{13}**.

D. DFT Calculations. The results of the density functional theory calculations generally track the key redox and optical properties of the chlorins under study (Figure II.5). The identical HOMO energies of **ZnC-E^{3}E^{12}** or **ZnC-E^{3}E^{13}** are in accord with the finding that the first oxidation potentials are the same to within 0.01 eV (Table II.2). The identical LUMO energies of the same two bis-ethynyl chlorins also are consistent with the finding that the first reduction potentials are the same to within 0.01 eV. The calculated HOMO of **ZnC-E^{3}A^{13}** being only 0.02 eV more negative than that for **ZnC-E^{3}A^{12}** is consistent with the measured $\Delta E_{1/2}^{ox}$ value of the former compound being only 0.02 eV more positive than that of the former, the values being within experimental error for the two compounds. Similarly, the calculated LUMO and measured $\Delta E_{1/2}^{red}$ values are the same for the two ethynyl-acetyl chlorins to within 0.01 eV. The findings from the measured redox potentials that the ethynyl-acetyl chlorins are perhaps slightly harder to oxidize but more substantially easier to reduce are also reproduced by the differences in HOMO energies and LUMO energies, respectively. Finally, the differences in the redox properties of the four substituted chlorins with the parent chlorin **ZnC** are qualitatively reproduced by the trends in orbital energies.

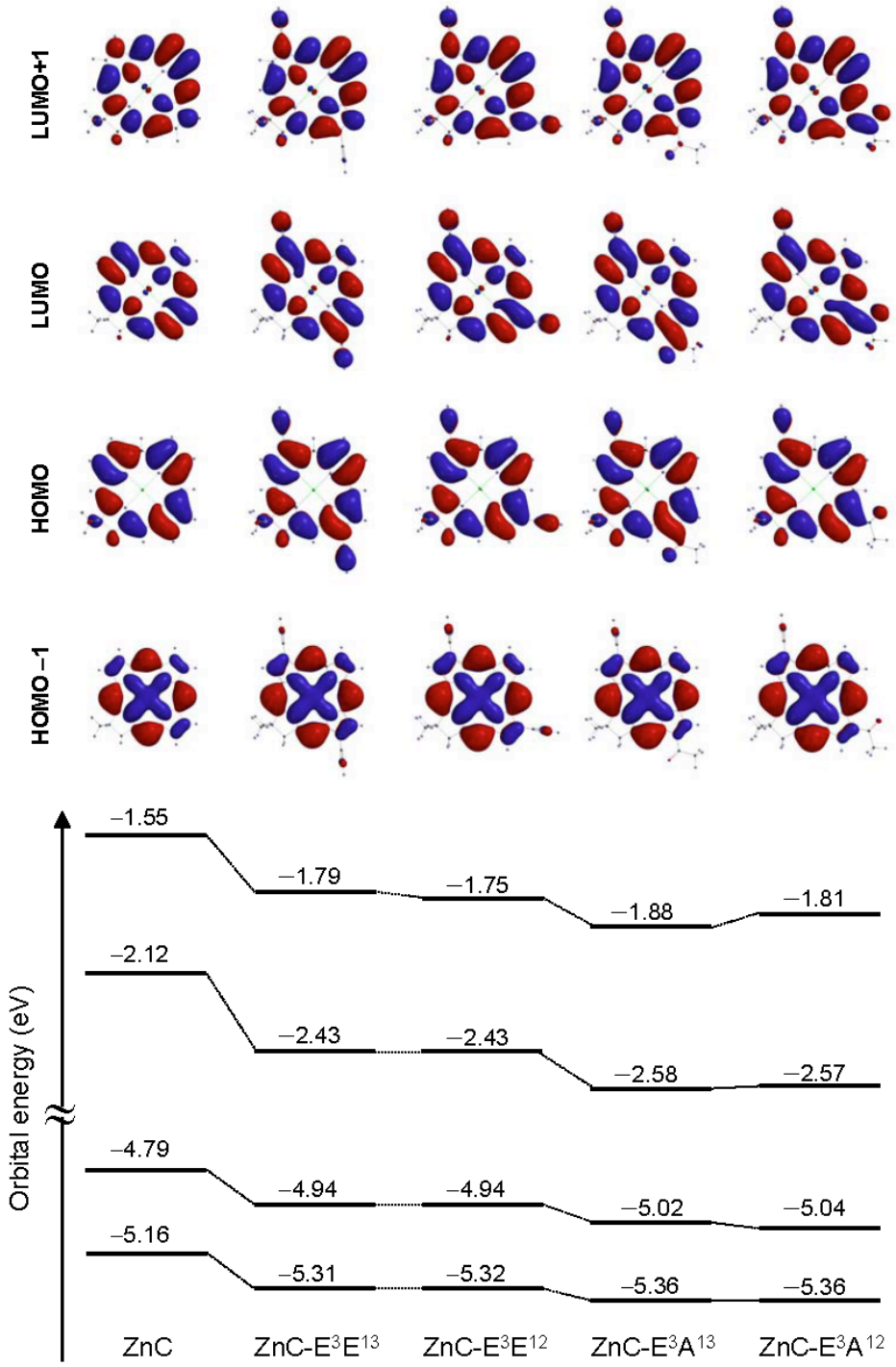

Figure II.5. Molecular orbital energies and electron-density distributions of 3,13- and 3,12-disubstituted chlorins obtained from DFT calculations.

The calculated orbital-energy difference $\Delta E_{MO} = E_{LUMO} - E_{HOMO}$ for **ZnC-E^{3}E^{12}** and **ZnC-E^{3}E^{13}** are the same as one another. This result matches the finding of the same value for the measured difference in first oxidation and reduction potentials $\Delta E_{redox} = \Delta E_{1/2}^{ox} - \Delta E_{1/2}^{red}$. These two quantities in turn match the finding of the same energy ($\Delta E_{0,0}$ within 0.01 eV) of the lowest singlet excited state derived from the optical spectra. One expects the latter result since the LUMO - HOMO energy gap is a major contributor to the energy of the S_1 excited state, along with a somewhat smaller (40%) contribution from the energy gap between LUMO+1 and HOMO-1.[58,59] The same basic agreement is found for the ΔE_{MO}, ΔE_{redox}, and $\Delta E_{0,0}$ values for **ZnC-E^{3}A^{12}** and **ZnC-E^{3}A^{13}**. In addition, the calculated ΔE_{MO} values are slightly (~0.05 eV) smaller for the ethynyl-acetyl chlorins than for the bis-ethynyl chlorins, consistent with the similarly smaller experimental ΔE_{redox}, and $\Delta E_{0,0}$ values for the former versus the latter chlorins.

II.3. Conclusions

Reexamination of the dibromination of dipyrromethanes **II-1** and **II-2** revealed an unexpected interplay of steric and electronic effects. In particular, the bromination of a 1-formyldipyrromethane with two equivalents of NBS proceeds at the 9- and 7-positions when there is no steric hindrance owing to a 5-aryl substituent; in the presence of a 5-aryl substituent, bromination proceeds at the 9- and 8-positions. The 7,9-dibromination pattern provides access to 12-substituted chlorins that lack a 10-substituent.

A rational route has been developed to 8,9-dibromo-1-formyldipyrromethane (**II-1-Br^{8,9}**, lacking a 5-substituent), which constitutes a key precursor for 13-substituted chlorins

lacking 10-substituents. Thus, chlorins bearing a single substituent at the 12-position or 13-position can now be unambiguously obtained, the former by regioselective bromination of the Eastern half precursor (1-formyldipyrromethane), the latter by a new synthesis of 8,9-dibromo-1-formyldipyrromethane.

The availability of both 12-substituted and 13-substituted chlorins provided an opportunity to probe the distinctions caused by this change in substitution pattern. The incorporation of an ethyne or acetyl group at the 12-position versus the 13 position of a 3-ethynyl chlorin results in (1) virtually the same first oxidation potential (within 0.01 eV), (2) virtually the same first reduction potential (within 0.02 eV), (3) a small blue shift in the $Q_y(0,0)$ absorption and emission bands (~ 2 nm for the bis-ethynyl and ~7 nm for the ethynyl-acetyl chlorins), (4) an increase in fluorescence yield (~30% for the bis-ethynyl and ~10% for the ethynyl-acetyl chlorins) and (5) an ~15% average lengthening of the lifetime of the lowest singlet excited state. The availability of chlorin isomers identical in all aspects except for the position of a substituent at the 12- or 13-position, which grew out of an effort to understand the unexpected regiochemistry of bromination of 1-formyldipyrromethanes, has provided deeper insight into the effects of substituents on the spectral, redox and photochemical features of analogues of chlorophyll.

II.4. Experimental Section

Absorption and fluorescence spectroscopy. Static absorption and fluorescence measurements were performed as described previously, typically for very dilute solutions of the compounds in toluene.[56,57] Fluorescence lifetimes were obtained using a phase

modulation technique.[57] Argon-purged solutions with an absorbance of ≤0.10 at the Soret-band λ_{exc} were used for the fluorescence spectral and lifetime measurements. For fluorescence spectra, the excitation and detection monochromators typically had a band pass of 1.5 and 3.7 nm, respectively, and spectra were obtained using 0.2 nm data intervals. The emission spectra were corrected for detection-system spectral response. Fluorescence quantum yields were determined for argon-purged solutions of the chlorin relative to chlorophyll *a* in benzene ($\Phi_f = 0.325$)[60] and were corrected for solvent refractive index.

For calculation of the integrated-intensity ratio of the Soret and Q_y absorption manifolds (Σ_B/Σ_{Q_y}), the Soret region was typically integrated from the red of the origin maximum (~450 nm) to ~350 nm in order to encompass the $B_x(0,0)$, $B_y(0,0)$, $B_x(1,0)$ and $B_y(1,0)$ features. Similarly, integration of the Q_y manifold encompassed the (0,0) band and the (1,0) feature(s), but not any (2,0) contributions. For each compound, the integration range for both the B and Q_y manifolds was chosen to attempt to best capture the associated oscillator strength while minimizing contributions from absorption to higher-energy electronic states (e.g., the Q_x bands in the case of the Q_y manifold).

Electrochemistry. The electrochemical measurements were made in a standard three-electrode cell using Pt working and counter electrodes and an Ag/Ag^+ reference electrode. The solvent/electrolyte was butyronitrile containing 0.1 M *n*-BuN_4PF_6. The potentials are reported versus $FeCp_2/FeCp_2^+ = 0.19$ V.

Molecular-Orbital Calculations. Density functional theory (DFT) calculations were performed as described previously[36] using the hybrid B3LYP functional and a 6-31G* basis

set. The equilibrium geometry of each complex was fully optimized using the complete structure and the default parameters of the program.

Bromination of 1-formyldipyrromethane (II-1). A solution of **II-1** (174 mg, 1.00 mmol) in anhydrous THF (10 mL) at –78 °C was treated with NBS (348 mg, 2.00 mmol) in one batch under argon. The reaction mixture was stirred for 1 h at –78 °C, after which the ice bath was removed. A thermometer was placed in the reaction mixture. The reaction mixture was allowed to warm up. Hexanes (10 mL) and water (10 mL) were added when the temperature of the reaction mixture reached –20 °C. The entire contents of the reaction flask were transferred to a separatory funnel. Ethyl acetate (20 mL) was added. The organic layer was separated, dried (K_2CO_3) and concentrated without heating to afford a brown solid. Column chromatography [silica, hexanes/CH_2Cl_2/ethyl acetate (7:2:1)] afforded three brominated dipyrromethanes in the following order: a trace of 3,7,9-tribromo-1-formyldipyrromethane (**II-1-Br^{3,7,9}**, estimated 80% purity, 8 mg, 2%); a dominant amount of 7,9-dibromo-1-formyldipyrromethane (**II-1-Br^{7,9}**, 219 mg, 66%); and finally a lesser amount of 8,9-dibromo-1-formyldipyrromethane (**II-1-Br^{8,9}**, 41 mg, 12%).

The three products were examined by ^{1}H NMR spectroscopy. The ^{1}H NMR data for **II-1-Br^{7,9}** were consistent with those described previously (reported as **II-1-Br^{8,9}**).[27] The ^{1}H NMR data for **II-1-Br^{8,9}** were consistent with those described for the compound prepared by rational synthesis (vide infra). Compound **II-1-Br^{3,7,9}** has not been previously described.

Data for **II-1-Br^{3,7,9}**: ^{1}H NMR (THF-d_8) δ 3.96 (s, 2H), 6.06 (d, J = 2.7 Hz, 1H), 6.92 (d, J = 2.6 Hz, 1H), 9.37 (s, 1H), 10.71 (br s, 1H), 11.45 (br s, 1H); ESI-MS obsd 408.8184 $(M + H)^+$ corresponds to 407.8111 (M), calcd 407.8109 ($C_{10}H_7Br_3N_2O$).

Bromination of 5-mesityl-1-formyldipyrromethane (II-2). Bromination of **II-2** (292 mg, 1.00 mmol) was carried out in exact analogy with that of **II-1**. Column chromatography [silica, hexanes/CH_2Cl_2/ethyl acetate (7:2:1)] afforded three brominated dipyrromethanes in the following order: a trace of 3,8,9-tribromo-1-formyl-5-mesityldipyrromethane (**II-2-Br^{3,8,9}**, estimated 90% purity, 9 mg, 1.7%); an amount of 7,9-dibromo-1-formyl-5-mesityldipyrromethane (**II-2-Br^{7,9}**, estimated 90% purity, 37 mg, 10%); and finally a dominant amount of 8,9-dibromo-1-formyl-5-mesityldipyrromethane (**II-2-Br^{8,9}**, 180 mg, 49%). The three products were examined by ^{1}H NMR spectroscopy. The ^{1}H NMR data for **2-Br^{8,9}** were consistent with those described previously.[26] Compounds **II-2-Br^{7,9}** and **II-2-Br^{3,8,9}** have not been previously described.

Data for **II-2-Br^{7,9}**: mp 66–68 °C (dec.); ^{1}H NMR (THF-d_8) δ 2.06 (s, 6H), 2.23 (s, 3H), 5.67–5.68 (m, 1H), 5.80 (s, 1H), 6.10 (s, 1H), 6. 76 (s, 1H), 6.81 (s, 2H), 9.42 (s, 1H), 10.46 (br s, 1H), 11.31 (br s, 1H); ^{13}C NMR (THF-d_8) δ 21.1, 21.2, 39.9, 96.7, 97.4, 112.0, 113.5, 121.1, 131.1, 132.0, 134.3, 135.4, 137.1, 137.9, 138.0, 139.8, 178.7; ESI-MS obsd 448.98618 $(M + H)^+$ corresponds to 447.97890 (M), calcd 447.97859 ($C_{19}H_{18}Br_2N_2O$).

Data for **II-2-Br^{3,8,9}**: mp 65 °C (dec.); ^{1}H NMR (THF-d_8) δ 2.06 (s, 6H), 2.23 (s, 3 H), 5.54–5.55 (m, 1H), 5.74 (s, 1H), 6.82 (s, 2H), 6.94–6.95 (m, 1H), 9.39 (s, 1H), 11.01 (br s, 1H), 11.26 (br s, 1H); ESI-MS obsd 526.8955 $(M + H)^+$ corresponds to 525.8883 (M), calcd 525.8891 ($C_{19}H_{17}Br_3N_2O$).

7,9-Dibromo-1-formyldipyrromethane (II-1-Br^{7,9}). Following the procedure for dibromination of 1-formyldipyrromethanes (described incorrectly to give **II-1-Br^{8,9}**),[26] a solution of **1** (174 mg, 1.00 mmol) in anhydrous THF (15 mL) at –78 °C was treated with

NBS (383 mg, 2.20 mmol) in one batch under argon. The reaction mixture was stirred for 1 h at –78 °C, after which the ice bath was removed, and the reaction mixture was allowed to warm up. Hexanes was added when the reaction mixture reached –20 °C, and water was added upon reaching 0 °C. Ethyl acetate was added. The organic layer was separated, dried (K_2CO_3) and concentrated without heating to afford a brown solid. Column chromatography [silica, hexanes/CH_2Cl_2/ethyl acetate (7:2:1)] afforded a pinkish-white solid (175 mg, 52%): mp 109–111 °C (dec.); ^{1}H NMR (THF-d_8) δ 3.94 (s, 2H), 5.89–5.91 (m, 1H), 6.06 (d, J = 2.7 Hz, 1H), 6.77–6.80 (m, 1H), 9.37 (s, 1H), 10.84 (br s, 1H), 11.17 (br s, 1H); ^{13}C NMR (THF-d_8) δ 96.2, 97.9, 110.0, 112.6, 121.6, 121.7, 128.8, 134.2, 138.9, 178.4; Anal. Calcd for $C_{10}H_8Br_2N_2$: C, 36.18; H, 2.43; N, 8.44. Found: C, 36.58; H, 2.50; N, 8.11.

Bromination of 5-phenyl-1-formyldipyrromethane (II-8). A solution of **II-8** (60 mg, 0.24 mmol) in anhydrous THF (2.4 mL) at –78 °C was treated with NBS (85 mg, 0.48 mmol) in one batch under argon. The reaction mixture was stirred for 1 h at –78 °C, after which the ice bath was removed. A thermometer was placed in the reaction mixture. The reaction mixture was allowed to warm up. Hexanes (5 mL) and water (5 mL) were added when the temperature of the reaction mixture reached –20 °C. The entire contents of the reaction flask were transferred to a separatory funnel. Ethyl acetate (10 mL) was added. The organic layer was separated, dried (K_2CO_3) and concentrated without heating to afford a yellow solid. Column chromatography [silica, hexanes/CH_2Cl_2/ethyl acetate (7:2:1)] was run twice but did not allow complete separation of isomers affording two brominated dipyrromethanes, each impure, in the following order: a minor amount of 7,9-dibromo-5-phenyl-1-formyldipyrromethane (**II-8-Br^{7,9}**, 15 mg, 15%); and a dominant amount of 8,9-

dibromo-5-phenyl-1-formyldipyrromethane (**II-8-Br**^{8,9}, 58 mg, 60%). The isolated sample of **II-8-Br**^{7,9} contained 0.5-1% of **II-8-Br**^{8,9}. The isolated sample of **II-8-Br**^{8,9} contained 7% of **II-8-Br**^{7,9}, 10% of **II-8-Br**^{9} and 5% of unidentified impurities. The two products were examined by ^{1}H NMR spectroscopy.

Data for **II-8-Br**^{8,9}: ^{1}H NMR (THF-d_8) δ 5.41 (s, 1H), 5.69–5.70 (m, 1H), 5.90-5.91 (m, 1H), 6.81-6.82 (m, 1H), 7.17-7.31 (m, 5H), 9.40 (s, 1H), 10.89 (br s, 1H), 11.27 (br s, 1H); ESI-MS 406.9382 $(M + H)^+$ corresponds to 405.9309 (M), calcd 405.9316 ($C_{16}H_{12}Br_2N_2O$).

Data for **II-8-Br**^{7,9}: ^{1}H NMR (THF-d_8) δ 5.65 (s, 1H), 5.98–6.00 (m, 1H), 6.09 (d, J = 2.6 Hz, 1H), 6.84-6.86 (m, 1H), 7.11-7.29 (m, 5H), 9.41 (s, 1H), 10.90 (br s, 1H), 11.29 (br s, 1H); obsd 406.9382 $(M + H)^+$ corresponds to 405.9309 (M), calcd 405.9316 ($C_{16}H_{12}Br_2N_2O$).

12-Bromo-17,18-dihydro-18,18-dimethylporphyrin (FbC-Br^{12}**).** A solution of **II-1-Br**^{7,9} (155 mg, 0.467 mmol) and **II-3** (88 mg, 0.47 mmol) in anhydrous CH_2Cl_2 (12 mL) was treated with a solution of $TsOH·H_2O$ (445 mg, 2.34 mmol) in anhydrous methanol (3 mL) under argon. The color of the reaction mixture changed immediately to orange-red. The mixture was stirred for 30 min under argon, then neutralized with 2,2,6,6-tetramethylpiperidine (970 μL, 5.15 mmol) and concentrated to dryness. The resulting brown solid was dissolved in acetonitrile (50 mL), and 2,2,6,6-tetramethylpiperidine (1.58 mL, 9.34 mmol), $Zn(OAc)_2$ (1.29 g, 7.01 mmol) and AgOTf (360 mg, 1.40 mmol) were added. The resulting suspension was refluxed for 16 h exposed to air. The reaction mixture was filtered though a silica pad, and the filtrate was concentrated to a green solid. The solid was dissolved in CH_2Cl_2 (12 mL), and the solution was stirred and treated dropwise with TFA (280 μL, 3.60 mmol). After 3 h the reaction mixture was diluted with CH_2Cl_2, and

washed (saturated aqueous $NaHCO_3$, water and brine). The organic phase was separated, concentrated and chromatographed [silica, CH_2Cl_2/hexanes (5:2)] to afford a green solid (15 mg, 8%): ^{1}H NMR δ –2.45 (br s, 2H), 2.06 (s, 6H), 4.64 (s, 2H), 8.96–8.99 (m, 4H), 9.06 (d, J = 3.9 Hz, 1H), 9.10 (d, J = 3.9 Hz, 1H), 9.25 (d, J = 5.6 Hz, 1H), 9.85 (s, 1H), 9.92 (s, 1H); LD-MS obsd 417.8; ESI-MS obsd 419.0869 $(M + H)^+$ corresponds to 418.0802 (M), calcd 418.0793 ($C_{22}H_{19}BrN_4$); λ_{abs} 391, 640 nm.

12-Acetyl-17,18-dihydro-18,18-dimethylporphyrin (FbC-A^{12}). Following a procedure for acetylation of aromatic compounds via Stille coupling,[45] a mixture of **FbC-Br^{12}** (14 mg, 0.034 mmol), tributyl(1-ethoxyvinyl)tin (45.0 μL, 0.134 mmol), and $(PPh_3)_2PdCl_2$ (4 mg, 0.005 mmol) was refluxed in acetonitrile/DMF [3 mL, (3:2)] for 2.5 h. The reaction mixture was treated with 10% aqueous HCl (1 mL) at room temperature for 40 min and then diluted with CH_2Cl_2. The organic phase was washed with saturated aqueous $NaHCO_3$, water, and brine. The organic layer was dried (Na_2SO_4), concentrated and chromatographed [silica, CH_2Cl_2/hexanes (2:1)] to afford a purple solid (9 mg, 70%): ^{1}H NMR δ –2.29 (br s, 1H), –2.08 (br s, 1H), 2.05 (s, 6H), 3.27 (s, 3H), 4.59 (s, 2H), 8.93 (s, 1H), 8.98 (d, J = 4.5 Hz, 1H), 8.99 (d, J = 4.1 Hz, 1H), 9.01 (s, 1H), 9.13 (d, J = 4.1 Hz, 1H), 9.20 (d, J = 4.5 Hz, 1H), 9.24 (s, 1H), 9.73 (s, 1H), 10.80 (s, 1H); LD-MS obsd 381.6; ESI-MS obsd 383.1869 $(M + H)^+$ corresponds to 382.1796 (M), calcd 382.1794 ($C_{24}H_{22}N_4O$); λ_{abs} 414, 662 nm.

Zn(II)-12-Acetyl-17,18-dihydro-18,18-dimethylporphyrin (ZnC-A^{12}). A solution of **FbC-A^{12}** (9 mg, 0.02 mmol) in $CHCl_3$ (4 mL) was treated with a solution of $Zn(OAc)_2 \cdot 2H_2O$ (78 mg, 0.35 mmol) in MeOH (1 mL). The reaction mixture was stirred for

6 h at room temperature. Then the reaction mixture was concentrated, and the crude solid was dissolved in CH_2Cl_2. The organic phase was washed (saturated aqueous $NaHCO_3$, water, and brine), dried (Na_2SO_4), and concentrated. The solid was washed three times with hexanes. The solid was dissolved in CH_2Cl_2 (1 mL), and hexanes (1 mL) was added. The resulting precipitate was isolated by centrifugation (9 mg, 80%): ^{1}H NMR (THF-d_8) δ 2.50 (s, 6H), 3.14 (s, 3H), 4.56 (s, 2H), 8.70 (s, 1H), 8.74 (s, 1H), 8.79–8.80 (m, 1H), 8.92–8.93 (m, 1H), 9.05–9.08 (m, 2H), 9.28 (s, 1H), 9.58 (s, 1H), 10.77 (s, 1H); LD-MS obsd 444.1; ESI-MS obsd 444.0928 (M^+) corresponds to 444.0934 (M), calcd 444.0929 ($C_{24}H_{20}N_4OZn$) λ_{abs} 418, 637 nm.

12-Acetyl-15-bromo-17,18-dihydro-18,18-dimethylporphyrin (FbC-A^{12}Br^{15}). A solution of **FbC-A^{12}** (14.0 mg, 0.0368 mmol) in CH_2Cl_2/TFA [18 mL (10:1)] was treated with NBS (368 μL, 0.100 M in CH_2Cl_2, 0.037 mmol). The reaction mixture was stirred for 1 h at room temperature. CH_2Cl_2 was added, and the mixture was washed with $NaHCO_3$. The organic layer was dried (Na_2SO_4), concentrated, and chromatographed [silica, CH_2Cl_2/hexanes (2:1)] to afford a purple solid (7 mg, 44 %): ^{1}H NMR δ –1.99 (br s, 2H), 2.03 (s, 3H), 3.25 (s, 3H), 4.58 (s, 2H), 8.75 (s, 1H), 8.76 (d, J = 4.2 Hz, 1H), 8.87 (d, J = 4.8 Hz, 1H), 8.95 (d, J = 4.2 Hz, 1H), 9.06 (d, J = 4.8 Hz, 1H), 9.44 (s, 1H), 9.48 (s, 1H), 10.63 (s, 1H); MALDI-MS obsd, 460.3; ESI-MS obsd 461.09692 $(M + H)^+$ corresponds to 460.08965 (M), calcd 460.08987 ($C_{24}H_{21}BrN_4O$); λ_{abs} 418, 664 nm**.**

2-Bromodipyrromethane (II-5). A solution of **II-4** (2.48 g, 14.4 mmol) in anhydrous THF/methanol (144 mL) at 0 °C was carefully treated with $NaBH_4$ (8.85 g, 233 mmol) in portions. The mixture was stirred for 2 h. Then water and ethyl acetate were

added, and the resulting mixture was stirred for 20 min. After thorough extraction with ethyl acetate the organic layer was separated, dried (Na_2SO_4) and concentrated to give a colorless oil, which was used in the next stage without purification. The oil was dissolved in pyrrole (20.0 mL, 287 mmol). The solution was degassed with a stream of argon for 10 min and then treated with $InCl_3$ (343 mg, 1.55 mmol). The mixture was stirred overnight under argon. The mixture turned dark brown during the first hour of reaction. The reaction mixture was quenched with 1 M NaOH (50 mL). After extraction with ethyl acetate, the organic layer was dried (Na_2SO_4) and concentrated. The excess pyrrole was recovered under high vacuum. The resulting crude brown oil was chromatographed [silica, hexanes/CH_2Cl_2/ethyl acetate (7:2:1)] to afford a pale yellow oil that turned brown when stored (2.02 g, 58%): ^{1}H NMR δ 3.89 (s, 2H), 6.02–6.03 (m, 2H), 6.13–6.16 (m, 1H), 6.58–6.59 (m, 1H), 6.65–6.66 (m, 1H), 7.66–7.84 (br s, 2H); ^{13}C NMR δ 26.5, 96.1, 107.1, 108.7, 109.2, 117.2, 117.9, 128.2, 130.2; ESI-MS obsd 225.00137 $(M + H)^+$ corresponds to 223.99409 (M), calcd 223.99491 ($C_9H_9BrN_2$).

8-Bromo-1-formyldipyrromethane (II-1-Br[8]). A sample of DMF (7.00 mL) was treated with $POCl_3$ (1.00 mL, 10.9 mmol) at 0 °C under argon, and the mixture was stirred for 10 min. Then a solution of **II-5** (1.94 g, 8.55 mmol) in DMF (25 mL) at 0 °C was treated with the freshly prepared Vilsmeier reagent (5.62 mL, 8.77 mmol) under argon. The resulting mixture was stirred for 2 h at 0 °C. The mixture was poured into a cooled mixture of 2 M NaOH (120 mL) and CH_2Cl_2 (80 mL) at 0 °C and stirred for 20 min. The organic phase was washed (saturated aqueous NH_4Cl, water, and brine), dried (Na_2SO_4), and concentrated to give a red-brownish oil. The oil was treated with hexanes and concentrated

to give a brown solid. Column chromatography [silica, hexanes/ethyl acetate (6:1)] afforded a brown solid. For recrystallization the solid was dissolved in the minimal amount of warm CH_2Cl_2, which upon cooling afforded pale brown crystals (868 mg, 40%): mp 134–135 ºC (dec.); ^{1}H NMR (acetone-d_6) δ 4.02 (s, 2H), 5.93–5.95 (m, 1H), 6.08–6.09 (m, 1H), 6.73–6.75 (m, 1H), 6.89–6.90 (m, 1H), 9.41 (s, 1H), 10.6 (br s, 1H), 10.9 (br s, 1H); ^{13}C NMR (acetone-d_6) δ 27.2, 96.2, 110.0, 110.8, 118.4, 122.4, 131.0, 134.1, 140.6, 179.2; Anal. Calcd for $C_{10}H_9BrN_2O$: C, 47.46; H, 3.58; N, 11.07. Found: C, 47.74, H, 3.52, N, 11.03; ESI-MS obsd 252.99694 $(M + H)^+$ corresponds to 251.98966 (M), calcd 251.98983 ($C_{10}H_9BrN_2O$).

8,9-Dibromo-1-formyldipyrromethane (II-1-Br[8,9]). A solution of **II-1-Br[8]** (506 mg, 2.00 mmol) in anhydrous THF (20 mL) was treated with NBS (356 mg, 2.00 mmol) in one batch under argon at –78 °C. The reaction mixture was stirred for 1 h at –78 °C, after which the ice bath was removed, and the reaction mixture was allowed to warm up. Upon reaching 5 °C, hexanes and water were added. The mixture was extracted with ethyl acetate. The organic layer was dried (K_2CO_3) and concentrated to a brown solid. The solid was suspended in warm CH_2Cl_2, and THF was added to achieve complete dissolution, whereupon hexanes was added. Pale yellow crystals were obtained (476 mg, 71%): mp 104–105 °C (dec.); ^{1}H NMR (acetone-d_6) δ 4.03 (s, 2H), 6.03 (s, 1H), 6.10 (d, J = 3.9 Hz, 1H), 6.89 (d, J = 3.9 Hz, 1H), 9.41 (s, 1H), 10.9 (br s, 1H), one NH was not observed presumably due to deuterium exchange; ^{13}C NMR (acetone-d_6) δ 27.2, 98.2, 98.8, 110.7, 111.0, 122.4, 132.2, 133.8, 139.9, 179.1; Anal. Calcd for $C_{10}H_8Br_2N_2O$: C, 36.18; H, 2.43; N, 8.44. Found: C, 36.08, H, 2.43, N, 8.28; ESI-MS obsd 330.9086 $(M + H)^+$ corresponds to 329.9013 (M), calcd 329.9003 ($C_{10}H_8Br_2N_2O$).

Zn(II)-3,13-Dibromo-17,18-dihydro-18,18-dimethylporphyrin (ZnC-Br^{3}Br^{13}). A solution of **II-1-Br**[8,9] (134 mg, 0.400 mmol) and **II-6** (107 mg, 0.400 mmol) in anhydrous CH_2Cl_2 (10.6 mL) was treated with a solution of $TsOH \cdot H_2O$ (380 mg, 2.00 mmol) in anhydrous methanol (2.8 mL) under argon. The reaction mixture changed immediately to orange-red. The mixture was stirred for 30 min under argon, then neutralized with 2,2,6,6-tetramethylpiperidine (746 μL, 4.40 mmol) and concentrated to dryness. The resulting brown solid was dissolved in acetonitrile (40 mL), and 2,2,6,6-tetramethylpiperidine (1.70 mL, 10.0 mmol), $Zn(OAc)_2$ (1.10 g, 6.00 mmol) and AgOTf (308 mg, 1.20 mmol) were added consecutively to the solution. The resulting suspension was refluxed for 22 h exposed to air. The crude mixture was filtered through a silica pad with CH_2Cl_2, and the filtrate was chromatographed [silica, CH_2Cl_2] to afford a green solid (21 mg, 9%): ^{1}H NMR (THF-d_8) δ 2.04 (s, 6H), 4.61 (s, 2H), 8.65 (s, 1H), 8.86–8.87 (m, 2H), 8.95 (d, J = 4.1 Hz, 1H), 9.01 (d, J = 4.1 Hz, 1H), 9.14 (s, 1H), 9.57 (s, 1H), 9.73 (s, 1H); ^{13}C NMR (THF-d_8) δ 31.5, 46.4, 51.7, 94.0, 95.1, 109.1, 109.2, 115.8, 128.6, 129.4, 129.8, 133.0, 133.7, 144.6, 147.6, 147.8, 148.3, 149.3, 155.1, 159.8, 171.6; MALDI-MS obsd 557.9; ESI-MS obsd 557.9021 (M^+) corresponds to 557.9024, calcd 557.9033 ($C_{22}H_{16}Br_2N_4Zn$); λ_{abs} 405, 619 nm.

Zn(II)-13-Bromo-17,18-dihydro-18,18-dimethyl-3-[2-(triisopropylsilyl)ethynyl]porphyrin (ZnC-E^{3}Br^{13}). A solution of **II-1-Br**[8,9] (117 mg, 0.350 mmol) and **II-7** (130 mg, 0.350 mmol) in anhydrous CH_2Cl_2 (10.0 mL) was treated with a solution of $TsOH \cdot H_2O$ (333 mg, 1.75 mmol) in anhydrous methanol (2.5 mL) under argon. The reaction mixture changed immediately to orange-red. The mixture was stirred for 40 min under argon, then neutralized with 2,2,6,6-tetramethylpiperidine (655 μL, 3.85

mmol) and concentrated to dryness. The resulting light brown solid was dissolved in acetonitrile (35 mL), and the solution was placed in an 80 mL pressurized microwave flask. The microwave apparatus has been described.[34] 2,2,6,6-Tetramethylpiperidine (1.48 mL, 8.75 mmol), $Zn(OAc)_2$ (966 mg, 5.25 mmol) and AgOTf (270 mg, 1.05 mmol) were added consecutively to the solution. The flask was inserted in a microwave reactor, and the reaction was carried out at 81 °C for 1.5 h. The crude mixture was filtered through a silica pad with ethyl acetate, and the filtrate was concentrated and chromatographed [silica, CH_2Cl_2/hexanes (3:2)] to afford a dark green solid (11 mg, 5%): ^{1}H NMR (THF-d_8) δ 1.44–1.46 (m, 27H), 2.04 (s, 6H), 4.62 (s, 2H), 8.67 (s, 1H), 8.86 (s, 1H), 8.91 (s, 1H), 8.95 (s, 1H + 1H), 9.14 (s, 1H), 9.56 (s, 1H), 9.87 (s, 1H); ^{13}C NMR (THF-d_8) δ 12.7, 19.5, 31.3, 46.1, 51.6, 94.2, 95.3, 98.8, 104.4, 106.7, 108.6, 116.5, 127.0, 130.0, 130.2, 130.7, 133.2, 145.3, 147.3, 147.9, 148.5, 149.5, 152.5, 160.3, 171.3; MALDI-MS obsd 660.4; ESI-MS obsd 660.1261 (M^+) corresponds to 660.1255 (M), calcd 660.1262 ($C_{33}H_{37}BrN_4SiZn$); λ_{abs} 412, 632 nm.

Zn(II)-17,18-Dihydro-18,18-dimethyl-3,13-bis[2-(triisopropylsilyl)ethynyl]porphyrin (ZnC-E^{3}E^{13}). Following a procedure for ethynylation of chlorins via Sonogashira coupling,[26] a mixture of **ZnC-Br^{3}Br^{13}** (38 mg, 0.068 mmol), (triisopropylsilyl)acetylene (95 μL, 0.41 mmol), $Pd_2(dba)_3$ (19 mg, 0.020 mmol), and P(*o*-tol)$_3$ (50 mg, 0.16 mmol) was heated in toluene/triethylamine [12 mL, (3:1)] at 60 °C for 8 h using a Schlenk line. The reaction mixture was concentrated and chromatographed [silica, hexanes/CH_2Cl_2 (3:1)] to afford a green solid (18 mg, 35%): ^{1}H NMR (THF-d_8) δ 1.43–1.46 (m, 54H), 2.06 (s, 6H), 4.60 (s, 2H), 8.64 (s, 1H), 8.91, (s, 1H), 8.93 (d, J = 4.2 Hz, 1H), 8.96

(d, J = 4.2 Hz, 1H), 9.03 (s, 1H), 9.18 (s, 1H), 9.58 (s, 1H), 9.85 (s, 1H); ^{13}C NMR (THF-d_8) δ 12.7, 13.0, 19.1, 19.5, 25.0, 31.4, 46.2, 51.5, 94.8, 95.0, 97.5, 98.8, 104.4, 104.7, 106.4, 109.4, 122.1, 127.0, 130.1, 130.8, 135.5, 145.7, 147.5, 148.2, 148.7, 152.7, 153.7, 160.2, 171.6; MALDI-MS obsd 762.8; ESI-MS obsd 763.3585 $(M + H)^+$ corresponds to 762.3512 (M), calcd 762.3492 ($C_{44}H_{58}N_4Si_2Zn$); λ_{abs} 416, 643 nm; λ_{em} (λ_{em} = 416 nm) 644 nm.

Zn(II)-13-Acetyl-17,18-dihydro-18,18-dimethyl-3-[2-(triisopropylsilyl)ethynyl]porphyrin (ZnC-E^{3}A^{13}). The following procedure entails zinc demetalation, Pd-mediated coupling with tributyl(1-ethoxyvinyl)tin, acidic hydrolysis and zinc metalation. A solution of **ZnC-E^{3}Br^{13}** (18 mg, 0.027 mmol) in CH_2Cl_2 (1 mL) was treated dropwise with TFA (42 μL, 0.54 mmol). After 5 h CH_2Cl_2 was added, and the organic layer was washed (saturated aqueous $NaHCO_3$, water, brine), dried (Na_2SO_4) and concentrated. The resulting crude solid was used in the next step. A mixture of crude solid, tributyl(1-ethoxyvinyl)tin (0.037 mL, 0.109 mmol) and $(PPh_3)_2PdCl_2$ (3 mg, 0.004 mmol) was stirred in acetonitrile/DMF [2.5 mL, (3:2)] at 85 °C using a Schlenk line. In 3.5 h the reaction mixture was treated with 10% aqueous HCl (3.5 mL) at room temperature. The mixture was stirred for 1 h. CH_2Cl_2 was added, and the organic layer was washed (saturated aqueous $NaHCO_3$, water, brine), dried (Na_2SO_4) and concentrated. The crude solid was dissolved in $CHCl_3$ (4 mL), and the solution was treated with $Zn(OAc)_2 \cdot 2H_2O$ (89 mg, 0.41 mmol) in MeOH (1 mL). The reaction mixture was stirred for 16 h at room temperature. Then the reaction mixture was concentrated and chromatographed [silica, CH_2Cl_2/hexanes (2:1)] to afford a green solid (10 mg, 59%): ^{1}H NMR (THF-d_8) δ 1.43 (s, 21H), 2.02 (s, 6H), 3.09 (s, 3H), 4.56 (s, 2H), 8.58 (s, 1H), 8.87 (s, 1H), 8.88 (d, J = 3.9 Hz, 1H), 8.95 (d, J = 3.9

Hz, 1H), 9.63 (s, 1H), 9.64 (s, 1H), 9.75 (s, 1H), 9.88 (s, 1H); ^{13}C NMR (THF-d_8) δ 12.7, 13.0, 19.1, 19.5, 25.0, 31.4, 46.2, 51.5, 94.8, 95.0, 97.5, 98.8, 104.4, 104.7, 106.4, 109.4, 122.1, 127.0, 130.1, 130.8, 135.5, 145.7, 147.5, 148.2, 148.7, 152.7, 153.7, 160.2, 171.6; MALDI-MS obsd 624.8; ESI-MS obsd 625.2320 $(M + H)^+$ corresponds to 624.2248 (M), calcd 624.2263 ($C_{35}H_{40}N_4SiZn$); λ_{abs} 420, 645 nm; λ_{em} (λ_{em} = 420 nm) 650 nm.

The results presented in this chapter have been published.[61]

II.5. References

(1) Stromberg, J. R.; Marton, A.; Kee, H. L.; Kirmaier, C.; Diers, J. R.; Muthiah, C.; Taniguchi, M.; Lindsey, J. S.; Bocian, D. F.; Meyer, G. J.; Holten, D. *J. Phys. Chem. C* **2007**, *111*, 15464–15478.

(2) (a) De Rosa, S. C.; Herzenberg, L. A.; Roederer, M. *Nature Med*. **2001**, *7*, 245–248. (b) De Rosa, S. C.; Brenchley, J. M.; Roederer, M. *Nature Med*. **2003**, *9*, 112–117.

(3) (a) Licha, K. *Top. Curr. Chem.* **2002**, *222*, 1–29. (b) Stefflova, K.; Li, H.; Chen, J.; Zheng, G. *Bioconjugate Chem*. **2007**, *18*, 379–388.

(4) Nyman, E. S.; Hynninen, P. H. *J. Photochem. Photobiol. B: Biol*. **2004**, *73*, 1–28.

(5) Strachan, J.-P.; O'Shea, D. F.; Balasubramanian, T.; Lindsey, J. S. *J. Org. Chem.* **2000**, *65*, 3160–3172.

(6) Taniguchi, M.; Ra, D.; Mo, G.; Balasubramanian, T.; Lindsey, J. S. *J. Org. Chem.* **2001**, *66*, 7342–7354.

(7) Ptaszek, M.; McDowell, B. E.; Taniguchi, M.; Kim, H.-J.; Lindsey, J. S. *Tetrahedron* **2007**, *63*, 3826–3839.

(8) Hynninen, P. H. In *Chlorophylls*; Scheer, H.; Ed.; CRC Press, Boca Raton, FL, 1991, pp 145–209.

(9) Osuka, A.; Wada, Y.; Shinoda, S. *Tetrahedron* **1996***, 52*, 4311–4326.

(10) Tamiaki, H.; Kouraba, M. *Tetrahedron* **1997**, *53*, 10677–10688.

(11) Gerlach, B.; Brantley, S. E.; Smith, K. M. *J. Org. Chem.* **1998**, *63*, 2314–2320.

(12) Kozyrev, A. N.; Suresh, V.; Das, S.; Senge, M. O.; Shibata, M.; Dougherty, T. J.; Pandey, R. K. *Tetrahedron* **2000**, *56*, 3353–3364.

(13) Wang, J.-J.; Shim,Y. K.; Jiang, G.-J.; Imafuku, K. *J. Heterocyc. Chem.* **2003**, *40*, 1075–1079.

(14) Kozyrev, A. N.; Alderfer, J. L.; Robinson, B. C. *Tetrahedron* **2003***, 59*, 499–504.

(15) Tamiaki, H. M.; Omoda, Y. S.; Morishita, H. *Tetrahedron* **2003**, *59*, 4337–4350.

(16) Li, G. A.; Graham, Y. C.; Dobhal, M. P.; Morgan, J.; Zheng, G.; Kozyrev, A.; Oseroff, A.; Dougherty, T. J.; Pandey, R. K. *J. Med. Chem.* **2003**, *46*, 5349–5359.

(17) Feofanov, A. V.; Nazarova, A. I.; Karmakova, T. A., Plyutinskaya, A. D.; Grishin, A. I.; Yakubovskaya, R. I.; Lebedeva, V. S.; Ruziev, R. D.; Mironov, A. F.; Maurizot, J. -C.; Vigny, P. *Russ. J. Bioorg. Chem.* **2004***, 30*, 374–384.

(18) Balaban, T. S.; Tamiaki, H.; Holzwarth, A. R. *Top. Curr. Chem.* **2005**, *258*, 1–38.

(19) Wang, J.-J.; Imafuku, K.; Shim, Y. K.; Jiang, G.-J. *J. Heterocyc. Chem.* **2005**, *42*, 835–840.

(20) Kunieda, M.; Tamiaki, H. *Eur. J. Org. Chem.* **2006**, 2352–2361.

(21) Kelley, R. F.; Tauber, M. J.; Wasielewski, R. W. *J. Am. Chem. Soc.* **2006**, *128*, 4779–4791.

(22) Balasubramanian, T.; Strachan, J.-P.; Boyle, P. D.; Lindsey, J. S. *J. Org. Chem.* **2000**, *65*, 7919–7929.

(23) Taniguchi, M.; Kim, H.-J.; Ra, D.; Schwartz, J. K.; Kirmaier, C.; Hindin, E.; Diers, J. R.; Prathapan, S.; Bocian, D. F.; Holten, D.; Lindsey, J. S. *J. Org. Chem.* **2002**, *67*, 7329–7342.

(24) Hindin, E.; Kirmaier, C.; Diers, J. R.; Tomizaki, K.-Y.; Taniguchi, M.; Lindsey, J. S.; Bocian, D. F.; Holten, D. *J. Phys. Chem. B* **2004**, *108*, 8190–8200.

(25) Taniguchi, M.; Kim, M. N.; Ra, D.; Lindsey, J. S. *J. Org. Chem.* **2005**, *70*, 275–285.

(26) Laha, J. K.; Muthiah, C.; Taniguchi, M.; McDowell, B. E.; Ptaszek, M.; Lindsey, J. S. *J. Org. Chem.* **2006**, *71*, 4092–4102.

(27) Laha, J. K.; Muthiah, C.; Taniguchi, M.; Lindsey, J. S. *J. Org. Chem.* **2006***, 71*, 7049–7052.

(28) Taniguchi, M.; Ptaszek, M.; McDowell, B. E.; Lindsey, J. S. *Tetrahedron* **2007***, 63*, 3840–3849.

(29) Taniguchi, M.; Ptaszek, M.; McDowell, B. E.; Boyle, P. D.; Lindsey, J. S. *Tetrahedron* **2007**, *63*, 3850–3863.

(30) Muthiah, C.; Ptaszek, M.; Nguyen, T. M.; Flack, K. M.; Lindsey, J. S. *J. Org. Chem*. **2007**, *72*, 7736–7749.

(31) Muthiah, C.; Taniguchi, M.; Kim, H.-J.; Schmidt, I.; Kee, H. L.; Holten, D.; Bocian, D. F.; Lindsey, J. S. *Photochem. Photobiol.* **2007**, *83*, 1513–1528.

(32) Kee, H. L.; Kirmaier, C.; Tang, Q.; Diers, J. R.; Muthiah, C.; Taniguchi, M.; Laha, J. K.; Ptaszek, M.; Lindsey, J. S.; Bocian, D. F.; Holten, D. *Photochem. Photobiol*. **2007**, *83*, 1110–1124.

(33) Muthiah, C.; Kee, H. L.; Diers, J. R.; Fan, D.; Ptaszek, M.; Bocian, D. F.; Holten, D.; Lindsey, J. S. *Photochem. Photobiol.* **2008**, *84*, 786–801.

(34) Ruzié, C.; Krayer, M.; Lindsey, J. S. *Org. Lett*. **2009**, *11*, 1761–1764.

(35) Muthiah, C.; Lahaye, D.; Taniguchi, M.; Ptaszek, M.; Lindsey, J. S. *J. Org. Chem*. **2009**, *74*, 3237–3247

(36) Kee, H. L.; Kirmaier, C.; Tang, Q.; Diers, J. R.; Muthiah, C.; Taniguchi, M.; Laha, J. K.; Ptaszek, M.; Lindsey, J. S.; Bocian, D. F.; Holten, D. *Photochem. Photobiol.* **2007**, *83*, 1125–1143.

(37) Scheer, H. In *Chlorophylls and Bacteriochlorophylls*; Grimm, B.; Porra, R. J.; Rüdiger, W.; Scheer, H.; Eds.; Springer: Dordrecht, 2006, pp 2–26.

(38) Kobayashi, M.; Akiyama, M.; Kano, H.; Kise, H. In *Chlorophylls and Bacteriochlorophylls*; Grimm, B.; Porra, R. J.; Rüdiger, W.; Scheer, H.; Eds.; Springer: Dordrecht, 2006, pp 79–94.

(39) Artico, M. In *Pyrroles. Part One*; Jones, R. A., Ed.; John Wiley & Sons, Inc.: New York, 1990, pp 329–395

(40) (a) Fischer, H.; Orth, H. *Die Chemie Des Pyrroles;* Johnson Reprint Corp.: New York, 1968, vol II. (b) Smith, K. M. In Porphyrins and Metalloporphyrins; Smith, K. M., Ed.; Elsevier Scientific Publishing Co.: Amsterdam, 1975, pp 29–58. (c) Paine, J. B. III in *The Porphyrins*; Dolphin, D., Ed.; Academic Press: New York, Vol 1, 1978, pp 101–234.

(41) Liu, Z.; Yasseri, A. A.; Loewe, R. S.; Lysenko, A. B.; Malinovskii, V. L.; Zhao, Q.; Surthi, S.; Li, Q.; Misra, V.; Lindsey, J. S.; Bocian, D. F. *J. Org. Chem*. **2004**, *69*, 5568–5577.

(42) Thamyongkit, P.; Bhise, A. D.; Taniguchi, M.; Lindsey, J. S. *J. Org. Chem*. **2006**, *71*, 903–910.

(43) Ptaszek, M.; McDowell, B. E.; Lindsey, J. S. *J. Org. Chem.* **2006**, *71*, 4328–4331.

(44) Ptaszek, M.; Bhaumik, J.; Kim, H.-J.; Taniguchi, M.; Lindsey, J. S. *Org. Process Res. Dev.* **2005**, *9*, 651–659.

(45) Kosugi, M.; Sumiya, T.; Obara, Y.; Suzuki, M.; Sano, H.; Migita, T. *Bull. Chem. Soc. Jpn*. **1987**, *60*, 767–768.

(46) Taniguchi, M.; Cramer, D. L.; Bhise, A. D.; Kee, H. L.; Bocian, D. F.; Holten, D.; Lindsey, J. S. *New J. Chem.* **2008**, *32*, 947–958.

(47) Wallace, D. M.; Leung, S. H.; Senge, M. O.; Smith, K. M. *J. Org. Chem*. **1993**, *58*, 7245–7257.

(48) Lee, C.-H.; Lindsey, J. S. *Tetrahedron* **1994**, *50*, 11427–11440.

(49) Noss, L.; Liddell, P. A.; Moore, A. L.; Moore, T. A.; Gust, D. *J. Phys. Chem. B* **1997**, *101*, 458–465.

(50) Abell, A. D.; Nabbs, B. K.; Battersby, A. R. *J. Org. Chem*. **1998**, *63*, 8163–8169

(51) Cho, W.-S.; Kim, H.-J.; Littler, B. J.; Miller, M. A.; Lee, C.-H.; Lindsey, J. S. *J. Org. Chem.* **1999**, *64*, 7890–7901.

(52) Littler, B. J.; Miller, M. A.; Hung, C.-H.; Wagner, R. W.; O'Shea, D. F.; Boyle, P. D.; Lindsey, J. S. *J. Org. Chem.* **1999**, *64*, 1391–1396.

(53) Balasubramanian, T.; Lindsey, J. S. *Tetrahedron* **1999**, *55*, 6771–6784.

(54) Dogutan, D. K.; Ptaszek, M.; Lindsey, J. S. *J. Org. Chem.* **2007***, 72,* 5008–5011.

(55) Srinivasan, N.; Haney, C. A.; Lindsey, J. S.; Zhang, W.; Chait, B. T. *J. Porphyrins Phthalocyanines* **1999**, *3*, 283–291.

(56) Li, F.; Gentemann, S.; Kalsbeck, W. A.; Seth, J.; Lindsey, J. S.; Holten, D.; Bocian, D. F. *J. Mater. Chem.* **1997**, *7*, 1245–1262.

(57) Kee, H. L.; Kirmaier, C.; Yu, L.; Thamyongkit, P.; Youngblood, W. J.; Calder, M. E.; Ramos, L.; Noll, B. C.; Bocian, D. F.; Scheidt, W. R.; Birge, R. R.; Lindsey, J. S.; Holten, D. *J. Phys. Chem*. *B* **2005**, *109*, 20433–20443.

(58) Gouterman, M. In *The Porphyrins;* Dolphin, D.; Academic Press: New York, 1978, Vol. 3, pp 1–165.

(59) Peti t, L.; Quartarolo, A.; Adamo, C.; Russo, N. *J. Phys. Chem. B* **2006**, *110*, 2398–2404.

(60) Weber, G.; Teale, F. W. J. *Trans. Faraday Soc.* **1957**, *53*, 646–655.

(61) Mass, O.; Ptaszek, M.; Taniguchi, M.; Diers, J. R.; Kee, H. L.; Bocian, D. F.; Holten,

D.; Lindsey, J. S. *J. Org. Chem*. **2009**, *74*, 5276–5289.

II.6. Supporting Information

II.6.1. NMR Characterization of Brominated Dipyrromethanes

The protons for bromodipyrromethane derivatives were assigned. The ^{1}H NMR chemical shifts for 5-mesityl and 5-unsubstituted bromodipyrromethane derivatives are shown in Table II.3. A NOE between H^3 and H^2 was observed for all dipyrromethanes. For compounds **II-1-Br^{9}** and **II-1-Br^{8,9}**, the proton H^5 had two cross peaks with pyrroline ring protons that were assigned as H^3 and H^7. The proton H^5 of **II-2-Br^{7,9}** and **II-1-Br^{7,9}** had only one single peak with pyrroline ring protons, and those protons in both compounds that did not exhibit any NOE were assigned as H^8. In compound **II-5** a proton that had no cross peaks was assigned as H^9. In 8,9-dibromodipyrromethane **II-8-Br^{8,9}** the NOE between the H^7 and aromatic protons of the phenyl ring was observed. In 7,9-dibromodipyrromethane **II-8-Br^{7,9}** the proton at the 8-position had the same NMR chemical shift as H^8 in 7,9-dibromo-5-mesityl-dipyrromethane **II-2-Br^{8,9}**

Table II.3. ^{1}H NMR chemical shifts of bromodipyrromethanes.

Compound	H^2	H^3	H^7	H^8	H^5	H-formyl
II-1-Br[9]	6.790–6.794	5.97	5.820–5.821	5.92–5.93	3.92	9.37
II-1-Br[7,9]	6.77–6.80	5.89-5.91	–	6.06–6.07	3.94	9.37
II-1-Br[8,9]	6.78–6.80	5.98–6.00	5.93–5.94	–	3.91	9.38
II-2-Br[9]	6.76–6.78	5.89–5.92	5.80–5.85	5.49–5.52	5.74	9.38
II-2-Br[8,9]	6.78–6.83	5.83–5.86	5.58–5.62	–	5.74	9.39
II-2-Br[7,9]	6.76	5.68	–	6.10	5.80	9.42

II.6.2. NMR Characterization of 12- and 13-Substituted Chlorins

Introduction of a bromine substituent to the 3-position in **ZnC-Br^{3}M^{10}** causes the resonance of the adjacent meso-proton (H^5) to shift downfield ($\Delta\delta$ = +0.21 ppm) and the resonances of the next adjacent meso-proton (H^{20}) to shift upfiled ($\Delta\delta$ = –0.08 ppm) (Table II.4). In similar manner, introduction of a bromine substituent to the 13-position in **ZnC-M^{10}Br^{13}** causes the resonance of the adjacent meso-proton (H^{15}) to shift downfield ($\Delta\delta$ = +0.26 ppm). Note that the next adjacent meso-position (10-position) is blocked by the mesityl group.

Effect of the ethynyl group (Table II.5): introduction of the ethynyl group causes the resonance of the adjacent meso-proton to shift downfield (0.22 to 0.33 ppm) and the resonance of the adjacent β-proton to shift downfield (0.10 to 0.15 ppm).

Effect of the acetyl group (Table II.5): introduction of the 12-acetyl group causes the resonance of the adjacent meso-proton (H^{10}) and β-proton (H^{13}) to shift downfield ($\Delta\delta$ = 1.11

and 0.61 ppm, respectively). Similarly, introduction of the 13-acetyl group causes the resonance of the adjacent meso-proton (H^{15}) and *β*-proton (H^{12}) to shift downfield (Δδ = 1.18 and 0.56 ppm, respectively).

The characteristic feature of the ^{1}H NMR spectra of 12-substituted chlorins is the downfield signal of H^{10} compared with the H^{10} resonance of 13-substituted chlorins (Table II.6). All protons were assigned with NOESY experiments. The H^{10} of all 13-substituted chlorins exhibited two cross peaks with β-protons, while in 12-substituted chlorins only one NOE for H^{10} was observed

Table II.4. ^{1}H NMR chemical shifts of zinc chlorins with 3- and 13-bromo substituents.[a]

Position		**ZnC-M^{10}** δ	**ZnC-Br^{3}M^{10}** δ (Δδ)	**ZnC-M^{10}Br^{13}** δ (Δδ)	**ZnC-Br^{3}M^{10}Br^{13}** δ (Δδ)	**ZnC-Br^{3}Ar^{10}Br^{13}**(*b*) δ (Δδ)
Meso	5	9.52	9.73 (**+0.21**)	9.54 (+0.02)	9.62 (+0.10)	9.62 (+0.10)
	10	–	–	–	–	–
	15	8.60[d]	8.68 (+0.08)	8.85 (**+0.25**)	8.81 (**+0.21**)	8.86 (+**0.26**)
	20	8.58[d]	8.50 (–0.08)	8.61 (+0.03)	8.41 (–0.17)	8.49 (–0.09)
β	2	8.70	8.77 (+0.07)	8.72 (+0.02)	8.78 (+0.08)	8.76 (+0.06)
	3	9.02	–	9.01 (–0.01)	–	–
	7	8.74	8.88 (+0.14)	8.80 (+0.06)	8.84 (+0.10)	8.82 (+0.08)
	8	8.24	8.37 (+0.13)	8.37 (+0.13)	8.26 (+0.02)	8.43 (+0.19)
	12	8.40	8.55 (+0.15)	8.57 (+0.17)	8.57 (+0.17)	8.64 (+0.24)
	13	8.53	8.60 (+0.07)	–	–	–

[a]In $CDCl_3$ (~20 mM) at 298 K. Significant shits (Δδ) are shown in bold. [b]Ar = 4-[2-(triisopropylsilyl)ethynyl]phenyl [c]Protons of the geminal dimethyl group (18-position). [d]The resonances could not be unambiguously distinguished and may be interchangeable.

Table II.5. ^{1}H NMR chemical shifts of zinc chlorins with 12- versus 13-substituents.[a]

Position		**ZnC**	**ZnC-E^{3}A^{12}**	**ZnC-E^{3}A^{13}**	**ZnC-E^{3}E^{12}**	**ZnC-E^{3}E^{13}**
		δ	δ (Δδ)	δ (Δδ)	δ (Δδ)	δ (Δδ)
Meso	5	9.63[c]	9.84 (+0.21)	9.75 (+0.12)	9.85[e] (+**0.22**)	9.85 (+**0.22**)
	10	9.61[c]	10.72 (+**1.11**)	9.63 (+0.02)	9.87[e] (+**0.26**)	9.58 (–0.03)
	15	8.70	8.78 (+0.08)	9.88 (+**1.18**)	8.69 (–0.01)	9.03 (+**0.33**)
	20	8.67	8.67 (0)	8.58 (–0.09)	8.65 (–0.02)	8.64 (–0.03)
β	2	8.76	8.92 (+0.16)	8.88 (+0.12)	8.90 (+0.14)	8.91 (+0.15)
	3	9.06[d]	–	–	–	–
	7	8.92	8.94 (+0.02)	8.87 (–0.05)	8.95 (+0.03)	8.91 (–0.01)
	8	8.92	9.06 (+0.14)	8.95 (+0.03)	8.95 (+0.03)	8.93 (+0.01)
	12	9.08[d]	–	9.64 (+**0.56**)	–	9.18 (+**0.10**)
	13	8.71	9.32 (+**0.61**)	–	8.86 (+**0.15**)	–
	17	4.58	4.57	4.56	4.57	4.60
	18[b]	2.05	2.04	2.02	2.03	2.06

[a]In THF (~20 mM) at 298 K. Significant shits (Δδ) are shown in bold. [b]Protons of the geminal dimethyl group (18-position). [c, d, e]The resonances could not be unambiguously distinguished and may be interchangeable.

Table II.6. ^{1}H NMR chemical shifts of free base chlorins with 12- versus 13-substituents.[a]

Position		**FbC**	**FbC-A^{12}Br^{15}**	**FbC-A^{13}Br^{15}**	**FbC-Br^{15}**	**FbC-A^{12}Br^{15}**	**FbC-A^{13}Br^{15}**
		δ	δ (Δδ)	δ (Δδ)	δ	δ (Δδ)	δ (Δδ)
	5	9.89	9.45 (–**0.44**)	9.61 (–0.28)	9.81	9.45 (–**0.64**)	9.61 (–0.20)
Meso	10	9.86	10.64 (+**0.78**)	9.73 (–0.13)	9.74	10.64 (+**0.80**)	9.73 (–0.01)
	15	9.08	–	–	–	–	–
	20	8.98	8.76 (–0.22)	8.82 (–0.16)	8.89	8.76 (–0.13)	8.82 (–0.07)
β	2	8.99	8.76 (–0.23)	8.91 (–0.08)	8.95	8.76 (–0.19)	8.91 (–0.04)
	3	9.26	8.96 (–0.30)	9.13 (–0.13)	9.17	8.96 (–0.21)	9.13 (–0.04)
	7	9.08	9.06 (–0.02)	8.88 (–0.20)	9.02	9.06 (+0.04)	8.88 (–0.14)
	8	9.08	8.89 (–0.19)	8.97 (–0.11)	8.98	8.89 (–0.09)	8.97 (–0.01)
	12	9.24	–	9.12 (–0.12)	9.19	–	9.12 (–0.07)
	13	8.94	9.49 (+**0.55**)	–	9.26	9.49 (+**0.23**)	–
	17	4.66	4.59	4.59	4.67	4.59	4.59
	18[b]	2.07	2.04	2.04	2.04	2.04	2.04

[a]In $CDCl_3$ (~20 mM) at 298 K. Significant shits (Δδ) are shown in bold. [b]Protons of the geminal dimethyl group (18-position).

CHAPTER III

Structural Characteristics that Make Chlorophylls Green: Interplay of Hydrocarbon Skeleton and Substituents

III.1. Introduction

Chlorophylls are the most famous members of the chlorin family.[1] The chlorin designation stems from the presence of one reduced ring in the tetrapyrrole macrocycle. However, the carbon skeleton of chlorophylls is not simply a cyclic tetrapyrrole, but also contains an annulated five-membered ring. This hydrocarbon framework is known as phorbine.[2] A phorbine that carries an oxo group at the 13^1-position, as is the case with all chlorophylls, is known as 13^1-oxophorbine. The structures of chlorin, phorbine, 13^1-oxophorbine, and chlorophyll *a* and chlorophyll *b* are shown in Chart III.1. Inspection of the chlorophyll structure leads naturally to questions concerning the requirements for the fifth ring, the given set of peripheral substituents, and the extent to which such features contribute to the distinct spectral and electronic properties of the chlorophylls.

The question of 'why chlorophyll?' has been asked a number of times from different perspectives. Mauzerall considered the features of chlorophyll with regards to the biosynthetic pathway, the electronic properties that give rise to spectral and photochemical properties, and how such properties are well matched for photosynthetic function.[3] A generation later the same question was addressed from the vantage point of a deeper molecular understanding of the diverse roles of chlorophylls in photosynthetic energy- and electron-transfer processes, including the apparently unique role of chlorophyll *a* in oxygenic

photosynthesis.[4] Björn considered the spectral matching of the chlorophyll absorption spectrum with solar radiation[5] and also the prospects for finding habitable exoplanets on the basis of chlorophyll spectral properties.[6] The spectroscopic properties of chlorophylls have been studied in detail.[7] Still, the role of the specific substituents about the perimeter of the tetrapyrrole macrocycle in engendering the characteristic features of chlorophylls has largely been unaddressed, at least in a systematic manner.

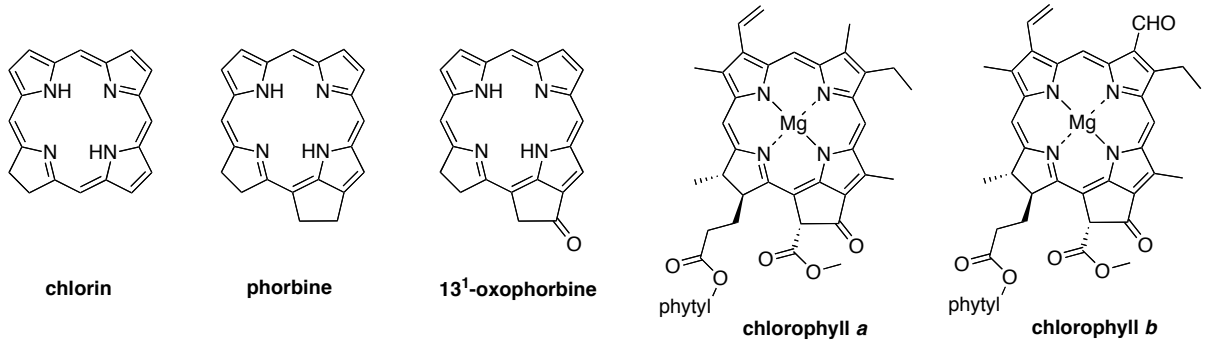

Chart III.1. Building the skeleton of chlorophyll *a*.

The presence of specific substituents at sites around the perimeter of the chlorophyll macrocycle can have a significant effect on the spectral, electronic, and photochemical properties. For example, the sole distinction between chlorophyll *a* and chlorophyll *b* is the presence of a 7-methyl versus 7-formyl group, yet this structural change results in a significant difference in spectral properties. This difference is exploited in nature, where chlorophyll *a* and *b* serve together to broaden spectral coverage in plant photosynthesis.[8]

The traditional route to probe the effects of substituents in chlorophylls has been to modify intact chlorophylls.[9-22] Such semisynthesis methods have resulted in structural

changes such as hydrogenation of the 3-vinyl group, reduction of the 13-keto group, and insertion of other metals. However, achieving more global changes such as removing all alkyl groups (2, 7, 8, 12 positions) has not been feasible via semisynthesis. An alternative entails total synthesis, which has been used to prepare analogues of the naturally occurring chlorophylls. The work in Lindsey group has been focused on the development of de novo synthetic methods for the preparation of stable synthetic analogues of the naturally occurring chlorophylls.[23-43]

Herein we report the use of recently developed synthetic methods (discussed in Chapter II) to gain access to a series of benchmark analogues of chlorophylls that lack any substituents other than the stabilizing geminal dimethyl group in the reduced ring. The compounds include phorbine **FbP**, chlorin **FbC-A**^{13}, and 13^{1}-oxophorbine **FbOP** (Chart III.2), as well as their zinc chelates (**ZnP**, **ZnC-A**^{13}, and **ZnOP**). The analogous chlorins **FbC** and **ZnC** have been synthesized previously,[31] as has the 17-oxochlorin **OxoFbC**.[32] The spectral and photophysical properties of each compound are also presented and are accompanied by density functional theory (DFT) calculations aimed at characterizing the frontier molecular orbitals. Collectively, these studies systematically address the issue of how structural modifications to the base chlorin macrocycle contribute to the electronic and spectral characteristics of chlorophylls.

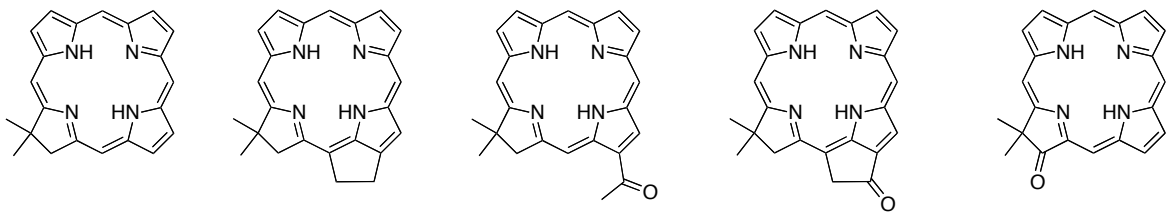

chlorin **FbC** phorbine **FbP** chlorin **FbC-A^{13}** 13^{1}-oxophorbine **FbOP** oxochlorin **FbOC**

Chart III.2. Benchmark molecules for chlorophylls.

A portion of the results presented in this chapter stemmed from a team effort including Marcin Ptaszek and Masahiko Taniguchi; photochemical studies were accomplished by Joseph W. Springer, Kaitlyn M. Faries and James R. Diers.

III.2. Results and Discussion

III.2.1. Synthesis

A. Reconnaissance. A method for installing the isocyclic ring was first reported nearly three-quarters of a century ago, when Fischer subjected (hydroxymethylcarbonyl)porphyrin to dehydrating conditions to give "pheoporphyrin" **III-A** (Chart III.3).[44] Fischer also used Dieckmann cyclization to convert chlorin e_6 trimethyl ester to methyl pheophorbide *a* **III-B**.[45] To our knowledge, the first mention of formation of a phorbine (lacking the keto group) appears in Fischer's work, where desoxy-pyropheophorbide *a* **III-C** was reported (but not characterized) as a side product during esterification of pheophorbide *a*.[46] Some 30 years later, Wolf reported the spectral properties of phorbine **III-C**.[47] The first report of the synthesis and characterization of a number of phorbines (**III-D**) was provided by Brockmann and Tacke-Karimdadian, who reduced bacteriopheophorbide *d* methyl ester with $LiAlH_4$ in the presence of zinc chloride to

deoxygenate the 13-keto group.[48] Lash *et al.* reported de novo methods of installing the isocyclic ring in a tetrapyrrole macrocycle, wherein the condensation of a dipyrromethane bearing an annulated ring affords the corresponding porphyrin (**III-E**) containing an five-membered exocyclic ring.[49] However, the resulting macrocycle is a porphyrin, not a chlorin, hence the skeleton is a 17,18-dehydrophorbine.

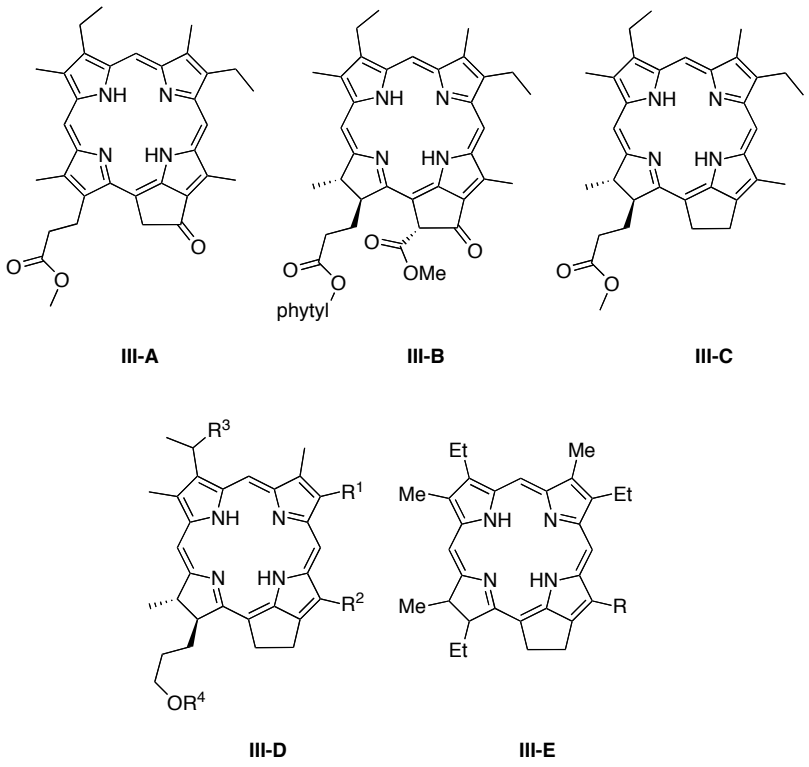

Chart III.3. Historical precedents in 13^1-oxophorbine and phorbine chemistry.

Each of the aforementioned syntheses of phorbines and 13^1-oxophorbines affords a macrocycle that contains a full complement of substituents at the β-pyrrole positions. The de novo synthesis of chlorins developed by Lindsey joins an Eastern half (rings B and C) and a Western half (rings A and D), where the latter contains a geminal methyl group in the

pyrroline ring to stabilize the resulting chlorin macrocycle toward adventitious dehydrogenation (Scheme III.1).[23-43] The de novo route requires far more synthetic effort than semisynthetic methods that begin with chlorophylls.[9-22] On the other hand, the de novo route affords greater versatility in the scope and range of substituents that can be introduced. The de novo route has been used to construct diverse substituted chlorins including a benchmark chlorin (**FbC**) that differs from chlorin itself only in the presence of the geminal dimethyl group in the reduced ring.[31] Methodology also has been developed to convert a synthetic 13-acetylchlorin to the corresponding 13^1-oxophorbine (via 15-bromination and intramolecular α-arylation). In this manner, seven free base 13^1-oxophorbines have been prepared, each of which bears a mesityl group at the 10-position and one or two other substituents. Four such 13^1-oxophorbines incorporate various substituents at the 7-position.[30,41] Nevertheless, a synthesis of the phorbine and 13^1-oxophorbine lacking any meso or β-pyrrole substituents has heretofore not been accomplished. Access to such macrocycles is fundamentally important because these molecules serve as benchmarks against which to compare the spectral and photophysical properties of the full library of synthetic chlorins, as well as the naturally occurring chlorophylls.

B. Unsubstituted 13^1-Oxophorbine. The de novo method was employed for the synthesis of the unsubstituted 13^1-oxophorbine **FbOP**. The condensation of 8,9-dibromo-1-formyldipyrromethane[42] **II-1-Br**[8,9] (Eastern half) and **II-3**[28] (Western half) was carried out in CH_2Cl_2 upon treatment with a solution of $TsOH \cdot H_2O$ in anhydrous MeOH under argon. The resulting crude tetrahydrobilene-*a* was subjected to zinc-mediated oxidative cyclization in CH_3CN for 20 h at reflux exposed to air.[31,38] Filtration through a silica pad and column

chromatography afforded chlorin **ZnC-Br**[13] in 16% yield, which upon demetalation with TFA in CH_2Cl_2 gave **FbC-Br**[13] in 87% yield (Scheme III.2).

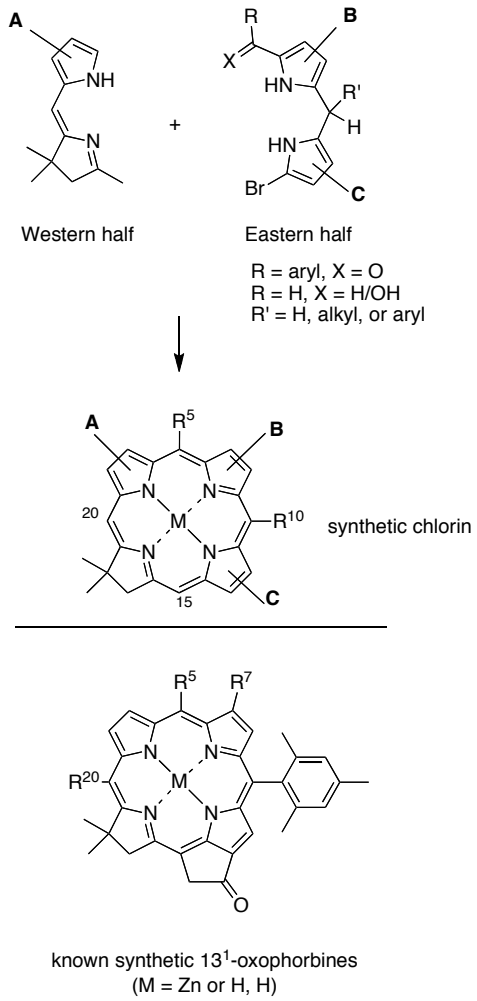

Scheme III.1. De novo synthesis of chlorins (top). All prior known synthetic 13[1]-oxophorbines incorporate a 10-mesityl group and one or two other substituents (bottom).

Stille coupling[50] of **FbC-Br**[13] was carried out under the same conditions employed in the synthesis of **FbC-A**[12] (Chapter II). Thus the reaction of **FbC-Br**[13] with tributyl(1-ethoxyvinyl)tin and $[(PPh_3)_2Pd]Cl_2$ in CH_3CN/DMF (3:2) for 2.5 h at 85 °C followed by

acidic workup afforded 13-acetylchlorin **FbC-A^{13}** in 81% yield. Regioselective 15-bromination of **FbC-A^{13}** was achieved with 1 mol equiv of NBS under acidic conditions[41] for 1 h at room temperature to give **FbC-A^{13}Br^{15}** in 73% yield. Acidic conditions cause deactivation of ring B of the macrocycle and thus prevent bromination at the 7-position. Intramolecular α-arylation[30,51] of the 13-acetyl group in the presence of $(PPh_3)_2PdCl_2$ and Cs_2CO_3 in toluene installed the isocyclic ring (spanning positions 13 and 15) in 55% yield. Metalation of **FbC-A^{13}** and **FbOP** with $Zn(OAc)_2 \cdot 2H_2O$ gave **ZnC-A^{13}** and **ZnOP** in 70% and 79% yield, respectively. The zinc oxophorbine **ZnOP** was successfully purified by precipitation; however, other attempts to purify by column chromatography using 1% TEA resulted in complete decomposition.

C. Conversion to Phorbine. The 13-keto group of naturally occurring chlorophylls has been reduced (mainly in acidic media[46,48,52-64]) to the methylene group. However, the absence of peripheral substituents on **FbOP** makes this macrocycle somewhat susceptible to the vigorous conditions generally employed for reduction of the 13-keto group. Hence, we turned to the use of milder conditions via the reduction of an intermediate tosylhydrazone.[65,66] Treatment of oxophorbine **FbOP** with tosylhydrazide in $CHCl_3$/ethanol (1:1) at 65 °C afforded crude tosylhydrazone-**FbP**, which upon reduction with sodium cyanoborohydride in the presence of $TsOH \cdot H_2O$ in MeOH/THF gave tosylhydrazide-**FbP**. The latter was converted to the target phorbine **FbP** in 42% overall yield in EtOH/DMF for 5 h at 80 °C in the presence of sodium acetate trihydrate. Metalation of phorbine **FbP** with $Zn(OAc)_2 \cdot 2H_2O$ gave the zinc chelate phorbine **ZnP** in 90% yield (Scheme III.3).

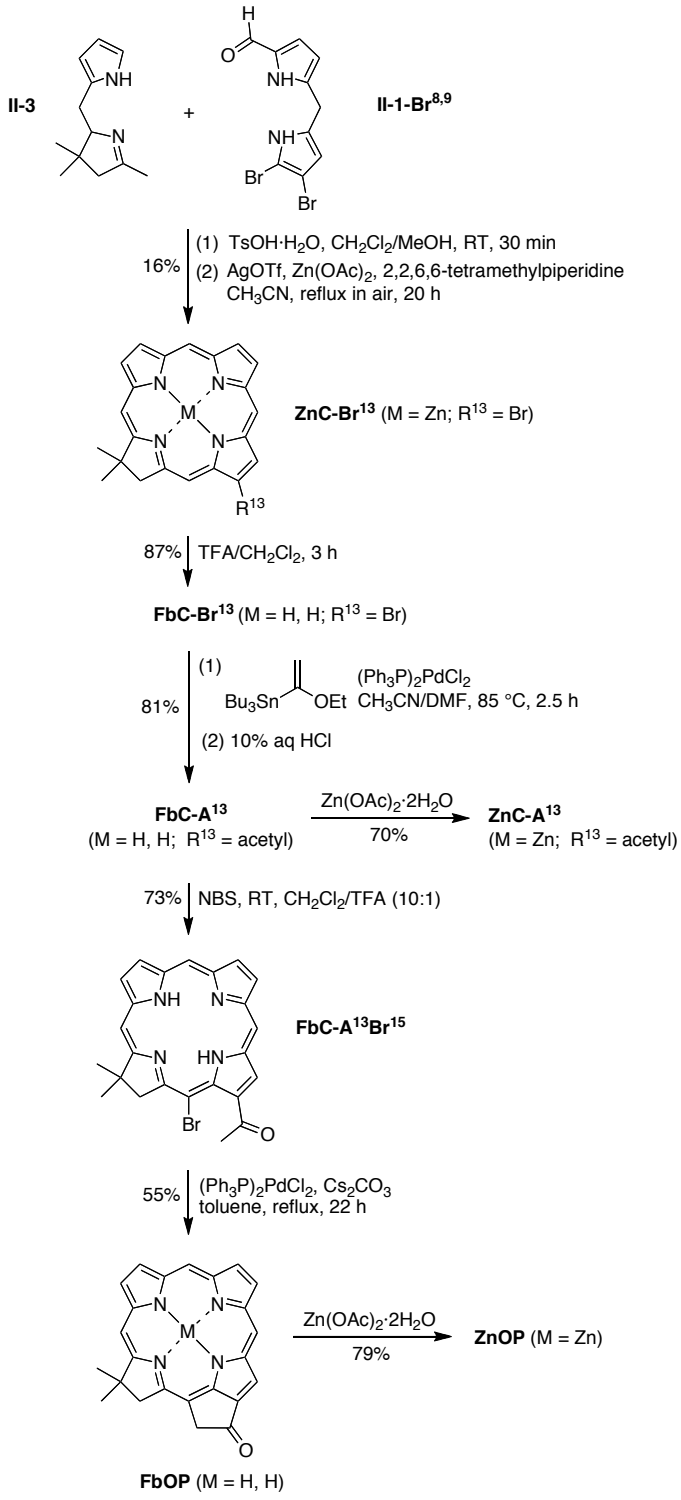

Scheme III.2. Synthesis of the 13^1-oxophorbines **FbOP** and **ZnOP**.

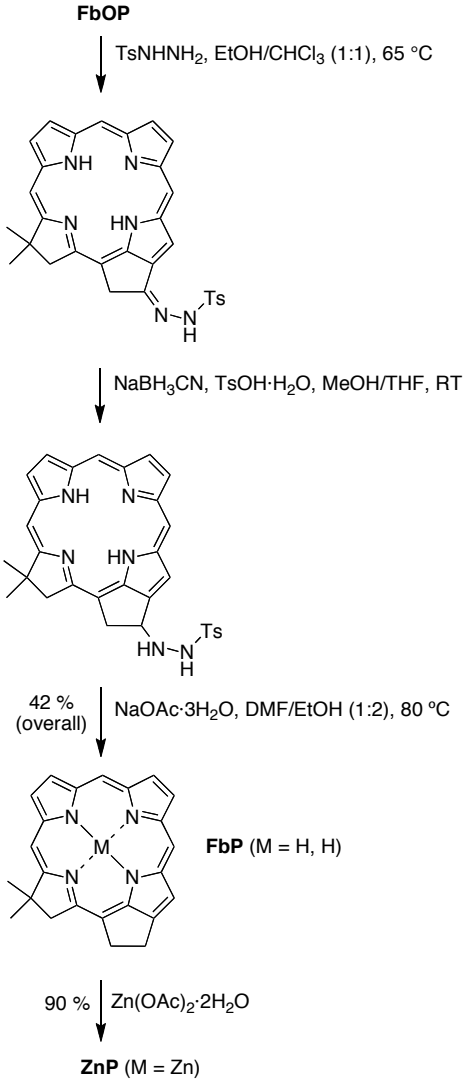

Scheme III.3. Synthesis of the free base **FbP** and zinc phorbines and **ZnP**.

III.2.2. Characterization

A. Molecular Identification. All of the phorbines and analogues were characterized by ^{1}H NMR spectroscopy (including gCOSY and NOESY), ^{13}C NMR spectroscopy, laser desorption mass spectrometry (without matrix or using a matrix of 1,4-bis(5-phenyloxazol-2-yl)benzene),[67] high-resolution electrospray ionization mass spectrometry, and absorption and

fluorescence spectroscopy.[68,69] Key electronic, spectral, and excited-state characteristics of the compounds are described in the following sections.

B. Absorption Spectra. The absorption spectra of the synthetic phorbine and 13^1-oxophorbine compounds are shown in Figure III.1 in the free base form (top panel) and zinc chelate form (bottom panel). The spectra for **ZnC**, **FbC**, **OxoZnC** and **OxoFbC** match those reported previously.[32,33] For comparison purposes, the spectral properties of sparsely substituted chlorins lacking any β-pyrrole substituents (**FbC** and **ZnC**) or only the 13-acetyl substituent (**FbC-A^{13}** and **ZnC-A^{13}**) also are provided. For exact comparison with species containing the full complement of substituents characteristic of chlorophylls, also displayed are the free base[70] and zinc[71] analogues of chlorophyll *a* [pheophytin *a* (**Pheo *a***) and zinc pheophytin *a* (**Zn-pheo *a***); Chart III.4].

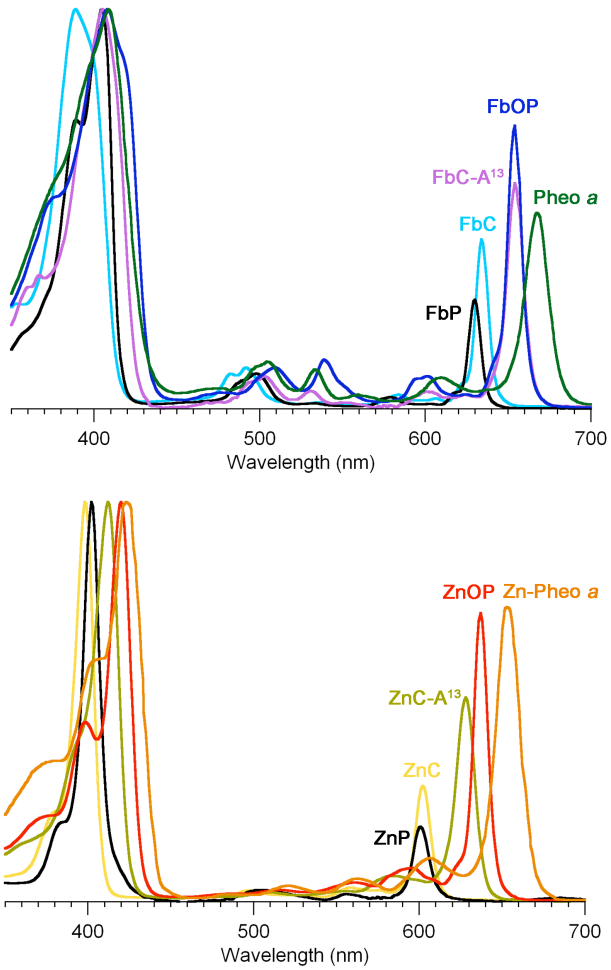

Figure III.1. Absorption spectra of synthetic chlorins and phorbines versus pheophytins[70,71] (normalized at the B-band maxima). Top panel: free base macrocycles. Bottom panel: zinc chelates. The solvent is diethyl ether (**Pheo *a*** and **Zn-Pheo *a***) or toluene (all other compounds).

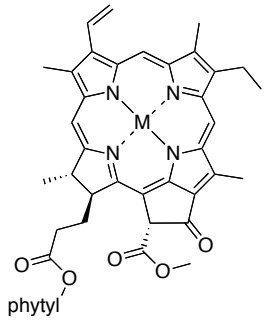

Pheophytin *a* (M = H, H)
Zinc Pheophytin *a* (M = Zn)

Chart III.4. Analogues of chlorophyll *a*.

The absorption spectrum of each compound is comprised of three main spectral regions. The strong red-region feature (600-670 nm) is the $Q_y(0,0)$ band; on average, this band lies ~30 nm to longer wavelength for the free base compound versus the corresponding zinc chelate. The weaker features in the blue-green to yellow spectral region (470-580 nm) are the Q_x bands; these features are somewhat stronger for the free base compounds than the zinc chelates. The intense bands in the near-ultraviolet region are the B_x and B_y features, also known as the Soret bands; these bands are generally superimposed for the zinc chelates but split for the free base compounds. The positions and relative intensities of the B and Q_y bands for the various macrocycles are listed in Table III.1.

Table III.1. Photophysical properties of oxophorbines and analogues.[a]

Compound	λ_B [fwhm] (nm)	Δ_B (cm^{-1})[b]	λ_{Q_y} [fwhm] (nm)	ΔQ_y (cm^{-1})[b]	I_B/I_{Q_y}[c]	Σ_{Q_y}/Σ_B[d]	HOMO– LUMO (eV)[e]	Φ_f[f]	τ_s (ns)[g]
FbC	389 [33]	–	633 [10]	–	2.4	0.19	2.69	0.20	8.8
FbP	404 [30]	–950	629 [9]	100	3.6	0.15	2.72	0.28	10.6
FbOP	408 [55]	–1170	654 [11]	–490	1.5	0.20	2.58	0.30	11.5
FbC-A[13]	405 [34]	–970	654 [12]	–500	1.8	0.24	2.59	0.24	7.8
OxoFbC	400 [27]	–710	634 [9]	–10	4.6	0.09	2.76	0.12	8.4
Pheo *a* [h]	409 [53]	–1200	668 [17]	–810	2.0	0.25	2.47		
ZnC	398 [13]	–	602 [11]	–	3.6	0.24	2.67	0.062	1.7
ZnP	402 [2]	–240	601 [12]	11	4.6	0.27	2.69	0.064	1.7
ZnOP	419 [19]	–1230	637 [17]	–910	1.6	0.42	2.55	0.23	5.1
ZnC-A[13]	411 [21]	–760	627 [14]	–680	1.9	0.40	2.56	0.23	4.3
OxoZnC	412 [14]	–810	602 [9]	–10	3.4	0.23	2.68	0.030	0.82
MgC	402 [10]	–220	607 [12]	–140	4.3	0.28	2.63[j]	0.26	6.9
Zn-Pheo *a* [i]	423 [38]	–1480	653 [17]	–1300	1.4	0.40	2.43		
Chl *a*	432 [40]	–1730	665 [18]	–1440	1.3	0.63	2.40	0.33	6.3

[a]In toluene at room temperature unless noted otherwise. [b]The redshift of the band relative to the corresponding band of the parent chlorin (**FbC** or **ZnC**). [c]Ratio of the peak intensities of the B and Q_y bands. [d]Ratio of the integrated intensities of the Q_y manifold [$Q_y(0,0)$ and $Q_y(1,0)$ bands] and B manifold [B_x and B_y origins and first vibronic overtones]. [e]Energy gap between the HOMO and LUMO orbitals. [f]Fluorescence quantum yield (error ± 7%). [g]Lifetime of the singlet excited state measured using fluorescence techniques (error ± 8%). [h]Absorption data from ref. 70 (in diethyl ether). [i]Absorption data from ref. 71 (in diethyl ether). [j]Essentially the same value (2.65 eV) is obtained with an H_2O axial ligand. [k]From ref. 34.

The characteristics of the main absorption features (B_x, B_y, Q_x, Q_y) depend on the nature of the macrocycle and peripheral substituents. **Pheo *a*** bears two major auxochromes, the 13-keto group (embedded in the isocyclic ring) and the 3-vinyl group. The 13^1-oxophorbines **FbOP** and **ZnOP** lack the 3-vinyl group; the phorbines **FbP** and **ZnP** additionally lack the 13-keto group; the chlorin **FbC-A^{13}** further lacks the five-membered ring; the base chlorins **FbC** and **ZnC** lack any substituents (except for the geminal dimethyl group in the reduced ring common to all of the synthetic compounds examined here). Of major interest is the manner in which the nature of the macrocycle influences the position and intensity of the $Q_y(0,0)$ band. This is so because this feature corresponds to excitation to lowest singlet excited state, from which key energy- and electron-transfer events of photosynthesis are initiated. The salient points concerning the Q_y band are as follows:

(1) In the free base series, **FbOP** has the most intense $Q_y(0,0)$ band (relative to the Soret maximum). The $Q_y(0,0)$ band of **FbC-A^{13}** exhibits the same (largest) bathochromic shift as **FbOP**, but is about 80% as intense. Both compounds nearly mimic the spectrum of **Pheo *a***. In the zinc-chelate series, **ZnOP** has the relatively most intense $Q_y(0,0)$ band and the largest bathochromic shift, with **ZnC-A^{13}** second in the series in both categories.

(2) The spectral properties of phorbines (**FbP** and **ZnP**) closely resemble those of chlorins (**FbC** or **ZnC**). Both sets of compounds exhibit a $Q_y(0,0)$ band that lacks the intensity and bathochromic shift of the keto-substituted analogues.

(3) The main absorption characteristics of unsubstituted chlorin **MgC**[33] closely resemble those of **ZnC** (Table III.1). This similarity parallels that for the native magnesium-containing chlorophyll *a* (**Chl *a***) and the zinc-bearing analogue **Zn-Pheo *a***.[71]

In summary, the chlorin chromophore alone affords a poor mimic of the spectral properties of chlorophylls. However, the addition of a 13-keto group to the chlorin is essential (and suffices) to closely mimic the absorption spectrum of the naturally occurring chlorin pigment; it is anticipated that the added effect of a 3-vinyl group would give a near complete match to the spectrum of chlorophyll *a*.

C. Fluorescence spectra and quantum yields and excited-state lifetimes. For each compound studied, the fluorescence spectrum (not shown) contains a prominent $Q_y(0,0)$ band and a much weaker Q (0,1) band, which together are in approximate mirror symmetry to the Q(0,0) and Q(1,0) absorption features. The Q(0,0) emission band has about the same spectral width as, and lies no more than 2 nm to longer wavelength of, the corresponding $Q_y(0,0)$ absorption feature. This very small (<60 cm^{-1}) absorption-fluorescence spacing (Stokes shift) indicates little change in the structure or solvent interactions of these macrocycles upon photoexcitation. The fluorescence quantum yields of **FbC**, **FbP**, **FbOP**, and **FbC-A**[13] are in the range 0.20-0.30, while the value for **OxoFbC** is somewhat smaller (0.12). For **ZnC**, **ZnP**, and **OxoZnC**, the fluorescence yields are each about one-quarter of those for the corresponding free base form, while the values for **ZnOP** (0.23) and **ZnC-A**[13] (0.23) are closer to those for **FbOP** and **FbC-A**[13] (Table III.1). The lifetime of the lowest singlet excited state (determined via fluorescence detection) is in the range 7.8 to 11.5 ns for all free

base compounds. The values are considerably shorter for **ZnC** (1.7 ns), **ZnP** (1.7 ns) and **OxoZnC** (0.82 ns), with the oxochlorin being the shortest. Such short excited-state lifetimes for peripherally substituted zinc oxochlorins was found previously,[26] and the current work shows that this effect is inherent to the parent macrocycle and not from substituent effects. The excited-state lifetimes for **ZnOP** (5.1 ns) and **ZnC-A**[13] (4.3 ns) are much longer than for the other zinc chelates and are about half of those for the free base forms, **FbOP** (11.5 ns) and **FbC-A**[13] (7.8 ns).

The fluorescence yield of the magnesium chlorin **MgC** is larger than those for the free base form **FbC** and zinc chelate **ZnC** (0.26, 0.20, 0.062) while the singlet excited-state lifetime is intermediate (6.9 ns, 8.8 ns, 1.7 ns). This trend follows those for the fluorescence yields (0.14, 0.09, 0.030) and excited-state lifetimes (13 ns, 8.9 ns, 2.1 ns) of magnesium, free base, and zinc tetraphenylporphyrins.[72-74]

The collective photophysical data show that the addition of a 13-keto group to the chlorin results in a more intense and bathochromically shifted $Q_y(0,0)$ absorption feature, accompanied by fluorescence yields and singlet excited-state lifetimes for the zinc chelates that are not nearly as diminished compared to the free base analogues as for the other macrocycles. The decreased excited-state energy and increased optical-transition strength affords better utilization of the red region of the solar spectrum. The 13-keto group also increases the excited-state lifetime, which is desirable for allowing a higher yield of the photoinduced energy- or charge-transfer reactions of photosynthesis. The lengthening of the excited-state lifetime is unexpected in that the lower excited-state energy would normally

(based on the energy-gap law[75]) lead to a shortening of the lifetime due to enhancement of the nonradiative (internal conversion) decay pathway. Thus, the incorporation of a 13-keto group in a chlorin or phorbine macrocycle results in a very favorable motif from a photophysical point of view.

D. Structural Studies. X-ray crystal structure analysis of the benchmark macrocycles porphine, **FbC**, **FbC-Br^{13}**, **FbP**, **FbOP** and **OxoFbC** allowed analysis of structural changes of the core macrocycle lacking any β- and *meso*-pyrrolic substituents along the series porphyrin, chlorin, phorbine, 13^1-oxophorbine and oxochlorin.[33,76] Such studies were accompanied by resonance Raman spectroscopy and DFT calculations.[76] Moving from chlorin to phorbine (upon a five-membered exocyclic ring insertion) and, finally, from phorbine to oxophorbine (upon 13-keto group introduction) causes numerous alterations in the core macrocycle size, shape and framework. The macrocycle changes from kite-shaped (**FbC**) to more trapezoidal (**FbP** and **FbOP**) and the size decreases along the series **FbC** > **FbP** ≈ **FbOP**. Suprisingly, alterations (e.g., shortening of the C13-C13^1 bond length) caused by introduction of the keto group are very small indicating that the unsymmetrical nature of the exocyclic ring (ring E) is probably due to the annulation with macrocycle rather than conjugation with 13-keto group.

E. Frontier Molecular Orbitals and Electronic Properties. The energies and electron-density distributions of the frontier molecular orbitals (MOs) of all the newly synthesized phorbins and chlorins were obtained from DFT calculations. Such methods were also applied to several fictive chlorins, incuding the 13,15-dimethylchlorin **FbC-Me^{13,15}** and

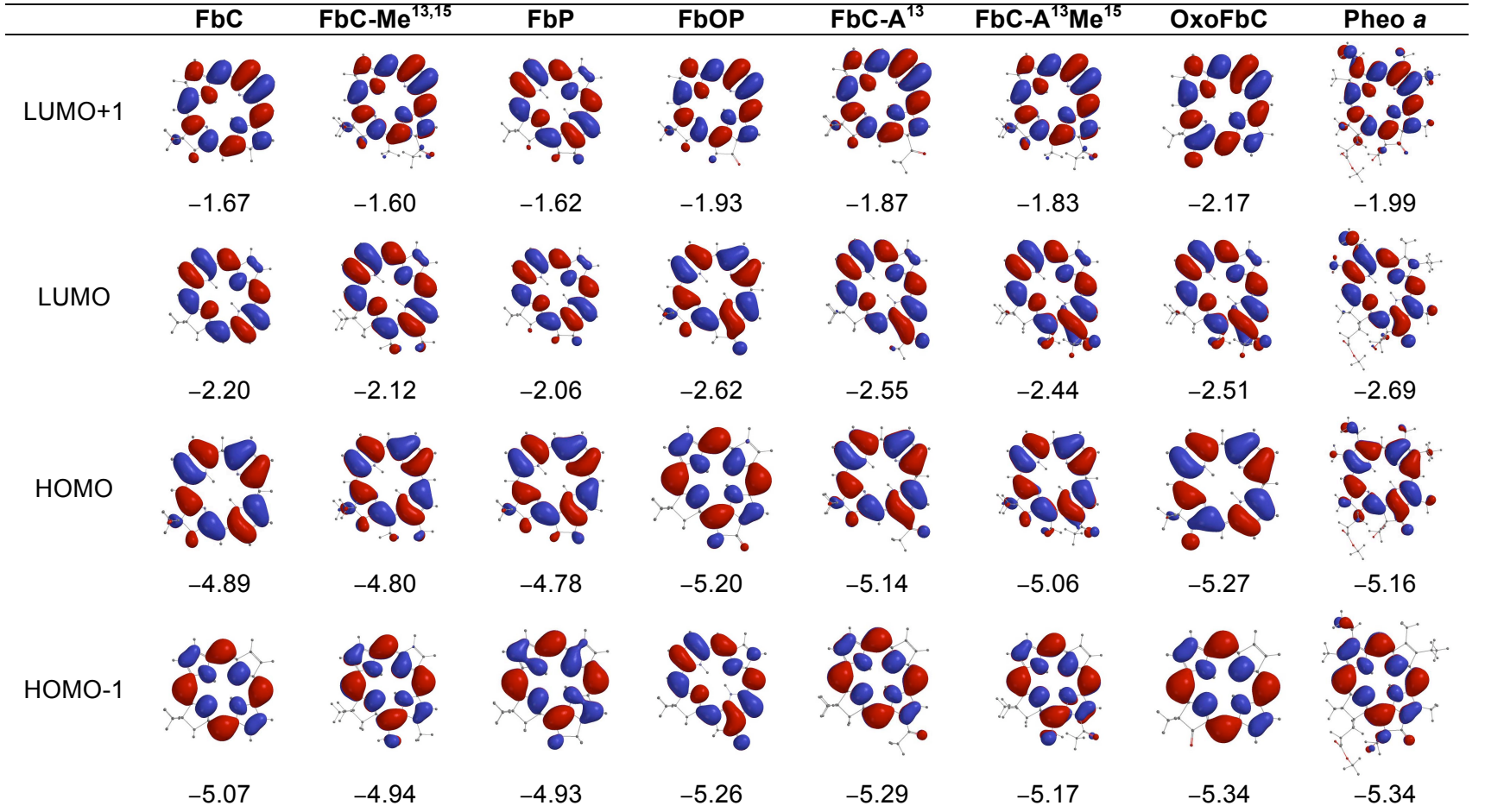

Figure III.2. Electron-density distributions and energies (eV) of the frontier MOs of the free base compounds.

	ZnC	ZnC-Me^{13,15}	ZnP	ZnOP	ZnC-A^{13}	ZnC-A^{13}Me^{15}	OxoZnC	Zn-Pheo *a*
LUMO+1	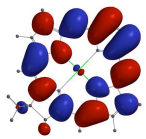	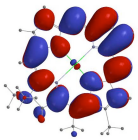	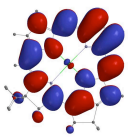	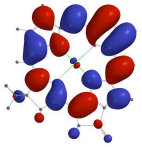	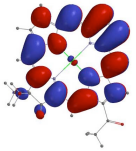	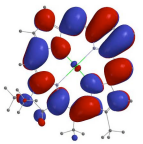	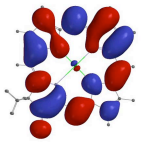	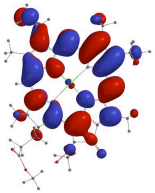
	–1.55	–1.48	–1.52	–1.83	–1.75	–1.71	–2.06	–1.89
LUMO	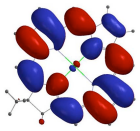	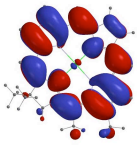	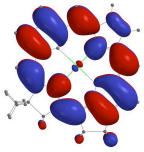	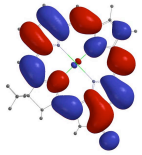	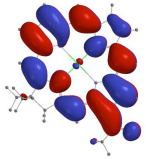	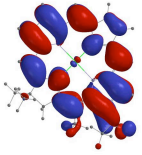	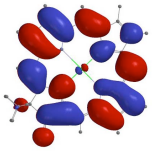	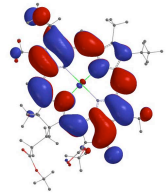
	–2.12	–2.07	–2.02	–2.57	–2.48	–2.39	–2.49	–2.64
HOMO	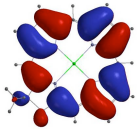	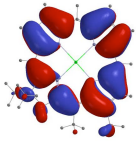	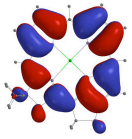	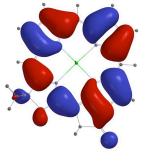	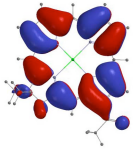	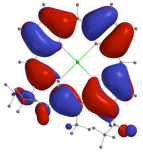	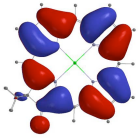	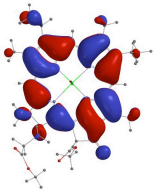
	–4.79	–4.71	–4.71	–5.12	–5.04	–4.98	–5.17	–5.07
HOMO-1	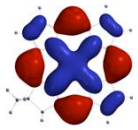	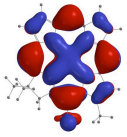	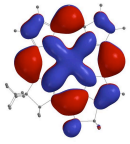	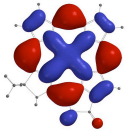	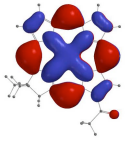	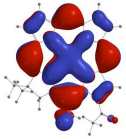	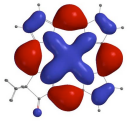	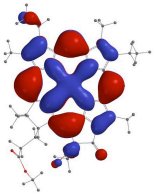
	–5.16	–5.03	–5.01	–5.35	–5.38	–5.27	–5.44	–5.43

Figure III. 3. Electron-density distributions and energies (eV) of the frontier MOs of the zinc chelates.

Macrocycle structure and MO energies. The key findings from the MO calculations are as follows:

(1) The conversion of the chlorin to a phorbine results in a small (0.08–0.14 eV) shift in the HOMO and LUMO energies to less negative values. Such shifts correspond to the phorbine being slightly easier to oxidize and slightly harder to reduce than the chlorin. This connection follows from our prior studies on about two dozen synthetic zinc chlorins that showed linear correlations between the calculated MO energies and measured redox potentials.[34,35] Moreover, the calculations reported herein on the fictive chlorins **FbC-Me^{13,15}** and **ZnC-Me^{13,15}** suggest that about half (free base) or almost the entire (zinc chelate) MO-energy shifts can be accounted for simply by the presence of the 13- and 15-substitutents and that closure to the five-membered ring (and associated ring strain) has only a small effect.

(2) Incorporation of a 13-keto group in a chlorin to produce **FbC-A^{13}** or **ZnC-A^{13}** gives a 0.25 eV shift in the HOMO energy and a 0.33–0.36 eV shift in the LUMO energy to more negative values. The analogous incorporation of a 13-keto group in a phorbine to produce the oxophorbine (e.g., **FbP** to **FbOP**) gives an even larger 0.41–0.42 eV shift in the HOMO energy and a larger still 0.55–0.56 eV shift in the LUMO energy to more negative values. The direction of the shifts is such that the presence of the 13-keto group will make the molecule harder to oxidize and easier to reduce. The calculations on the fictive chlorin **ZnC-A^{13}M^{15}**, together with those described above for **ZnC-M^{13,15}**, suggest that closure to the five-membered ring (and associated ring strain) has a somewhat greater effect on the frontier-MO

energies when the 13-keto group is present (e.g. **FbP** to **FbOP**) than in its absence (e.g. **FbC** to **FbC-A**^{13}).

(3) The effect of the 13-keto group on the LUMO energy is larger than the effect on the HOMO energy by an average of 0.11 eV for the four cases (13-keto addition to chlorin or oxophorbine and for free base and zinc forms). This effect can be understood by the generally larger electron density on the 13-group for the LUMO compared to the HOMO (Figures III.2 and III.3). The unequal effect of the 13-keto group on the LUMO and HOMO alters the HOMO-LUMO energy gap and thus affects the energy/wavelength of the $Q_y(0,0)$ absorption band, as described further below.

(4) The 13-keto substituted chlorins **FbC-A**^{13} and **ZnC-A**^{13} have HOMO energies that are only slightly (0.02–0.03 eV) less negative and LUMO energies that are modestly (0.14-0.16 eV) less negative than those of the corresponding natural pigments **Pheo *a*** and **Zn-Pheo *a***. Thus, the simple presence of a 13-keto group, without closure to the five-membered ring to give the oxophorbine, is sufficient to give a macrocycle which is almost as easy to oxidize and only modestly harder to reduce than the related photosynthetic pigment (i.e., **Pheo *a***). Carrying the comparison one step further, the unsubstituted oxophorbines **FbOP** and **ZnOP** have HOMO energies that are actually slightly (0.04–0.05 eV) more negative and LUMO energies that are slightly (0.07 eV) less negative than those of the **Pheo *a*** and **Zn-Pheo *a***. Thus, the oxophorbine macrocycle encodes the primary electronic properties that dictate the redox potentials of the native photosynthetic pigments, with only small net adjustments due to the substituents at the eight β-pyrrole positions.

Absorption spectra and MO energies. Figure III.4 (top) plots the energies of the HOMO, LUMO, HOMO-1, and LUMO+1 versus $Q_y(0,0)$ absorption energy/wavelength (Table III.1) for the various macrocycles, along with linear fits to the data and values indicating the slopes of the trend lines. For both the free base macrocycles (open symbols and dashed lines) and zinc chelates (closed symbols and solid lines), the LUMO exhibits a much greater dependence on macrocycle characteristics than the HOMO or other orbitals (HOMO-1 and LUMO+1). In particular, the slope of the trend lines encompassing the addition of a 13-keto group to a chlorin (e.g. **FbC** to **FbC-A**[13]) or to a phorbine (e.g. **FbP** to **FbOP**) is twice as large for the LUMO than for the other three frontier MOs.

Close inspection of the orbital energies listed in Figures III.2 and III.3 shows that the trends depicted in Figure III.4 (top) reflect a correlation between a decrease in the $Q_y(0,0)$ absorption-band energy (an increase in wavelength) and a decrease in the HOMO – LUMO energy gap upon addition of a 13-keto group (to either a chlorin or phorbine). This tracking of the $Q_y(0,0)$ energy/wavelength with the HOMO – LUMO energy gap is shown explicitly in Figure III.4 (bottom) for the free base macrocycles (open downward triangles and dashed line) and zinc chelates (closed downward triangles and solid line). The bottom panel of Figure III.4 also shows that, in contrast, the energy gap between the LUMO+1 and HOMO-1 increases slightly as the $Q_y(0,0)$ energy decreases (wavelength increases), and with a trend-line slope that is about one-third that of the HOMO – LUMO energy gap.

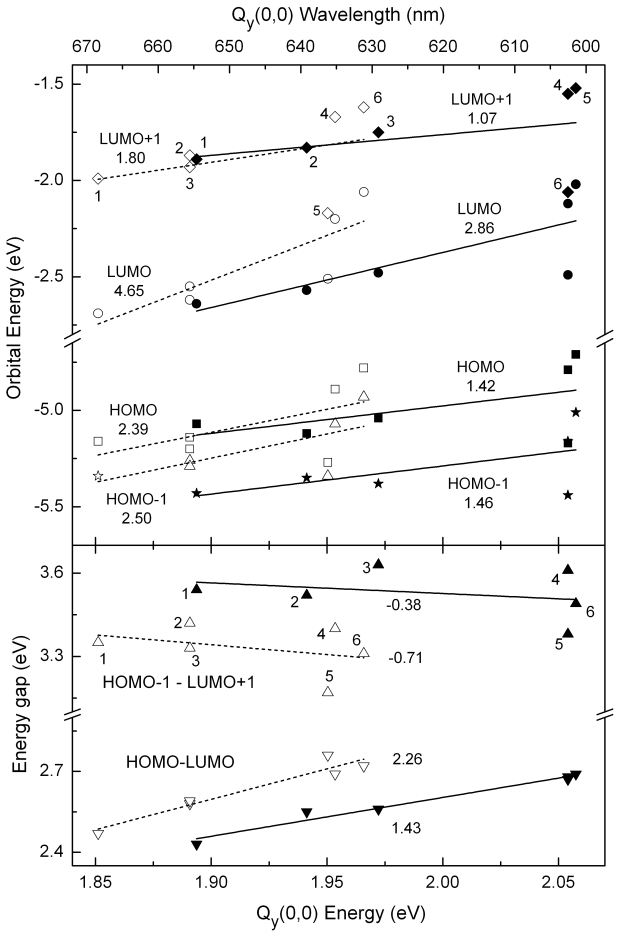

Figure III.4. Calculated frontier MO energies (top panel) and energy gaps (bottom panel) versus the measured $Q_y(0,0)$ absorption-band energy (bottom axis) and wavelength (top axis) for free base macrocycles (open symbols) and zinc chelates (closed symbols). Top: energies LUMO+1 (diamonds), LUMO (circles), HOMO (squares), HOMO-1 (stars). Bottom: energy gaps HOMO-1 – LUMO+1 (up triangles), and HOMO – LUMO (down triangles). The indicated values are the slopes of the trend lines for free base macrocycles (dashed lines) and zinc chelates (solid lines). The points for the different macrocycles are labeled as follows: **Pheo *a*** (1), **FbC-A**[13] (2), **FbOP** (4), **FbC** (4), **OxoFbC** (5), and **FbP** (6), and similarly for the zinc chelates.

The collective results depicted in Figure III.4 show that (1) the bathochromic shift in the position of the $Q_y(0,0)$ absorption band is driven by a reduction in the HOMO – LUMO energy gap. (2) The reduction in the HOMO – LUMO energy gap is in turn driven by a

stronger effect of the 13-keto substituent on the LUMO energy than the HOMO energy. (3) These effects can be understood by the greater electron density on the 13-keto group for the LUMO compared to the other frontier MOs.

The results above can be taken one step further by application of Gouterman's four-orbital model.[77-79] Within this model, the energy/wavelength of the $Q_y(0,0)$ absorption band depends on the quantity ΔE_{avg} defined in Eq (III.1), namely the average of the HOMO – LUMO and LUMO+1 – HOMO-1 energy gaps, whereas the intensity of the band depends on the quantity ΔE_{dif} defined in Eq (III.2), namely the difference in these two orbital energy gaps:

$$\Delta E_{avg} = [(\text{HOMO-1} - \text{LUMO+1}) + (\text{HOMO} - \text{LUMO})]/2 \qquad \text{(III.1)}$$

$$\Delta E_{dif} = [(\text{HOMO-1} - \text{LUMO+1}) - (\text{HOMO} - \text{LUMO})] \qquad \text{(III.2)}$$

Figure III.5 (top) shows a good overall correlation between ΔE_{avg} and the $Q_y(0,0)$ absorption energy/wavelength for both the free base macrocycles and zinc chelates. Figure III.5 (bottom) shows a good correlation between ΔE_{dif} and the integrated intensity of the $Q_y(0,0)$ absorption band (Table III.1), especially for the free base compounds (open symbols and dashed line). We have previously utilized the four-orbital model to understand how the macrocycle-substituent pattern controls the MO energies and the spectral characteristics of a large set of synthetic free base and zinc chlorins.[34,35]

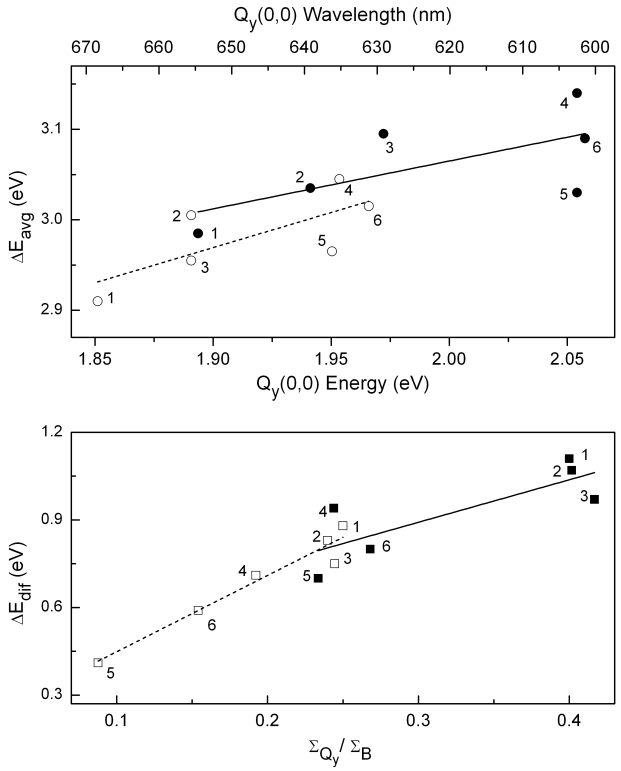

Figure III.5. (Top) Calculated average of the HOMO-1 – LUMO+1 and HOMO – LUMO energy gaps versus the measured $Q_y(0,0)$ absorption-band energy (bottom axis) and wavelength (top axis) for free base macrocycles (open symbols and dashed trendline) and zinc chelates (closed symbols and solid trend line). (Bottom) Calculated difference in the HOMO-1 – LUMO+1 and HOMO – LUMO energy gaps versus the ratio of the integrated intensities of the Q_y and B absorption manifolds for the free base macrocycles (open symbols and dashed trend line) and zinc chelates (closed symbols and solid trend line). The points for the different macrocycles are labeled as follows: **Pheo *a*** (1), **FbC-A**[13] (2), **FbOP** (4), **FbC** (4), **OxoFbC** (5), and **FbP** (6), and similarly for the zinc chelates.

In the present study of unsubstituted parent macrocycles (chlorin, phorbine, oxophorbine), the use of the four-orbital framework (involving simple sums and differences of MO energy gaps) provides additional fundamental insights into the intimate relationship between the hydrocarbon skeleton, electronic structure, and characteristics of the long-

wavelength absorption band of the natural photosynthetic pigments. Moreover, this framework and understanding has predictive value in aiding the design of synthetic analogues of the parent macrocycles and the fully substituted photosynthetic pigments to allow better coverage of the solar spectrum toward artificial systems for solar-energy conversion. The ability to mimic the spectral properties of chlorophylls with far simpler and synthetically accessible macrocycles augurs well for the use of such hydroporphyrins in a variety of artificial photosynthetic architectures.

Finally, we note that the studies here have employed zinc chelates rather than magnesium as is present in the chlorophylls. Compared with zinc, magnesium affords a bathochromic shift of the Qy band of about 10 nm, 3–4-fold longer singlet excited-state lifetime, more facile groud-state oxidation, a more potent excited-state reductant, and tighter binding of oxygenic apical ligands. On the other hand, magnesium is more susceptible to demetalation. Any application would need to balance the advantageous photophysical properties of magnesium chlorins versus the greater chemical stability of the zinc chelates.

III.3. Experimental Section

General Synthetic Methods. All ^{1}H NMR (300 MHz and 400 MHz) and ^{13}C NMR (100 MHz) spectra were obtained in $CDCl_3$ unless noted otherwise. Mass spectra of chlorins were obtained via laser desorption ionization mass spectrometry without matrix or using a matrix of 1,4-bis(5-phenyloxazol-2-yl)benzene. Electrospray ionization mass spectrometry (ESI-MS) data are reported for the molecule ion or protonated molecule ion. Column chromatography was performed with flash silica. Melting points are uncorrected. All

commercially available materials were used as received. Absorption and fluorescence spectra were obtained in toluene at room temperature unless noted otherwise. All of the Pd-mediated coupling reactions were carried out under argon using standard Schlenk-line procedures (e.g., three freeze-pump-thaw cycles were performed prior to and after the addition of the palladium reagent, for a total of six such cycles).

Zn(II)-13-Bromo-17,18-dihydro-18,18-dimethylporphyrin (ZnC-Br[13]). Following a standard procedure,[31,38] a solution of **II-1-Br**[8,9] (151 mg, 0.452 mmol) and **II-3** (86 mg, 0.45 mmol) in anhydrous CH_2Cl_2 (12 mL) was treated with a solution of $TsOH \cdot H_2O$ (430 mg, 2.26 mmol) in anhydrous methanol (3 mL) under argon. The reaction mixture changed immediately to orange-red. The mixture was stirred for 30 min under argon, then treated with 2,2,6,6-tetramethylpiperidine (845 μL, 4.97 mmol) and concentrated to dryness, thereby affording a brown solid. The solid was suspended in acetonitrile (45 mL), whereupon 2,2,6,6-tetramethylpiperidine (1.92 mL, 11.3 mmol), $Zn(OAc)_2$ (1.25 g, 6.78 mmol) and AgOTf (349 mg, 1.36 mmol) were consecutively added. The resulting suspension was refluxed for 20 h exposed to air. The crude mixture was filtered through a silica pad with CH_2Cl_2, and the filtrate was chromatographed [silica, CH_2Cl_2/hexanes (2:1)] to afford a green solid (35 mg, 16%): ^{1}H NMR (400 MHz, THF-d_8) δ 2.06 (s, 6H), 4.63 (s, 2H), 8.72 (s, 1H), 8.80 (d, J = 4.1 Hz, 1H), 8.89 (s, 1H), 8.94–8.96 (m, 2H), 9.09 (d, J = 4.1 Hz, 1H), 9.15 (s, 1H), 9.58 (s, 1H), 9.64 (s, 1H); ^{13}C NMR (THF-d_8) δ 31.5, 46.4, 51.7, 94.0, 95.1, 109.08, 109.17, 115.8, 128.6, 129.4, 129.8, 133.0, 133.7, 144.6, 147.6, 147.8, 148.3, 149.3, 155.1, 159.8, 171.6; MALDI-MS obsd 479.9; ESI-MS obsd 481.00126 $(M + H)^+$

corresponds to 479.99398 (M), calcd 479.99281 (M = $C_{22}H_{17}BrN_4Zn$); λ_{abs} 401, 610 nm; λ_{em} 614 nm (λ_{ex} 401 nm).

13-Bromo-17,18-dihydro-18,18-dimethylporphyrin (FbC-Br[13]). A solution of **ZnC-Br[13]** (33 mg, 0.069 mmol) in CH_2Cl_2 (11 mL) was treated with TFA (0.256 mL, 3.44 mmol). The reaction mixture was stirred for 3 h at room temperature, and then was quenched by the addition of saturated aqueous $NaHCO_3$. Following extraction with CH_2Cl_2, the organic phase was dried (Na_2SO_4) and concentrated to afford a green solid. Purification by column chromatography [silica, CH_2Cl_2/hexanes (1:1)] afforded a purple solid (25 mg, 87%): ^{1}H NMR (400 MHz, THF-d_8) δ –2.45 (br, 2H), 2.06 (s, 6H), 4.70 (s, 2H), 9.015–9.017 (m, 2H), 9.06 (d, J = 4.4 Hz, 1H), 9.11 (s, 1H), 9.19 (s, 1H), 9.31 (d, J = 4.4 Hz, 1H), 9.39 (s, 1H), 9.82 (s, 1H), 9.89 (s, 1H); ^{13}C NMR (THF-d_8) δ 31.3, 47.4, 52.7, 95.0, 95.9, 106.9, 107.5, 112.4, 125.0, 128.8, 129.1, 133.5, 133.7, 133.9, 136.4, 136.9, 141.8, 153.1, 153.5, 164.1, 176.1; LD-MS obsd 417.9; ESI-MS obsd 419.08744 $(M + H)^+$ corresponds to 418.08017 (M), calcd 418.07931 (M = $C_{22}H_{19}BrN_4$); λ_{abs} 391, 641 nm.

13-Acetyl-17,18-dihydro-18,18-dimethylporphyrin (FbC-A[13]). Following a procedure for Stille coupling of aromatic compounds[50] with the modifications employed in the synthesis of **FbC-A[12]**, a mixture of **FbC-Br[13]** (52 mg, 0.12 mmol), tributyl(1-ethoxyvinyl)tin (169 μL, 0.500 mmol), and $(PPh_3)_2PdCl_2$ (13 mg, 0.018 mmol) in the solvent mixture of acetonitrile (3.5 mL) and DMF (2.5 mL) was heated at 85 °C for 2.5 h. The reaction mixture was treated with 10% aqueous HCl (2 mL) at room temperature for 40 min and then diluted with CH_2Cl_2. The organic phase was washed with saturated aqueous $NaHCO_3$, water, and brine. The organic layer was dried (Na_2SO_4), concentrated and

chromatographed [silica, CH_2Cl_2/hexanes (2:1)] to afford a purple solid (37 mg, 81%): ^{1}H NMR (300 MHz) δ –1.80 (br, 2H), 2.03 (s, 6H), 3.24 (s, 3H), 4.61 (s, 2H), 8.82 (s, 1H), 8.91 (d, *J* = 4.4 Hz, 1H), 8.92 (d, *J* = 4.2 Hz, 1H), 9.00 (d, *J* = 4.2 Hz, 1H), 9.14 (d, *J* = 4.4 Hz, 1H), 9.53 (s, 1H), 9.64 (s, 1H), 9.76 (s, 1H), 10.1 (s, 1H); ^{13}C NMR δ 29.9, 31.2, 47.0, 51.9, 95.0, 97.7, 106.1, 109.5, 125.7, 128.9, 129.4, 130.4, 132.6, 134.0, 136.9, 137.3, 142.3, 151.6, 154.3, 165.0, 177.6, 197.0, 203.0; MALDI-MS obsd 381.9; ESI-MS obsd 383.18648 $(M + H)^+$ corresponds to 382.1792 (M), calcd 382.1794 ($M = C_{24}H_{22}N_4O$); λ_{abs} 405 (log ε = 4.91), 654 (log ε = 4.64) nm.

13-Acetyl-15-bromo-17,18-dihydro-18,18-dimethylporphyrin (FbC-A^{13}Br^{15}). Following a procedure for regioselective 15-bromination,[41] a solution of **FbC-A^{13}** (34 mg, 0.089 mmol) in CH_2Cl_2 (40 mL) and TFA (4 mL) was treated with NBS (890 μL, 0.100 M in CH_2Cl_2, 0.0890 mmol) at room temperature. The reaction mixture was stirred for 1 h at room temperature. CH_2Cl_2 was added, and the reaction mixture was washed with saturated aqueous $NaHCO_3$, water, and brine. The organic layer was dried (Na_2SO_4), concentrated, and chromatographed [silica, CH_2Cl_2/hexanes (2:1)] to give a purple solid (30 mg, 73%): ^{1}H NMR (300 MHz) δ –2.14 (br, 1H), –1.90 (br, 1H), 2.04 (s, 6H), 3.19 (s, 3H), 4.59 (s, 2H), 8.82 (s, 1H), 8.88 (d, *J* = 4.3 Hz, 1H), 8.91 (d, *J* = 5.0 Hz, 1H), 8.97 (d, *J* = 4.3 Hz, 1H), 9.13 (d, *J* = 5.0 Hz, 1H), 9.13 (s, 1H), 9.61 (s, 1H), 9.73 (s, 1H); ^{13}C NMR δ 31.6, 34.8, 46.8, 55.2, 95.0, 95.7, 105.9, 109.7, 126.37, 126.46, 129.2, 130.5, 132.7, 133.8, 134.6, 136.9, 137.6, 141.5, 151.3, 155.0, 163.1, 177.4, 202.3; LD-MS obsd 460.0; ESI-MS obsd 461.09695 $(M + H)^+$ corresponds to 460.08968 (M); calcd 460.08987 ($M = C_{24}H_{21}BrN_4O$); λ_{abs} 399, 664 nm.

Zn(II)-13-Acetyl-17,18-dihydro-18,18-dimethylporphyrin (ZnC-A^{13}). A solution of **FbC-A^{13}** (7 mg, 0.02 mmol) in $CHCl_3$ (2 mL) was treated with a solution of $Zn(OAc)_2 \cdot 2H_2O$ (61 mg, 0.28 mmol) in MeOH (1 mL). The reaction mixture was stirred overnight at room temperature. Then the reaction mixture was concentrated and chromatographed [silica, CH_2Cl_2/hexanes (2:1)] to afford a green solid (5 mg, 70%): ^{1}H NMR (400 MHz, THF-d_8) δ 2.02 (s, 6H), 3.08 (s, 3H), 4.55 (s, 2H), 8.58 (s, 1H), 8.73 (d, J = 4.4 Hz, 1H), 8.85 (d, J = 4.4 Hz, 1H), 8.93 (d, J = 4.4 Hz, 1H), 9.01 (d, J = 4.4 Hz, 1H), 9.48 (s, 1H), 9.60 (s, 1H), 9.63 (s, 1H), 9.87 (s, 1H); MALDI-MS 444.2; ESI-MS obsd 445.09909 $(M + H)^+$ corresponds to 444.09181 (M), calcd 444.09286 ($M = C_{24}H_{20}N_4OZn$); λ_{abs} 412, 628 nm, λ_{em} 632 nm (λ_{ex} 412 nm).

17,18-Dihydro-18,18-dimethyl-13^1-oxophorbine (FbOP). Following a standard procedure,[30,51] a mixture of **FbC-A^{13}Br^{15}** (27 mg, 0.058 mmol), Cs_2CO_3 (96 mg, 0.29 mmol), and $(PPh_3)_2PdCl_2$ (8 mg, 0.02 mmol) in toluene (6 mL) was refluxed in a Schlenk line. After 22 h CH_2Cl_2 was added, and the organic layer was washed with water and brine. The organic layer was isolated, dried (Na_2SO_4) and concentrated. The resulting residue was purified by column chromatography [silica, hexanes/ethyl acetate (2:1)] to afford a purple solid (12 mg, 55%): ^{1}H NMR (300 MHz) δ –2.23 (br, 1H), –0.17 (br, 1H), 1.98 (s, 6H), 4.18 (s, 2H), 5.03 (s, 2H), 8.64 (s, 1H), 8.73 (d, J = 4.3 Hz, 1H), 8.81 (d, J = 4.3 Hz, 1H), 8.85–8.87 (m, 1H), 9.91 (s, 1H), 9.03–9.06 (m, 1H), 9.37 (s, 1H), 9.50 (s, 1H); ^{13}C NMR δ 31.1, 47.8, 48.57, 48.74, 95.1, 103.8, 106.1, 111.1, 115.6, 126.8, 130.3, 132.5, 132.8, 134.3, 138.1, 138.9, 143.1, 149.2, 152.6, 154.9, 157.3, 177.1, 195.8; MALDI-MS obsd 380.0; ESI-MS obsd

381.17088 $(M + H)^+$ corresponds to 380.16360 (M); calcd 380.16371 ($M = C_{24}H_{20}N_4O$); λ_{abs} 408 (log ε = 4.74), 654 (log ε = 4.53) nm; λ_{em} 657 nm (λ_{ex} 408 nm).

Zn(II)-17,18-Dihydro-18,18-dimethyl-13^1-oxophorbine (ZnOP). A solution of **FbOP** (11 mg, 0.029 mmol) in $CHCl_3$/MeOH (4:1, 6 mL) was treated with $Zn(OAc)_2 \cdot 2H_2O$ (95 mg, 0.43 mmol). The reaction mixture was stirred for 20 h at room temperature. CH_2Cl_2 was added, and the mixture was concentrated. The resulting solid was dissolved in CH_2Cl_2, and the resulting organic solution was washed (saturated aqueous $NaHCO_3$, water), dried (Na_2SO_4), and concentrated to afford a green solid. The solid was washed with hexanes three times and then was dissolved in the minimal amount of CH_2Cl_2. A double volume of hexanes subsequently was added, which afforded a precipitate that was isolated by centrifugation (10 mg, 78%): ^{1}H NMR (400 MHz, THF-d_8) δ 2.05 (s, 6H), 4.34 (s, 2H), 5.04 (s, 2H), 8.59 (s, 1H), 8.78–8.80 (m, 2H), 8.95 (d, J = 4.4 Hz, 1H), 9.01, (d, J = 4.2 Hz, 1H), 9.05 (s, 1H), 9.39 (s, 1H), 9.74 (s, 1H); LD-MS obsd 442.1; ESI-MS obsd 443.08407 $(M + H)^+$ corresponds to 442.07679; calcd 442.07587 ($C_{24}H_{18}N_4OZn$); λ_{abs} 420, 637 nm, λ_{em} 640 (λ_{ex} 420 nm).

18,18-Dimethylphorbine (FbP). A sample of **FbOP** (30 mg, 0.079 mmol) in ethanol/$CHCl_3$ (5 mL, 1:1) was treated with tosylhydrazide (44 mg, 0.24 mmol) at 65 °C. The reaction mixture was stirred for 2 h at 65 °C and then 2 h at room temperature. The reaction mixture was concentrated, and the solid was washed three times [H_2O/methanol (1:4)] and dried under high vacuum. The crude solid was dissolved in THF (4 mL), and the resulting solution was treated with sodium cyanoborohydride (22 mg, 0.32 mmol) followed by a solution of $TsOH \cdot H_2O$ (48 mg, 0.25 mmol) in MeOH (1 mL). After 2 h, the reaction

mixture was diluted with CH_2Cl_2 and quenched by the addition of saturated aqueous $NaHCO_3$. The organic phase was washed with water, dried over Na_2SO_4, and filtered. The filtrate was concentrated to afford a green solid. The solid was dissolved in DMF/EtOH (5 mL, 1:2), and the solution was treated with sodium acetate trihydrate (54 mg, 0.40 mmol). After heating at 80 °C for 5 h, the mixture was allowed to cool to room temperature, whereupon CH_2Cl_2 and water were added. The organic phase was washed (water and brine), dried (Na_2SO_4) and concentrated. Column chromatography (silica, CH_2Cl_2/hexanes [1:1] afforded a green solid (12 mg, 42%): ^{1}H NMR (400 MHz) δ –3.42 (br, 1H), –1.67 (br, 1H), 2.10 (s, 6H), 4.17–4.19 (m, 2H), 4.46 (s, 2H), 4.78–4.80 (m, 2H), 8.79 (s, 1H), 9.04–9.06 (m, 2H), 9.08 (d, *J* = 4.1 Hz, 1H), 9.16 (d, *J* = 4.1 Hz, 1H), 9.31–9.33 (m, 1H), 9.73 (s, 1H), 9.98 (s, 1H); ^{13}C NMR δ 25.9, 31.9, 37.6, 47.4, 49.9, 95.1, 103.4, 105.8, 112.3, 116.2, 122.6, 127.4, 131.1, 132.5, 133.5, 139.2, 143.0, 145.2, 147.9, 149.2, 152.7, 160.1, 171.4; LD-MS obsd 366.1; ESI-MS obsd 367.19219 $(M + H)^+$ corresponds to 366.18492 (M), calcd 366.18445 ($M = C_{24}H_{22}N_4$); λ_{abs} 405 (log ε = 5.16), 630 (log ε = 4.59) nm.

Zn(II)-18,18-Dimethylphorbine (ZnP). A solution of **FbP** (12 mg, 0.033 mmol) in $CHCl_3$ (4 mL) was treated with a methanolic solution (1 mL) of $Zn(OAc)_2 \cdot 2H_2O$ (108 mg, 0.492 mmol). The reaction mixture was stirred for 1 h at room temperature. CH_2Cl_2 was added, and the mixture was concentrated. The resulting solid was dissolved in CH_2Cl_2, and the resulting organic solution was washed (saturated aqueous $NaHCO_3$ and water), dried (Na_2SO_4), and concentrated to afford a green solid. The solid was dissolved in CH_2Cl_2 (1 mL), and hexanes (1 mL) was added. The resulting precipitate was isolated by centrifugation (13 mg, 90%): ^{1}H NMR (400 MHz) δ 2.07 (s, 6H), 3.74–3.76 (m, 2H), 4.28 (s, 2H), 4.36–

4.39 (m, 2H), 8.27 (s, 1H), 8.75 (s, 1H). 8.86 (d, J = 4.1 Hz, 1H), 8.89 (d, J = 4.4 Hz, 1H), 8.93 (d, J = 4.1 Hz, 1H), 9.17 (d, J = 4.4 Hz, 1H), 9.30 (s, 1H), 9.67 (s, 1H); LD-MS obsd 428.0; ESI-MS obsd 428.0971, calcd 428.0974 ($C_{24}H_{20}N_4Zn$); λ_{abs} 402 (log ε = 4.89), 601 (log ε = 4.23) nm, λ_{em} 605 (λ_{ex} 410 nm).

Photophysical Measurements. Static absorption (Varian Cary 100) and fluorescence (Spex Fluorolog Tau 2 or PTI Quantamaster 40) measurements were performed as described previously.[68,69] Argon-purged solutions of the samples in toluene with an absorbance of ≤0.10 at the excitation wavelength were used for the fluorescence spectral, quantum yield, and lifetime measurements. Fluorescence lifetimes were obtained using a phase modulation technique and Soret-band excitation[69] (Spex Fluorolog Tau 2) or via decay measurements using excitation pulses at 337 nm from a nitrogen laser and time-correlate-single-photon-counting detection (Photon Technology International LaserStrobe TM-3). Emission measurements employed 2-4 nm excitation- and detection-monochromator bandwidths and 0.2 nm data intervals. Emission spectra were corrected for detection-system spectral response. Fluorescence quantum yields were determined relative to chlorophyll *a* in benzene (Φ_f = 0.325)[80] or chlorophyll *a* in toluene, which was found to have the same value as in benzene.

Density Functional Theory Calculations. DFT calculations were performed with Spartan '08 for Windows (Wavefunction, Inc.) on a PC (Dell Optiplex GX270) equipped with a 3.2 GHz CPU and 3 GB of RAM.[81] The hybrid B3LYP functional and the 6-31G* basis set were employed. The equilibrium geometries were fully optimized using the default

parameters of the Spartan ‘08 program. A methyl group was substituted for the phytyl chain in the calculations on Pheo *a* and Zn Pheo *a*.

The results presented in this chapter have been published.[82]

III.4. References

(1) Scheer, H. In *Chlorophylls and Bacteriochlorophylls*; Grimm, B.; Porra, R. J.; Rüdiger, W.; Scheer, H.; Eds.; Springer: Dordrecht, 2006, pp 2–26.

(2) Moss, G. P. *Pure Appl. Chem*. **1987**, *59*, 779–832.

(3) Mauzerall, D. *Ann. N. Y. Acad. Sci.* **1973**, *206*, 483–494.

(4) Björn, L. O.; Papageorgiou, G. C.; Blankenship, R. E.; Govindjee, *Photosyn. Res*. **2009**, *99*, 85–98.

(5) Björn, L. O. *Photosynthetica* **1976**, *10*, 121–129.

(6) Björn, L. O.; Papageorgiou, G. C.; Dravins, D.; Govindjee, *Curr. Sci.* **2009**, *96*, 1171–1175.

(7) Kobayashi, M.; Akiyama, M.; Kano, H.; Kise, H. In *Chlorophylls and Bacteriochlorophylls*; Grimm, B.; Porra, R. J.; Rüdiger, W.; Scheer, H.; Eds.; Springer: Dordrecht, 2006, pp 79–94.

(8) Butler, W. L. In *The Chlorophylls*; Vernon L. P.; Seely, G. P.; Eds.; Academic Press: New York, 1966, pp 343–379.

(9) Flitsch, W. *Adv. Heterocyclic Chem*. **1988**, *43*, 73–126.

(10) Hynninen, P. H. In *Chlorophylls*; Scheer, H.; Ed.; CRC Press: Boca Raton, FL, 1991, pp 145–209.

(11) Smith, K. M. In *Chlorophylls*; Scheer, H.; Ed.; CRC Press: Boca Raton, FL, 1991, pp 115–143.

(12) Montforts, F.-P.; Gerlach, B.; Höper, F. *Chem. Rev*. **1994**, *94*, 327–347.

(13) Montforts, F.-P.; Glasenapp-Breiling, M. *Prog. Heterocycl. Chem*. **1998**, *10*, 1–24.

(14) Jaquinod, L. In *The Porphyrin Handbook*; Kadish, K. M.; Smith, K. M.; Guilard, R.; Eds.; Academic Press: San Diego, CA, 2000, vol. 1, pp 201–237.

(15) Vicente, M. G. H. In *The Porphyrin Handbook*; Kadish, K. M.; Smith, K. M.; Guilard, R.; Eds.; Academic Press: San Diego, 2000, vol. 1, pp 149–199.

(16) Pandey, R. K.; Zheng, G. In *The Porphyrin Handbook*; Kadish, K. M.; Smith, K. M.; Guilard, R.; Eds.; Academic Press: San Diego, 2000, vol. 6, pp 157–230.

(17) Montforts, F.-P.; Glasenapp-Breiling, M. *Fortschr. Chem. Org. Naturst*. **2002**, *84*, 1–51.

(18) Pavlov, V. Y.; Ponomarev, G. V. *Chem. Heterocycl. Cmpds*. **2004**, *40*, 393–425.

(19) Senge, M. O.; Wiehe, A.; Ryppa, C. In *Chlorophylls and Bacteriochlorophylls. Biochemistry, Biophysics, Functions and Applications*; Grimm, B.; Porra, R. J.; Rüdiger, W.; Scheer, H.; Eds.; *Advances in Photosynthesis and Respiration*, Springer: Dordrecht, The Netherlands, 2006, vol. 25, pp 27–37.

(20) Fox, S.; Boyle, R. W. *Tetrahedron* **2006**, *62*, 10039–10054.

(21) Galezowski, M; Gryko, D. T. *Curr. Org. Chem*. **2007**, *11*, 1310–1338.

(22) Silva, A. M. G.; Cavaleiro, J. A. S. In *Progress in Heterocyclic Chemistry*; Gribble, G. W.; Joule, J. A.; Eds.; Elsevier: Amsterdam, 2008, vol. 19, ch. 2, pp 44–69.

(23) Strachan, J.-P.; O'Shea, D. F.; Balasubramanian, T.; Lindsey, J. S. *J. Org. Chem.* **2000**, *65*, 3160–3172.

(24) Balasubramanian, T.; Strachan, J.-P.; Boyle, P. D.; Lindsey, J. S. *J. Org. Chem.* **2000**, *65*, 7919–7929.

(25) Taniguchi, M.; Ra, D.; Mo, G.; Balasubramanian, T.; Lindsey, J. S. *J. Org. Chem.* **2001**, *66*, 7342–7354.

(26) Taniguchi, M.; Kim, H.-J.; Ra, D.; Schwartz, J. K.; Kirmaier, C.; Hindin, E.; Diers, J. R.; Prathapan, S.; Bocian, D. F.; Holten, D.; Lindsey, J. S. *J. Org. Chem.* **2002**, *67*, 7329–7342.

(27) Taniguchi, M.; Kim, M. N.; Ra, D.; Lindsey, J. S. *J. Org. Chem.* **2005**, *70*, 275–285.

(28) Ptaszek, M.; Bhaumik, J.; Kim, H.-J.; Taniguchi, M.; Lindsey, J. S. *Org. Process Res. Dev.* **2005**, *9*, 651–659.

(29) (a) Laha, J. K.; Muthiah, C.; Taniguchi, M.; McDowell, B. E.; Ptaszek, M.; Lindsey, J. S. *J. Org. Chem.* **2006**, *71*, 4092–4102. (b) Ibid. *J. Org. Chem.* **2009**, *74*, 5122.

(30) Laha, J. K.; Muthiah, C.; Taniguchi, M.; Lindsey, J. S. *J. Org. Chem.* **2006**, *71*, 7049–7052.

(31) Ptaszek, M.; McDowell, B. E.; Taniguchi, M.; Kim, H.-J.; Lindsey, J. S. *Tetrahedron* **2007**, *63*, 3826–3839.

(32) Taniguchi, M.; Ptaszek, M.; McDowell, B. E.; Lindsey, J. S. *Tetrahedron* **2007**, *63*, 3840–3849.

(33) Taniguchi, M.; Ptaszek, M.; McDowell, B. E.; Boyle, P. D.; Lindsey, J. S. *Tetrahedron* **2007**, *63*, 3850–3863.

(34) Kee, H. L.; Kirmaier, C.; Tang, Q.; Diers, J. R.; Muthiah, C.; Taniguchi, M.; Laha, J. K.; Ptaszek, M.; Lindsey, J. S.; Bocian, D. F.; Holten, D. *Photochem. Photobiol*. **2007**, *83*, 1110–1124.

(35) Kee, H. L.; Kirmaier, C.; Tang, Q.; Diers, J. R.; Muthiah, C.; Taniguchi, M.; Laha, J. K.; Ptaszek, M.; Lindsey, J. S.; Bocian, D. F.; Holten, D. *Photochem. Photobiol*. **2007**, *83*, 1125–1143.

(36) Muthiah, C.; Bhaumik. J.; Lindsey, J. S. *J. Org. Chem*. **2007**, *72*, 5839–5842.

(37) Borbas, K. E.; Chandrashaker, V.; Muthiah, C.; Kee, H. L.; Holten, D.; Lindsey, J. S. *J. Org. Chem*. **2008**, *73*, 3145–3158.

(38) Muthiah, C.; Ptaszek, M.; Nguyen, T. M.; Flack, K. M.; Lindsey, J. S. *J. Org. Chem*. **2007**, *72*, 7736–7749.

(39) Muthiah, C.; Kee, H. L.; Diers, J. R.; Fan, D.; Ptaszek, M.; Bocian, D. F.; Holten, D.; Lindsey, J. S. *Photochem. Photobiol.* **2008**, *84*, 786–801.

(40) Ruzié, C.; Krayer, M.; Lindsey, J. S. *Org. Lett*. **2009**, *11*, 1761–1764.

(41) Muthiah, C.; Lahaye, D.; Taniguchi, M.; Ptaszek, M.; Lindsey, J. S. *J. Org. Chem*. **2009**, *74*, 3237–3247.

(42) Mass, O.; Ptaszek, M.; Taniguchi, M.; Diers, J. R.; Kee, H. L.; Bocian, D. F.; Holten, D.; Lindsey, J. S. *J. Org. Chem*. **2009**, *74*, 5276–5289.

(43) Ptaszek, M.; Lahaye, D.; Krayer, M.; Muthiah, C.; J. S. Lindsey, J. S. *J. Org. Chem*. **2010**, *75*, 1659–1673.

(44) Fischer, H.; Laubereau, O. *Justus Liebigs Ann*. **1938**, *535*, 17–37.

(45) Fischer, H.; Oestreicher, A. *Justus Liebigs Ann. Chem*. **1940**, *546*, 49–57.

(46) Fischer, H.; Siebel, H. *Justus Liebigs Ann. Chem*. **1932**, *499*, 84–108.

(47) Wolf, H. *Liebigs Ann. Chem.* **1966**, *695*, 98–111.

(48) Brockman, H. J.; Tackekarimdadian, R. *Liebigs Ann. Chem.* **1979**, 419–430.

(49) Lash, T. D.; Balasubramaniam, R. P.; Catarello, J. J.; Johnson M. C.; May, D. A.; Bladel, K. A.; Feeley, J. M.; Hoehner, M. C.; Marron, T. G.; Nguyen, T. H.; Perun, T. J.; Quizon, D. M.; Shiner, C. M.; Watson, A. *Energy&Fuels* **1990**, *4*, 668–674.

(50) Kosugi, M.; Sumiya, T.; Obara, Y.; Suzuki, M.; Sano, H.; Migita, T. *Bull. Chem. Soc. Jpn*. **1987**, *60*, 767–768.

(51) (a) Muratake, H.; Natsume, M. *Tetrahedron Lett*. **1997**, *38*, 7581–7582. (b) Muratake, H.; Natsume, M.; Nakai, H. *Tetrahedron* **2004**, *60*, 11783–11803.

(52) Brockman, H. J.; Bode, J. *Liebigs Ann. Chem.* **1974**, 1017–1027.

(53) Smith, K. M.; Goff, D. A. *J. Am. Chem. Soc.* **1985**, *107*, 4954–4964.

(54) Maruyama, K.; Yamada, H.; Osuka, A. *Chem. Lett.* **1989**, 833–836.

(55) Smith, N. W.; K. M. Smith, K. M. *Energy Fuels* **1990**, *4*, 675–688.

(56) Maruyama, K.; Yamada, H.; Osuka, A. *Photochem. Photobiol.* **1991**, *53*, 617–626.

(57) Abraham, R. J.; Rowan, A. E.; Smith, N. W.; Smith, K. M. *J. Chem. Soc., Perkin Trans.* **1993***, 2*, 1047–1059.

(58) Tamiaki, H.; Amakawa, M.; Shimono, Y.; Tanikaga, R.; Holzwarth, A. R.; Schaffner, K. *Photochem. Photobiol.* **1996**, *63*, 92–99.

(59) Pandey, R. K.; Constantine, S.; Tsuchida, T.; Zheng, G.; Medforth, C. J.; Aoudia, M.; Kozyrev, A. N.; Rodgers, M. A. J.; Kato, H.; Smith, K. M.; Dougherty, T. J. *J. Med. Chem.* **1997**, *40*, 2770–2779.

(60) Tamiaki, H.; Miyatake, T.; Tanikaga, R. *Tetrahedron Lett.* **1997**, *38*, 267–270.

(61) Mettath, S.; Shibata, M.; Alderfer, J. L.; Senge, M. O.; Smith, K. M.; Rein, R.; Dougherty, T. J.; Pandey, R. K. *J. Org. Chem.* **1998**, *63*, 1646–1656.

(62) Tamiaki, H.; Yagai, S.; Miyatake, T. *Bioorg. Med. Chem.* **1998**, *6*, 2171–2178.

(63) Katterle, M.; Holzwarth A. R.; Jesorka, A. *Eur. J. Org. Chem.* **2006**, 414–422.

(64) Miyatake, T.; Tanigawa, S.; Kato, S.; Tamiaki, H. *Tetrahedron Lett.* **2007**, *48*, 2251–2254.

(65) Hutchins, R. O.; Milewski, C. A.; Maryanoff, B. E. *J. Am. Chem. Soc.* **1973**, *95*, 3662–3668.

(66) Nair, V.; Sinhababu, A. K. *J. Org. Chem*. **1978**, *43*, 5013–5017.

(67) Srinivasan, N.; Haney, C. A.; Lindsey, J. S.; Zhang, W.; Chait, B. T. *J. Porphyrins Phthalocyanines* **1999**, *3*, 283–291.

(68) Li, F.; Gentemann, S.; Kalsbeck, W. A.; Seth, J.; Lindsey, J. S.; Holten, D.; Bocian, D. F. *J. Mater. Chem.* **1997**, *7*, 1245–1262.

(69) Kee, H. L.; Kirmaier, C.; Yu, L.; Thamyongkit, P.; Youngblood, W. J.; Calder, M. E.; Ramos, L.; Noll, B. C.; Bocian, D. F.; Scheidt, W. R.; Birge, R. R.; Lindsey, J. S.; Holten, D. *J. Phys. Chem*. *B* **2005**, *109*, 20433–20443.

(70) Zass, E.; Isenring, H. P.; Etter, R.; Eschenmoser, A. *Helv. Chim. Acta* **1980**, *63*, 1048–1067.

(71) Jones, I. D.; White, R. C.; Gibbs, E.; Denard, C. D. *J. Agric. Food Chem*. **1968**, *16*, 80–83.

(72) Yang, S. I.; Seth, J.; Strachan, J.-P.; Gentemann, S.; Kim, D.; Holten, D.; Lindsey, J. S.; Bocian, D. F. *J. Porphyrins and Phthalocyanines* **1999**, *3*, 117–147.

(73) Gradyushko, A. T.; Sevchenko, A. N.; Solovyov, K. N.; Tsvirko, M. P. *Photochem. Photobiol.* **1970**, *11*, 387–400.

(74) Seybold, P. G.; Gouterman, M. *J. Mol. Spectrosc.* **1969**, *31*, 1–13.

(75) Birks, J. B. In *Photophysics of Aromatic Molecules*; Wiley-Interscience: London, 1970, pp 140–192.

(76) Taniguchi, M.; Mass, O.; Boyle, P. D.; Tang, Q.; Diers, J. R.; Bocian, D. F.; Holten, D.; Lindsey, J. S. *J. Mol. Structure* **2010**, *979*, 27–45.

(77) Gouterman, M. In *The Porphyrins*; Dolphin, D.; Ed.; Academic Press: New York, 1978, vol. 3, pp 1–165.

(78) Gouterman, M. *J. Chem. Phys.* **1959**, *30*, 1139–1161.

(79) Gouterman, M. *J. Mol. Spectroscopy* **1961**, *6*, 138–163.

(80) Weber, G.; Teale, F. W. J. *Trans. Faraday Soc.* **1957**, *53*, 646–655.

(81) Except for molecular mechanics and semi-empirical models, the calculation methods used in Spartan have been documented in: Shao, Y.; Molnar, L. F.; Jung, Y.; Kussmann, J.; Ochsenfeld, C.; Brown, S. T.; Gilbert, A. T .B.; Slipchenko, L. V.; Levchenko, S.V.; O'Neill, D. P.; DiStasio, R. A., Jr.; Lochan, R. C.; Wang, T.; Beran,

G. J. O.; Besley, N. A.; Herbert, J. M.; Lin, C. Y.; Van Voorhis, T.; Chien, S. H.; Sodt, A.; Steele, R. P.; Rassolov, V. A.; Maslen, P. E.; Korambath, P. P.; Adamson, R. D.; Austin, B.; Baker, J.; Byrd, E. F. C.; Dachsel, H.; Doerksen, R. J.; Dreuw, A.; Dunietz, B. D.; Dutoi, A. D.; Furlani, T. R.; Gwaltney, S. R.; Heyden, A.; Hirata, S.; Hsu, C.-P.; Kedziora, G.; Khalliulin, R. Z.; Klunzinger, P.; Lee, A. M.; Lee, M. S.; Liang, W.-Z.; Lotan, I.; Nair, N.; Peters, B.; Proynov, E. I.; Pieniazek, P. A.; Rhee, Y. M.; Ritchie, J.; Rosta, E.; Sherrill, C. D.; Simmonett, A. C.; Subotnik, J. E.; Woodcock, H. L., III; Zhang, W.; Bell, A. T.; Chakraborty, A. K.; Chipman, D. M.; Keil, F. J.; Warshel, A.; Hehre, W. J.; Schaefer, H. F., III; Kong, J.; Krylov, A. I.; Gill, P. M. W.; Head-Gordon, M. *Phys. Chem. Chem. Phys.* **2006**, 8, 3172–3191.

(82) Mass, O.; Taniguchi, M.; Ptaszek, M.; Springer, J. W.; Faries, K. M.; Diers, J. R.; Bocian, D. F.; Holten, D.; Lindsey, J. S. *New J. Chem.* **2011**, *35,* 76–88.

CHAPTER IV

De novo Synthesis and Properties of Analogues of the Self-Assembling Chlorosomal Bacteriochlorophylls

IV.1. Introduction

The light-harvesting antennas in photosynthetic organisms contain highly organized, three dimensional systems of pigments that absorb light and funnel the resulting excitation energy to the reaction centers.[1] In plants and purple bacteria, photosynthetic pigments (chlorophylls and bacteriochlorophylls) are bound to protein scaffolds to elaborate the proper distance and orientation of each pigment to assure efficient energy transfer. On the other hand, in green photosynthetic bacteria, the tetrapyrrole macrocycles are organized in self-assembled structures (chlorosomes) with little or no aid from a proteinaceous scaffolding.[2,3] This highly organized system encompassing as many as 250,000 pigment molecules collects light and supports rapid excitation energy migration. Chlorosomes are perhaps Nature's most spectacular light-harvesting antennas and enable photosynthesis under conditions of low ambient light intensity.

It is important to note that the tetrapyrrole macrocycles in the chlorosomes are termed bacteriochlorophylls but in fact are chlorins (i.e., dihydroporphyrins) rather than true bacteriochlorins (i.e., tetrahydroporphyrins). The chlorosomal bacteriochlorophylls (bacteriochlorophylls *c*, *d*, and *e*) are structurally heterogeneous (i.e., not pure compounds) yet differ only slightly from the plant photosynthetic pigments chlorophylls *a* and *b* (Chart IV.1). Key structural differences include the presence of a mixture of stereoisomeric 3-(1-

hydroxyethyl) groups rather than the 3-vinyl unit; the absence of the 13^2-methoxycarbonyl substituent in the isocyclic ring; diverse substituents at the R^8, R^{12}, and propionate ester positions; and the presence of a methyl group at position 20 (Bchl *c* and *e*).[4]

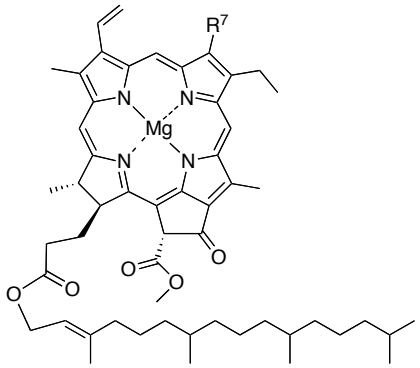

Plant chlorophylls

chlorophyll *a* ($R^7 = CH_3$)
chlorophyll *b* ($R^7 = CHO$)

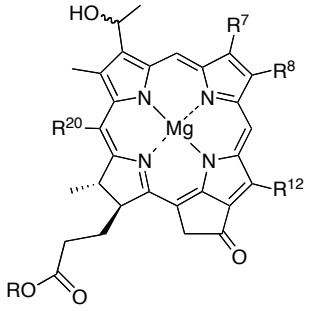

Chlorosomal bacteriochlorophylls

R = mixture of hydrocarbon chains
R^8 = Et, Pr, *iso*-Bu, neopentyl
R^{12} = Me, Et

bacteriochlorophyll *c* ($R^7 = R^{20} = CH_3$)
bacteriochlorophyll *d* ($R^7 = CH_3$, $R^{20} = H$)
bacteriochlorophyll *e* ($R^7 = CHO$, $R^{20} = CH_3$)

13^1-Oxophorbine

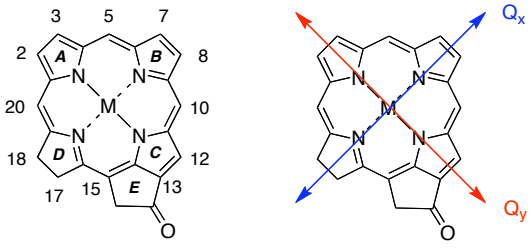

nomenclature *spectroscopic axes*

Chart IV.1. Chief pigments of plants (top) and green bacteria (middle). Nomenclature of 13^1-oxophorbine showing the reduced ring (D), isocyclic ring (E), and spectroscopic axes (bottom).

The structure of chlorosomes has been investigated by diverse methods including cryoelectron microscopy,[5-7] X-ray scattering,[5,7,8] absorption linear dichroism spectroscopy,[9] resonance Raman spectroscopy,[10] and solid-state NMR spectroscopy.[8,11,12] The pattern of self-assembly of chlorosomal bacteriochlorophyll molecules – which may differ across diverse organisms – remains a subject of intense debate. One of the longstanding models proposed for the self-assembled architecture is illustrated in Figure IV.1.[13] In the proposed model, the hydroxyl oxygen of one macrocycle coordinates to the apical Mg(II) site of a second macrocycle, and the hydroxyl proton forms a hydrogen bond with the carbonyl oxygen from a third macrocycle. The resulting two-dimensional lattice results in π–π interactions between the chlorin macrocycles, which additionally stabilize the self-assembled system. The organization shown in Figure IV.1, which implies long-range order of crystal-like periodicity, likely represents an idealized limiting form given the heterogeneity of the bacteriochlorophylls themselves. Several alternative models have recently been proposed that retain key features of apical coordination (and typically hydrogen bonding) yet pack the macrocycles in other patterns.[12,14,15] Structural issues that remain poorly understood include the fundamental assembly pattern of the tetrapyrrole macrocycles; the role and effect of length of diverse long-chain alcohols incorporated to form the ester at the 17-propionate position;[7] the effects of stereoisomeric mixtures derived from the presence of *R/S* epimers of the 3-(1-hydroxyethyl substituent);[16] and the size, internal regularity, and relative orientations of self-assembled domains of bacteriochlorophylls within the chlorosome.[7]

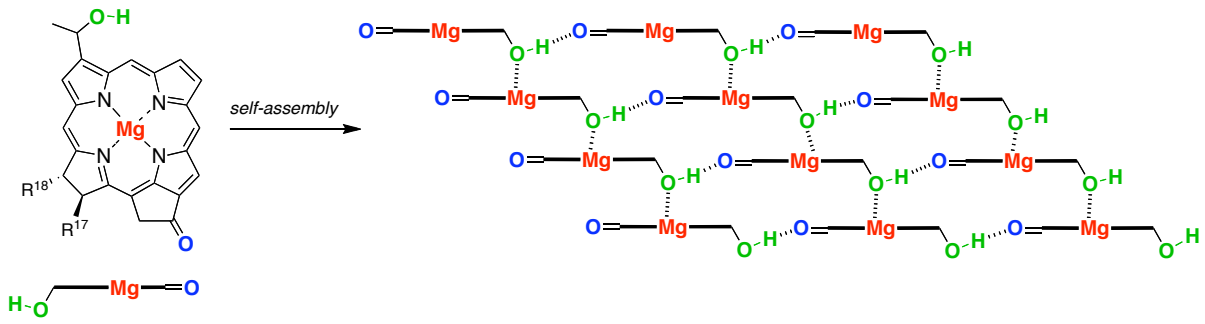

Figure IV.1. One model for the assembly pattern of chlorosomal bacteriochlorophylls, showing coordination of the hydroxyl group to the apical site on magnesium, hydrogen bonding, and π–π stacking.

The complexity and size of the chlorosomes has prompted a large body of synthetic and structural work on synthetic macrocycles to determine the essential features necessary to induce self-assembly.[13,17-19] The groups of Tamiaki[13,18,20-25] and Würthner[26-29] extensively investigated semisynthetic chlorophyll and bacteriochlorophyll derivatives to probe the influence of the nature and position of substituents on the self-assembly pattern. Balaban[13,14,16,17,19,30-34] explored synthetic porphyrins bearing oxygenic (hydroxyalkyl and keto groups, **IV-A**, Chart IV.2) at the meso or β-positions, as well as cyano substituents (**IV-B**). Balaban also prepared chlorins by derivatization of porphyrins (**IV-H**).[17] Tamiaki also developed methodology for converting octaethylporphyrin to porphyrin-based chlorosomal bacteriochlorophyll mimics (**IV-C** – **IV-F**).[35] Almost all studies to date of wholly synthetic macrocycles have employed zinc(II) porphyrins, though a recent study of magnesium(II) porphyrins (analogues of **IV-A**) was reported.[36] We synthesized porphyrin derivatives with two oxygenic substituents at the meso or β-positions (**IV-G**).[37] However, X-ray structural studies of **IV-G** (5-hydroxymethyl and 5,15-diphenyl; 3-hydroxymethyl- and 5,15-di-*p*-tolyl)

revealed intermolecular interactions and packing patterns quite different from those suggested in Figure IV.1. Balaban has reported similar results.[14,16] At a minimum, such results point to the subtlety of structural features that engender assembly.

Construction of structural and functional mimics of the chlorosomes requires access to model compounds that possess essential structural features of the natural bacteriochlorophylls *c*, *d* and *e*. The minimum structural features appear to include an α-hydroxyalkyl group and carbonyl group at the perimeter of a metallochlorin. In the chlorosome neighboring tetrapyrrole macrocycles are believed to be oriented such that their respective Q_y transition dipole moments are close to collinear, thereby affording strong exciton coupling. Because porphyrins are planar oscillators whereas chlorins are linear oscillators,[38,39] it does not appear feasible to mimic the photophysical features of the chlorosome with porphyrins alone, though valuable insights concerning the structural requirements for assembly undoubtedly can be gleaned by examination of diverse tetrapyrrole macrocycles.

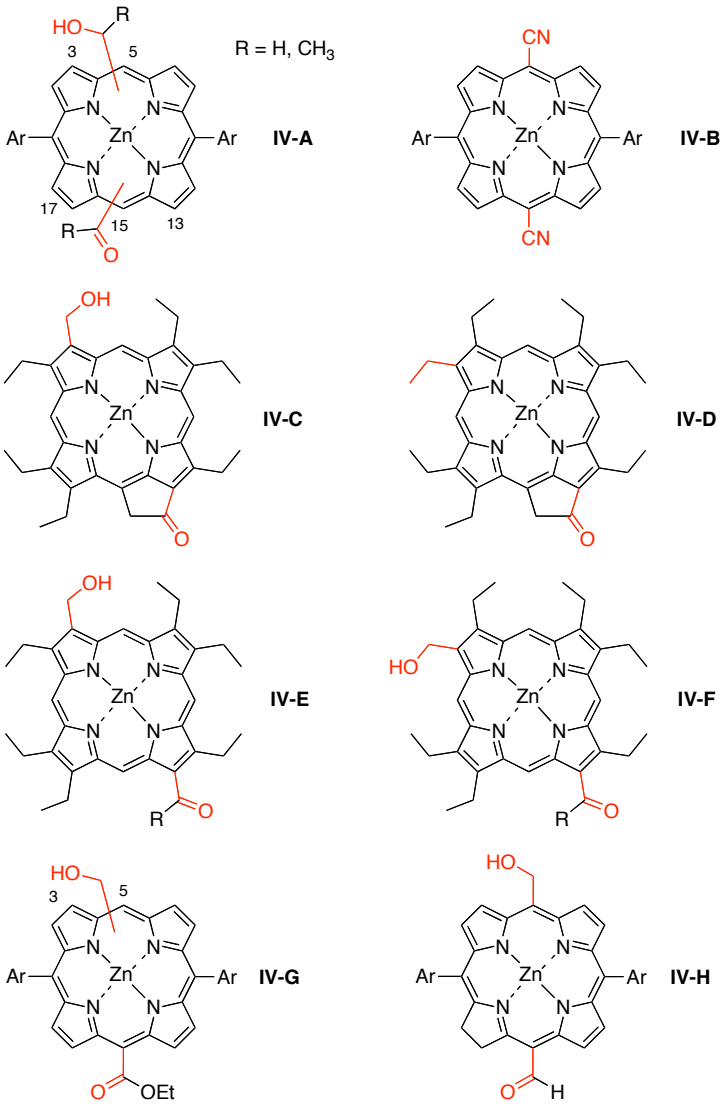

Chart IV.2. Synthetic porphyrin and chlorin mimics of chlorosomal bacteriochlorophylls.

Over the years we have been working to develop de novo synthetic methods for preparing chlorins (a part of these studies is reported in Chapters II and III). A key feature of the de novo methods is the ability to introduce substituents at will at the various β-pyrrolic and meso positions, and to install the 5-membered isocyclic ring (ring E, spanning positions

13 and 15).[40-45] Chlorins that contain the isocyclic ring are termed phorbines,[46] which is the hydrocarbon skeleton for all naturally occurring chlorophylls (including the chlorosomal bacteriochlorophylls).[4] Herein we report extension of this methodology to the synthesis of mimics of chlorosomal bacteriochlorophylls. The resulting mimics are equipped with the structural features that are believed to be essential for self-assembly: (i) central metal with apical ligation site, (ii) coplanar keto group, and (iii) α-hydroxyethyl group, with the latter two substituents disposed on opposite sites of the macrocycle. For appropriate electronic coupling to give rise to efficient energy transfer, as in the natural systems, the α-hydroxyethyl and 13-keto groups are positioned along the Q_y axis. Three such 13^1-oxophorbines have been prepared, which differ only in the nature of a substituent (phenyl, mesityl, or pentafluorophenyl) at the 10-position. For comparison purposes, a chlorin was prepared that contains a coplanar keto group and an α-hydroxyethyl group located along the Q_x axis, which is perpendicular to the Q_y axis. This de novo approach to the synthesis of chlorin/13^1-oxophorbine macrocycles complements the existing strategies for the semisynthesis of naturally derived tetrapyrroles and the chemical synthesis of porphyrins.

A portion of the results presented in this chapter stemmed from a team effort including Dinesh R. Pandithavidana, Marcin Ptaszek and Koraliz Santiago; photochemical studies were accomplished by Joseph W. Springer, Jieying Jiao, Qun Tang, and Christine Kirmaier.

IV.2. Results and Discussion

IV.2.1. Synthesis of 13^1-Oxophorbines

A. Retrosynthetic Analysis. Our approach to chlorosomal bacteriochlorophyll analogues relies on a de novo route to 3,13-dibromochlorins.[40] The route entails the directed formation of the chlorin macrocycle by reaction of an Eastern half and a Western half. Extension therefrom to the key precursor 3-acetyl-13^1-oxophorbine **FbOP-A^{3}R^{10}** includes (a) palladium-mediated acetylation of a 3,13-dibromochlorin (**FbC-Br^{3,13}R^{10}**),[40] (b) selective 15-bromination (under acidic conditions) of the resulting 3,13-diacetylchlorin,[44] and (c) installation of the isocyclic ring by palladium-mediated, intramolecular α-arylation.[41] The resulting 13^1-oxophorbine possesses two keto groups, one embedded in the isocyclic ring and the second as the 3-acetyl substituent. Selective reduction of the carbonyl group at the 3-position of the chlorin will afford the target 3-(1-hydroxyethyl)-13^1-oxophorbine **FbOP-He^{3}R^{10}**.

B. Chlorins FbC-Br^{3,13}R^{10}. The requisite Western half (8-bromo-2,3,4,5-tetrahydro-1,3,3-trimethyldipyrrin, **II-6**) for the syntheses of the target 13^1-oxophorbines has been prepared in multigram quantities.[47] The Eastern halves for the phenyl (**II-8-Br^{8,9}**, Chapter II) and mesityl (**II-8-Br^{8,9}**)[40] substituted target compounds also have been reported. The synthesis of the pentafluorophenyl substituted Eastern half (**IV-1-Br^{8,9}**) is shown in Scheme IV.1. Treatment of 1-formyl-5-(pentafluorophenyl)dipyrromethane[49] with two mol equiv of NBS at –78 °C afforded the corresponding 8,9-dibromo derivative **IV-1-Br^{8,9}**.

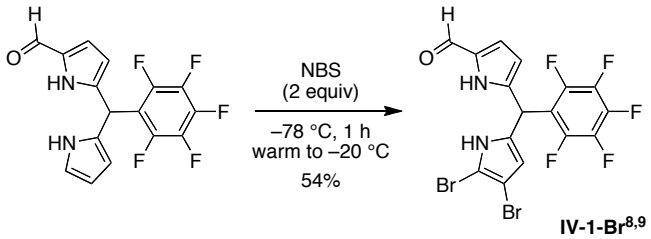

Scheme IV.1. Preparation of the Eastern half for the pentafluorophenyl-substituted 13[1]-oxophorbine.

The dibromochlorin **FbC-Br^{3,13}M^{10}** was recently prepared via a streamlined procedure[45] from 0.5 mmol quantities of 8-bromo-2,3,4,5-tetrahydro-1,3,3-trimethyldipyrrin (**II-6**, Western half)[47] and 8,9-dibromo-1-formyl-5-mesityldipyrromethane (**II-2-Br^{8,9}**, Eastern half).[40] Here, the same procedure at the 1.7 mmol scale afforded **FbC-Br^{3,13}M^{10}** in 24% yield (versus 25% previously) (Scheme IV.2). Dibromochlorin **FbC-Br^{3,13}P^{10}** or **FbC-Br^{3,13}Pf^{10}** bearing a 10-phenyl or 10-(pentafluorophenyl) substituent was synthesized in the same manner in 29% or 9% yield, respectively. It is noteworthy that the three dibromochlorins were prepared in 0.13–0.53-g quantities, facilitating subsequent elaboration.

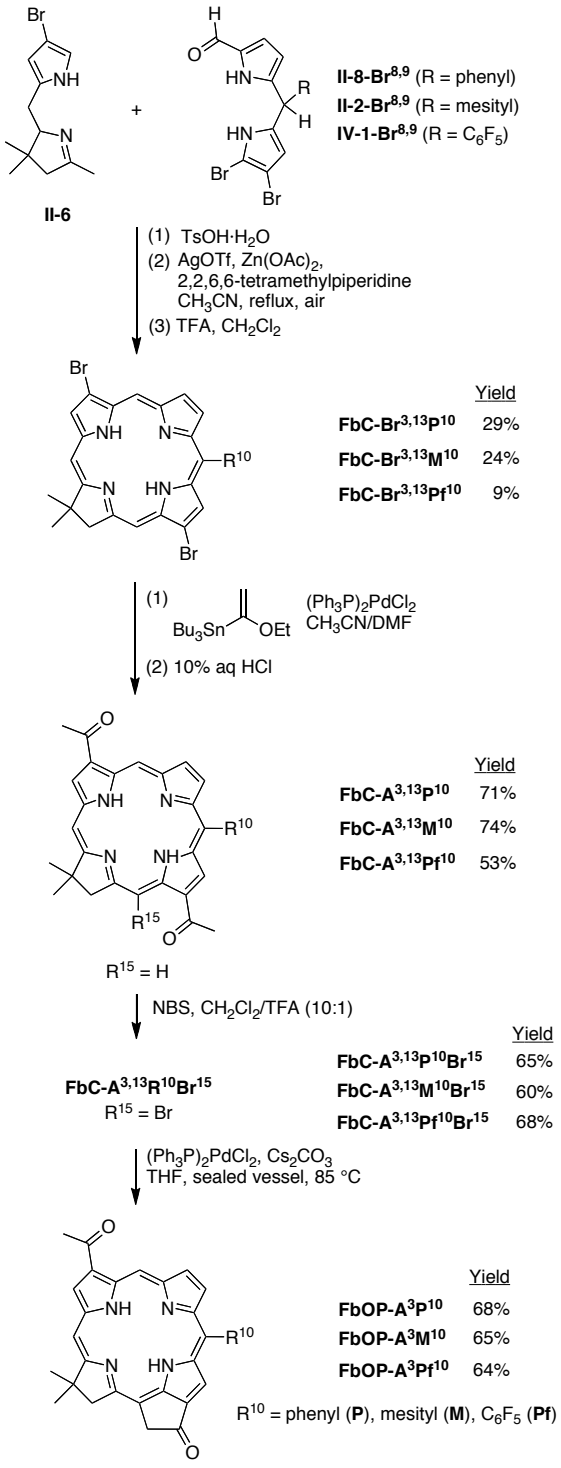

Scheme IV.2. Synthesis of 3-acetyl-13^1-oxophorbine compounds.

C. 3,13-Diacetylchlorins. The Pd-coupling of dibromochlorin **FbC-Br^{3,13}R^{10}** employed five mol equiv of tributyl(1-ethoxyvinyl)tin[41] in the presence of 20 mol% of $(Ph_3P)_2PdCl_2$ in CH_3CN/DMF (3:2) at 83 °C for 3.5 – 4 h. Hydrolysis with 10% aqueous HCl and purification of the crude product gave 3,13-diacetylchlorin **FbC-A^{3,13}R^{10}** (53–74% yield). Note that the free base 3,13-diacetylchlorin **FbC-A^{3,13}M^{10}** was previously prepared from the zinc chelate **ZnC-A^{3,13}M^{10}** via demetalation,[42] and the latter was obtained from the zinc chelate of the dibromochlorin **ZnC-Br^{3,13}M^{10}** via a multistep procedure that includes demetalation, Pd-coupling, acidic work up, and remetalation.[40]

D. Synthesis of 3-Acetyl-13^1-oxophorbines. Installation of the isocyclic ring on the free base 3,13-diacetylchlorin **FbC-A^{3,13}R^{10}** was achieved by intramolecular ring closure of the 13-acetyl group and the 15-position of the chlorin macrocycle. The 15-bromo analogue of the 3,13-diacetylchlorin was synthesized using a selective bromination strategy.[44] The conditions of selective bromination were studied with **FbC-A^{3,13}M^{10}**. Thus, treatment of **FbC-A^{3,13}M^{10}** with 1 mol equiv of NBS in CH_2Cl_2/TFA (10:1) resulted in incomplete reaction, affording a ~2:1 ratio of starting material/**FbC-A^{3,13}M^{10}Br^{15}**. The mixture was not readily separable by column chromatography. Prolonged reaction or higher temperature (50 °C, 1,2-dichloroethane/TFA mixture) did not improve the outcome. The stepwise treatment of **FbC-A^{3,13}M^{10}** with 1.3 mol equiv of NBS in CH_2Cl_2/TFA (10:1) at room temperature provided complete consumption of the starting material and also yielded 30% of dibrominated side product (according to the ^{1}H NMR spectrum of the crude mixture). Analogous bromination of **FbC-A^{3,13}P^{10}** and **FbC-A^{3,13}Pf^{10}** afforded **FbC-A^{3,13}P^{10}Br^{15}** and

FbC-A^{3,13}Pf^{10}Br^{15}, respectively (Scheme IV.2). With the 15-bromo-13-acetylchlorins in hand, intramolecular ring closure[41] upon treatment with $(Ph_3P)_2PdCl_2$ (20 mol%) in the presence of 5–6 mol equiv of Cs_2CO_3 in THF at 85 °C in a sealed Schlenk flask for 4 h gave in 64–68% yield the desired 3-acetyl-13^1-oxophorbines **FbOP-A^{3}R^{10}**.

E. Reduction of the 3-Acetyl Group. The selective reduction of the 3-acetyl group of oxophorbine **FbOP-A^{3}M^{10}** to give the macrocycle containing the 3-α-hydroxyethyl moiety (**FbOP-He^{3}M^{10}**) is shown in Scheme II.3. Several methods have been described for the reduction (using $NaBH_4$,[24] $BH_3 \cdot THF$,[20] $BH_3 \cdot Me_2S$,[20] $BH_3 \cdot {}^t BuNH_2$,[25] and $BH_3 \cdot PhNEt_2$)[20] of the 3-acetyl group in chlorophylls and their derivatives. We examined a number of such reductants under various conditions to achieve selective reduction of the 3-acetyl moiety (Table IV.1).

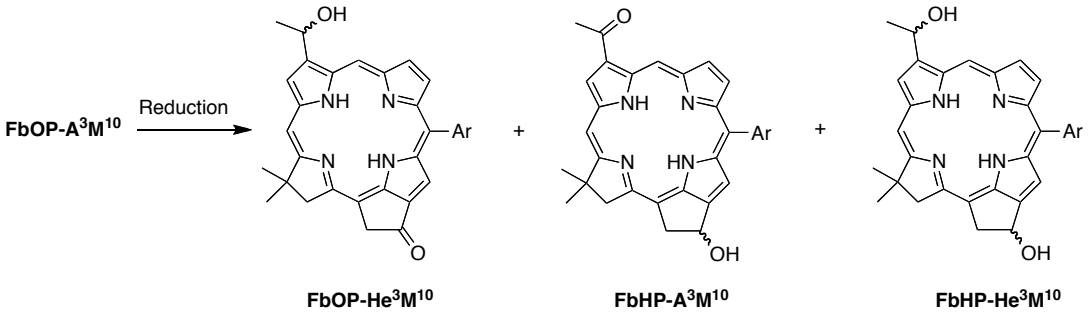

Scheme IV.3. Reduction to form a free base 3-(1-hydroxyethyl)-13^1-oxophorbine.

Table IV.1. Reduction of **FbOP-A^{3}M^{10}**.

Entry	Reductant	Solvent	Temp.	Product(s)
1	$NaBH_4$, excess	THF/MeOH	RT	**FbHP-He^{3}M^{10}**
2	$NaBH_4$, excess	THF/MeOH	–78 °C	no reaction
3	$NaBH_4$, excess	THF/MeOH	–20 to 0 °C	**FbOP-He^{3}M^{10}** + **FbHP-A^{3}M^{10}** + **FbHP-He^{3}M^{10}** (~ 1:1:1)
4	BH_3·THF	THF	0 °C	**FbOP-He^{3}M^{10}** (42%)[a]
5	BH_3·^{t}BuNH$_2$	$CHCl_3$	RT	**FbOP-He^{3}M^{10}** (77%)[a]

[a]Isolated yield.

Treatment of **FbOP-A^{3}M^{10}** with excess $NaBH_4$ in THF/MeOH (10:1) at room temperature resulted in fast reduction of both keto groups to produce the corresponding diol **FbHP-He^{3}M^{10}** (Table IV.1, entry 1). Reaction of **FbOP-A^{3}M^{10}** with $NaBH_4$ did not proceed at –78 °C (entry 2) whereas at –20 °C to 0 °C (entry 3) a mixture of three products was obtained: expected **FbOP-He^{3}M^{10}** (presumably as a racemic mixture), 13^1-hydroxyphorbine **FbHP-A^{3}M^{10}** (presumably as a racemic mixture) and 3,13^1-dihydroxyphorbine **FbHP-**

He^{3}M^{10} (presumably as a mixture of diastereomers). The expected product could be separated by column chromatography; however, it was difficult to obtain fully reproducible results, presumably due to the inaccuracy in temperature control and the relative amount of sodium borohydride employed in these vigorous, small-scale reactions. Stepwise treatment of **FbOP-A^{3}M^{10}** with 2 mol equiv of a 1 M solution of BH_3·THF in THF at 0 °C (entry 4) provided the expected **FbOP-He^{3}M^{10}** as the major product in 42% isolated yield, together with small amounts of **FbHP-A^{3}M^{10}** and **FbHP-He^{3}M^{10}**. The best selectivity upon reduction was achieved when **FbOP-A^{3}M^{10}** was treated with 6 mol equiv of BH_3·^{t}BuNH$_2$ in anhydrous $CHCl_3$ at room temperature for 4.5 h (entry 5). Quenching the reaction mixture with 5% aqueous HCl and stirring for 20 minutes followed by organic extraction and column chromatography [silica, CH_2Cl_2, then CH_2Cl_2/ethyl acetate (9:1)] gave **FbOP-He^{3}M^{10}** in 77% isolated yield; the side products 3-acetyl-13^1-hydroxyphorbine **FbHP-A^{3}M^{10}** (10% yield) and diastereomers of 3,13^1-dihydroxyphorbine **FbHP-He^{3}M^{10}** (3% and 5% yield) also were isolated. The workup procedure proved critical to obtain the desired product: attempted quenching of the reaction with saturated aqueous NH_4Cl followed by the same workup described above resulted in full reduction of **FbOP-A^{3}M^{10}** to a diastereomeric mixture of 3,13^1-dihydroxyphorbine **FbHP-He^{3}M^{10}** (presumably because the excess BH_3·^{t}BuNH$_2$ was not removed completely). Application of the best conditions (6 mol equiv of BH_3·^{t}BuNH$_2$ in $CHCl_3$) to oxophorbines **FbOP-A^{3}P^{10}** and **FbOP-A^{3}Pf^{10}** afforded the corresponding free base analogues of the chlorosomal bacteriochlorophyll mimics **FbOP-He^{3}P^{10}** and **FbOP-He^{3}Pf^{10}** in 72% and 55% yield respectively (Chart IV.3).

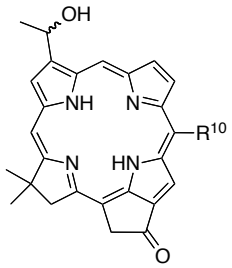

FbOP-He^{3}P^{10}
(R^{10} = phenyl, 72% yield)

FbOP-He^{3}Pf^{10}
(R^{10} = C_6F_5, 55% yield)

Chart IV.3. Free base 3-(1-hydroxyethyl)-13^1-oxophorbines with various R^{10} substituents.

F. Zinc Insertion. Metalation of each of the three hydroxyethyl–oxophorbines (**FbOP-He^{3}R^{10}**) with 15 mol equiv of zinc acetate in $CHCl_3$/MeOH afforded the corresponding zinc(II) chelate. Thus, **ZnOP-He^{3}P^{10}**, **ZnOP-He^{3}M^{10}** and **ZnOP-He^{3}Pf^{10}** were obtained in good yield (Chart IV.4). The zinc chelates (**ZnOP-He^{3}R^{10}**) are unstable in solution, especially in chlorinated solvents (CH_2Cl_2, $CHCl_3$) resulting in demetalation and decomposition. Compound **ZnOP-He^{3}Pf^{10}** turned out to be poorly soluble in organic solvents (CH_2Cl_2, THF, ethyl acetate, MeOH, DMF), and hence the failure to obtain a ^{1}H NMR spectrum. For spectroscopic studies, the 3-acetyl-10-phenyl-13^1-oxophorbine **FbOP-A^{3}P^{10}** also was converted to the zinc chelate **ZnOP-A^{3}P^{10}**.

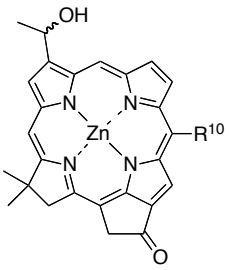

ZnOP-He^{3}P^{10}
(R^{10} = phenyl, 80% yield)

ZnOP-He^{3}M^{10}
(R^{10} = mesityl, 70% yield)

ZnOP-He^{3}Pf^{10}
(R^{10} = C_6F_5, 80% yield)

Chart IV.4. Target zinc(II) 3-(1-hydroxethyl)-13^1-oxophorbines.

IV.2.2. Synthesis of a 7-Substituted Oxochlorin

A. Selective Bromination of Oxochlorins. Chlorins that contain a keto group integral to the reduced ring (ring D) are known as oxochlorins. Oxochlorins exhibit greater redox stability than chlorins.[50] Retrosynthetic analysis of a chlorosomal bacteriochlorophyll analogue built around a 17-oxochlorin macrocycle relies on: (1) regioselective bromination at the 7-position of the macrocycle; (2) selective reduction of the 7-acetyl group in the presence of the 17-keto group. Results concerning the interplay of electronic and steric factors in dictating the regioselectivity of bromination warrant mention as a preface to the studies described below. First, bromination of the chlorin **FbC** (which bears no substituents other than the 18,18-dimethyl group) with 1 mol equiv of NBS at room temperature proceeds selectively at the 15-position given the hindrance of the 20-position owing to the 18,18-dimethyl group, while the second preferable sites of bromination are carbons 7 and 8 in equal extent (Chart IV.5).[44] Second, the presence of aryl groups at the 10- and 15-positions (e.g., **FbC-M^{10}P^{15}**) results in preference for bromination at the 7-position.[43] Third, the zinc chelate of a 5,10-diaryloxochlorin (e.g., **OxoFbC-Ar^{5,10}**) undergoes bromination selectively at the 20-position.[51] Fourth, the 20-position is >6-times more reactive than the 15-position in a fully unsubstituted oxochlorin (**OxoFbC**) toward electrophilic deuteration.[52] Here, we investigated bromination of both the zinc chelate and free base forms of a 10-phenyl-17-oxochlorin.

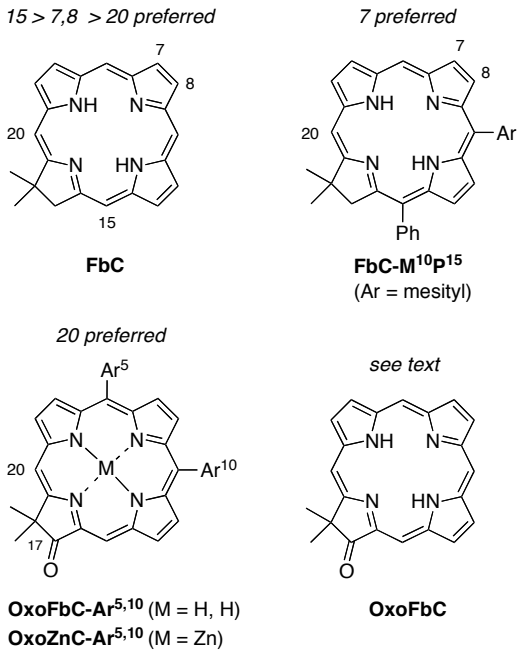

Chart IV.5. Preferred sites of bromination of chlorins and oxochlorins.

The 10-phenyl-17-oxochlorin (**OxoZnC-P^{10}**) was prepared in 52% yield from chlorin[53] **ZnC-P^{10}** via a two-step oxidation procedure[50] [basic alumina (activity I) in toluene at 60 °C, DDQ for 5 min at room temperature] (Scheme IV.4). Treatment of **OxoZnC-P^{10}** with one mol equiv of NBS in THF at room temperature gave a mixture of several brominated products that was not separable by column chromatography. Demetalation of the mixture with TFA in CH_2Cl_2 enabled separation of the free base products. The major product was identified by NOESY as **OxoFbC-P^{10}Br^{20}** rather than the desired 7-bromo derivative required for the target oxochlorin analogue of the chlorosomal bacteriochlorophylls. On the other hand, demetalation of **OxoZnC-P^{10}** with TFA followed by treatment of the resulting free base **OxoFbC-P^{10}** with 1 mol equiv of NBS in THF at

room temperature afforded the desired 7-bromo-17-oxochlorin **OxoFbC-Br^{7}P^{10}** in 58% yield (Scheme IV.4). The strong preference for 7- versus 8-substitution stems from shielding of the latter site by the 10-phenyl substituent.[43] The position of the bromo group in **OxoFbC-Br^{7}P^{10}** was established by NOESY. In summary, for the 10-phenyl-substituted macrocycles, the free base oxochlorin exhibits a bromination pattern (7 > 15, 20) that is distinct from that of the zinc oxochlorin (20 > 15, 7) and the free base chlorin (15 > 7 > 20).

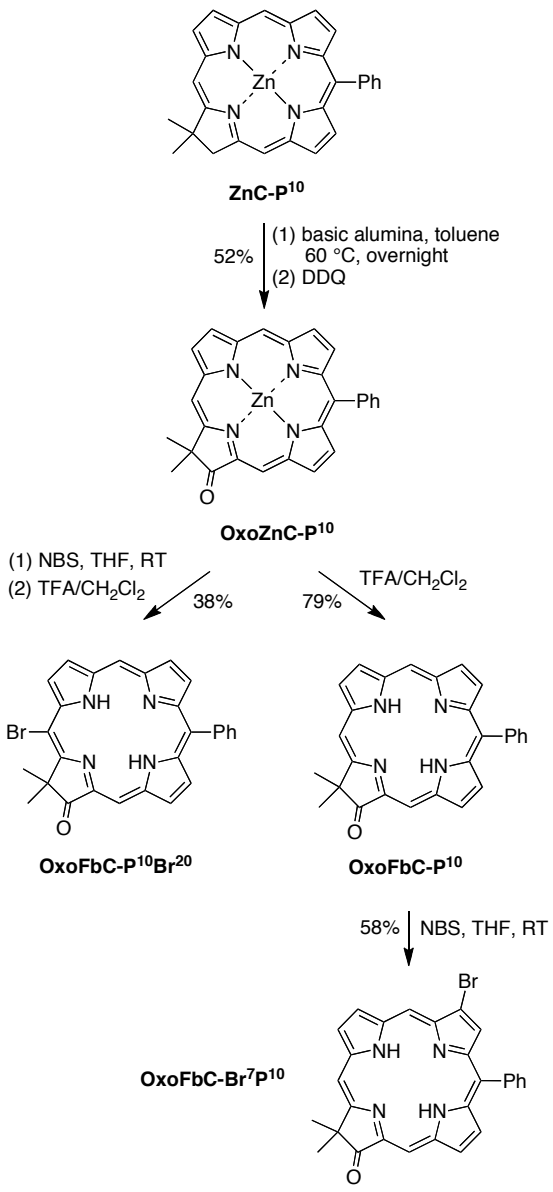

Scheme IV.4. Regioselective bromination of a 10-phenyl-17-oxochlorin.

B. Selective Reduction. The 7-acetyl group was introduced through palladium-coupling of **OxoFbC-Br^{7}P^{10}** with tributyl(1-ethoxyvinyl)tin[41] in the presence of 14 mol% of $(Ph_3P)PdCl_2$ in CH_3CN/DMF for 3 h at 85 °C followed by acidic hydrolysis to give 7-acetyl-

oxochlorin **OxoFbC-A^{7}P^{10}** in 55% yield (Scheme IV.5). The reduction of the 7-acetyl group of **OxoFbC-A^{7}P^{10}** was first examined under conditions used for selective reduction of the aforementioned 3-acetyl-13^{1}-oxophorbines, namely treatment of **OxoFbC-A^{7}P^{10}** with 6 mol equiv of $BH_3 \cdot {}^{t}BuNH_2$ in $CHCl_3$ at room temperature. The conditions afforded the 17-hydroxychlorin **FbC-A^{7}P^{10}HO^{17}** in 70% yield. The mixture of diastereomers (**FbC-He^{7}P^{10}HO^{17}**) was isolated as a trace byproduct, but no presence of the desired 7-(1-hydroxyethyl)-17-oxochlorin **OxoFbC-He^{7}P^{10}** was observed by TLC analysis and ^{1}H NMR spectroscopy. The decreased reactivity of the carbonyl group adjacent to the C_7=C_8 double bond was discussed previously by Tamiaki.[25] The C_7=C_8 double bond is relatively isolated from the chlorin 18π-electron aromatic system, which increases the conjugation of the carbonyl group. The presence of diastereomers of **FbC-He^{7}P^{10}HO^{17}** and the absence of **OxoFbC-He^{7}P^{10}** together indicate that the 7-acetyl group in **OxoFbC-A^{7}P^{10}** can be reduced with a stronger reductant, albeit sacrificing selectivity.

To overcome the problem of the reduction of the 7-acetyl group of **OxoFbC-A^{7}P^{10}**, the 17-keto group was protected (Scheme IV.6). Thus, following a procedure for ketalization,[54] **OxoFbC-Br^{7}P^{10}** was heated under reflux with ethylene glycol and $TsOH \cdot H_2O$ in toluene for 20 h to afford **OxoFbC′-Br^{7}P^{10}** in 46% yield. Subsequent Pd-mediated acetylation in the manner described for **OxoFbC-A^{7}P^{10}** afforded **OxoFbC′-A^{7}P^{10}** (84% yield), which upon treatment with excess $NaBH_4$ in THF at room temperature afforded **OxoFbC′-He^{7}P^{10}** in 71% yield. Deprotection using reported conditions with some modifications[55] (10% aqueous HCl in THF at room temperature for 1.5 days) gave the

desired **OxoFbC-He^{7}P^{10}** in 50% yield. The oxochlorin **OxoFbC-He^{7}P^{10}** was metalated with $Zn(OAc)_2 \cdot 2H_2O$ to afford **OxoZnC-He^{7}P^{10}** in 70% yield.

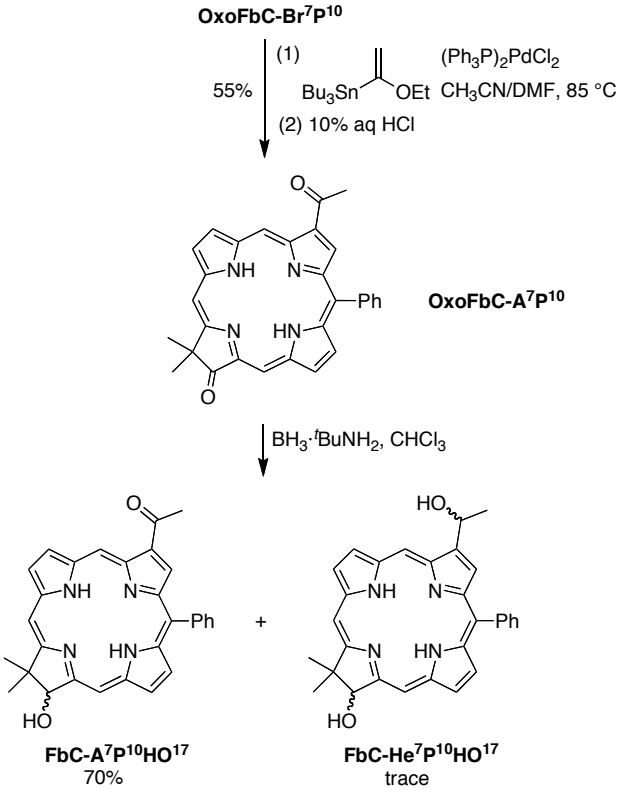

Scheme IV.5. Reduction of a 7-acetyl-10-phenyl-17-oxochlorin.

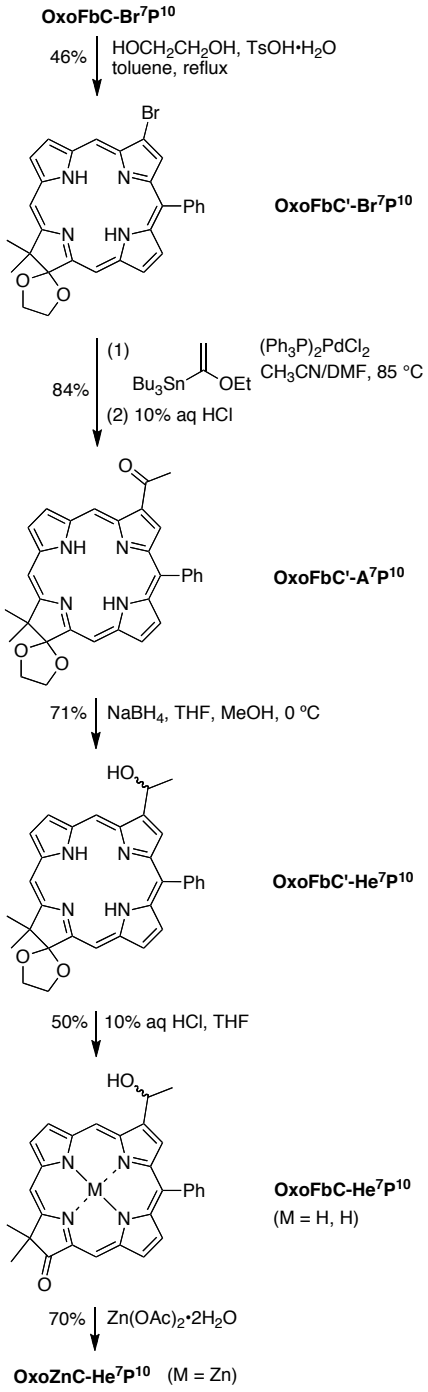

Scheme IV.6. Formation of the target 7-(1-hydroxyethyl)-17-oxochlorin.

IV.2.3. Chemical Characterization.

Altogether, 30 new macrocycles (chlorin, oxochlorin, oxophorbine and derivatives thereof) were prepared and 4 macrocyclic byproducts were isolated. Each macrocycle was characterized by low-resolution (LD-MS) and high-resolution (ESI-MS) mass spectrometry, and by UV-Vis absorption spectroscopy. Each macrocycle also was characterized by ^{1}H NMR spectroscopy, with the exception of **ZnOP-He^{3}Pf^{10}**, for which a solvent that afforded sufficient solubility was not identified. The hydroxyethyl proton was not observed for any of the mesityl-substituted chlorosomal mimics. ^{13}C NMR spectroscopy was attempted in a number of cases; in many cases satisfactory spectra were obtained whereas in other cases only a subset of the expected set of signals was observed. Such cases have been noted in the Experimental section.

The synthetic oxophorbine bearing the 10-mesityl group (**ZnOP-He^{3}M^{10}**) was characterized by the aforementioned set of techniques as well as by ^{13}C NMR and NOESY methods. The ^{1}H NMR spectrum of **ZnOP-He^{3}M^{10}** exhibits a doublet at δ = 2.04 ppm, attributed to the protons from the CH_3 unit of the 3-(1-hydroxyethyl) group, as well as a multiplet at δ = 6.15–6.70 ppm, attributed to the proton from the CH unit of the same substituent. The NOESY spectrum exhibited the characteristic NOE between the CH in the 1-hydroxyethyl substituent and aromatic proton at the 2-position of the macrocycle.

In general, the three other target macrocycles with the requisite structural features for self-assembly (zinc(II) chelate and apposite keto and 1-hydroxyethyl groups) proved difficult to fully characterize by NMR methods. (i) The free base analogue of the 10-phenyl

substituted oxophorbine (**FbOP-He^{3}P^{10}**) gave a satisfactory ^{1}H and ^{13}C NMR spectra, whereas the zinc chelate was only characterized by ^{1}H NMR spectroscopy. (ii) The free base analogue of the immediate precursor to the 10-(pentafluorophenyl) substituted oxophorbine (**FbOP-A^{3}Pf^{10}**) gave a satisfactory ^{1}H and ^{13}C NMR spectra, whereas the zinc chelate target compound (**ZnOP-He^{3}Pf^{10}**) was quite insoluble and was not characterized by any form of NMR spectroscopy. (iii) The zinc chelate target compound (**OxoZnC-He^{7}P^{10}**) was only characterized by ^{1}H NMR spectroscopy. Regardless of the lack of NMR spectroscopic characterization, the mass spectra were as expected throughout the series of compounds that constitute each synthetic pathway.

IV.2.4. Photophysical Properties.

The electronic absorption spectra of representative free base oxophorbines are shown in Figure IV.2. Reduction of the acetyl group results in a significant hypsochromic shift of the Q_y band (603 cm^{-1}, λ_{max} = 656 nm for **FbOP-He^{3}M^{10}** versus 683 nm for **FbOP-A^{3}M^{10}**). The position of the wavelength maximum and the relative intensity of the Q_y and B_x bands in **FbOP-He^{3}M^{10}** are similar to those reported for 3-unsubstituted **FbOP-M^{10}**.[44] The Q_y band maximum in isomeric **FbHP-A^{3}M^{10}** appears at 662 nm and has a lower relative intensity. The spectral band positions and band intensity ratios are summarized in Table IV.2.

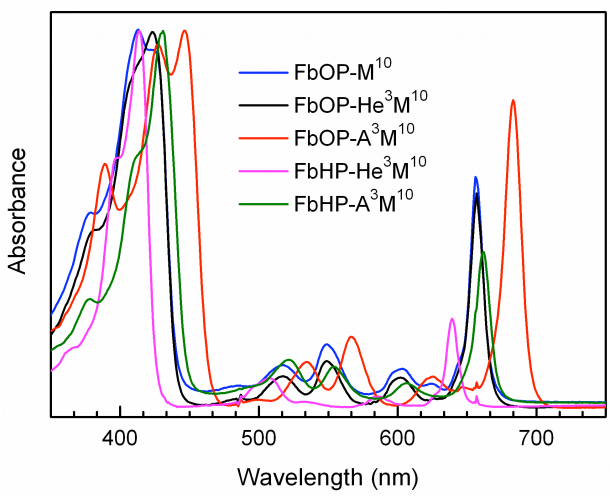

Figure IV.2. Absorption spectra (normalized at the B bands) in toluene at room temperature of free base species including the 3-alkylphorbine **FbHP-He^{3}M^{10}** (magenta), the 3-alkyl-13^1-oxophorbine **FbOP-He^{3}M^{10}** (black), the 3-unsubstituted 13^1-oxophorbine **FbOP-M^{10}** (blue), the 3-acetylphorbine **FbHP-A^{3}M^{10}** (green) and the 3-acetyl-13^1-oxophorbine **FbOP-A^{3}M^{10}** (red).

The fluorescence yield and singlet excited-state lifetimes for the target zinc oxophorbines **ZnOP-He^{3}M^{10}**, **ZnOP-He^{3}P^{10}** and **ZnOP-He^{3}Pf^{10}**, the corresponding free base oxophorbines **FbOP-He^{3}M^{10}**, **FbOP-He^{3}P^{10}** and **FbOP-He^{3}Pf^{10}**, and of several analogues are listed in Table IV.2. The various zinc oxophorbines have similar fluorescence yields (0.23–0.30) and excited-state lifetimes (5.1–6.3 ns). The various free base oxophorbines have comparable fluorescence yields to each other (0.26–0.32) and to the zinc chelates, but longer excited-state lifetimes (9.9–13.0 ns). Note that the sets of zinc and free base oxophorbines each include the parent compound for which the only substituents are the geminal dimethyl groups (**ZnOP** and **FbOP**);[56] thus, the results indicate that the substituents at the 3- and 13-positions have little effect on these photophysical properties. Similarly,

replacement of the ring E keto group with a hydroxyl group gives compounds (**FbHP-A^{3}M^{10}** and **FbHP-He^{3}M^{10}**) that have photophysical properties comparable to the oxophorbines (**FbOP-A^{3}M^{10}** and **FbOP-He^{3}M^{10}**).

Turning to the oxochlorins, the unsubstituted free base compound **OxoFbC** studied in Chapter III and used here as a benchmark has a fluorescence yield (0.12) that is 2.4-fold smaller than the average value for the free base oxophorbines (0.29) and a singlet excited-state lifetime (8.4 ns) that is only 1.4-fold shorter than the oxophorbine average (11.6 ns). On the other hand, zinc oxochlorin **OxoZnC-He^{7}P^{10}**, and the parent **OxoZnC** studied in Chapter III, have an average fluorescence yield (0.031) and excited-state lifetime (0.84) that are both about 7-fold smaller than those for the zinc oxophorbines (Table IV.2). The latter values are comparable to those reported previously for 5,10-substituted zinc oxochlorins.[50,57]

Table IV.2. Photophysical properties.[a]

Compound	B_{max} (nm)	$Q_y(0,0)$ abs (nm)	$Q_y(0,0)$ emis (nm)	$\frac{I_B}{I_{Q_y}}$ [b]	$\frac{\Sigma_B}{\Sigma_{Q_y}}$ [c]	Φ_f	τ_f (ns)
zinc chelates							
ZnOP-He^{3}M^{10}	426	642	644	1.9	2.4	0.24	5.7
ZnOP-He^{3}P^{10}	426	640	643	1.9	2.4	0.23	6.1
ZnOP-He^{3}Pf^{10}	426	648	653	1.7	2.7	0.25	5.7
ZnOP-A^{3}P^{10}	449	665	672	1.5	2.1	0.30	6.3
ZnOP [e]	419	637	639	1.6	2.4	0.23	5.1
OxoZnC-He^{7}P^{10}	419	609	612	4.8	4.2	0.032	0.86
OxoZnC [e]	411	602	602	3.4	4.3	0.030	0.82
free base cmpds							
FbOP-He^{3}M^{10}	423	657	660	1.9	4.3	0.30	12.3
FbOP-He^{3}P^{10}	423	656	659	2.0	4.8	0.29	12.0
FbOP-He^{3}Pf^{10}	422	663	667	1.9	4.4	0.27	9.9
FbOP-A^{3}M^{10}	446[f]	683	686	1.3	3.5	0.26	10.9
FbOP-A^{3}P^{10}	446[f]	682	686	1.3	4.2	0.28	10.5
FbOP-M^{10} [g]	413	656	659	1.7	4.4	0.32	13.0
FbOP [e]	408	654	656	1.5	4.1	0.30	11.5
OxoFbC [e]	400	634	636	4.6	11.1	0.12	8.4
FbHP-A^{3}M^{10}	430	661	664	3.2	6.3	0.32	10.5
FbHP-He^{3}M^{10}	413	639	641	4.4	8.0	0.35	10.7

[a]Data were acquired at room temperature for solutions in toluene, except for **ZnOP-He^{3}P^{10}**, **ZnOP-He^{3}Pf^{10}** and **ZnOP-A^{3}P^{10}**, which employed THF solutions. [b]Ratio of the peak intensities of the $Q_y(0,0)$ band to the Soret (B) maximum, which could be either the $B_y(0,0)$ or $B_x(0,0)$ band. [c]Ratio of the integrated intensities of the Q_y manifold [$Q_y(0,0)$, $Q_y(1,0)$] to the Soret manifold [$B_y(0,0)$, $B_y(1,0)$, $B_x(0,0)$, $B_x(1,0)$], for spectra plotted in cm^{-1}. [d]Comparable data are found in dilute solutions of the compound in THF and in toluene, with a small amount of assembly present in the latter case. [e]Previously studied in Chapter III. [f]Two peaks with comparable intensities are observed at 427 and 446 nm. [g]From ref. 44.

IV.2.5. Spectroscopic Studies on Self-Assembly of ZnOP-He^{3}M^{10}

A. Electronic Absorption Spectroscopy. The self-assembly of **ZnOP-He^{3}M^{10}** in solution was investigated using UV-vis absorption spectroscopy and a variety of solution and preparative conditions, all at room temperature. The parameters varied included concentration of the compound, solvent (toluene, THF, *n*-hexane/THF mixture, Triton X-100 micellar solutions) and use of sonication. Somewhat limiting cases are illustrated in Figure IV.3, which shows absorption spectra of **ZnOP-He^{3}M^{10}** in THF or in *n*-hexane containing 0.3% THF. The spectra have been normalized to have the same integrated area (oscillator strength) across the spectral region shown (to reflect the same total pigment content; see also below).

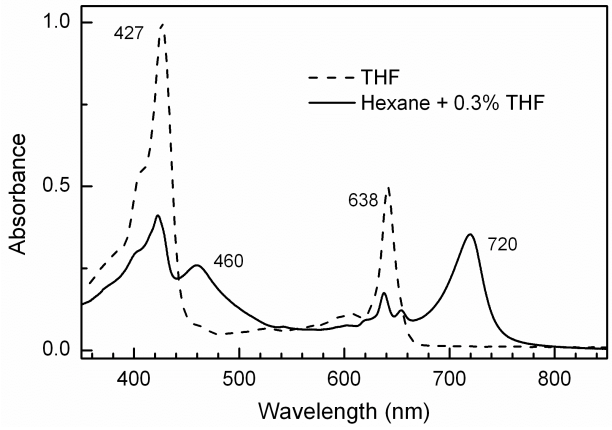

Figure IV.3. Absorption spectra at room temperature of 3-(1-hydroxyethyl)-13^1-oxophorbine **ZnOP-He^{3}M^{10}** in THF (solid) and in *n*-hexane containing 0.3% THF (dashed).

In THF solution, **ZnOP-He^{3}M^{10}** exhibits a strong, sharp Q_y band with maximum centered at 638 nm, characteristic for monomeric species. In *n*-hexane containing 0.3% THF

(v/v), the Q_y band is intense and broad, and shifts to 720 nm (a bathochromic shift of 82 nm, or 1785 cm^{-1}). The Soret (B) band similarly shifts from 427 to 460 nm (33 nm; 1680 cm^{-1}). Such spectral shifts, particularly that in the Q_y band, are characteristic for self-assembled natural[58] and semisynthetic[27,59] analogues of the chlorosomal bacteriochlorophylls in nonpolar solvents.

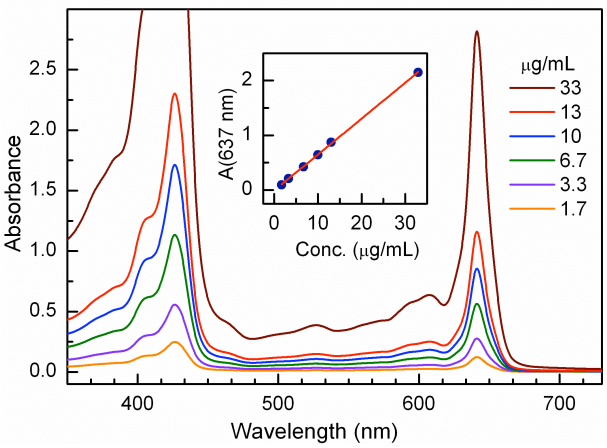

Figure IV.4. Absorption spectra as a function of concentration of **ZnOP-He^{3}M^{10}** in THF. The inset shows the absorbance at 637 nm as a function of concentration along with a linear fit. (Note that a 10 μg/mL solution of **ZnOP-He^{3}M^{10}** is 17 μM.)

The monomeric form and formation of the assemblies of **ZnOP-He^{3}M^{10}** were studied using a variety of conditions. Figure IV.4 shows spectra as a function of the concentration of this compound in THF, in which solvent coordination to the central zinc ion is expected to inhibit formation of the assembly. As expected, the spectra can be ascribed to the monomeric species throughout the concentration range studied; the absorbance at 637 nm depends linearly on **ZnOP-He^{3}M^{10}** concentration (Figure IV.4 inset). At the highest concentrations, which are far above those normally used for photophysical characterization

studies, the sample is highly absorbant and virtually opaque, yet remains a solution of the monomeric species.

As illustrated in Figure IV.3 (solid spectrum), the formation of assemblies (aggregates) is apparent for **ZnOP-He^{3}M^{10}** in *n*-hexane containing a small amount of THF to aid initial solubilization of the compound. Figure IV.5 shows absorption spectra for a 3.3 μg/mL (5.5 μM) solution as a function of the percentage of THF in the medium. With 7% THF the spectrum is that of the monomer and essentially equivalent to that in 100% THF. With 3.7% THF, the red-shifted absorption at 720 nm due to the assembly begins to be seen (Figure IV.5 inset). With 0.3% THF the monomer feature at ~640 nm is dramatically reduced as one would expect due to greater formation of the assembly; however, a proportionate rise in the intensity of the long-wavelength feature at 720 nm is not observed, and in fact a diminution is observed. (Similarly the absorption of the 1% THF solution is slightly smaller than with 2% THF.) These observations reflect the inhomogeneous nature of the solutions with low THF concentrations due to the large fraction of assemblies that precipitate from solution and thus do not contribute to the associated red-region absorption feature.

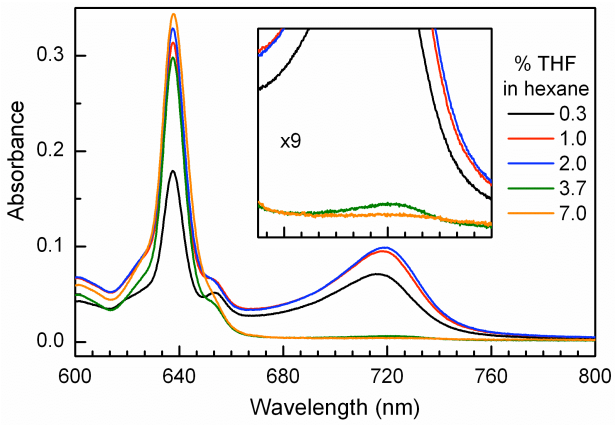

Figure IV.5. Absorption spectra of a 3.3 μg/mL (5.5 μM) solutions of **ZnOP-He^{3}M^{10}** as a function of %THF in n-hexane.

It was anticipated that the formation of the assemblies may depend on interplay between the amount of THF in the n-hexane solution and the concentration of the oxophorbine. To complement the %THF dependence depicted in Figure IV.5, a study was performed in which the concentration of **ZnOP-He^{3}M^{10}** was varied. The solvent consisted of *n*-hexane containing 3% THF, which is the approximate proportion at which the onset of formation of the assemblies was observed for a 3.3 μg/mL solution of **ZnOP-He^{3}M^{10}** (Figure IV.5). The results are shown in Figure IV.6, panel A.

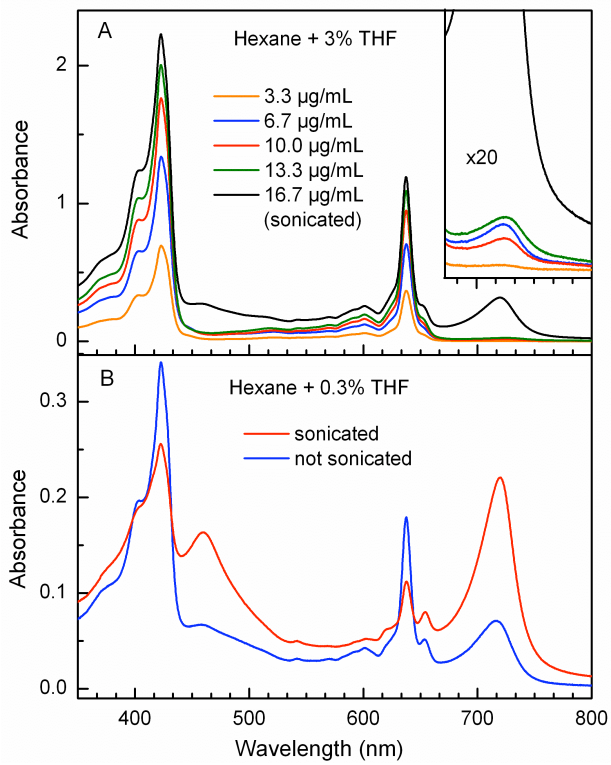

Figure IV.6. Absorption spectra of **ZnOP-He^{3}M^{10}** as a function of concentration in n-hexane containing 3% THF (A) and for two different preparations of a 3.3 µg/mL (5.5 µM) solution in *n*-hexane containing 0.3% THF with and without sonication (B).

The 3.3 µg/mL solution in Figure IV.6, panel A, is essentially the same as that observed in pure THF (Figure IV.3, blue) and ascribed to monomeric **ZnOP-He^{3}M^{10}**. Increasing concentrations (6.7 µg/mL and above) show the presence of assemblies as is evidenced by the absorption at 720 nm (Figure IV.6, panel A inset). However, quantitation of assembly formation on the basis of absorption in the red-region band is difficult. As noted above, the assemblies (aggregates) fall out of solution and adhere to the cuvette walls. The spectrum recorded depends on the extent of mixing upon preparation and the subsequent time to spectral acquisition. For example, the absorbance of the assembly at 720 nm (Figure IV.6,

panel A inset) for a 10 μg/mL solution (red) is less than that for a 6.7 μg/mL solution even though a larger amount of assemblies are produced in the former case, but fall out of solution. Figure IV.6B shows that assemblies (or some fraction of them) can be returned to solution via sonication, greatly enhancing the red-region feature. Due to such issues concerning quantitation (and comparisons), the spectrum of the monomeric species and that dominated by the assembly in Figure IV.3 are normalized to the same integrated intensity over the near-UV and near-IR regions to correspond to approximately the same total pigment content.

Several other points regarding the formation of assemblies of **ZnOP-He^{3}M^{10}** can be noted. The assemblies formed in n-hexane with a small amount of THF can be returned significantly (but typically not completely) to the monomeric form by dilution in the same solvent. The assemblies can be formed in aqueous Triton X-100 micellar solutions (the compound is insoluble in water alone). The extent of formation of the assemblies (as expected) depends on the concentration of the oxophorbine and the detergent; starting near the critical micelle concentration, appreciable assemblies are formed. Increasing the pigment concentration shifts the system towards assembly, while increasing the detergent concentration improves monomer solubility and shifts the system towards the monomeric form.

Zinc oxophorbine **ZnOP-He^{3}M^{10}** is also soluble in toluene to give solutions of the monomeric species. This point is illustrated in Figure IV.7 (dashed) for a 0.8 μg/mL (1.3 μM) solution. Upon increasing the concentration about 5-fold (Figure IV.7 solid), the formation of the assembly is apparent by the growth of the absorption at 720 nm relative to

the 638-nm Q_y band of the monomeric species (and by the sloping baseline due to assembly particulates in the solution). Thus, for **ZnOP-He^{3}M^{10}** the photophysical properties (fluorescence yields and excited-state lifetimes) of the monomeric species could be investigated in dilute toluene solutions, as is our standard protocol for synthetic chlorins and related macrocycles (Table IV.2).[42,56,57] The replacement of the 10-mesityl group with a phenyl group in **ZnOP-He^{3}P^{10}** affords a complex that is somewhat less soluble in toluene. This is evidenced for very dilute (~1 μM) solutions by the presence of a red-shifted feature similar to that found for **ZnOP-He^{3}M^{10}** in addition to pronounced features due to the monomeric form (data not shown). Incorporation of a 10-pentafluorophenyl group in **ZnOP-He^{3}Pf^{10}** affords a compound that is virtually insoluble in toluene and gives assemblies with little if any monomeric species even for very dilute (< 1 μM) solutions. On the other hand, the analogous zinc oxochlorin **OxoZnC-He^{7}P^{10}** is highly soluble in toluene. This compound remains in the monomeric form without the appearance of spectral manifestations (red shifted or broadened bands) or physical manifestations (precipitates, cloudy solutions) of aggregation at far higher concentrations than those at which **ZnOP-He^{3}M^{10}** or **ZnOP-He^{3}P^{10}** readily form assemblies.

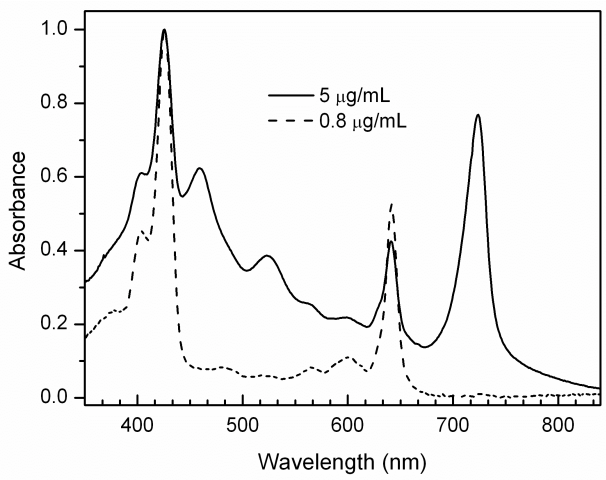

Figure IV.7. Absorption spectra of **ZnOP-He^{3}M^{10}** in toluene. The spectra are normalized at the Soret (B) maximum to facilitate comparisons.

The above-noted results indicate that the propensity for assembly formation increases in the following order **OxoZnC-He^{7}P^{10}** < **ZnOP-He^{3}M^{10}** < **ZnOP-He^{3}P^{10}** < **ZnOP-He^{3}Pf^{10}**. The presence of the germinal dimethyl groups in the same ring that bears the keto group in the zinc oxochlorin must provide substantial steric constraints toward assembly formation. This particular inhibition is removed in the zinc oxophorbines, in which the geminal dimethyl group and keto group are in separate rings. In turn, the greater assembly formation for oxophorbines bearing a 10-phenyl versus 10-mesityl complex can be understood by diminished steric hindrance involving the aryl group. The greater extent of assembly for the 10-pentafluorophenyl-substituted oxophorbine likely arises from both decreased steric hindrance (versus 10-mesityl) and increased intermolecular interactions (e.g., π-stacking) derived from the electronic characteristics of the pentafluorophenyl rings. On the other hand, the free base analogues of all three zinc oxophorbines, **FbOP-He^{3}M^{10}**, **FbOP-He^{3}P^{10}** and **FbOP-He^{3}Pf^{10}** (like oxochlorin **OxoFbC-He^{7}P^{10}**) are soluble in toluene to give the

monomeric species. Collectively, the results demonstrate the ability to tune the structural and electronic properties of the chlorosomal bacteriochlorophyll analogues toward the formation of assemblies for further study of their light-harvesting and energy-transport properties.

B. Vibrational Spectroscopy. The assembly of **ZnOP-He^{3}M^{10}** was further investigated using both resonance Raman (RR) and IR spectroscopy. The focal point of these studies was the 13-keto substituent whose frequency is sensitive to hydrogen-bonding interactions such as those that would occur in the hypothetical assemblies shown in Figure IV.1. The initial aim of the vibrational spectroscopic studies was to probe the assemblies in solution using RR spectroscopy that parallel the absorption spectroscopic studies described above. However, examination of the RR spectra of **ZnOP-He^{3}M^{10}** in solution (and in solid films) revealed that the band associated with the 13-keto stretching vibration is too weak to identify with certainty. Consequently, the focus turned to the IR spectra of **ZnOP-He^{3}M^{10}**. The interpretation of the IR spectra of **ZnOP-He^{3}M^{10}** in solution is severely compromised by interference from solvent bands. Thus, the IR spectra were acquired of solids, both in KBr pellets and neat films.

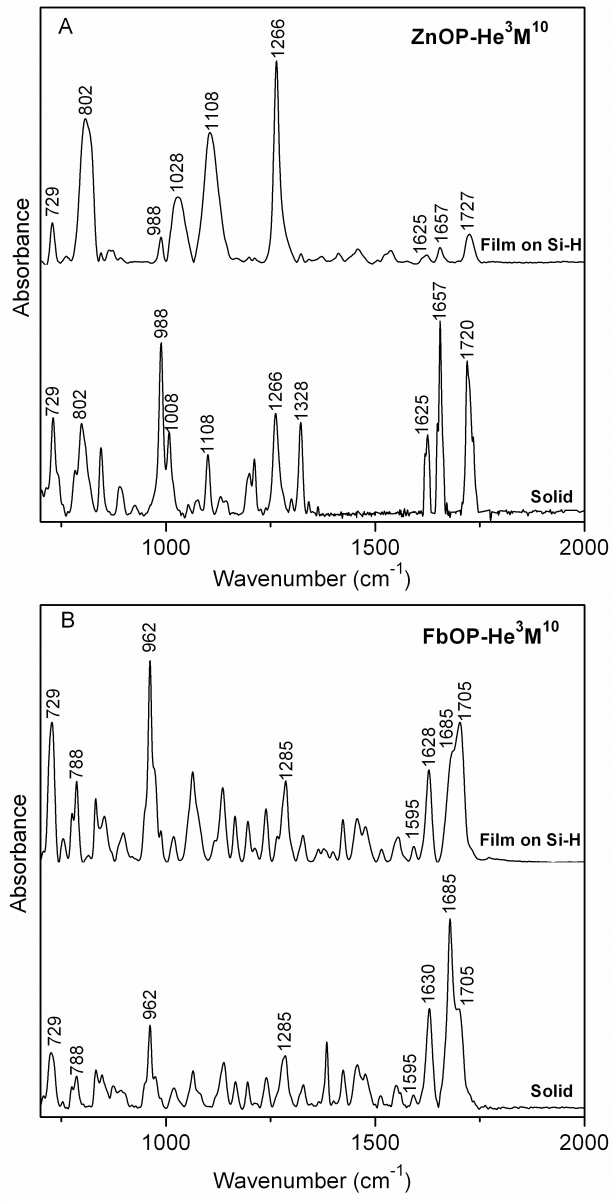

Figure IV.8. IR spectra at room temperature of (A) **ZnOP-He^{3}M^{10}** and (B) **FbOP-He^{3}M^{10}**.

The pellet and film IR spectra of **ZnOP-He^{3}M^{10}** are shown in Figure IV.8, panel A. For comparison, the pellet and film IR spectra of the free base analogue, **FbOP-He^{3}M^{10}**, are also shown in Figure IV.8, panel B. The key spectral region is 1650–1710 cm^{-1}, where the

band associated with the 13-keto stretching vibration is expected. [Note that the band in the 1720–1730 cm^{-1} region is not due to the 13-keto stretching vibration as this band is observed for complexes that lack the 13-keto group (unpublished results).]

In the case of **FbOP-He^{3}M^{10}**, the pellet and film samples exhibit bands near 1685 cm^{-1} and 1705 cm^{-1} that are assignable to the 13-keto stretching vibration. The relative intensity of these bands depends on the concentration of the samples in the pellet or in the solutions from which the films were deposited. Previous studies of chlorophylls have shown that 13-keto stretching frequencies near 1705 cm^{-1} are associated with 13-keto groups that are free from any type of interactions.[60] On the other hand, 13-keto stretching frequencies that are downshifted to the 1685 cm^{-1} region are indicative of a subset of molecules in the solid wherein the 13-keto group experiences hydrogen-bonding interactions. The downshifted 13-keto stretching vibrations observed for **FbOP-He^{3}M^{10}** could arise from hydrogen bonding of the 13-keto group on one molecule with the α-hydroxyethyl group of a neighboring molecule in the solid. This view is supported by the observation that the relative amounts of free versus interacting 13-keto groups in the solid samples are dependent on concentration in the pellet or the solution from which the film was deposited.

The pellet and film IR spectra of **ZnOP-He^{3}M^{10}** in the 13-keto region are quite different from those of **FbOP-He^{3}M^{10}**. In particular, the spectra of **ZnOP-He^{3}M^{10}** do not exhibit bands attributable to the 13-keto stretching vibrations in the 1680-1705 cm^{-1} region. Instead, a band attributable to this vibration is observed at near 1657 cm^{-1}. The frequency of this band does not depend on the concentration in the pellet or the solution from which the

film was deposited. The much lower frequency for the 13-keto stretching vibration of **ZnOP-He^{3}M^{10}** versus **FbOP-He^{3}M^{10}** indicates that the nature of the interactions experienced by the 13-keto group are different for the two complexes in the solids. One plausible explanation for the much lower 13-keto stretching frequency observed for the zinc chelate is that the hydrogen-bonding interaction is stronger for this complex. The enhanced hydrogen bonding could arise if **ZnOP-He^{3}M^{10}** forms an assembly with the types of interactions shown in Figure IV.1. In particular, ligation of the hydroxyl oxygen of one molecule to the zinc ion of a neighboring molecule would weaken the hydroxyl bond owing to transfer of electron density from the oxygen atom to the metal ion. This in turn could result in a stronger hydrogen bond between the hydroxyl group and the 13-keto group of an adjacent **ZnOP-He^{3}M^{10}** molecule.

IV.3. Conclusions

The synthetic approaches developed previously to mimic chlorosomal assembly and function rely on (i) modification of naturally occurring tetrapyrrole macrocycles (pioneered chiefly by Tamiaki),[18] and (ii) synthesis and derivatization of porphyrins (pioneered chiefly by Balaban).[17,19] Here we have introduced a third approach that relies on *de novo* synthesis of chlorin macrocycles. While synthetically more intensive than the aforementioned methods, greater control over structure ultimately is available. This versatility is realized in the target synthetic zinc oxophorbines that differ in the 10-substituent (mesityl, phenyl, pentafluorophenyl), which differ in the propensity to form assemblies, although all do so readily. The ability to tune the steric and electronic characteristics of the synthetic

chlorosomal-bacterichlorophyll mimics augurs well for the use of these constructs for bioinspired light-harvesting systems.

IV.4. Experimental Section

General. ^{1}H NMR and ^{13}C NMR (100 MHz) spectra were collected at room temperature in $CDCl_3$ unless noted otherwise. All tetrapyrrole macrocycles were analyzed by laser desorption mass spectrometry (LD-MS) in the absence of a matrix. Electrospray ionization mass spectrometry (ESI-MS) data are reported for the molecular ion or protonated molecular ion. All commercially available materials were used as received. All of the Pd-mediated coupling reactions were carried out under argon using standard Schlenk-line procedures (e.g., three freeze-pump-thaw cycles were performed prior to and after the addition of the palladium reagent, for a total of six such cycles). Bromination reactions were performed using freshly recrystallized NBS (from water). Anhydrous solvents ($CHCl_3$, CH_2Cl_2, CH_3OH) were obtained from commercial suppliers and used as received. Chromatography often was performed with hexanes (a mixture of hexane isomers with bp ~ 68–70 °C). Sonication was performed in a benchtop bath.

Noncommercial Compounds. Compounds 8-bromo-2,3,4,5-tetrahydro-1,3,3-trimethyldipyrrin (**II-6**),[47] 8,9-dibromo-1-formyl-5-phenyldipyrromethane (**II-8-Br^{8,9}**),[48] 8,9-dibromo-1-formyl-5-mesityldipyrromethane (**II-2-Br^{8,9}**),[40] 1-formyl-5-(pentafluorophenyl)dipyrromethane[49] and oxochlorin[51] **OxoZnC-P^{10}** were prepared following literature procedures.

Mesityl-Substituted Compounds:

3,13-Dibromo-17,18-dihydro-10-mesityl-18,18-dimethylporphyrin (FbC-Br^{3,13}M^{10}). Following a streamlined procedure,[45] a solution of **II-2-Br^{8,9}** (762 mg, 1.70 mmol) and **II-6** (456 mg, 1.70 mmol) in anhydrous CH_2Cl_2 (45 mL) was treated with a solution of $TsOH \cdot H_2O$ (1.62 g, 8.50 mmol) in anhydrous methanol (11 mL) under argon. The red reaction mixture was stirred at room temperature for 40 min. A sample of 2,2,6,6-tetramethylpiperidine (2.5 mL, 15 mmol) was added. The reaction mixture was concentrated. The resulting solid was dissolved in CH_3CN (170 mL) and subsequently treated with 2,2,6,6-tetramethylpiperidine (5.5 mL, 33 mmol), $Zn(OAc)_2$ (4.69 g, 25.5 mmol), and AgOTf (1.31 g, 5.10 mmol). The resulting suspension was refluxed for 20 h exposed to air. The crude mixture was filtered through a pad of silica (ethyl acetate), and the filtrate was concentrated. The resulting solid was dissolved in CH_2Cl_2 (70 mL), and the solution was treated dropwise with TFA (1.90 mL, 24.7 mmol). After stirring for 2.5 h, saturated aqueous $NaHCO_3$ was slowly added to the reaction mixture. The organic phase was washed (water and brine), dried (Na_2SO_4) and concentrated. Column chromatography [silica, hexanes/CH_2Cl_2 (3:1)] afforded a green solid (250 mg, 24%): ^{1}H NMR (300 MHz) δ –1.80 (br, 2H), 1.84 (s, 6H), 2.04 (s, 6H), 2.60 (s, 3H), 4.62 (s, 2H), 7.24 (s, 2H), 8.40 (d, J = 4.4 Hz, 1H), 8.62 (s, 1H), 8.74 (s, 1H), 8.89 (d, J = 4.4 Hz, 1H), 8.94 (s, 1H), 9.07 (s, 1H), 9.82 (s, 1H); LD-MS obsd 613.3; ESI-MS obsd 615.0759, calcd 615.0753 [$(M + H)^+$, M = $C_{31}H_{28}Br_2N_4$]; λ_{abs} (toluene) 413, 651 nm. This compound has been prepared previously in smaller quantity.[45]

3,13-Diacetyl-17,18-dihydro-10-mesityl-18,18-dimethylporphyrin (FbC-A^{3,13}M^{10}). Following a procedure for Stille coupling of chlorins,[40] a sample of **FbC-**

Br^{3,13}M^{10} (225 mg, 0.365 mmol), tributyl(1-ethoxyvinyl)tin (620 μL, 1.84 mmol) and $(Ph_3P)_2PdCl_2$ (51 mg, 0.073 mmol) was stirred in CH_3CN/DMF [18.5 mL (3:2)] under argon for 4 h at 83 °C in a Schlenk line. The reaction mixture was treated with 10% aqueous HCl (25 mL) at room temperature for 20 min. CH_2Cl_2 was added. The organic layer was separated, washed (saturated aqueous $NaHCO_3$, water, and brine), dried (Na_2SO_4), and concentrated. Column chromatography [silica, hexanes/CH_2Cl_2 (1:2)] afforded a purple solid (147 mg, 74%): ^{1}H NMR (300 MHz) δ –1.27 (br, 2H), 1.85 (s, 6H), 2.03 (s, 6H), 2.63 (s, 3H), 3.07 (s, 3H), 3.27 (s, 3H), 4.61 (s, 2H), 7.25 (s, 2H), 8.35 (d, J = 4.4 Hz, 1H), 8.82 (s, 1H), 8.87 (d, J = 4.4 Hz, 1H), 8.94 (s, 1H), 9.31 (s, 1H), 10.09 (s, 1H), 10.64 (s, 1H); LD-MS obsd 541.9; ESI-MS obsd 543.2751, calcd 543.2755 [$(M + H)^+$, M = $C_{35}H_{34}N_4O_2$]; λ_{abs} (toluene) 431, 687 nm. This compound has been prepared previously in smaller quantity via a more elaborate route.[42]

3,13-Diacetyl-15-bromo-17,18-dihydro-10-mesityl-18,18-dimethylporphyrin (FbC-A^{3,13}M^{10}Br^{15}). Following a known procedure[44] with modification, a sample of **FbC-A^{3,13}M^{10}** (140 mg, 0.258 mmol) in CH_2Cl_2/TFA [142 mL (10:1)] was treated with NBS (36 mg, 0.26 mmol) at room temperature. After 1 h, an additional amount of NBS (14 mg, 0.078 mmol) was added. After 30 min, CH_2Cl_2 was added. The mixture was washed with saturated aqueous $NaHCO_3$ and water. The organic layer was separated, dried (Na_2SO_4) and concentrated. Column chromatography [silica, CH_2Cl_2/hexanes (2:1)] afforded a purple solid (96 mg, 60%): ^{1}H NMR (300 MHz) δ –1.47 (br, 2H), 1.81 (s, 6H), 2.05 (s, 6H), 2.60 (s, 3H), 3.06 (s, 3H), 3.27 (s, 3H), 4.59 (s, 2H), 7.23 (s, 2H), 8.35 (d, J = 4.5 Hz, 1H), 8.50 (s, 1H), 8.83 (s, 1H), 8.86 (d, J = 4.5 Hz, 1H), 9.33 (s, 1H), 10.61 (s, 1H); LD-MS obsd 620.4; ESI-

MS obsd 621.1854, calcd 621.1860 [$(M + H)^+$, M = $C_{35}H_{33}BrN_4O_2$]; λ_{abs} (toluene) 425, 677 nm.

3-Acetyl-17,18-dihydro-10-mesityl-18,18-dimethyl-13^1-oxophorbine (FbOP-A^{3}M^{10}). Following a known procedure[41] with modification, a mixture of **FbC-A^{3,13}M^{10}Br^{15}** (94 mg, 0.15 mmol), Cs_2CO_3 (248 mg, 0.759 mmol) and $(Ph_3P)_2PdCl_2$ (21 mg, 0.030 mmol) in freshly distilled THF (13 mL) under argon was stirred for 4 h at 85 °C in a sealed Schlenk flask. The reaction mixture was concentrated, and the resulting crude solid was dissolved in CH_2Cl_2. The organic phase was washed with water, dried (Na_2SO_4) and filtered. The filtrate was concentrated to afford a brown solid. Column chromatography [silica, CH_2Cl_2/hexanes (2:1), then CH_2Cl_2] afforded a purple solid (53 mg, 65%): ^{1}H NMR (400 MHz) δ –1.64 (br, 1H), 0.72 (br, 1H), 1.87 (s, 6H), 2.03 (s, 6H), 2.58 (s, 3H), 3.23 (s, 3H), 4.30 (s, 2H), 5.15 (s, 2H), 7.23 (s, 2H), 8.43 (d, J = 4.4 Hz, 1H), 8.63 (s, 1H), 8.74 (s, 1H), 8.82 (d, J = 4.4 Hz, 1H), 9.31 (s, 1H), 10.56 (s, 1H); LD-MS obsd 539.8; ESI-MS obsd 541.2594, calcd 541.2598 [$(M + H)^+$, M = $C_{35}H_{32}N_4O_2$]; λ_{abs} (toluene) 427, 446, 683 nm.

3-(1-Hydroxyethyl)-10-mesityl-18,18-dimethyl-13^1-oxophorbine (FbOP-He^{3}M^{10}). A sample of **FbOP-A^{3}M^{10}** (52 mg, 0.096 mmol) in anhydrous $CHCl_3$ (7 mL) was treated with $BH_3{\cdot}^t$BuNH$_2$ (49 mg, 0.56 mmol) at room temperature. After stirring for 4.5 h under argon, the reaction mixture was diluted with $CHCl_3$ and treated with 5% aqueous HCl (5 mL). The reaction mixture was stirred vigorously for 20 min. The organic phase was washed (5% aqueous HCl, water, saturated aqueous $NaHCO_3$, and brine), dried (Na_2SO_4) and filtered. The filtrate was concentrated to afford a brown solid. Column chromatography [silica, CH_2Cl_2, then CH_2Cl_2/ethyl acetate (9:1)] afforded a trace of unreacted starting

material (first fraction), **FbHP-A^{3}M^{10}** (second fraction), title compound **FbOP-He^{3}M^{10}** (third fraction), diastereomer 1 of **FbHP-He^{3}M^{10}** (fourth fraction), and diastereomer 2 of **FbHP-He^{3}M^{10}** (fifth fraction).

Data for **FbOP-He^{3}M^{10}** (40 mg, 77%): ^{1}H NMR (300 MHz) δ –1.38 (br, 1H), 1.22 (br, 1H), 1.88 (s, 6H), 1.98 (s, 6H), 2.19 (d, J = 6.6 Hz, 3H), 2.58 (s, 3H), 4.21 (s, 2H), 5.08 (s, 2H), 6.38–6.45 (m, 1H), 7.22 (s, 2H), 8.39 (d, J = 4.4 Hz, 1H), 8.51 (s, 1H), 8.52 (s, 1H), 8.64 (d, J = 4.4 Hz, 1H), 8.76 (s, 1H), 9.44 (s, 1H), note that the hydroxy proton was not observed; ^{13}C NMR δ 21.4, 21.6, 26.1, 47.6, 48.5, 48.8, 65.4, 94.9, 101.4, 106.6, 115.9, 122.9, 126.4, 128.1, 132.73, 132.77, 133.1, 135.6, 135.8, 138.3, 138.9, 139.5, 142.2, 147.6, 150.0, 153.0, 154.6, 157.3, 177.8, 195.8; LD-MS obsd 542.2; ESI-MS obsd 543.2764, calcd 543.2755 [$(M + H)^+$, M = $C_{35}H_{34}N_4O_2$]; λ_{abs} (toluene) 423, 657 nm.

Data for **FbHP-A^{3}M^{10}** (5 mg, 10%): ^{1}H NMR (300 MHz) δ –2.60 (br, 1H), –0.57 (br, 1H), 1.87 (s, 6H), 2.07 (s, 6H), 2.59 (s, 3H), 3.31 (s, 3H), 4.40 (s, 2H), 4.59 (d, J = 20 Hz, 1H), 5.21 (dd, J = 20 Hz, J = 6.4 Hz, 1H), 6.44–6.46 (m, 1H), 7.24–7.26 (m, 2H), 8.46 (s, 1H), 8.46 (d, J = 3.8 Hz, 1H), 8.94 (s, 1H), 9.02 (d, J = 3.8 Hz, 1H), 9.41 (s, 1H), 10.9 (s, 1H), note that the hydroxy proton was not observed; LD-MS obsd 542.6; ESI-MS obsd 543.2757, calcd 543.2755 [$(M + H)^+$, M = $C_{35}H_{34}N_4O_2$]; λ_{abs} (toluene) 430, 661 nm.

Data for **FbHP-He^{3}M^{10}** (diastereomer 1) (2 mg, 3%): ^{1}H NMR (400 MHz) δ –2.98 (br, 1H), 1.25 (br, 1H), 1.87 (s, 3H), 1.88 (s, 3H), 2.07 (s, 6H), 2.27 (d, J = 5.6 Hz, 3H), 2.6 (s, 3H), 4.40 (m, 2H), 4.60 (d, J = 19.5 Hz, 1H), 5.23 (dd, J = 19.5 Hz, J = 6.4 Hz, 1H), 6.46 (d, J = 6.4 Hz, 1H), 6.64–6.69 (m, 1H), 7.25 (s, 2H), 8.49 (s, 1H), 8.52 (d, J = 4.3 Hz, 1H),

8.88 (s, 1H), 8.94 (d, J = 4.3 Hz, 1H), 8.99 (s, 1H), 9.93 (s, 1H), note that the two hydroxy protons were not observed; LD-MS obsd 544.6; ESI-MS obsd 545.2910, calcd 545.2911 [(M + H)$^+$, M = $C_{35}H_{36}N_4O_2$]; λ_{abs} (toluene) 413, 639 nm.

Data for **FbHP-He^{3}M^{10}** (diastereomer 2) (3 mg, 5%): ^{1}H NMR (400 MHz) δ –2.98 (br, 1H), 1.25 (br, 1H), 1.87 (s, 3H), 1.88 (s, 3H), 2.07 (s, 3H), 2.08 (s, 3H), 2.27 (d, J = 6.4 Hz, 3H), 2.60 (s, 3H), 4.40–4.41 (m, 2H), 4.60 (d, J = 19.0 Hz, 1H), 5.22 (dd, J = 19.0 Hz, J = 5.6 Hz 1H), 6.47 (d, J = 5.6 Hz, 1H), 6.64–6.69 (m, 1H), 7.25 (s, 2H), 8.49 (s, 1H), 8.52 (d, J = 4.3 Hz, 1H), 8.88 (s, 1H), 8.94 (d, J = 4.3 Hz, 1H), 8.99 (s, 1H), 9.94 (s, 1H), note that the two hydroxy protons were not observed; LD-MS obsd 544.5; ESI-MS obsd 545.2917, calcd 545.2911 [(M + H)$^+$, M = $C_{35}H_{36}N_4O_2$]; λ_{abs} (toluene) 414, 639 nm.

Zn(II)-3-(1-Hydroxyethyl)-10-mesityl-18,18-dimethyl-13^1-oxophorbine (ZnOP-He^{3}M^{10}). A sample of **FbOP-He^{3}M^{10}** (6 mg, 0.01 mmol) in $CHCl_3$ was treated with $Zn(OAc)_2 \cdot 2H_2O$ (37 mg, 0.17 mmol) in methanol (1 mL). The reaction mixture was stirred for 8 h at room temperature. The reaction mixture was concentrated. The crude solid was dissolved in CH_2Cl_2, and the organic phase was washed (saturated aqueous $NaHCO_3$, water and brine), dried (Na_2SO_4) and filtered. The product, which adhered to the Na_2SO_4, was liberated by washing with methanol. The CH_2Cl_2 and methanol filtrates were combined and concentrated to afford a bright green solid. Column chromatography [silica, CH_2Cl_2/MeOH (25:1)] afforded a green solid (5 mg, 70%): ^{1}H NMR (400 MHz, THF-d_8) δ 1.87 (s, 3H), 1.88 (s, 3H), 2.01 (s, 6H), 2.04 (d, J = 6.6 Hz, 3H), 2.57 (s, 3H), 4.25 (s, 2H), 4.93 (s, 2H), 6.15–6.70 (m, 1H), 7.23 (s, 2H), 8.26 (d, J = 4.6 Hz, 1H), 8.30 (s, 1H), 8.39 (s, 1H), 8.60 (s, 1H),

8.61 (d, J = 4.6 Hz, 1H), 9.46 (s, 1H); ^{13}C NMR (THF-d_8) δ 21.5, 21.7, 27.3, 30.8, 31.4, 47.3, 49.0, 65.5, 94.2, 104.1, 106.6, 120.5, 126.8, 128.2, 128.7, 129.4, 131.0, 135.6, 138.3, 139.0, 139.5, 142.2, 148.6, 149.2, 152.2, 154.2, 155.3, 174.3, 194.9 (other signals expected were not observed); LD-MS obsd 604.5; ESI-MS obsd 605.1879, calcd 605.1889 [$(M + H)^+$, M = $C_{35}H_{32}N_4O_2Zn$]; λ_{abs} (toluene) 426, 642 nm.

Phenyl-Substituted Compounds:

3,13-Dibromo-17,18-dihydro-18,18-dimethyl-10-phenylporphyrin (FbC-Br^{3,13}P^{10}). A solution of **II-8-Br**^{8,9} (1.28 g, 3.16 mmol) and **II-6** (851 mg, 3.16 mmol) in anhydrous CH_2Cl_2 (80 mL) under argon was treated with $TsOH \cdot H_2O$ (3.00 g, 15.8 mmol) in anhydrous methanol (20 mL). The red reaction mixture was stirred at room temperature for 40 min. A sample of 2,2,6,6-tetramethylpiperidine (4.5 mL, 27 mmol) was added. The reaction mixture was concentrated. The resulting solid was dissolved in CH_3CN (300 mL) and subsequently treated with 2,2,6,6-tetramethylpiperidine (10.7 mL, 63.2 mmol), $Zn(OAc)_2$ (8.70 g, 47.4 mmol), and AgOTf (2.43 g, 9.46 mmol). The resulting suspension was refluxed for 20 h exposed to air. The crude mixture was filtered through a pad of silica (ethyl acetate), and the filtrate was concentrated. The resulting solid was dissolved in CH_2Cl_2 (200 mL), and the solution was treated dropwise with TFA (3.65 mL, 47.4 mmol). After stirring for 2.5 h, saturated aqueous $NaHCO_3$ was slowly added to the reaction mixture. The organic phase was washed (water and brine), dried (Na_2SO_4) and concentrated. Column chromatography [silica, hexanes/CH_2Cl_2 (3:1)] afforded a green solid (530 mg, 29%): ^{1}H NMR (300 MHz) δ –1.80 (br, 2H), 2.04 (s, 6H), 4.64 (s, 2H), 7.72–7.75 (m, 3H), 8.08–8.11 (m, 2H), 8.57 (d, J = 4.4 Hz, 1H), 8.77 (s, 1H), 8.80 (s, 1H), 8.94 (d, J = 4.4 Hz, 1H), 9.96 (s, 1H), 9.12 (s, 1H),

9.87 (s, 1H); ^{13}C NMR δ 31.3, 52.1, 94.6, 95.5, 106.0, 124.6, 127.2, 128.1, 129.3, 132.7, 133.1, 134.2 (other signals expected were not observed); LD-MS obsd 572.6; ESI-MS obsd 573.0281, calcd 573.0284 [$(M + H)^+$, M = $C_{28}H_{22}Br_2N_4$]; λ_{abs} (toluene) 400, 651 nm.

3,13-Diacetyl-17,18-dihydro-18,18-dimethyl-10-phenylporphyrin (FbC-A^{3,13}P^{10}). Following a procedure for Stille coupling of chlorins,[40] a sample of **FbC-Br^{3,13}P^{10}** (150 mg, 0.260 mmol), tributyl(1-ethoxyvinyl)tin (700 μL, 2.10 mmol) and $(Ph_3P)_2PdCl_2$ (36 mg, 0.052 mmol) was stirred in CH_3CN/DMF [20 mL (3:2)] under argon for 4 h at 83 °C in a Schlenk line. The reaction mixture was treated with 10% aqueous HCl (20 mL) at room temperature for 20 min. CH_2Cl_2 was added. The organic layer was separated, washed (saturated aqueous $NaHCO_3$, water, and brine), dried (Na_2SO_4), and concentrated. Column chromatography (silica, CH_2Cl_2) afforded a purple solid (93 mg, 71%): ^{1}H NMR (300 MHz) δ –1.27 (br, 2H), 2.08 (s, 6H), 3.07 (s, 3H), 3.24 (s, 3H), 4.60 (s, 2H), 7.73–7.77 (m, 3H), 8.07–8.10 (m, 2H), 8.51 (d, *J* = 4.4 Hz, 1H), 8.82 (s, 1H), 8.91 (d, *J* = 4.4 Hz, 1H), 9.01 (s, 1H), 9.29 (s, 1H), 10.13 (s, 1H), 10.66 (s, 1H); ^{13}C NMR δ 29.9, 31.2, 46.5, 52.3, 96.4, 99.1, 109.2, 123.9, 127.2, 127.4, 128.3, 130.1, 131.9, 133.0, 133.7, 134.2, 134.5, 134.8, 135.4, 137.6, 138.1, 141.1, 154.4, 154.8, 165.8, 176.8, 196.9, 197.2; LD-MS obsd 500.3; ESI-MS obsd 501.2281, calcd 501.2285 [$(M + H)^+$, M = $C_{32}H_{28}N_4O_2$]; λ_{abs} (toluene) 428, 686 nm.

3,13-Diacetyl-15-bromo-17,18-dihydro-18,18-dimethyl-10-phenylporphyrin (FbC-A^{3,13}P^{10}Br^{15}). Following a known procedure[44] with modification, a sample of **FbC-A^{3,13}P^{10}** (100 mg, 0.200 mmol) in CH_2Cl_2/TFA [110 mL (10:1)] was treated with NBS (46 mg, 0.26 mmol) at room temperature. After 1 h, a further amount of NBS (35 mg, 0.20

mmol) was added. After 30 min, CH_2Cl_2 was added. The mixture was washed with saturated aqueous $NaHCO_3$ and water. The organic layer was separated, dried (Na_2SO_4) and concentrated. Column chromatography (silica, CH_2Cl_2) afforded a purple solid (75 mg, 65%): ^{1}H NMR (300 MHz) δ –1.42 (br, 2H), 2.04 (s, 6H), 3.05 (s, 3H), 3.25 (s, 3H), 4.59 (s, 2H), 7.71–7.74 (m, 3H), 8.03–8.06 (m, 2H), 8.48 (d, J = 4.5 Hz, 1H), 8.61 (s, 1H), 8.82 (s, 1H), 8.88 (d, J = 4.5 Hz, 1H), 9.31 (s, 1H), 10.62 (s, 1H); ^{13}C NMR δ 29.9, 31.6, 34.7, 46.2, 55.6, 127.1, 127.6, 128.4, 128.6, 134.1, 134.4, 134.7, 141.2, 196.8, 202.1 (other signals expected were not observed); LD-MS obsd 579.6; ESI-MS obsd 579.1389, calcd 579.1390 [$(M + H)^+$, M = $C_{32}H_{27}BrN_4O_2$]; λ_{abs} (toluene) 425, 677 nm.

3-Acetyl-17,18-dihydro-18,18-dimethyl-10-phenyl-13^1-oxophorbine (FbOP-A^{3}P^{10}). Following a known procedure[41] with modification, a mixture of **FbC-A^{3,13}P^{10}Br^{15}** (60 mg, 0.10 mmol), Cs_2CO_3 (196 mg, 0.600 mmol), and $(Ph_3P)_2PdCl_2$ (15 mg, 0.021 mmol) in freshly distilled THF (15 mL) under argon was stirred for 4 h at 85 °C in a sealed Schlenk flask. The reaction mixture was concentrated, and the resulting crude solid was dissolved in CH_2Cl_2. The organic phase was washed with water, dried (Na_2SO_4) and filtered. The filtrate was concentrated to afford a brown solid. Column chromatography [silica, CH_2Cl_2/ethyl acetate (20:1)] afforded a dark purple solid (35 mg, 68%): ^{1}H NMR (400 MHz) δ –1.62 (br, 1H), 0.74 (br, 1H), 2.02 (s, 6H), 3.24 (s, 3H), 4.28 (s, 2H), 5.10 (s, 2H), 7.73–7.76 (m, 3H), 8.09–8.13 (m, 2H), 8.63 (d, J = 4.4 Hz, 1H), 8.74 (s, 1H), 8.83 (s, 1H), 8.87 (d, J = 4.4 Hz, 1H), 9.32 (s, 1H), 10.57 (s, 1H); ^{13}C NMR δ 30.1, 31.2, 48.2, 48.3, 48.7, 96.7, 106.8, 107.6, 118.2, 126.8, 127.7, 128.2, 128.4, 129.8, 130.7, 133.9, 134.1, 134.4, 134.6, 134.9, 135.3,

139.0, 139.5, 141.2, 149.6, 153.9, 155.0, 158.5, 176.5, 195.6, 196.8; LD-MS obsd 498.5; ESI-MS obsd 499.2129, calcd 499.2129 [$(M + H)^+$, M = $C_{32}H_{26}N_4O_2$]; λ_{abs} (toluene) 428, 446, 682 nm.

3-(1-Hydroxyethyl)-18,18-dimethyl-10-phenyl-13^1-oxophorbine (FbOP-He^{3}P^{10}). A sample of **FbOP-A^{3}P^{10}** (14 mg, 0.028 mmol) in anhydrous $CHCl_3$ (5 mL) was treated with $BH_3 \cdot {}^t BuNH_2$ (15 mg, 0.17 mmol) at room temperature. After stirring for 4.5 h under argon, the reaction mixture was diluted with $CHCl_3$ and treated with 5% aqueous HCl (5 mL). The reaction mixture was stirred vigorously for 20 min. The organic phase was washed (5% aqueous HCl, water, saturated aqueous $NaHCO_3$, and brine), dried (Na_2SO_4) and filtered. The filtrate was concentrated to afford a brown solid. Column chromatography [silica, CH_2Cl_2/ethyl acetate (20:1)] afforded a dark purple solid (10 mg, 72%): ^{1}H NMR (300 MHz) δ –1.38 (br, 1H), 1.16 (br, 1H), 1.95 (s, 6H), 2.20 (d, J = 6.9 Hz, 3H), 2.62 (br, 1H), 4.15 (s, 2H), 5.02 (s, 2H), 6.23–6.25 (m, 1H), 7.72–7.74 (m, 3H), 8.09–8.11 (m, 2H), 8.51 (s, 1H), 8.60 (d, J = 4.4 Hz, 1H), 8.70 (d, J = 4.4 Hz, 1H), 8.73 (s, 1H), 8.77 (s, 1H), 9.47 (s, 1H); ^{13}C NMR δ 25.9, 30.8, 30.9, 47.7, 48.5, 48.6, 65.3, 94.8, 101.6, 106.5, 117.3, 122.8, 127.5, 127.6, 128.4, 132.5, 132.8, 134.0, 134.3, 135.6, 139.6, 140.1, 142.2, 147.6, 149.7, 152.7, 154.3, 157.4, 177.8, 195.9; LD-MS obsd 500.9; ESI-MS obsd 501.2278, calcd 501.2285 [$(M + H)^+$, M = $C_{32}H_{28}N_4O_2$]; λ_{abs} (toluene) 423, 656 nm.

Zn(II)-3-(1-Hydroxyethyl)-18,18-dimethyl-10-phenyl-13^1-oxophorbine (ZnOP-He^{3}P^{10}). A sample of **FbOP-He^{3}P^{10}** (7 mg, 0.01 mmol) in $CHCl_3$ (2 mL) was treated with $Zn(OAc)_2$ (44 mg, 0.24 mmol) in methanol (1 mL) for 8 h at room temperature. The reaction mixture was concentrated. The crude solid was dissolved in CH_2Cl_2, and the organic phase

was washed (saturated aqueous $NaHCO_3$, water and brine), dried (Na_2SO_4), and filtered. The title compound, which adhered to the Na_2SO_4, was liberated by washing with methanol. The CH_2Cl_2 and methanol filtrates were combined and concentrated to afford a bright green solid (6 mg, 80%): ^{1}H NMR (300 MHz, THF-d_8) δ 2.02 (s, 6H), 2.05 (d, J = 6.3 Hz, 3H), 4.27 (s, 2H), 4.85 (d, J = 4.4 Hz, 1H), 4.95 (s, 2H), 6.23–6.25 (m, 1H), 7.68–7.71 (m, 3H), 8.06–8.09 (m, 2H), 8.42 (s, 1H), 8.46 (d, J = 4.4 Hz, 1H), 8.51 (s, 1H), 8.62 (s, 1H), 8.67 (d, J = 4.4 Hz, 1H), 9.53 (s, 1H); LD-MS obsd 562.3; ESI-MS obsd 562.1343, calcd 562.1347 ($C_{32}H_{26}N_4O_2Zn$); λ_{abs} (THF) 426, 640 nm.

Zn(II)-3-Acetyl-17,18-dihydro-18,18-dimethyl-10-phenyl-13^1-oxophorbine (ZnOP-A^{3}P^{10}). A sample of **FbOP-A^{3}P^{10}** (6 mg, 0.01 mmol) in $CHCl_3$ (2 mL) was treated with $Zn(OAc)_2$ (37 mg, 0.20 mmol) in methanol (1 mL). The reaction mixture was stirred for 8 h at room temperature. The reaction mixture was concentrated. The crude solid was dissolved in CH_2Cl_2. The solution was washed (saturated aqueous $NaHCO_3$, water and brine), dried (Na_2SO_4), concentrated and chromatographed [alumina, CH_2Cl_2/MeOH (25:1)] to afford a green solid (5 mg, 70%): ^{1}H NMR (300 MHz, THF-d_8) δ 2.01 (s, 6H), 3.06 (s, 3H), 4.37 (s, 2H), 5.03 (s, 2H), 7.71–7.73 (m, 3H), 8.09–8.11 (m, 2H), 8.55 (d, J = 4.3 Hz, 1H), 8.63 (s, 1H), 8.68 (s, 1H), 8.85 (d, J = 4.3 Hz, 1H), 9.44 (s, 1H), 10.54 (s, 1H); LD-MS obsd 560.7; ESI-MS obsd 561.1257, calcd 561.1263 [$(M + H)^+$, M = $C_{32}H_{24}N_4O_2Zn$]; λ_{abs} (THF) 449, 665 nm.

Pentafluorophenyl-Substituted Compounds:

8,9-Dibromo-1-formyl-5-(pentafluorophenyl)dipyrromethane (IV-1-Br^{8,9}). Following a reported procedure,[48] a solution of 1-formyl-5-

(pentafluorophenyl)dipyrromethane[49] (1.83 g, 5.39 mmol) in anhydrous THF (54 mL) at –78 °C under argon was treated with NBS (1.92 g, 10.8 mmol) in one batch. The reaction mixture was stirred for 1 h at –78 °C, and then allowed to warm up. When the temperature of the reaction mixture reached –20 °C, hexanes and water were added. The contents of the reaction flask were transferred to a separatory funnel. Ethyl acetate was added. The organic layer was separated, dried (K_2CO_3) and concentrated without heating to afford a yellow solid. Column chromatography [silica, hexanes/CH_2Cl_2/ethyl acetate (7:2:1)] afforded a brown solid (1.44 g, 54%): mp 76–78 °C (dec.); ^{1}H NMR (THF-d_8) δ 5.83 (s, 1H), 5.98 (d, J = 3.0 Hz, 1H), 6.10–6.12 (m, 1H), 6.85–6.87 (m, 1H), 9.42 (s, 1H), 11.12 (br, 1H), 11.43 (br, 1H); ESI-MS obsd 496.8920, calcd 496.8918 [$(M + H)^+$, M = $C_{16}H_7Br_2F_5N_2O$]. Note: Compound **IV-1-Br**[8,9] is relatively unstable but can be stored in the solid form at –20 °C under argon for many weeks without decomposition.

3,13-Dibromo-17,18-dihydro-18,18-dimethyl-10-(pentafluorophenyl)porphyrin (FbC-Br^{3,13}Pf^{10}). Following a streamlined procedure,[45] a solution of **IV-1-Br**[8,9] (1.06 g, 2.13 mmol) and **II-6** (570 mg, 2.13 mmol) in anhydrous CH_2Cl_2 (56.8 mL) under argon was treated with a solution of TsOH·H_2O (2.02 g, 10.6 mmol) in anhydrous methanol (14.2 mL). The red reaction mixture was stirred at room temperature for 40 min. A sample of 2,2,6,6-tetramethylpiperidine (2.70 mL, 16.0 mmol) was added. The reaction mixture was concentrated. The resulting solid was dissolved in CH_3CN (213 mL) and subsequently treated with 2,2,6,6-tetramethylpiperidine (7.2 mL, 43 mmol), $Zn(OAc)_2$ (5.88 g, 32.0 mmol), and AgOTf (1.64 g, 6.38 mmol). The resulting suspension was refluxed for 18 h exposed to air. The crude mixture was filtered through a pad of silica (ethyl acetate), and the

filtrate was concentrated. The resulting solid was dissolved in CH_2Cl_2 (50 mL), and the solution was treated dropwise with TFA (2.6 mL, 34 mmol). After stirring for 2 h, saturated aqueous $NaHCO_3$ was slowly added to the reaction mixture. The organic phase was washed (water and brine), dried (Na_2SO_4) and concentrated. Column chromatography [silica, hexanes/CH_2Cl_2 (3:2)] afforded a green solid (132 mg, 9%): ^{1}H NMR (300 MHz) δ –2.32 (br, 1H), –2.00 (br, 1H), 2.05 (s, 6H), 4.68 (s, 2H), 8.51 (d, J = 4.3 Hz, 1H), 8.76 (s, 1H), 8.88 (s, 1H), 9.02 (s, 1H), 9.05 (d, J = 4.3 Hz, 1H), 9.23 (s, 1H), 9.94 (s, 1H); ^{13}C NMR δ 12.0, 14.7, 23.2, 28.1, 31.7, 32.1, 47.0, 52.7, 96.3, 96.9, 106.7, 115.6, 119.2, 125.3, 127.5, 131.0, 133.0, 135.0, 137.6, 140.2, 151.3 152.1, 165.0, 176.4; LD-MS obsd 662.4; ESI-MS obsd 662.9815, calcd 662.9813 [$(M + H)^+$, M = $C_{28}H_{17}Br_2F_5N_4$]; λ_{abs} (toluene) 400, 654 nm.

3,13-Diacetyl-17,18-dihydro-18,18-dimethyl-10-(pentafluorophenyl)porphyrin (FbC-A^{3,13}Pf^{10}). Following a procedure for Stille coupling of chlorins,[40] a mixture of **FbC-Br^{3,13}Pf^{10}** (132 mg, 0.199 mmol), tributyl(1-ethoxyvinyl)tin (340 μL, 1.00 mmol) and $(Ph_3P)_2PdCl_2$ (28 mg, 0.040 mmol) was stirred in CH_3CN/DMF [10 mL (3:2)] under argon for 3.5 h at 83 °C in a Schlenk line. The reaction mixture was treated with 10% aqueous HCl (5 mL) at room temperature for 20 min. CH_2Cl_2 was added. The organic layer was separated, washed (saturated aqueous $NaHCO_3$, water, and brine), dried (Na_2SO_4), and concentrated. Column chromatography [silica, hexanes/CH_2Cl_2 (2:3)] afforded a purple solid (62 mg, 53%; 95% purity): ^{1}H NMR (400 MHz) δ –1.73 (br, 1H), –1.62 (br, 1H), 2.04 (s, 6H), 2.18 (s, 3H), 3.28 (s, 3H), 4.66 (s, 2H), 8.47 (d, J = 4.4 Hz, 1H), 8.96 (s, 1H), 9.04 (d, J = 4.4 Hz, 1H), 9.06 (s, 1H), 9.38 (s, 1H), 10.25 (s, 1H), 10.77 (s, 1H); ^{13}C NMR δ 13.8, 17.7,

27.1, 28.1, 30.0, 30.2, 31.3, 46.6, 52.5, 97.8, 100.3, 128.2, 129.3, 131.2, 133.5, 134.4, 136.4, 137.4, 138.0, 153.5, 155.3, 166.5, 176.9 196.78, 196.86; LD-MS obsd 590.4; ESI-MS obsd 591.1816, calcd 591.1814 [$(M + H)^+$, M = $C_{32}H_{23}F_5N_4O_2$]; λ_{abs} (toluene) 432, 688 nm.

3,13-Diacetyl-15-bromo-17,18-dihydro-18,18-dimethyl-10-(pentafluorophenyl)porphyrin (FbC-A^{3,13}Pf^{10}Br^{15}). Following a known procedure[44] with modification, a sample of **FbC-A^{3,13}Pf^{10}** (60 mg, 0.10 mmol) in CH_2Cl_2/TFA [50.1 mL (10:1)] was treated with NBS (18 mg, 0.10 mmol) at room temperature. After 1 h, a further amount of NBS (5 mg, 0.03 mmol) was added. After 30 min, CH_2Cl_2 was added. The mixture was washed with saturated aqueous $NaHCO_3$ and water. The organic layer was separated, dried (Na_2SO_4) and concentrated. Column chromatography [silica, CH_2Cl_2/hexanes (3:1)] afforded a brown solid (46 mg, 68%): ^{1}H NMR (400 MHz, 40 °C) δ – 2.02 (br, 1H), –1.71 (br, 1H), 2.07 (s, 6H), 3.13 (s, 3H), 3.29 (s, 3H), 4.65 (s, 2H), 8.47 (d, J = 4.0 Hz, 1H), 8.61 (s, 1H), 8.99 (s, 1H), 9.02 (d, J = 4.7 Hz, 1H), 9.42 (s, 1H), 10.74 (s, 1H); LD-MS obsd 668.0; ESI-MS obsd 669.0912, calcd 669.0919 [$(M + H)^+$, M = $C_{32}H_{22}BrF_5N_4O_2$]; λ_{abs} (toluene) 432, 678 nm.

3-Acetyl-17,18-dihydro-18,18-dimethyl-10-(pentafluorophenyl)-13^1-oxophorbine (FbOP-A^{3}Pf^{10}). Following a known procedure[41] with modification, a mixture of **FbC-A^{3,13}Pf^{10}Br^{15}** (45 mg, 0.067 mmol), Cs_2CO_3 (110 mg, 0.336 mmol), and $(Ph_3P)_2PdCl_2$ (9 mg, 0.01 mmol) in freshly distilled THF (5.6 mL) under argon was stirred for 4 h at 85 °C in a sealed Schlenk flask. The reaction mixture was concentrated, and the resulting crude solid was dissolved in CH_2Cl_2. The organic phase was washed with water, dried (Na_2SO_4) and filtered. The filtrate was concentrated to afford a brown solid. Column chromatography

(silica, CH_2Cl_2) afforded a purple solid (25 mg, 64%): ^{1}H NMR (400 MHz) δ –2.16 (br, 1H), 0.24 (br, 1H), 2.07 (s, 6H), 3.29 (s, 3H), 4.39 (s, 2H), 5.23 (s, 2H), 8.55 (d, J = 4.7 Hz, 1H), 8.78 (s, 1H), 8.94 (s, 1H), 9.00 (d, J = 4.3 Hz, 1H), 9.44 (d, J = 1.7 Hz 1H), 10.73 (s, 1H); ^{13}C NMR δ 14.4, 21.3, 26.1, 30.0, 31.0, 47.9, 48.6, 48.4, 60.6, 65.4, 96.4, 101.8, 107.6, 114.9, 123.4, 132.1, 133.6, 134.1, 136.1, 138.7, 141.7, 147.8, 149.3, 152.6, 155.0, 158.4, 177.9, 195.4; LD-MS obsd 588.5; ESI-MS obsd 589.1661, calcd 589.1657 [$(M + H)^+$, M = $C_{32}H_{21}F_5N_4O_2$]; λ_{abs} (toluene) 428, 445, 686 nm.

3-(1-Hydroxyethyl)-18,18-dimethyl-10-(pentafluorophenyl)-13^1-oxophorbine (FbOP-He^{3}Pf^{10}). A sample of **FbOP-A^{3}Pf^{10}** (25 mg, 0.043 mmol) in anhydrous $CHCl_3$ (3 mL) was treated with $BH_3 \cdot {}^t$Bu NH_2 (22 mg, 0.25 mmol) at room temperature. After stirring for 4 h under argon, the reaction mixture was diluted with $CHCl_3$ and treated with 5% aqueous HCl (5 mL). The reaction mixture was stirred vigorously for 20 min. The organic phase was washed (5% aqueous HCl, water, saturated aqueous $NaHCO_3$, and brine), dried (Na_2SO_4) and filtered. The filtrate was concentrated to afford a brown solid. Column chromatography [silica, CH_2Cl_2, then CH_2Cl_2/ethyl acetate (9:1)] afforded a brown solid (14 mg, 55%): ^{1}H NMR (300 MHz) δ –2.07 (br, 1H), 0.54 (br, 1H), 1.97 (s, 6H), 2.22 (d, J = 6.6 Hz, 3H), 2.64 (br, 1H), 4.23 (s, 2H), 5.10 (s, 2H), 6.43–6.50 (m, 1H), 8.52 (d, J = 4.5 Hz, 1H), 8.70 (s, 2H), 8.83 (d, J = 4.5 Hz, 1H), 8.88 (s, 1H), 9.63 (s, 1H); LD-MS obsd 590.3; ESI-MS obsd 591.1814, calcd 591.1813 [$(M + H)^+$, M = $C_{32}H_{23}F_5N_4O_2$]; λ_{abs} (toluene) 422, 663 nm.

Zn(II)-3-(1-Hydroxyethyl)-10-(pentafluorophenyl)-18,18-dimethyl-13^1-oxophorbine (ZnOP-He^{3}Pf^{10}). A sample of **FbOP-He^{3}Pf^{10}** (7 mg, 0.01 mmol) in $CHCl_3$ (1.9 mL) was treated with $Zn(OAc)_2 \cdot 2H_2O$ (40 mg, 0.18 mmol) in methanol (1.5 mL) for 8 h at room temperature. The reaction mixture was diluted with ethyl acetate/MeOH (10:1). The organic phase was washed (saturated aqueous $NaHCO_3$, water and brine) and concentrated to a minimum volume, which was freeze-dried overnight. The resulting solid was treated with Et_2O and sonicated. The resulting suspension was centrifuged, and the supernatant (which contained the free base starting material) was removed. The procedure (treatment with Et_2O, sonication, centrifugation, and supernatant removal) was performed two further times to afford the title compound as a green solid (6 mg, 80%). The title compound exhibited poor solubility in organic solvents (e.g., CH_2Cl_2, ethyl acetate, THF, and DMF and did not afford a satisfactory ^{1}H NMR spectrum (DMF-d_7, THF-d_8); LD-MS obsd 652.3; ESI-MS obsd 653.0923, calcd 653.0949 [$(M + H)^+$, M = $C_{32}H_{21}F_5N_4O_2Zn$]; λ_{abs} (THF) 426, 648 nm.

Oxochlorins:

Zn(II)-17,18-Dihydro-18,18-dimethyl-10-phenyl-17-oxoporphyrin (OxoZnC-P^{10}). Following a reported procedure for the synthesis of oxochlorins,[51] a mixture of **ZnC-P^{10}** (800 mg, 1.66 mmol) and basic alumina (activity I, 60 g) in 100 mL of toluene was stirred overnight at 60 °C exposed to air. The reaction mixture was filtered and washed with CH_2Cl_2/CH_3OH (19:1). The filtrate was concentrated, and the resulting solid was dissolved in toluene (600 mL). DDQ (940 mg, 4.15 mmol) was added, and the mixture was stirred for 5 min at room temperature. Triethylamine (20 mL) was added, and the solvent was removed under reduced pressure. The residue was immediately chromatographed (silica, CH_2Cl_2) to

afford a purple solid (428 mg, 52%): ^{1}H NMR (400 MHz) δ 2.08 (s, 6H), 7.74–7.76 (m, 3H), 8.11–8.14 (m, 2H), 8.75 (d, J = 4.0 Hz, 1H), 8.84 (d, J = 4.4 Hz, 1H), 9.01–9.03 (m, 3H), 9.05 (d, J = 4.4 Hz, 1H), 9.23 (d, J = 4.4 Hz, 1H), 9.65 (s, 1H), 9.80 (s, 1H); ^{13}C NMR δ 24.1, 50.6, 76.9, 95.2, 98.3, 108.5, 126.7, 128.1, 129.3, 129.8, 130.5, 132.1, 133.3, 133.9, 134.1, 142.2, 150.9, 151.6, 154.1, 165.2, 171.6 (other signals expected were not observed); LD-MS obsd 491.9; ESI-MS obsd 492.0915, calcd 492.0923 ($C_{28}H_{20}N_4OZn$); λ_{abs} (toluene) 417, 606 nm.

20-Bromo-17,18-dihydro-18,18-dimethyl-10-phenyl-17-oxoporphyrin (OxoFbC-P^{10}Br^{20}). A solution of **OxoZnC-P^{10}** (35 mg, 0.071 mmol) in distilled THF (44 mL) under argon was treated with NBS (13 mg, 0.073 mmol) at room temperature. The reaction mixture was stirred for 30 min at room temperature under argon. CH_2Cl_2 and saturated aqueous $NaHCO_3$ were added. The organic layer was washed (water, brine), dried (Na_2SO_4) and concentrated. Column chromatography did not afford separation of the brominated products. The mixture was dissolved in CH_2Cl_2 (0.6 mL) and treated with TFA (0.6 mL, 8 mmol) at room temperature for 2 h to achieve demetalation. Saturated aqueous $NaHCO_3$ was added. The reaction mixture was extracted with CH_2Cl_2. The organic phase was washed (water and brine), dried (Na_2SO_4) and concentrated. Column chromatography [silica, CH_2Cl_2/hexanes (2:3)] afforded a purple solid (11 mg, 38%): ^{1}H NMR (400 MHz) δ –2.66 (br, 1H), –1.85 (br, 1H), 2.20 (s, 6H), 7.78–7.80 (m, 3H), 8.16–8.18 (m, 2H), 8.71 (d, J = 4.3 Hz, 1H), 8.98 (d, J = 4.7 Hz, 1H), 9.09 (d, J = 4.3 Hz, 1H), 9.36–9.38 (m, 1H), 9.47–9.48 (m,

1H), 9.63 (d, J = 4.7 Hz, 1H), 9.94 (s, 1H), 10.13 (s, 1H); LD-MS obsd 508.2; ESI-MS obsd 509.0966, calcd 509.0972 [$(M + H)^+$, M = $C_{28}H_{21}BrN_4O$]; λ_{abs} (toluene) 410, 645 nm.

17,18-Dihydro-18,18-dimethyl-10-phenyl-17-oxoporphyrin (OxoFbC-P^{10}). A solution of **OxoZnC-P^{10}** (320 mg, 0.65 mmol) in CH_2Cl_2 (20 mL) was treated with TFA (750 μL, 9.74 mmol) for 2 h at room temperature. Saturated aqueous solution of $NaHCO_3$ was added. The reaction mixture was extracted with CH_2Cl_2. The organic phase was washed (water and brine), dried (Na_2SO_4) and concentrated. Column chromatography [silica, CH_2Cl_2/hexanes (3:2)] afforded a purple solid (220 mg, 79%): ^{1}H NMR (400 MHz) δ –2.76 (br, 1H), –2.28 (br, 1H), 2.10 (s, 6H), 7.76–7.79 (m, 3H), 8.16–8.18 (m, 2H), 8.78 (d, J = 4.4 Hz, 1H), 8.94 (dd, J = 4.6 Hz, J = 1.7 Hz, 1H), 9.06 (d, J = 4.4 Hz, 1H), 9.19–9.21 (m, 2H), 9.25 (s, 1H), 9.35 (dd, J = 4.6 Hz, J = 1.7 Hz, 1H), 9.92 (s, 1H), 9.98 (s, 1H); ^{13}C NMR δ 24.1, 50.2, 95.3, 96.8, 106.5, 126.3, 126.4, 127.2, 128.1, 128.4. 129.3, 133.9, 134.5, 134.6, 136.8, 137.7, 140.7, 146.4, 153.9, 168.6 (other signals expected were not observed); LD-MS obsd 430.3; ESI-MS obsd 431.1860, calcd 431.1866 [$(M + H)^+$, M = $C_{28}H_{22}N_4O$]; λ_{abs} (toluene) 405, 637 nm.

7-Bromo-17,18-dihydro-18,18-dimethyl-10-phenyl-17-oxoporphyrin (OxoFbC-Br^{7}P^{10}). A solution of **OxoFbC-P^{10}** (100 mg, 0.232 mmol) in distilled THF (60 mL) under argon was treated with NBS (41 mg, 0.23 mmol) for 45 min at room temperature. CH_2Cl_2 and saturated aqueous $NaHCO_3$ were added. The organic layer was washed (water, brine), dried (Na_2SO_4) and concentrated. Column chromatography [silica, CH_2Cl_2/hexanes (3:2)] afforded a purple solid (68 mg, 58%): ^{1}H NMR (400 MHz, THF-d_8) δ –2.69 (br, 1H), –2.27

(br, 1H), 2.06 (s, 6H), 7.78–7.81 (m, 3H), 8.15–8.18 (m, 2H), 8.74 (s, 1H), 8.92–8.94 (m, 1H), 9.33–9.35 (m, 2H), 9.51 (s, 1H), 9.57–9.59 (m, 1H), 9.89 (s, 1H), 10.22 (s, 1H); ^{13}C NMR δ 24.1, 96.9, 127.3, 127.8, 128.1, 129.2, 129.5, 131.0, 134.8, 135.2, 137.3, 139.4, 141.9, 142.5, 148.3, 150.3, 170.6 (other signals expected were not observed); LD-MS obsd 508.0; ESI-MS obsd 509.0972, calcd 509.0970 [$(M + H)^+$, M = $C_{28}H_{21}BrN_4O$]; λ_{abs} (toluene) 411, 637 nm.

7-Acetyl-17,18-dihydro-18,18-dimethyl-10-phenyl-17-oxoporphyrin (OxoFbC-A^{7}P^{10}). Following a procedure for Stille coupling of chlorins,[40] a mixture of **OxoFbC-Br^{7}P^{10}** (37 mg, 0.072 mmol), tributyl(1-ethoxyvinyl)tin (0.10 mL, 0.30 mmol) and $(Ph_3P)_2PdCl_2$ (8 mg, 0.01 mmol) in anhydrous CH_3CN/DMF [3.6 mL (3:2)] under argon was stirred for 3 h at 85 °C in a Schlenk flask. The reaction mixture was treated with 10% aqueous HCl at room temperature for 20 min. CH_2Cl_2 was added. The organic layer was washed (saturated aqueous $NaHCO_3$, water, brine), dried (Na_2SO_4), and filtered. The filtrate was concentrated. Column chromatography (silica, CH_2Cl_2) afforded a red solid (19 mg, 55%): ^{1}H NMR (400 MHz) δ –2.36 (br, 1H), –1.94 (br, 1H), 2.07 (s, 6H), 3.05 (s, 3H), 7.78–7.83 (m, 3H), 8.12–8.14 (m, 2H), 8.84 (d, J = 4.8 Hz, 1H), 9.08–9.12 (m, 3H), 9.16 (s, 1H), 9.39 (d, J = 4.4 Hz, 1H), 9.76 (s, 1H), 11.07 (s, 1H); LD-MS obsd 472.6; ESI-MS obsd 473.1976, calcd 473.1976 [$(M + H)^+$, M = $C_{30}H_{24}N_4O_2$]; λ_{abs} (toluene) 422, 639 nm.

7-Acetyl-17,18-dihydro-17-hydroxy-18,18-dimethyl-10-phenylporphyrin (FbC-A^{7}P^{10}HO^{17}). A sample of **OxoFbC-A^{7}P^{10}** (7 mg, 0.02 mmol) in anhydrous $CHCl_3$ (1.5 mL) under argon was treated with $BH_3 \cdot {}^t$BuNH$_2$ (7 mg, 0.08 mmol) at room temperature for 6 h.

The reaction mixture was diluted with $CHCl_3$ and treated with 5% aqueous HCl (1 mL). The reaction mixture was stirred vigorously for 20 min. The organic phase was washed (5% aqueous HCl, water, saturated aqueous $NaHCO_3$, and brine), dried (Na_2SO_4) and filtered. The filtrate was concentrated to afford a brown solid. Column chromatography [silica, CH_2Cl_2, then CH_2Cl_2/ethyl acetate (20:1)] afforded three fractions, of which the first was the title compound and the latter two were trace amounts of the doubly reduced products. Data for the title compound: brown solid (5 mg, 70%); ^{1}H NMR (400 MHz) δ –1.85 (br, 1H), –1.52 (br, 1H), 1.93 (s, 3H), 2.08 (s, 3H), 2.76 (d, J = 8.3 Hz, 1H), 3.02 (s, 3H), 6.25 (d, J = 8.3 Hz, 1H), 7.76–7.79 (m, 3H), 8.08–8.15 (m, 2H), 8.74 (dd, J = 3.3 Hz, J = 1.7 Hz, 1H), 8.80–8.83 (m, 2H), 8.89 (dd, J = 3.3 Hz, J = 1.4 Hz, 1H), 9.02 (s, 1H), 9.15 (s, 1H), 9.27 (dd, J = 3.0 Hz, J = 1.7 Hz, 1H), 10.9 (s, 1H); LD-MS obsd 474.7; ESI-MS obsd 475.2123, calcd 475.2129 [$(M + H)^+$, M = $C_{30}H_{26}N_4O_2$]; λ_{abs} (toluene) 419, 633 nm.

Data for **FbC-He^{7}P^{10}HO^{17}** (diastereomer 1): LD-MS obsd 475.5; ESI-MS obsd 477.2286, calcd 477.2285 [$(M + H)^+$, M = $C_{30}H_{28}N_4O_2$].

Data for **FbC-He^{7}P^{10}HO^{17}** (diastereomer 2): LD-MS obsd 475.6; ESI-MS obsd 477.2288, calcd 477.2285 [$(M + H)^+$, M = $C_{30}H_{28}N_4O_2$].

7-Bromo-17-(1,3-dioxolan-2-yl)-17,18-dihydro-18,18-dimethyl-10-phenylporphyrin (OxoFbC′-Br^{7}P^{10}). Following a literature procedure,[54] a solution of **OxoFbC-Br^{7}P^{10}** (40 mg, 0.093 mmol) in toluene (25 mL) and ethylene glycol (140 mg, 2.26 mmol) was treated with $TsOH \cdot H_2O$ (9 mg, 0.05 mmol). The resulting mixture was stirred under reflux for 20 h, cooled, poured into ice-water, and extracted with ethyl acetate. The organic extract was dried ($MgSO_4$) and concentrated under reduced pressure. Column

chromatography [silica, CH_2Cl_2/hexanes (3:2)] afforded a green solid (23 mg, 46%): ^{1}H NMR (400 MHz) δ –2.44 (br, 1H), –2.16 (br, 1H), 1.99 (s, 6H), 4.50–4.59 (m, 2H), 4.76–4.84 (m, 2H), 7.71–7.75 (m, 3H), 8.10–8.12 (m, 2H), 8.67 (s, 1H), 8.81–8.83 (m, 1H), 8.90–8.93 (m, 1H), 8.97–8.99 (m, 1H), 9.02 (s, 1H), 9.18 (s, 1H), 9.29–9.30 (m, 1H), 10.07 (s, 1H); ^{13}C NMR δ 24.1, 96.7, 126.3, 127.9, 129.1, 129.7, 130.5, 131.0, 134.8, 135.2, 135.8, 139.7, 142.9, 143.5 (other signals expected were not observed); LD-MS obsd 552.1; ESI-MS obsd 553.1233, calcd 553.1234 [$(M + H)^+$, M = $C_{30}H_{25}BrN_4O_2$]; λ_{abs} (toluene) 405, 632 nm.

7-Acetyl-17-(1,3-dioxolan-2-yl)-17,18-dihydro-18,18-dimethyl-10-phenylporphyrin (OxoFbC′-A^{7}P^{10}). Following a procedure for Stille coupling of chlorins,[40] a mixture of **OxoFbC′-Br^{7}P^{10}** (23 mg, 0.042 mmol), tributyl(1-ethoxyvinyl)tin (57 μL, 0.17 mmol), and $(Ph_3P)_2PdCl_2$ (8 mg, 0.01 mmol) in anhydrous CH_3CN/DMF [3.6 mL (3:2)] under argon was stirred for 3 h at 85 °C in a Schlenk flask. The reaction mixture was treated with 10% aqueous HCl at room temperature for 20 min. CH_2Cl_2 was added. The organic layer was washed (saturated aqueous $NaHCO_3$, water, brine), dried (Na_2SO_4), and filtered. The filtrate was concentrated. Column chromatography [silica, hexanes/CH_2Cl_2/ethyl acetate (7:2:1)] afforded a brownish-red solid (18 mg, 84%): ^{1}H NMR (400 MHz) δ –1.91 (br, 1H), –1.63 (br, 1H), 2.05 (s, 6H), 3.03 (s, 3H), 4.50–4.58 (m, 2H), 4.75–4.83 (m, 2H), 7.76–7.79 (m, 3H), 8.12–8.15 (m, 2H), 8.76 (dd, *J* = 4.9 Hz, *J* = 2.0 Hz, 1H), 8.86 (dd, *J* = 4.9 Hz, *J* = 2.0 Hz, 1H),), 8.88 (s, 1H), 8.93 (dd, *J* = 4.8 Hz, *J* = 1.6 Hz, 1H), 9.056 (s, 1H), 9.064 (s, 1H), 9.31(dd, *J* = 4.8 Hz, *J* = 1.6 Hz, 1H), 10.98 (s, 1H); LD-

MS obsd 516.2; ESI-MS obsd 517.2241, calcd 517.2234 [$(M + H)^+$, M = $C_{32}H_{28}BrN_4O_3$]; λ_{abs} (toluene) 403, 636 nm.

17-(1,3-Dioxolan-2-yl)-17,18-dihydro-3-(1-hydroxyethyl)-18,18-dimethyl-10-phenylporphyrin (OxoFbC′-He^{7}P^{10}). A sample of **OxoFbC′-A^{7}P^{10}** (15 mg, 0.029 mmol) in anhydrous THF/methanol [11 mL (10:1)] was slowly treated with $NaBH_4$ (83 mg, 2.18 mmol) at 0 °C. The mixture was stirred for 1.5 h. Water and ethyl acetate were added, and the resulting mixture was stirred for 20 min. The organic layer was separated, dried (Na_2SO_4), and concentrated. Column chromatography [silica, CH_2Cl_2/ethyl acetate (20:1)] afforded a green solid (11 mg, 71%): ^{1}H NMR (400 MHz) δ –2.45 (br, 1H), –2.21 (br, 1H), 2.01 (s, 6H), 2.14 (d, J = 4.8 Hz, 3H), 2.42–2.44 (m, 1H), 4.53–4.61 (m, 2H), 4.79–4.87 (m, 2H), 6.44–6.46 (m, 1H), 7.71–7.75 (m, 3H), 8.12–8.14 (m, 2H), 8.55 (s, 1H), 8.80–8.82 (m, 1H), 8.94–8.95 (m, 1H), 9.00–9.03 (m, 2H), 9.19 (s, 1H), 9.27–9.29 (m, 1H), 10.14 (s, 1H); LD-MS obsd 518.3; ESI-MS obsd 519.2384, calcd 519.2391 [$(M + H)^+$, M = $C_{32}H_{30}N_4O_3$]; λ_{abs} (toluene) 399, 636 nm.

17,18-Dihydro-7-(1-hydroxyethyl)-18,18-dimethyl-10-phenyl-17-oxoporphyrin (OxoFbC-He^{7}P^{10}). Following a literature procedure,[55] a solution of **OxoFbC′-He^{7}P^{10}** (10 mg, 0.019 mmol) in THF (15 mL) was treated with 10% aqueous HCl (5 mL). The reaction mixture was stirred at room temperature for 36 h. Ethyl acetate was added, and the organic layer was separated. The organic layer was washed (aqueous $NaHCO_3$ and brine), dried (Na_2SO_4), and concentrated. Column chromatography [silica, CH_2Cl_2/ethyl acetate (20:1)] afforded a purple solid (5 mg, 50%): ^{1}H NMR (400 MHz) δ –2.71 (br, 1H), –2.33 (br, 1H),

2.09 (s, 6H), 2.19 (d, J = 5.1 Hz, 3H), 2.47–2.50 (m, 1H), 6.48–6.48 (m, 1H), 7.74–7.79 (m, 3H), 8.14–8.15 (m, 2H), 8.64 (s, 1H), 8.88 (d, J = 4.4 Hz, 1H), 9.16 (d, J = 4.4 Hz, 1H), 9.21 (d, J = 4.4 Hz, 1H), 9.24 (s, 1H), 9.38 (d, J = 4.4 Hz, 1H), 9.89 (s, 1H), 10.25 (s, 1H); LD-MS obsd 474.3; ESI-MS obsd 475.2122, calcd 475.2129 [$(M + H)^+$, M = $C_{30}H_{26}N_4O_2$]; λ_{abs} (toluene) 407, 641 nm.

Zn(II)-17,18-Dihydro-7-(1-hydroxyethyl)-18,18-dimethyl-10-phenyl-17-oxoporphyrin (OxoZnC-He^{7}P^{10}). A sample of **OxoFbC-He^{7}P^{10}** (5 mg, 0.01 mmol) in $CHCl_3$ (3 mL) was treated with $Zn(OAc)_2 \cdot 2H_2O$ (35 mg, 0.16 mmol) in methanol (1 mL) for 12 h at room temperature. The reaction mixture was concentrated. The crude solid was dissolved in CH_2Cl_2, and the organic phase was washed (saturated aqueous $NaHCO_3$, water and brine), dried (Na_2SO_4), and filtered. The filtrate was concentrated. The resulting crude solid was treated with hexanes followed by sonication. The resulting suspension was centrifuged, and supernatant was removed leaving the title compound as a solid (4 mg, 70%): ^{1}H NMR (400 MHz, THF-d_8) δ 2.03 (s, 6H), 2.05 (d, J = 5.6 Hz, 3H), 4.86 (d, J = 4.7 Hz, 1H), 6.33–6.35 (m, J = 4.7 Hz, 1H), 7.71–7.74 (m, 3H), 8.10–8.15 (m, 2H), 8.55 (s, 1H), 8.68 (d, J = 4.4 Hz, 1H), 8.98 (d, J = 4.4 Hz, 1H), 9.02 (d, J = 4.5 Hz, 1H), 9.07 (s, 1H), 9.23 (d, J = 4.5 Hz, 1H), 9.55 (s, 1H), 10.12 (s, 1H); LD-MS obsd 536.9; ESI-MS obsd 537.1262, calcd 537.1263 [$(M + H)^+$, M = $C_{30}H_{24}N_4O_2Zn$]; λ_{abs} (toluene) 419, 609 nm.

Static and Time-resolved Optical Spectroscopy. Argon-purged solutions of the samples in toluene (or THF for **ZnOP-He^{3}P^{10}**, **ZnOP-He^{3}Pf^{10}** and **ZnOP-A^{3}P^{10}**) with an absorbance of ≤0.10 at the excitation wavelength were used for the fluorescence spectral, quantum yield, and lifetime measurements. Solutions used for absorption studies in the same

solvents contained ambient O_2. Solutions of **ZnOP-He^{3}M^{10}** in *n*-hexane containing a small percentage of THF (and ambient O_2) were prepared by adding a small amount of a concentrated pigment solution in THF to *n*-hexane followed by mixing. Static absorption (Varian Cary 100 or Shimadzu UV-1800) and fluorescence (Spex Fluorolog Tau 2 or PTI Quantamaster 40) measurements were performed at room temperature, as were all other studies. Static emission measurements employed 2-4 nm excitation- and detection-monochromator bandwidths and 0.2 nm data intervals. Emission spectra were corrected for detection-system spectral response. Fluorescence quantum yields were determined relative to chlorophyll *a* in benzene[61] or toluene (Chapter III) and were equal: Φ_f = 0.325. Fluorescence lifetimes were obtained by two methods (and typically averaged) as follows: (i) A phase-modulation technique in which samples were excited at various wavelengths in the Soret region and detected through appropriate colored glass filters (Spex Fluorolog Tau 2). Modulation frequencies from 20–300 MHz were utilized and both the fluorescence phase shift and modulation amplitude were analyzed. (ii) Decay measurements using time-correlated-single-photon-counting detection on an apparatus with an approximately Gaussian instrument response function with a full-width-at-half-maximum of ~0.5 ns (Photon Technology International LaserStrobe TM-3). Samples were excited in the Soret or Q regions using excitation pulses at 337 nm from a nitrogen laser or in the blue to green spectral regions from a dye laser pumped by the nitrogen laser.

FTIR Spectroscopy. The FTIR spectra of the solid compounds in either pellet or film forms were collected at room temperature using a Bruker Tensor 27 spectrometer with a spectral resolution of 4 cm^{-1}. The spectra of the solids in pellets were obtained in KBr (~1-2

wt % compound). These spectra were collected in transmission mode using a room-temperature DTGS detector, averaging over 32 scans. The spectra of the solids as films, deposited on a commercially available Si(100) substrate that was hydrogen-passivated, were obtained using a Harrick Scientific Ge attenuated total reflection accessory (GATR™, 65° incidence angle relative to the surface normal). The Si(100) substrates were placed in contact with the flat surface of a semispherical Ge crystal that serves as the optical element. The IR spectra were collected with *p*-polarized light using a liquid-nitrogen cooled medium-bandwidth (600 – 4000 cm^{-1}) MCT detector, averaging over 256 scans. The spectra of the films were referenced against a bare hydrogen-passivated Si(100) substrate. The Ge crystal was cleaned with neat 2-butanone before every experiment, and the GATR™ accessory was purged with dry N_2 during data acquisition.

Resonance Raman Spectroscopy. Resonance Raman (RR) spectra were acquired for both solution and solid film samples. The solution measurements were made on samples dissolved in CH_2Cl_2; the sample cell was a sealed 4 mm i.d. NMR tube, which was spun to mitigate photodecomposition. The film measurements were made on samples deposited on a copper tip that was mounted in an evacuated chamber. All of the RR spectra were acquired at ambient temperature.

The RR spectra were acquired with a triple spectrograph (Spex 1877) equipped with a holographically etched 1200 or 2400 grooves⁄mm grating in the first or third stage. The excitation wavelengths were provided by the discrete outputs of a krypton ion (Coherent Innova 200-K3) laser using 415 nm excitation. The scattered light was collected in a 90° configuration using a 50 mm f⁄1.4 Canon camera lens. A UV-enhanced charge-coupled

device (CCD) was used as the detector (Princeton Instruments LN/CCD equipped with an EEV 1152-UV chip). The data acquisition times were typically 0.5 h (180 • 10 s frames). Cosmic spikes were removed prior to addition of the datasets. The laser power at the samples was 5–10 mW. The spectral resolution was ~2.5 cm^{-1}. The frequencies were calibrated using the known frequencies of indene, fenchone, and 50/50 toluene/acetonitrile.

The results presented in this chapter have been published.[62]

IV.5. References

(1) Green, B. R.; Anderson, J. M.; Parson, W. W. In *Light-Harvesting Antennas in Photosynthesis*; Green, B. R.; Parson, W. W.; Eds.; Kluwer Academic Publishers: The Netherlands, 2003, pp 1–28.

(2) Blankenship, R. E.; Olson, J. M.; Miller, M. In *Anoxygenic Photosynthetic Bacteria*; Blankenship, R. E.; Madigan, M. T.; Bauer, C. E.; Eds.; Kluwer Academic Publishers: The Netherlands, 1995, pp 399–435.

(3) Oostergetel, G. T.; van Amerongen, H.; Boekema, E. J. *Photosynth. Res*. **2010**, *104*, 245–255.

(4) Scheer, H. In *Chlorophylls and Bacteriochlorophylls: Biochemistry, Biophysics, Functions and Applications*; Grimm, B.; Porra, R. J.; Rüdiger, W.; Scheer, H.; Eds.; Kluwer Academic Publishers: The Netherlands, 2006, pp 1–26.

(5) Pšenčik, J.; Ikonen, T. P.; Laurinmäki, P.; Merckel, M. C.; Butcher, S. J.; Serimaa, R. E.; Tuma, R. *Biophys. J.* **2004**, *87*, 1165–1172.

(6) Oostergetel, G. T.; Reus, M.; Gomez Maqueo Chew, A.; Bryant, D. A.; E. J. Boekema, E. J.; Holzwarth, A. R. *FEBS Lett.* **2007**, *581*, 5435–5439.

(7) Pšenčik, J.; Collins, A. M.; Liljeroos, L.; Torkkelli, M.; Laurinmäki, P.; Ansink, H. M.; Ikonen, T. P.; Serimaa, R. E.; Blankenship, R. E.; Tuma, R.; Butcher, S. J. *J. Bacteriol.* **2009**, *191*, 6701–6708.

(8) Kakitani, Y.; Koyama, Y.; Shimoikeda, Y.; Nakai, T.; Utsumi, H.; Shimizu T.; Nagae, H. *Biochemistry* **2009**, *48*, 74–86.

(9) Furamaki, S.; Vacha, F.; Habuchi, S.; Tsukatani, Y.; Bryant, D. A.; Vacha, M. *J. Am. Chem. Soc.* **2011**, *133*, 6703–6710.

(10) Nozawa, T.; Noguchi, T.; Tasumi, M. *J. Biochem.* **1990**, *108*, 737–740.

(11) Egawa, A.; Fujiwara, T.; Mizoguchi, T.; Kakitani, Y.; Koyama, Y.; Akutsu, H. *Proc. Natl. Acad. Sci. U.S.A.* **2007**, *104*, 790–795.

(12) Akutsu, H.; Egawa, A.; Fujiwara, T. *Photosynth. Res.* **2010**, *104*, 221–231.

(13) Balaban, T. S.; Tamiaki, H.; Holzwarth, A. R. *Top. Curr. Chem*. **2005**, *258*, 1–38.

(14) Jochum, T.; Reddy, C. M.; Eichhöfer, A.; Buth, G.; Szmytkowski, J.; Kalt, H.; Moss, D.; Balaban, T. S. *Proc. Natl. Acad. Sci. U.S.A.* **2008**, *105*, 12736–12741.

(15) Ganapathy, S.; Oostergetel, G. T.; Wawrzyniak, P. K.; Reus, M.; Gomez Maqueo Chew, A.; Buda, F.; Boekema, E. J.; Bryant, D. A.; Holzwarth, A. R.; de Groot, H. J. M. *Proc. Natl. Acad. Sci. U.S.A.* **2009**, *106*, 8525–8530.

(16) Balaban, T S.; Bhise, A. D.; Bringmann, G.; Bürck, J.; Chappaz-Gillot, C.; Eichhöfer, A.; Fenske, D.; Götz, D. C. G.; Knauer, M.; Mizoguchi, T.; Mössinger, D.; Rösner, H.; Roussel, C.; Schraut, M.; Tamiaki, H.; Vanthuyne, N. *J. Am. Chem. Soc.* **2009**, *131*, 14480–14492.

(17) Balaban, T. S. *Acc. Chem. Res.* **2005**, *38*, 612–623.

(18) Miyatake, T.; Tamiaki, H. *Coord. Chem. Rev.* **2010**, *254*, 2593–2602.

(19) Balaban, T. S. In *Handbook of Porphyrin Science*; Kadish, K. M.; Smith, K. M.; Guilard, R.; Eds.; World Scientific Publishing Co.: Singapore, vol. 1, 2010, pp 221–306.

(20) Tamiaki, H.; Kouraba, M.; Takeda, K.; Kondo, S.-i.; Tanikaga, R. *Tetrahedron: Asymmetry* **1998**, *9*, 2101–2111.

(21) Miyatake, T.; Tamiaki, H.; Holzwarth, A. R.; Schaffner, K. *Helv. Chim. Acta* **1999**, *82*, 797–810.

(22) Prokhorenko, V. I.; Holzwarth, A. R.; Müller, M. G.; Schaffner, K.; Miyatake, T.; Tamiaki, H. *J. Phys. Chem. B* **2002**, *106*, 5761–5768.

(23) Saga, Y.; Akai, S.; Miyatake, T.; Tamiaki, H. *Chem. Lett.* **2004**, *33*, 544–545.

(24) Sasaki, S.-i.; Tamiaki, H. *J. Org. Chem.* **2006**, *71*, 2648–2654.

(25) Tamiaki, H.; Hamada, K.; Kunieda, M. *Tetrahedron* **2008**, *64*, 5721–5727.

(26) Röger, C.; Müller, M. G; Lysetska, M.; Miloslavina, Y.; Holzwarth, A. R.; Würthner, F. *J. Am. Chem. Soc.* **2006**, *128*, 6542–6543.

(27) Huber, V.; Lysetska, M.; Würthner, F. *Small* **2007**, *3*, 1007–1014.

(28) Röger, C.; Miloslavina, Y.; Brunner, D.; Holzwarth, A. R.; Würthner, F. *J. Am. Chem. Soc.* **2008**, *130*, 5929–5939.

(29) Huber, V.; Sengupta, S.; Würthner, F. *Chem. Eur. J.* **2008**, *14*, 7791–7807.

(30) Balaban, T. S.; Eichhöfer, A.; Lehn, J.-M. *Eur. J. Org. Chem.* **2000**, 4047–4057.

(31) Balaban, T. S.; Bhise, A. D.; Fischer, M.; Linke-Schaetzel, M.; Roussel, C.; Vanthuyne, N. *Angew. Chem. Int. Ed.* **2003**, *42*, 2140–2144.

(32) Balaban, T. S.; Linke-Schaetzel, M.; Bhise, A. D.; Vanthuyne, N.; Roussel, C. *Eur. J. Org. Chem.* **2004**, 3919–3930.

(33) Balaban, T. S.; Linke-Schaetzel, M.; Bhise, A. D.; Vanthuyne, N.; Roussel, C.; Anson, C. E.; Buth, G.; Eichhöfer, A.; Foster, K.; Garab, G.; Gliemann, H.; Goddard, R.; Javorfi, T.; Powell, A. K.; Rösner, H.; Schimmel, T.; *Chem. Eur. J.* **2005**, *11*, 2267–2275.

(34) Balaban, M. C.; Eichhöfer, A.; Buth, G.; Hauschild, R.; Szmytkowski, J.; Kalt, H.; Balaban, T. S. *J. Phys. Chem. B.* **2008**, *112*, 5512–5521.

(35) Kunieda, M.; Tamiaki, H. *J. Org. Chem.* **2009**, *74*, 5803–5809.

(36) Szymtkowski, J.; Conradt, J.; Kuhn, H.; Reddy, C. M.; Balaban, M. C.; Balaban, T. S.; Kalt, H. *J. Phys. Chem. C* **2011**, *115*, 8832–8839.

(37) Ptaszek, M.; Yao, Z.; Savithri, D.; Boyle, P. D.; Lindsey, J. S. *Tetrahedron* **2007**, ***63***, 12629–12638.

(38) Gurinovich, G. P.; Sevchenko, A. N.; Solov'ev, K. N. *Opt. Spectrosc.* **1961**, *10*, 396–401.

(39) Gouterman, M.; Stryer, L.; *J. Chem. Phys.* **1962**, *37*, 2260–2266.

(40) Laha, J. K.; Muthiah, C.; Taniguchi, M.; McDowell, B. E.; Ptaszek, M.; Lindsey, J. S. *J. Org. Chem.* **2006**, *71*, 4092–4102.

(41) Laha, J. K.; Muthiah, C.; Taniguchi, M.; Lindsey, J. S. *J. Org. Chem.* **2006**, *71*, 7049–7052.

(42) Kee, H. L.; Kirmaier, C.; Tang, Q.; Diers, J. R.; Muthiah, C.; Taniguchi, M.; Laha, J. K.; Ptaszek, M.; Lindsey, J. S.; Bocian, D. F.; Holten, D. *Photochem. Photobiol*. **2007**, *83*, 1110–1124.

(43) Muthiah, C.; Ptaszek, M.; Nguyen, T. M.; Flack, K. M.; Lindsey, J. S. *J. Org. Chem*. **2007**, *72*, 7736–7749.

(44) Muthiah, C.; Lahaye, D.; Taniguchi, M.; Ptaszek, M.; Lindsey, J. S. *J. Org. Chem*. **2009**, *74*, 3237–3247.

(45) Ptaszek, M.; Lahaye, D.; Krayer, M.; Muthiah, C.; Lindsey, J. S. *J. Org. Chem*. **2010**, *75*, 1659–1673.

(46) Moss, G. P.; *Pure Appl. Chem.* **1987**, *59*, 779–832.

(47) Krayer, M.; Balasubramanian, T.; Ruzié, C.; Ptaszek, M.; Cramer, D. L.; Taniguchi, M.; Lindsey, J. S. *J. Porphyrins Phthalocyanines* **2009**, *13*, 1098–1110.

(48) Mass, O.; Ptaszek, M.; Taniguchi, M.; Diers, J. R.; Kee, H. L.; Bocian, D. F.; Holten, D.; Lindsey, J. S. *J. Org. Chem*. **2009**, *74*, 5276–5289.

(49) Ptaszek, M.; McDowell, B. E.; Lindsey, J. S. *J. Org. Chem.* **2006**, *71*, 4328–4331.

(50) Taniguchi, M.; Kim, H.-J.; Ra, D.; Schwartz, J. K.; Kirmaier, C.; Hindin, E.; Diers, J. R.; Prathapan, S.; Bocian, D. F.; Holten, D.; Lindsey, J. S. *J. Org. Chem.* **2002**, *67*, 7329–7342.

(51) Taniguchi, M.; Kim, M. N.; Ra, D.; Lindsey, J. S. *J. Org. Chem*. **2005**, *70*, 275–285.

(52) Taniguchi, M.; Ptaszek, M.; McDowell, B. E.; Lindsey, J. S. *Tetrahedron* **2007**, *63*, 3840–3849.

(53) Ptaszek, M.; McDowell, B. E.; Taniguchi, M.; Kim, H.-J.; Lindsey, J. S. *Tetrahedron* **2007**, *63*, 3826–3839.

(54) Smith, E. M.; Swiss, G. F.; Neustadt, B. R.; Gold, E. H.; Sommer, J. A.; Brown, A. D.; Chiu, P. J. S.; Moran, R.; Sybertz, E. J.; Baum, T. *J. Med. Chem*. **1988**, *31*, 875–885.

(55) Grieco, P. A.; Nishizawa, M.; Oguri, T.; Burke, S. D.; Marinovic, N. *J. Am. Chem. Soc*. **1978**, *99*, 5773–5780.

(56) Mass, O.; Taniguchi, M.; Ptaszek, M.; Springer, J. W.; Faries, K. M.; Diers, J. R.; Bocian, D. F.; Holten, D.; Lindsey, J. S. *New J. Chem*. **2011**, *35*, 76–88.

(57) Kirmaier, C.; Hinden, E.; Schwartz, J. K.; Sazanovich, I. V.; Diers, J. R.; Muthukumaran, K.; Taniguchi, M.; Bocian, D. F.; Lindsey, J. S.; Holten, D. *J. Phys. Chem*. *B* **2003**, *107*, 3443–3454.

(58) Smith, K. M.; Kehres, L. A.; Fajer, J. *J. Am. Chem. Soc*. **1983**, *105*, 1387–1389.

(59) Tamiaki, H.; Yoshimura, H.; Shimamura, Y.; Kunieda, M. *Photosynth. Res.* **2008**, *95*, 223–228.

(60) Lutz, M.; Robert, B. In *Biological Applications of Raman Spectroscopy. Resonance Raman Spectra of Heme and Metalloproteins*; Spiro, T. G.; Ed.; Wiley: New York, 1988, vol. 3, pp 347–412.

(61) Weber, G.; Teale, F. W. J. *Trans. Faraday Soc.* **1957**, *53*, 646–655.

(62) Mass, O.; Pandithavidana, D. R.; Ptaszek, M.; Santiago, K.; Springer, J. W.; Jiao, J. Y.; Tang, Q.; Kirmaier, C.; Bocian, D.F.; Holten, D.; Lindsey, J. S. *New J. Chem.*, **2011**, *35,* 2671–2690.

CHAPTER V

Investigation of Essential Motifs in Hydrodipyrrin Precursors Leads to a *trans*-AB-Bacteriochlorin Building Block

V.1. Introduction

A longstanding theme in tetrapyrrole chemistry has been the de novo synthesis of building blocks for use in studies encompassing the broad fields of biomimetic chemistry, materials science, and clinical medicine. Porphyrins with up to four distinct meso-substituents are readily available.[1,2] The chemistry of chlorins is less developed, but chlorin macrocycles with substituents at designated meso- and β-pyrrole sites have been prepared.[3,4] For bacteriochlorins, synthetic access is under active development. Bacteriochlorins are of considerable interest owing to their strong absorption in the near-infrared spectral region, which is attractive for solar energy applications, low-energy photochemistry, and deep-tissue light-mediated medical therapies.[5,6] Realizing the scientific potential of bacteriochlorins has been largely crimped, however, by the limited means for synthesis of stable, tailorable bacteriochlorin building blocks.[7]

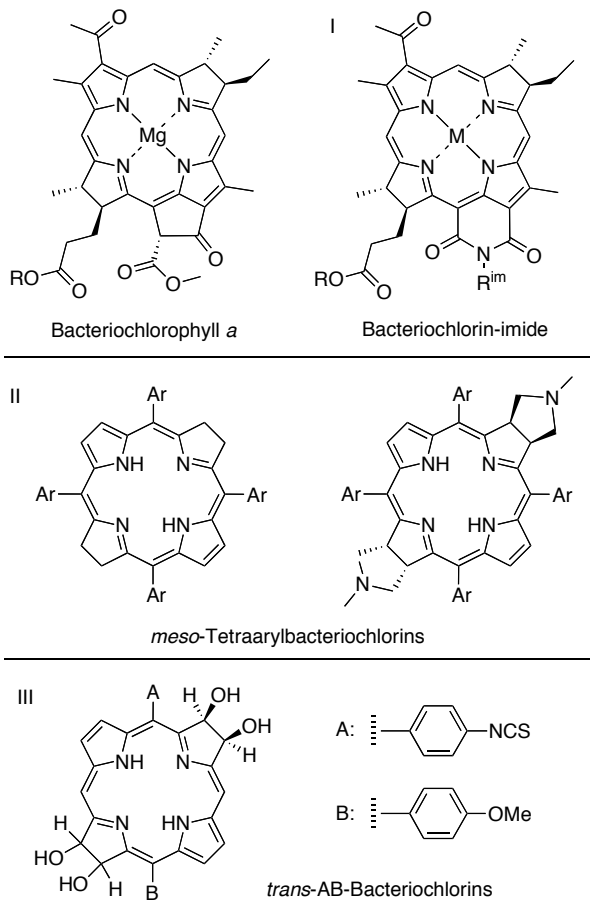

Chart V.1. Bacteriochlorophyll *a* and bacteriochlorin building blocks.

Distinct methods for the synthesis of bacteriochlorins entail semisynthesis procedures beginning with bacteriochlorophyll *a*;[8-14] hydrogenation[15,16] of (or addition to)[4,17-22] synthetic porphyrins and chlorins; and de novo routes.[5,23-28] Each has strengths and limitations. Representative building blocks available via such methods are shown in Chart V.1. Derivatization of bacteriochlorophyll *a* to form the imide ring stabilizes the macrocycle and provides a convenient handle at the *N*-imide site for derivatization (entry I).[29] Still, few other sites are available given the nearly full complement of β-substituents. *meso*-

Tetraarylbacteriochlorins (entry II) are readily synthesized yet the presence of four identical substituents may limit the accessible architectures. Two variants on this approach include (i) a strategy by Brückner to achieve wavelength tunability,[30] and (ii) a strategy by Boyle wherein *trans*-AB-porphyrins undergo vicinal dihydroxylation to afford the corresponding *trans*-AB-bacteriochlorin building blocks (albeit composed of a mixture of diastereomers, entry III).[31]

A rational, de novo route to synthetic bacteriochlorins[25,28] that we have been developing affords the following features: (1) resiliency of the macrocycles toward dehydrogenation upon routine handling by virtue of a geminal-dimethyl group in each reduced ring;[25] (2) a relatively concise (8-step) synthesis;[27,28] (3) characteristic bacteriochlorin absorption and photophysical features;[6,32] and (4) ability to introduce a variety of β-pyrrole substituents.[5,26,28] The synthetic route employs the acid-mediated, room-temperature self-condensation of a dihydrodipyrrin–acetal (Scheme V.1). The use of TMSOTf in the presence of 2,6-di-*tert*-butylpyridine (2,6-DTBP) results in the formation of the 5-methoxybacteriochlorin in 8.4–63% yield depending on the nature of the β-pyrrolic substituents.[28] The 5-methoxybacteriochlorin **BC-1** undergoes regioselective electrophilic bromination at the 15-position,[33] enabling further derivatization at this site via diverse palladium-coupling processes.[29,33] In contrast, bromination of the 5-unsubstituted bacteriochlorin **BC-2** (available via $BF_3{\cdot}OEt_2$ or other catalysis)[28] results in a mixture of mono- and dibromobacteriochlorins.[33]

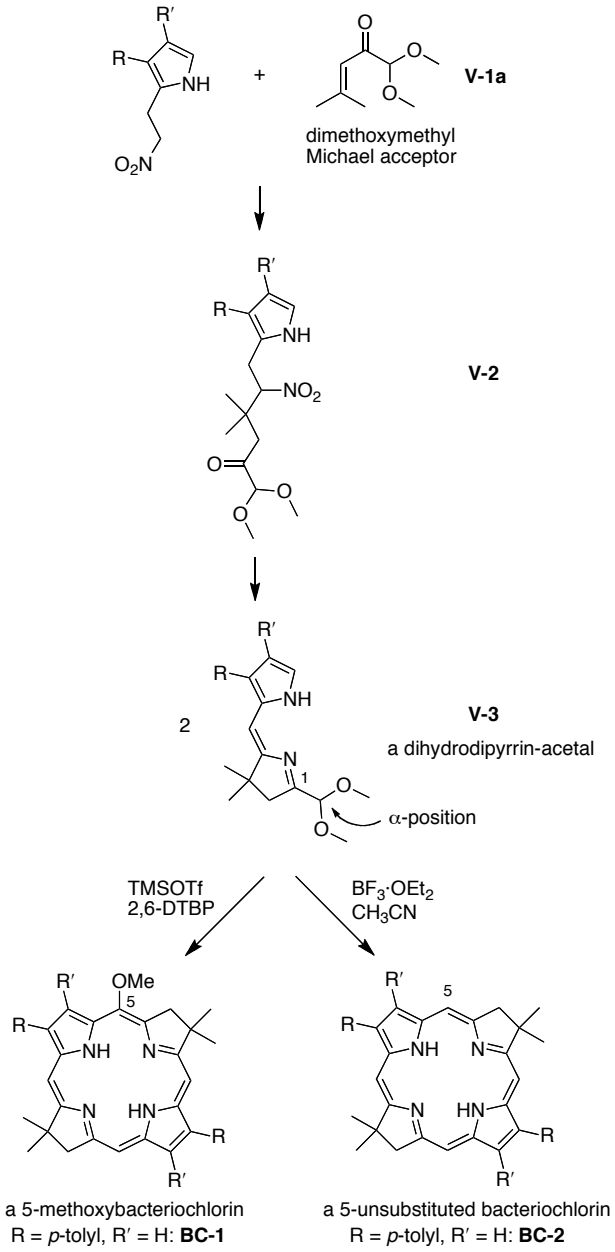

Scheme V.1. De novo route to bacteriochlorins.

While the de novo method has provided access to a larger palette of substituted bacteriochlorins versus those via semisynthesis or porphyrin/chlorin reductive

transformations, numerous limitations have persisted: (1) the substituents at the 2- and 12-positions are identical with each other (R), as are those at the 3- and 13-position (R′); and (2) the 5-position has heretofore been occupied either by –H or –OCH_3. Accordingly, access to *trans*-AB-bacteriochlorins akin to those of Boyle has not been available. A linear pattern of meso-AB-substituents is attractive for the design of diverse molecular architectures.

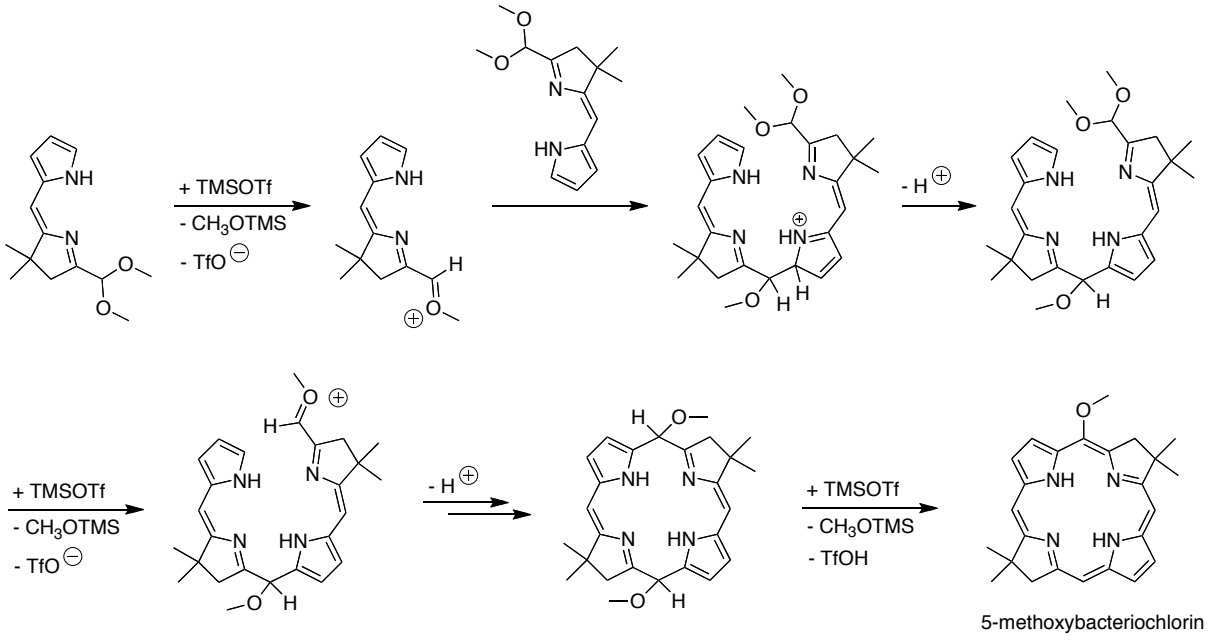

Scheme V.2. Key steps in the formation of 5-methoxybacteriochlorin.

To achieve a *trans*-AB substituent pattern in bacteriochlorins, we considered that alternative dihydrodipyrrin units could be employed in the self-condensation. Because the acetal carbon of the dihydrodipyrrin–acetal (i.e., the α-carbon at the 1-position) forms the 5- and 15- carbons of the bacteriochlorin, alternative substituents at the "acetal" α-carbon in lieu of the methoxy group could be conveyed to the bacteriochlorin 5-position. The 15-

position would then be accessible for bromination and subsequent substitution processes. This analysis is consistent with our current conceptualization of the mechanism of formation of the 5-methoxybacteriochlorin (Scheme V.2). Treatment of the dihydrodipyrrin–acetal with TMSOTf affords an oxocarbenium ion and eliminates one molecule of methanol (as the trimethylsilyl ether); the oxocarbenium ion serves as the electrophile for attack by the pyrrole of the other dihydrodipyrrin–acetal. Repetition of this process eliminates a second molecule of methanol and affords the 5,15-dimethoxy-5,15-dihydrobacteriochlorin. Elimination of the third molecule of methanol results in the aromatic bacteriochlorin macrocycle containing the 5-methoxy substituent.[25]

Here, we report the synthesis of a handful of dihydrodipyrrins (containing diverse substituents at the 1-position) and investigate their conversion to bacteriochlorins. The synthesis of the dihydrodipyrrins was facilitated by the development of a new route to the α,β-unsaturated ketone–acetal **V-1a** (the Michael acceptor in formation of the dihydrodipyrrin–acetal), which also is reported herein. Among four new dihydrodipyrrins, one was found to afford the corresponding bacteriochlorin, which contains a 5-(2-hydroxyethoxy) substituent. Bromination of the 5-(2-hydroxyethoxy)bacteriochlorin proceeded smoothly at the 15-position, affording the bacteriochlorin with reactive functional groups in a *trans*-AB architecture.

V.2. Results and Discussion

V.2.1. Synthesis of New Michael Acceptors

A. Reconnaissance. The first reported synthesis of Michael acceptor **V-1a** was carried out in 56% yield when 2 mmol of mesityl oxide was treated with 10 mol % of diphenyl diselenide and excess ammonium peroxydisulfate in methanol (Scheme V.3).[34] A subsequent scaled-up procedure employed a catalytic amount of diphenyl diselenide and afforded **V-1a** in 29% yield.[25] Significant drawbacks to the synthesis of **V-1a** remain: (i) use of expensive and toxic diphenyl diselenide; (ii) difficult purification including distillation followed by extensive chromatography, and (iii) relatively low yield. Moreover, the method has limited scope for introduction of substituents other than the dimethoxymethyl unit, which gives rise to the 5-methoxy substituent in the bacteriochlorin. Here, a scalable and more versatile synthesis of Michael acceptors was envisaged to entail reaction of 2-methyl-1-propenylmagnesium bromide (**V-4**) with an acetal-containing nitrile or Weinreb amide (*N*-methoxy-*N*-methylamide; Scheme V.3). To our knowledge, preparation of α,β-unsaturated ketones by reaction of a nitrile and a vinyl Grignard reagent has not been reported previously. Our attempts to prepare the 1,1-dialkoxy-α,β-unsaturated ketones via the Weinreb amide method were not successful; however, we did prepare such compounds via the nitrile method. The α,β-unsaturated ketones bearing a single alkoxy group or other substituents examined herein were prepared via the Weinreb amide method (vide infra).

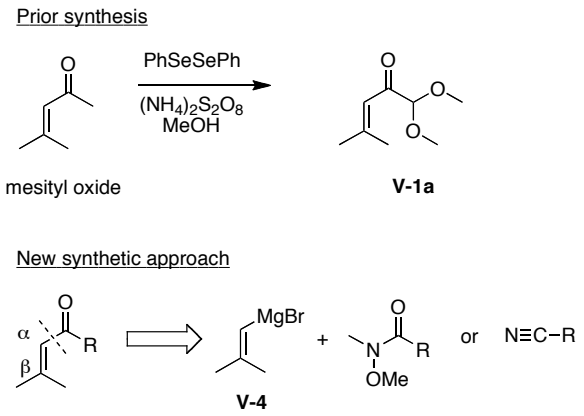

Scheme V.3. Prior and envisaged routes to Michael acceptors.

B. Attempted synthesis of dimethoxymethyl ketone V-1a. In our initial studies we attempted to convert methyl dimethoxyacetate to dimethoxymethyl ketone **V-1a** via treatment of the *N*-methoxy-*N*-methylamide (Weinreb amide) intermediate with an organomagnesium reagent.[35] The Weinreb amide is prepared by treatment of an ester with *i*-PrMgCl and Me(MeO)NH·HCl.[36] However, when the slurry of methyl dimethoxyacetate and 1.25 mol equiv of *N,O*-dimethylhydroxylamine hydrochloride in THF was treated with 2.5 mol equiv of *i*-PrMgCl at –20 °C according to a general procedure,[36] putative isopropylketone **V-A** and unreacted methyl dimethoxyacetate were obtained in 1:1 ratio (Scheme V.4). Reversal of the order of addition (treatment of *i*-PrMgCl with Me(MeO)NH·HCl at –25 °C for 40 min followed by methyl dimethoxyacetate)[37] gave the same result. On the other hand, the attempted direct conversion by treatment of methyl dimethoxyacetate and Me(MeO)NH·HCl with 3.3 mol equiv of 2-methyl-1-propenylmagnesium bromide at –20 °C afforded an inseparable mixture that contained the

desired **V-1a** and a putative tertiary alcohol (**V-B**) in 3:5 ratio as determined by GC-MS and ^{1}H NMR analysis.

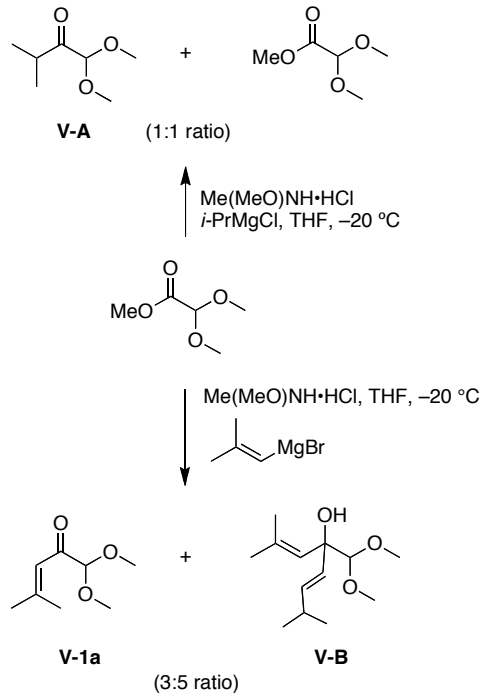

Scheme V.4. Attempted synthesis of the dimethoxymethyl-containing Michael acceptor **V-1a**.

C. Synthesis of Michael Acceptors via Nitrile Method. Treatment of trimethyl orthoformate with an equimolar amount of trimethylsilyl cyanide in the presence of 10 mol % of $BF_3 \cdot OEt_2$ afforded dimethoxyacetonitrile (**V-5a**).[38,39] The reaction was carried out at 255-mmol scale (11-fold larger than the literature procedure[38]). Reaction of **V-5a** with 1.2 mol equiv of Grignard reagent **V-4** at room temperature for 2.5 h followed by hydrolysis with saturated aqueous NH_4Cl afforded **V-1a** as the major product (Scheme V.5). The 2-step synthesis was carried out with streamlined workup procedures: distillation at atmospheric

pressure gave **V-5a** in 90% yield (>90% purity), whereas distillation at reduced pressure gave **V-1a** in 57% yield (16.5 g, 90% purity). The formation of **V-1a** is accompanied by trace quantities of multiple products that could not be fully separated by distillation; on the other hand, when column chromatography [silica, hexanes/ethyl acetate] was employed, **V-1a** was obtained in high purity yet only 29% yield. The 2-step synthesis of **V-1a** also uses little solvent. The conversion of trimethyl orthoformate to **V-5a** is solvent-free, and the conversion of **V-5a** to **V-1a** employs 2-methyl-1-propenylmagnesium bromide (**V-4**, available commercially as a 0.5 M solution in THF) and no other solvent. In this regard, both reactions are carried out at the highest possible concentration, an approach commensurate with the objective of preparing multigram quantities of the valuable intermediate **V-1a**. While the yield of this transformation is not high, the nitrile method overcomes the limitations of the prior synthesis with diphenyl diselenide, and moreover, can be employed to prepare α,β-unsaturated ketones with diverse functionalities at the methyl site.

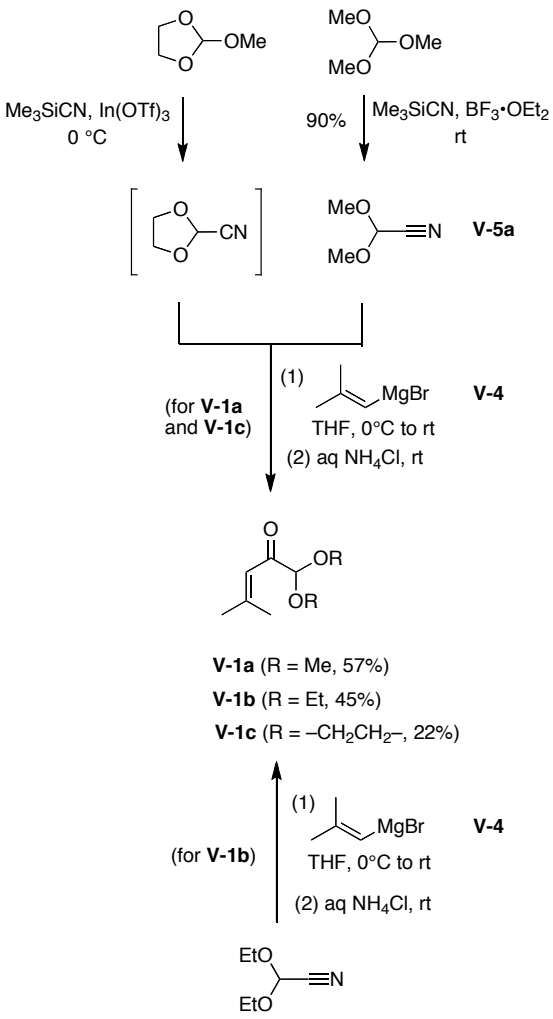

Scheme V.5 New scalable synthesis of Michael acceptors via a nitrile intermediate.

The new route established for **V-1a** was extended to two other Michael acceptors. First, commercially available diethoxyacetonitrile afforded diethoxymethyl Michael acceptor **V-1b** in 45% yield (Scheme V.5). Second, treatment of 2-methoxy-1,3-dioxolane with 1 mol equiv of trimethylsilyl cyanide in the presence of a catalytic amount of $In(OTf)_3$ for 1 h at 0 °C afforded 1,3-dioxolane-2-carbonitrile. (An exploratory survey showed $BF_3 \cdot OEt_2$, $InCl_3$ and $Yb(OTf)_3$ to give additional byproducts as observed upon ^1H NMR analysis of crude

samples.) The ^{1}H NMR spectrum of the crude 1,3-dioxolane-2-carbonitrile was consistent with literature data.[40] The dioxolane–nitrile was found to be unstable, and for this reason was used directly in the next step. Treatment of the crude nitrile with **V-4** afforded **V-1c** in 22% overall yield. Compound **V-1c** was found to be very unstable in air, but could be stored in a degassed ether solution at –20 °C for several months without decomposition.

Transacetalization of diethoxyacetal **V-1b** with 1,3-propanediol in benzene/TsOH afforded 1,3-dioxane **V-1d** in 64% yield (Eqs V.1). This apparently simple approach could not be generalized: attempted transacetalization of **V-1b** with ethylene glycol afforded a chromatographically inseparable mixture of **V-1c** and a putative byproduct **V-C** (Eqs V.2).

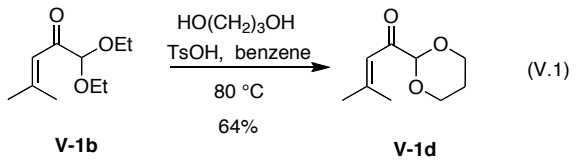

V-1b **V-1d** (V.1)

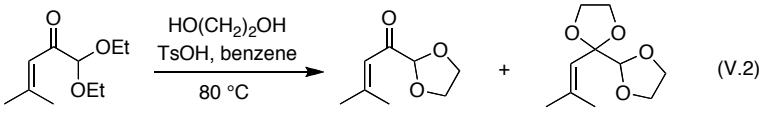

V-1b **V-1c** **V-C** (1:1 ratio) (V.2)

D. Synthesis of New Michael Acceptors via Weinreb Amides. Treatment of α-methoxyacetic acid (**V-6e**) with 1,1′-carbonyldiimidazole (CDI) and *N,O*-dimethylhydroxylamine hydrochloride followed by **V-4** afforded methoxymethyl Michael acceptor **V-1e** in 22% yield (Table V.1). The reaction of known phenoxymethyl Weinreb amide **V-7f** (prepared from phenoxyacetic acid (**V-6f**) and *N,O*-dimethylhydroxylamine

hydrochloride with CDI)[41] with 1.1 mol equiv of **V-4** afforded phenoxymethyl Michael acceptor **V-1f** in nearly quantitative yield. Similarly, treatment of α-methoxyphenylacetic acid (**V-6g**) with CDI followed by triethylamine and *N,O*-dimethylhydroxylamine hydrochloride afforded amide **V-7g** in 58% yield. (The *S*-enantiomer of **V-7g** is described in the literature.[42]) The reaction of **V-7g** with 1.1 mol equiv of **V-4** afforded α-methoxybenzyl Michael acceptor **V-1g** in 87% yield.

A general procedure was followed to convert an ester to a Weinreb amide.[36] Thus, treatment of ethyl 1,3-dithiolane-2-carboxylate (**V-6h**) and 2.5 mol equiv of *N,O*-dimethylhydroxylamine hydrochloride in THF with 5 mol equiv of isopropylmagnesium chloride at –78 °C afforded **V-7h** in 49% yield. Compound **V-7h** was prepared previously in three steps from glyoxylic acid in 47% overall yield.[43] The reaction of Weinreb amide **V-7h** with 1.1 mol equiv of **V-4** afforded Michael acceptor **V-1h** in 77% yield (Table V.1).

Table V.1. Synthesis of Michael acceptors via Weinreb amides.

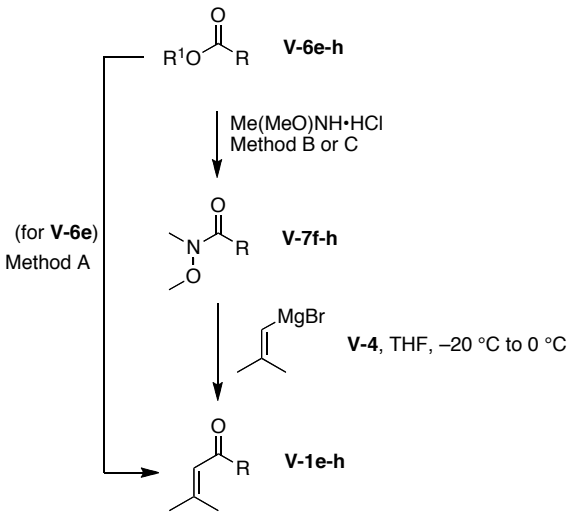

Entry	R	Acid derivative	Weinreb amide	Method	Yield %	**V-1**	Yield %
1	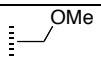	**V-6e** (R^1 = H)	n/a	A[a]	n/a	**V-1e**	22
2		**V-6f** (R^1 = H)	**V-7f**	B[b]	91	**V-1f**	97
3		**V-6g** (R^1 = H)	**V-7g**	B[b]	58	**V-1g**	87
4		**V-6h** (R^1 = Et)	**V-7h**	C[c]	49	**V-1h**	77

[a]Method A: (1) CDI, CH_2Cl_2, 0 °C to rt; (2) Me(MeO)NH·HCl, Et_3N, CH_2Cl_2, 0 °C to rt; (3) **V-4**, THF, –20 °C to 0 °C. [b]Method B: (1) CDI, CH_2Cl_2, 0 °C to rt; (2) Me(MeO)NH·HCl, Et_3N, CH_2Cl_2, 0 °C to rt. [c]Method C: (1) Me(MeO)NH·HCl; (2) *i*-PrMgCl, THF, –78 °C.

V.2.2. Synthesis of New Dihydrodipyrrins

Following a general approach to the synthesis of dihydrodipyrrins,[28] nitroethylpyrrole **V-8**[28] was treated with 1.1–2.4 mol equiv of a Michael acceptor (**V-1c-h**) in the presence of 3 mol equiv of DBU at room temperature to afford the corresponding hexanone (**V-2c-h**). The results are summarized in Table V.2. The yields obtained with the benchmark compounds for the series **V-1a** → **V-2a** → **V-3a** are provided for comparison (entry 1).[28] The $TiCl_3$-mediated reductive cyclization of **V-2c-f** afforded dihydrodipyrrins **V-3c-f** (entries 2–5); however, analogous reaction of **V-2g** or **V-2h** did not afford the corresponding dihydrodipyrrin yet all starting material was consumed (entries 6,7). The crude **V-3g** decomposed immediately after the reaction work-up. The reaction with **V-2h** afforded unidentified products.

Table V.2. Synthesis of dihydrodipyrrins.

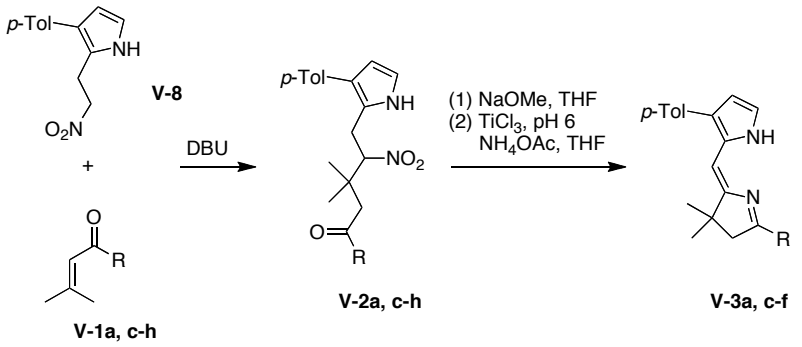

Entry	V-1	R	V-2	Yield, %	V-3	Yield, %
1	**V-1a**[a]		**V-2a**	63	**V-3a**	54
2	**V-1c**		**V-2c**	54	**V-3c**	31
3	**V-1d**	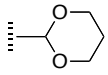	**V-2d**	35	**V-3d**	18
4	**V-1e**		**V-2e**	70	**V-3e**	22
5	**V-1f**	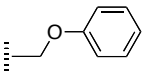	**V-2f**	60	**V-3f**	37
6	**V-1g**	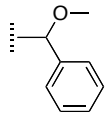	**V-2g**	63	**V-3g**	0
7	**V-1h**		**V-2h**	36	**V-3h**	0

[a]Ref. 28.

V.2.3. Self-condensation Study

The self-condensation conditions (5 equiv of TMSOTf and 20 equiv of 2,6-DTBP in CH_2Cl_2) employed previously for dihydrodipyrrin–acetals bearing a 1-(dimethoxymethyl) unit and diverse β-pyrrole substituents[28] were recently modified to use a lesser amount of reagents (4 equiv of TMSOTf and 8 equiv of 2,6-DTBP).[44] The latter conditions were applied with dihydrodipyrrins **V-3c-f**. The crude reaction mixtures (neutralized with aqueous saturated $NaHCO_3$, and washed with water) were analyzed for the presence of bacteriochlorin macrocycles by TLC, laser-desorption mass spectrometry (LD-MS) and UV-Vis spectroscopy. The results are shown in Table V.3. For comparison, dihydrodipyrrin–acetal **V-3a** affords bacteriochlorin **BC-1** (entry 1). Dihydrodipyrrin–dioxolane **V-3c** also successfully afforded a bacteriochlorin (entry 2; vide infra), whereas dihydrodipyrrin–dioxane **V-3d** resulted in partial decomposition and no bacteriochlorin (entry 3). Dihydrodipyrrin **V-3e**, bearing a methoxymethyl group, gave only a small LD-MS peak corresponding to a tetradehydrocorrin[25,46] macrocycle, but the product was not isolated (entry 4). Dihydrodipyrrin **V-3f**, bearing a phenoxymethyl group, gave decomposition with no starting material or macrocycle observed (entries 5, 6).

Table V.3. Self-Condensation survey of dihydrodipyrrins.

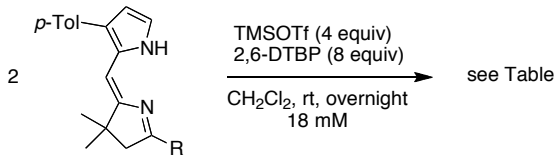

V-3a, c-f

Entry	R	Dihydrodipyrrin	Result
1[a]		**V-3a**	**BC-1**, 40.7%
2		**V-3c**	**BC-3**, 30%
3	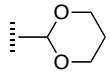	**V-3d**	0[b]
4		**V-3e**	0[b]
5	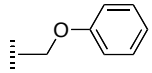	**V-3f**	0[c]

[a]Ref.44. [b]Unreacted starting material and decomposition observed. [c]Decomposition.

V.2.4. Synthesis of *trans*-AB-bacteriochlorin Building Block

The success of dihydrodipyrrin **V-3c** in the survey reaction prompted scale-up to fully characterize the resulting bacteriochlorin. Thus, the self-condensation of dihydrodipyrrin **V-3c** (0.76 mmol) in the presence of 4 mol equiv of TMSOTf and 8 mol equiv of 2,6-DTBP in CH_2Cl_2 afforded bacteriochlorin **BC-3** in 30% yield; no other macrocycles were observed by

TLC and LD-MS analyses. Consistent with the mechanistic picture shown in Scheme V.2, bacteriochlorin **BC-3** contained a 2-(trimethylsilyloxy)ethoxy group at the 5-position (Scheme V.6). Treatment with 1.5 mol equiv of TBAF at room temperature under argon cleaved the TMS group and afforded the 5-(2-hydroxyethoxy)bacteriochlorin **BC-4** in 83% yield.

Bacteriochlorins with a 5-methoxy group undergo smooth and selective bromination at the 15-position, whereas bacteriochlorins lacking a 5-methoxy group typically afford a mixture of bromobacteriochlorins.[28,33] To examine whether the hydroxyethoxy group directed selective bromination, bacteriochlorin **BC-4** was treated with 1 mol equiv of NBS at room temperature. The resulting bacteriochlorin (**BC-5**) was obtained in 64% yield and contained a bromine atom at the 15-position (established by NOESY). When TMS-protected bacteriochlorin **BC-3** was treated with 1 mol equiv of NBS, bacteriochlorin **BC-5** was obtained as well in 65% yield indicating that NBS acted both as a deprotecting and brominating agent. Bacteriochlorin **BC-5** contains two reactive functional groups at opposing meso positions. Analogues of **BC-5** that bears diverse β-pyrrole substituents and the same *trans*-AB substituents are expected to afford valuable building blocks.

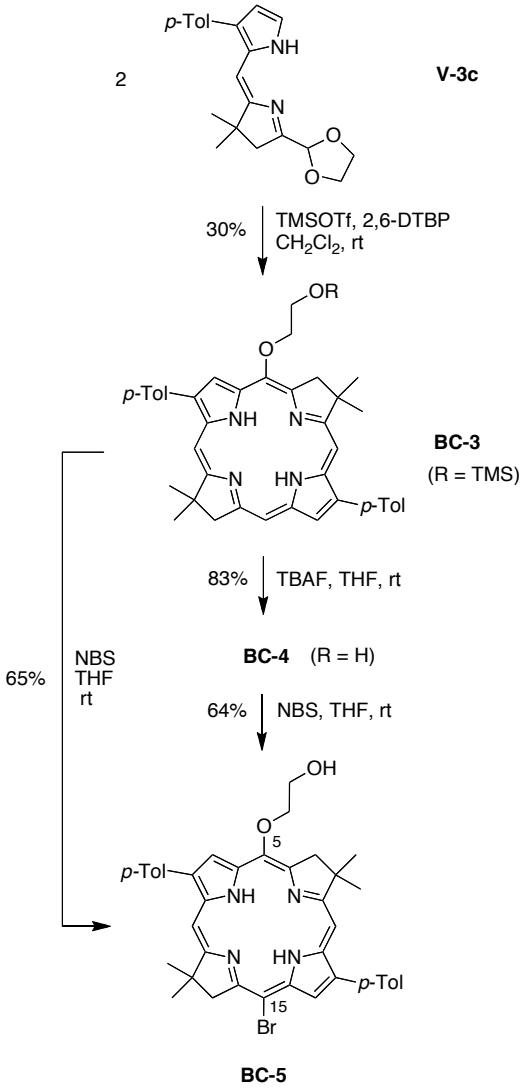

Scheme V.6. Synthesis of a *trans*-AB-bacteriochlorin.

V.3. Outlook

A scalable synthesis was developed to gain access to α,β-unsaturated ketones for use as Michael acceptors in the preparation of bacteriochlorins. One method employed the reaction of a nitrile and vinyl Grignard reagent. This new approach and that with Weinreb amides afforded diverse substituents in place of the dimethoxymethyl unit. Upon screening

of four new dihydrodipyrrins that bear distinct electrophilic centers, the dihydrodipyrrin bearing a 1,3-dioxolan-2-yl group (**V-3c**) was found to afford the corresponding 5-(2-hydroxyethoxy)bacteriochlorin (**BC-4**). Consistent with the mechanism of 5-methoxybacteriochlorin formation, the condensation of two molecules of a dihydrodipyrrin bearing a 1,3-dioxolan-2-yl group is accompanied by formal release of three alcohol units, yet here the first two are integral to an ethylene glycol molecule whereas the third moiety is the terminus of the hydroxyethoxy unit anchored at the 5-position of the bacteriochlorin. Previously, the only type of 1-substituent in a dihydrodipyrrin that afforded a bacteriochlorin was a dimethoxymethyl unit (e.g., **V-3a**).[25,28] Although a singular success from a broad survey, the resulting bacteriochlorin **BC-4** and its 15-brominated derivative (**BC-5**) are expected to be valuable building blocks given the orthogonality and linear arrangement of the functional groups disposed at the 5- and 15-positions. The singular success with the new dihydrodipyrrin–acetal highlights the exacting structural features of the dihydrodipyrrin electrophilic site for successful self-condensation.

V.4. Experimental Section

General Methods. ^{1}H NMR (300 MHz) and ^{13}C NMR (100 MHz) spectra were collected at room temperature in $CDCl_3$ unless noted otherwise. Absorption spectra were obtained in toluene at room temperature unless noted otherwise. Electrospray ionization mass spectrometry [HRMS (ESI)] data are reported for the molecular ion or cationized molecular ion. Laser-desorption mass spectrometry was performed without a matrix. All commercially available materials (including **V-4**, **V-6e-h**) were used as received. Non-

commercially available compounds **V-5a** (11-fold larger scale),[38,39] **V-7f**,[41] and **V-8**[28], **V-9**[28] were prepared as described in the literature; in each case the identity and purity were established by ^{1}H NMR spectroscopy.

1,1-Dimethoxy-4-methyl-3-penten-2-one (V-1a). Dimethoxyacetonitrile (**V-5a**, 18.7 g, 185 mmol) in a 1-L round bottom flask equipped with a stirring bar and a 500-mL addition funnel (all oven-dried) was treated under argon with **V-4** (445 mL, 222 mmol, 0.5 M in THF) over 30 min at 0 °C following by stirring for 2 h at room temperature. The bright yellow-orange solution was treated with saturated aqueous NH_4Cl (500 mL), and the reaction mixture was vigorously stirred for 2 h. ^{1}H NMR spectroscopy indicated the completion of hydrolysis (disappearance of peaks at 5.89 ppm and 4.61 ppm (imine) and appearance of peaks at 6.34 ppm and 4.49 ppm). The aqueous phase was extracted with Et_2O (3 x 350 mL), and each organic extract was washed (brine). The combined organic extract was dried (Na_2SO_4) and concentrated to an orange liquid. Bulb-to-bulb distillation (95 °C/0.05 mmHg) afforded a yellow liquid (16.5 g, 57%, 90% purity). When the procedure was repeated on the same scale, but the crude product was purified by column chromatography [silica, EtOAc/hexanes (5:1)], the title compound was obtained in 29% yield. The characterization values (^{1}H NMR) were consistent with those in the literature.[25,34] IR (neat) 3518, 2937, 2834, 1699, 1620, 1445, 1381, 1192, 1106, 1073, 988, 846 cm^{-1}.

1,1-Diethoxy-4-methyl-3-penten-2-one (V-1b). A sample of diethoxyacetonitrile (5.00 g, 38.7 mmol) was subjected to the procedure described for **V-1a**. Chromatography [silica, EtOAc/hexanes (1:9)] afforded a yellow liquid (3.27 g, 45%): ^{1}H NMR δ 1.25 (t, J = 7.4 Hz, 6H), 1.95 (s, 3H), 2.20 (s, 3H), 3.52–3.74 (m, 4H), 4.58 (s, 1H), 6.40–6.42 (m, 1H);

^{13}C NMR δ 15.4, 21.5, 28.4, 63.2, 103.3, 119.2, 160.1, 194.9. HRMS (ESI). Calcd for $C_{10}H_{18}O_3Na$ $(M + Na)^+$: 209.1148. Found 209.1148. IR (neat) 2976, 2880, 1697, 1620, 1444, 1380, 1317, 1235, 1104, 1060, 986, 845 cm^{-1}.

1-(1,3-Dioxolan-2-yl)-3-methyl-2-buten-1-one (V-1c). A solution of 2-methoxy-1,3-dioxolane (5.00 mL, 53.7 mmol) and trimethylsilyl cyanide (7.16 mL, 53.7 mmol) in CH_2Cl_2 (107 mL) at 0 °C was treated under argon with $In(OTf)_3$ (377 mg, 0.671 mmol). After stirring for 1 h at 0 °C, the reaction mixture was quenched with saturated aqueous $NaHCO_3$. After extraction, the organic phase was washed (water), dried (Na_2SO_4) and concentrated. The characterization values (^{1}H NMR, ^{13}C NMR) of the crude 1,3-dioxolane-2-carbonitrile were consistent with reported values.[40] A solution of the crude 1,3-dioxolane-2-carbonitrile in THF (10 mL) at –20 °C under argon was treated dropwise with **V-4** (107.4 mL, 53.7 mmol, 0.5 M in THF). After stirring for 1 h at –10 °C, saturated aqueous NH_4Cl (150 mL) was added, and the reaction mixture was stirred vigorously for 1 h at room temperature. The reaction mixture was extracted with Et_2O (3 x 150 mL). The combined organic extract was washed (water, brine), dried and concentrated. Column chromatography [silica, hexanes/EtOAc (5:1)] afforded a pale yellow liquid (1.80 g, 22%). The title compound was found to be unstable in air even as a neat liquid, but could be stored without decomposition in a degassed solution of Et_2O (~0.4 M) for 2 months at –20 °C. Data for the title compound: ^{1}H NMR δ 1.96 (s, 3H), 2.20 (s, 3H), 3.96–4.09 (m, 4H), 5.05 (s, 1H), 6.29–6.30 (m, 1H); ^{13}C NMR δ 21.6, 28.5, 65.8, 102.7, 118.8, 161.2, 194.5. HRMS (ESI). Calcd for $C_8H_{12}O_3Na$ $(M + Na)^+$: 179.0679. Found: 179.0678. IR (neat) 3525, 2978, 2893, 1697, 1618, 1445, 1380, 1236, 1162, 1101, 1033, 841 cm^{-1}.

Attempted Synthesis of V-1c via transacetalization. A solution of **V-1b** (902 mg, 4.85 mmol) and ethylene glycol (0.35 mL, 6.26 mmol) in benzene (9.7 mL) was treated with *p*-toluenesulfonic acid (92 mg, 0.48 mmol). The reaction mixture was stirred at 80 °C for 3.5 h. Saturated aqueous $NaHCO_3$ was added, and the mixture was extracted with Et_2O. The organic extract was washed (water), dried (Na_2SO_4), concentrated to a brown liquid, and chromatographed [silica, hexanes/EtOAc (5:1)] to afford two fractions. The ^{1}H NMR spectrum of the first fraction showed starting material **V-1b**. The ^{1}H NMR spectrum of the second fraction (major product) showed a mixture of the desired **V-1c** and a byproduct [a putative bis(1,3-dioxolane), **V-C**] in a 1:1 ratio

1-(1,3-Dioxan-2-yl)-3-methyl-2-buten-1-one (V-1d). A solution of **V-1b** (1.06 g, 5.69 mmol) and 1,3-propanediol (0.600 mL, 8.30 mmol) in benzene (11.5 mL) was treated with *p*-toluenesulfonic acid (542 mg, 2.85 mmol) at 80 °C for 4.5 h. Saturated aqueous $NaHCO_3$ was added, and the mixture was extracted with Et_2O. The organic extract was washed (water), dried (Na_2SO_4), concentrated to a brown liquid, and chromatographed [silica, hexanes/EtOAc (5:1)] to afford a yellow liquid (620 mg, 64%, ≥ 95% purity): ^{1}H NMR δ 1.40–1.45 (m, 1H), 1.96 (s, 3H), 2.20 (s, 3H), 2.12–2.25 (m, 1H), 3.83–3.92 (m, 2H), 4.20–4.26 (m, 2H), 4.79 (s, 1H), 6.40–6.42 (m, 1H); ^{13}C NMR δ 21.7, 25.9, 28.5, 67.3, 101.4, 119.0, 161.2, 192.1. HRMS (ESI). Calcd for $C_9H_{14}O_3Na$ $(M + Na)^+$: 193.0835. Found 193.0833. IR (neat) 3480, 2975, 2863, 1726, 1618, 1446, 1380, 1240, 1149, 1103, 1034 cm^{-1}.

1-Methoxy-4-methyl-3-penten-2-one (V-1e). According to a reported procedure[41] with some modifications, a solution of α-methoxyacetic acid (**V-6e**, 1.17 g, 13.0 mmol) in

anhydrous CH_2Cl_2 (20 mL) was treated portionwise with 1,1′-carbonyldiimidazole (2.54 g, 15.7 mmol) at 0 °C under argon. The reaction mixture was stirred for 30 min at room temperature, treated with triethylamine (2.18 mL, 15.7 mmol) and *N,O*-dimethylhydroxylamine hydrochloride (1.53 g, 15.6 mmol) at 0 °C, and stirred overnight at room temperature under argon. Saturated aqueous NH_4Cl was added. The organic phase was washed with water, dried (Na_2SO_4) and concentrated to a transparent oil. The crude amide at –20 °C under argon was treated dropwise with **V-4** (28.7 mL, 14.4 mmol, 0.5 M in THF). The reaction mixture was stirred for 2 h under argon at 0 °C upon which a white precipitate was formed. The mixture was diluted with Et_2O and treated with saturated aqueous NH_4Cl. The ethereal extract was washed (water, brine), dried (Na_2SO_4), concentrated and chromatographed [silica, hexanes/EtOAc (3:1)] to afford an orange liquid (360 mg, 22%): ^{1}H NMR δ 1.93 (s, 3H), 2.20 (s, 3H), 3.43 (s, 3H), 4.01 (s, 2H), 6.19–6.20 (m, 1H); ^{13}C NMR δ 21.4, 28.2, 59.4, 78.5, 119.6, 158.3, 159.9, 197.9. HRMS (ESI). Calcd for $C_7H_{12}O_2Na$ $(M + Na)^+$: 151.0730. Found 151.0731. IR (neat) 3451, 2979, 2935, 2825, 1699, 1618, 1447, 1379, 1227, 1200, 1109, 1038, 986, 934, 815 cm^{-1}.

4-Methyl-1-phenoxy-3-penten-2-one (V-1f). A solution of amide **V-7f** (508 mg, 2.60 mmol) in THF (5.1 mL) at –20 °C under argon was treated dropwise with **V-4** (5.70 mL, 2.85 mmol, 0.5 M in THF). The reaction mixture was stirred for 2 h under argon at 0 °C upon which a white precipitate formed. The mixture was diluted with Et_2O and treated with saturated aqueous NH_4Cl. The ethereal extract was washed (water, brine), dried (Na_2SO_4), and concentrated to a slightly yellow oil (480 mg, 97%) of sufficient purity to not require further purification: ^{1}H NMR δ 1.95 (s, 3H), 2.23 (s, 3H), 4.56 (s, 2H), 6.35–6.37 (m, 1H),

6.88 (m, 2H), 6.91–7.00 (m, 1H), 7.27–7.32 (m, 2H); ^{13}C NMR δ 21.6, 28.4, 73.4, 114.8, 119.4, 121.7, 129.8, 159.9, 196.4. HRMS (ESI). Calcd for $C_{12}H_{14}O_2Na$ $(M + Na)^+$: 213.0892. Found 213.0886. IR (neat) 3520, 3041, 2911, 1702, 1686, 1600, 1495, 1436, 1379, 1211, 1152, 1121, 1031, 844, 754 cm^{-1}.

1-Methoxy-4-methyl-1-phenyl-3-penten-2-one (V-1g). Compound **V-7g** (585 mg, 2.80 mmol) was subjected to the procedure described for **V-1f**. Chromatography [silica, hexanes/EtOAc (5:1)] afforded the title compound (495 mg, 87%): ^{1}H NMR δ 1.87 (s, 3H), 2.14 (s, 3H), 3.39 (s, 3H), 4.64 (s, 1H), 6.27–6.28 (m, 1H), 7.32–7.38 (m, 5H); ^{13}C NMR δ 21.4, 28.3, 57.4, 89.7, 119.3, 127.1, 128.4, 128.8, 136.8, 159.4, 197.8. HRMS (ESI). Calcd for $C_{13}H_{16}O_2Na$ $(M + Na)^+$: 227.1043. Found: 227.1041. IR (neat) 2933, 2826, 1686, 1618, 1445, 1379, 1199, 1099, 989 cm^{-1}.

1-(1,3-Dithiolan-2-yl)-3-methyl-2-buten-1-one (V-1h). Compound **V-7h** (250 mg, 1.30 mmol) was subjected to the procedure described for **V-1f**. Chromatography [silica, hexanes/EtOAc (3:1)] afforded a yellow oil (189 mg, 77%): ^{1}H NMR δ 1.95 (s, 3H), 2.19 (s, 3H), 3.31–3.35 (m, 4H), 4.87 (s, 1H), 6.23–6.24 (m, 1H); ^{13}C NMR δ 21.4, 28.4, 39.2, 58.5, 120.3, 159.8, 193.3. HRMS (ESI). Calcd for $C_8H_{12}OS_2Na$ $(M + Na)^+$: 211.0222. Found: 211.0227. IR (neat) 3434, 2928, 1674, 1619, 1441, 1379, 1237, 1121, 1039 cm^{-1}.

1-(1,3-Dioxolan-2-yl)-3,3-dimethyl-4-nitro-5-(3-*p*-tolylpyrrol-2-yl)-1-pentanone (V-2c). Following a literature procedure,[28] a mixture of **V-1c** (1.56 g, 9.99 mmol) and **V-8** (950 mg, 4.13 mmol) was treated with DBU (2.54 mL, 13.1 mmol) at room temperature. When no starting material was observed upon TLC analysis (3 h in this case), the reaction

mixture was diluted with EtOAc, and water was added. The combined organic extract was washed (brine), dried (Na_2SO_4) and concentrated to a brown oil. Column chromatography [silica, hexanes/EtOAc (3:1)] afforded a brown oil (861 mg, 54%): ^{1}H NMR δ 1.11 (s, 3H), 1.20 (s, 3H), 2.37 (s, 3H), 2.50 (d, *J* = 18.4 Hz, 1H), 2.71 (d, *J* = 18.4 Hz, 1H), 3.19 (dd, *J* = 2.6 Hz, *J* = 15.5 Hz, 1H), 3.40 (dd, *J* = 11.4 Hz, *J* = 15.5 Hz, 1H), 3.98–4.03 (m, 4H), 4.93 (s, 1H), 5.13 (dd, *J* = 2.6 Hz, *J* = 11.4 Hz, 1H), 6.23–6.24 (m, 1H), 6.67–6.69 (m, 1H), 7.18 (d, *J* = 8.8 Hz, 2H), 7.26 (d, *J* = 8.8 Hz, 2H), 8.07 (br, 1H); ^{13}C NMR δ 21.2, 23.9, 24.1, 25.3, 36.7, 44.4, 65.7, 94.9, 102.0, 109.4, 117.7, 121.8, 123.4, 128.2, 129.3, 133.5, 135.5, 204.1. HRMS (ESI). Calcd for $C_{21}H_{27}N_2O_5$ $(M + H)^+$: 387.1914. Found: 387.1906.

1-(1,3-Dioxan-2-yl)-3,3-dimethyl-4-nitro-5-(3-*p*-tolylpyrrol-2-yl)-1-pentanone (V-2d). Samples of **V-1d** (268 mg, 1.58 mmol), **V-8** (302 mg, 1.31 mmol) and DBU (0.765 mL, 3.93 mmol) were subjected (overnight) to the general procedure described for **V-2c**. Chromatography [silica, CH_2Cl_2/EtOAc (9:1)] afforded a brown solid (186 mg, 35%): mp 45 °C (dec.); ^{1}H NMR δ 1.11 (s, 3H), 1.19 (s, 3H), 1.40–1.44 (m, 1H), 2.07–2.21 (m, 1H), 2.37 (s, 3H), 2.60 (d, *J* = 18.8 Hz, 1H), 2.75 (d, *J* = 18.8 Hz, 1H), 3.20 (dd, *J* = 2.5 Hz, *J* = 15.6 Hz, 1H), 3.39 (dd, *J* = 11.7 Hz, *J* = 15.6 Hz, 1H), 3.79–3.88 (m, 2H), 4.17–4.23 (m, 2H), 4.68 (s, 1H), 5.16 (dd, *J* = 2.5 Hz, *J* = 11.7 Hz, 1H), 6.22–6.24 (m, 1H), 6.67–6.68 (m, 1H), 7.17–7.24 (m, 4H), 8.05–8.10 (br, 1H); ^{13}C NMR δ 21.4, 24.2, 24.3, 25.4, 25.8, 36.8, 45.1, 67.3, 95.1, 100.7, 109.6, 117.7, 122.1, 123.7, 128.4, 129.5, 133.6, 135.6, 201.0. HRMS (ESI). Calcd for $C_{22}H_{28}N_2O_5Na$ $(M + Na)^+$: 423.1890. Found: 423.1890.

1-Methoxy-4,4-dimethyl-5-nitro-6-[3-*p*-tolylpyrrol-2-yl]-2-hexanone (V-2e). Samples of **V-1e** (187 mg, 1.46 mmol), **V-8** (250 mg, 1.09 mmol) and DBU (0.636 mL, 3.27

mmol) were subjected (for 8 h) to the general procedure described for **V-2c**. Chromatography [silica, hexanes/EtOAc (3:1)] afforded a brown oil which solidified upon storage at 1 °C (274 mg, 70%): mp 103–104 °C (dec); ^{1}H NMR δ 1.09 (s, 3H), 1.20 (s, 3H), 2.36 (d, *J* = 17.6 Hz, 1H), 2.37 (s, 3H), 2.56 (d, *J* = 17.6 Hz, 1H), 3.22 (dd, *J* = 1.8 Hz, *J* = 15.8 Hz, 1H), 3.40 (s, 3H), 3.38 (dd, *J* = 9.9 Hz, *J* = 15.8 Hz, 1H), 3.90 (s, 2H), 5.14 (dd, *J* = 1.8 Hz, *J* = 9.9 Hz, 1H), 6.22–6.24 (m, 1H), 6.67–6.68 (m, 1H), 7.19 (d, *J* = 8.2 Hz, 2H), 7.23 (d, *J* = 8.2 Hz, 2H), 8.19 (br, 1H); ^{13}C NMR δ 21.3, 24.2, 24.5, 25.3, 37.0, 46.5, 59.5, 78.4, 95.0, 109.5, 117.7, 122.0, 123.7, 128.4, 129.4, 133.6, 135.7, 206.8. HRMS (ESI). Calcd for $C_{20}H_{26}N_2O_4Na$ $(M + Na)^+$: 381.1785. Found: 381.1782. Anal. Calcd for $C_{20}H_{26}N_2O_4$: C, 67.02; H, 7.31; N, 7.82. Found: C, 67.04; H, 7.25; N, 7.62.

4,4-Dimethyl-5-nitro-1-phenoxy-6-(3-*p*-tolylpyrrol-2-yl)-2-hexanone (V-2f). Samples of **V-1f** (256 mg, 1.35 mmol), **V-8** (250 mg, 1.09 mmol) and DBU (0.635 mL, 3.26 mmol) were subjected (overnight) to the general procedure described for **V-2c**. Chromatography (silica, CH_2Cl_2) afforded a brown oil (274 mg, 60%): ^{1}H NMR δ 1.10 (s, 3H), 1.21 (s, 3H), 2.34 (s, 3H), 2.50 (d, *J* = 18.2 Hz, 1H), 2.72 (d, *J* = 18.2 Hz, 1H), 3.23 (dd, *J* = 2.7 Hz, *J* = 15.6 Hz, 1H), 3.40 (dd, *J* = 11.4 Hz, *J* = 15.6 Hz, 1H), 4.43 (d, *J* = 3.6 Hz, 2H), 5.20 (dd, *J* = 2.7 Hz, *J* = 11.4 Hz, 1H), 6.23–6.24 (m, 1H), 6.69–6.67 (m, 1H), 6.86 (d, *J* = 8.8 Hz, 2H), 6.99–7.03 (m, 1H), 7.18–7.33 (m, 6H), 8.08 (br, 1H); ^{13}C NMR δ 21.3, 24.2, 24.5, 25.3, 37.0, 46.7, 73.3, 94.8, 109.5, 114.6, 117.7, 121.9, 122.1, 123.7, 128.4, 129.4, 129.9, 133.5, 135.7, 157.7, 205.6. HRMS (ESI). Calcd for $C_{25}H_{28}N_2O_4Na$ $(M + Na)^+$: 443.1941. Found: 443.1940.

1-Methoxy-4,4-dimethyl-5-nitro-6-[3-*p*-tolylpyrrol-2-yl]-1-phenyl-2-hexanone (V-2g). Samples of **V-1g** (250 mg, 1.23 mmol), **V-8** (235 mg, 1.02 mmol) and DBU (0.600 mL, 3.06 mmol) were subjected (overnight) to the general procedure described for **V-2c**. Chromatography [silica, hexanes/EtOAc (5:1)] afforded a brown oil (280 mg, 63%, a mixture of diastereomers): ^{1}H NMR δ 0.96 (s, 3H), 0.97 (s, 3H), 1.04 (s, 3H), 1.09 (s, 3H), 2.36 (s, 3H), 2.37 (s, 3H), 2.40 (m, 2H), 2.56–2.62 (m, 1H), 2.69–2.75 (m, 1H), 3.09–3.12 (m 1H), 3.14–3.18 (m, 1H), 3.29–3.33 (m, 2H), 3.35 (s, 3H), 3.36 (s, 3H), 4.57 (s, 1H), 4.58 (s, 1H), 5.14–5.15 (m, 1H), 5.17–5.19 (m, 1H) 6.21–6.22 (m, 2H), 6.64–6.67 (m, 2H), 7.14–7.25 (m, 8H), 7.31–7.40 (m, 10H), 8.03 (br, 1H), 8.07 (br, 1H); ^{13}C NMR δ 21.23, 21.25, 23.95, 23.99, 24.04, 24.2, 25.3, 25.4, 36.8, 36.9, 45.1, 45.5, 57.35, 57.42, 89.7, 89.8, 95.0, 95.1, 109.4, 109.5, 117.65, 117.66, 121.96, 122.00, 123.5, 123.6, 127.2, 127.4, 128.25, 128.33, 128.89, 128.98, 129.01, 129.1, 129.3, 133.59, 133.61, 135.5, 135.6, 206.4, 206.7. HRMS (ESI). Calcd for $C_{26}H_{31}N_2O_4$ $(M + H)^+$: 435.2278. Found: 435.2275.

1-(1,3-Dithiolan-2-yl)-3,3-dimethyl-4-nitro-5-(3-*p*-tolylpyrrol-2-yl)-1-pentanone (V-2h). Samples of **V-1h** (180 mg, 0.958 mmol), **V-8** (200 mg, 0.869 mmol) and DBU (0.508 mL, 2.61 mmol) were subjected (for 3.5 h) to the general procedure described for **V-2c**. Chromatography [silica, hexanes/EtOAc (3:1)] afforded a brown oil (129 mg, 36%): ^{1}H NMR (400 MHz) δ 1.12 (s, 3H), 1.16 (s, 3H), 2.37 (s, 3H), 2.63 (d, J = 18.0 Hz, 1H), 2.76 (d, J = 18.0 Hz, 1H), 3.23 (dd, J = 2.8 Hz, J = 15.5 Hz, 1H), 3.25–3.32 (m, 4H), 3.38 (dd, J = 11.4 Hz, J = 15.5 Hz, 1H), 4.74 (s, 1H), 5.14 (dd, J = 2.8 Hz, J = 11.4 Hz, 1H), 6.22–6.23 (m, 1H), 6.66–6.68 (m, 1H), 7.18 (d, J = 8.4 Hz, 2H), 7.23 (d, J = 8.4 Hz, 2H), 8.12 (br, 1H); ^{13}C NMR δ 21.6, 24.4, 24.5, 25.7, 37.6, 39.4, 46.4, 58.6, 95.6, 109.9, 118.1, 122.3, 123.9,

128.6, 129.7, 133.9, 136.0, 202.1. HRMS (ESI). Calcd for $C_{21}H_{27}N_2O_3S_2$ $(M + H)^+$: 419.1453. Found: 419.1458.

1-(1,3-Dioxolan-2-yl)-2,3-dihydro-3,3-dimethyl-7-*p*-tolyldipyrrin (V-3c). Following a reported procedure,[28] in a first flask a solution of **V-2c** (940 mg, 2.43 mmol) in THF/MeOH (11.4 mL, 5:1) at 0 °C under argon was treated with NaOMe (395 mg, 7.32 mmol) for 40 min. In a second flask, $TiCl_3$ (20 wt % $TiCl_3$ in 3 wt % HCl, 9.30 mL, 14.7 mmol) in THF (9.5 mL) was treated with a solution of NH_4OAc (7.52 g, 97.7 mmol) in H_2O (6.0 mL) that had been bubbled with argon for 1 h. The solution from the first flask was transferred to the second flask. The resulting reaction mixture was stirred overnight under argon at room temperature. Ethyl acetate and water were added. The organic extract was washed (brine), dried (Na_2SO_4), concentrated and chromatographed [alumina, hexanes/EtOAc (3:1)] to afford a yellow solid (255 mg, 31%): mp 185 °C (dec); ^{1}H NMR (400 MHz) δ 1.20 (s, 6H), 2.39 (s, 3H), 2.61 (s, 2H), 4.01–4.12 (m, 4H), 5.64 (s, 1H), 6.10 (s, 1H), 6.26–6.29 (m, 1H), 6.85–6.87 (m, 1H), 7.21 (d, *J* = 8.1 Hz, 2H), 7.36 (d, *J* = 8.1 Hz, 2H), 10.82 (br, 1H); ^{13}C NMR δ 21.3, 29.2, 40.7, 47.1, 66.0, 101.4, 106.6, 109.2, 119.4, 124.8, 126.8, 128.7, 129.4, 134.2, 135.4, 160.0, 173.4. HRMS (ESI). Calcd for $C_{21}H_{25}N_2O_2$ $(M + H)^+$: 337.1911. Found: 337.1911.

1-(1,3-Dioxan-2-yl)-2,3-dihydro-3,3-dimethyl-7-*p*-tolyldipyrrin (V-3d). A sample of **V-2d** (255 mg, 0.422 mmol) was subjected to the procedure described for **V-3c**. Chromatography [silica, hexanes/EtOAc (2:1)] afforded a light yellow solid (27 mg, 18%): mp 145 °C (dec.); ^{1}H NMR (400 MHz) δ 1.18 (s, 6H), 1.44–1.47 (m, 1H), 2.17–2.23 (m, 1H), 2.38 (s, 3H), 2.67 (s, 2H), 3.92–3.98 (m, 2H), 4.21–4.24 (m, 2H), 5.39 (s, 1H), 6.10 (s,

1H), 6.26–6.28 (m, 1H), 6.85–6.87 (m, 1H), 7.21 (d, J = 8.3 Hz, 2H), 7.34 (d, J = 8.3 Hz, 2H), 10.92 (br, 1H); ^{13}C NMR δ 21.4, 26.0, 29.3, 40.4, 48.0, 67.3, 99.9, 106.6, 109.1, 119.3, 124.6, 126.9, 128.7, 129.4, 134.3, 135.3, 160.2, 173.4. HRMS (ESI). Calcd for $C_{22}H_{27}N_2O_2$ $(M + H)^+$: 351.2067. Found: 351.2064.

2,3-Dihydro-1-(methoxymethyl)-3,3-dimethyl-7-*p*-tolyldipyrrin (V-3e). A sample of **V-2e** (150 mg, 0.419 mmol) was subjected to the procedure described for **V-3c**. Chromatography [alumina, hexanes/EtOAc (5:1)] afforded a brown solid (28 mg, 22%). (The title compound decomposed upon attempted column chromatography on silica gel.) Data for the title compound: mp 93–95 °C; ^{1}H NMR δ 1.20 (s, 6H), 2.39 (s, 3H), 2.61 (s, 2H), 3.44 (s, 3H), 4.33 (s, 2H), 6.06 (s, 1H), 6.27–6.30 (m, 1H), 6.85–6.87 (m, 1H), 7.21 (d, J = 7.8 Hz, 2H), 7.35 (d, J = 7.8 Hz, 2H), 10.90 (br, 1H); ^{13}C NMR δ 21.7, 29.7, 41.0, 50.6, 59.6, 73.3, 105.3, 109.5, 119.2, 124.5, 127.4, 129.0, 129.7, 134.7, 135.6, 160.8, 176.8. HRMS (ESI). Calcd for $C_{20}H_{25}N_2O$ $(M + H)^+$: 309.1961. Found: 309.1971.

2,3-Dihydro-3,3-dimethyl-1-(phenoxymethyl)-7-*p*-tolyldipyrrin (V-3f). A sample of **V-2f** (270 mg, 0.642 mmol) was subjected to the procedure described for **V-3c**. Chromatography [silica, CH_2Cl_2/hexanes (1:1)] afforded a light brown oil which quickly turned dark brown (87.5 mg, 37%): ^{1}H NMR δ 1.18 (s, 6H), 2.39 (s, 3H), 2.66 (s, 2H), 4.97 (s, 2H), 6.07 (s, 1H), 6.28–6.30 (m, 1H), 6.82–6.84 (m, 1H), 6.94–6.98 (m, 3H), 7.20–7.23 (d, J = 7.7 Hz, 2H), 7.29–7.37 (m, 4H), 10.78 (br, 1H); ^{13}C NMR δ 21.4, 29.3, 40.8, 50.3, 68.3, 105.3, 109.3, 114.8, 119.1, 121.7, 122.7, 124.4, 128.7, 129.4, 129.9, 134.3, 135.4, 160.3, 175.4. HRMS (ESI). Calcd for $C_{25}H_{27}N_2O$ $(M + H)^+$: 371.2118. Found: 371.2105.

***N*-Methoxy-*N*-methyl-2-methoxy-2-phenylacetamide (V-7g).** According to a reported procedure with some modifications,[40] a solution of **V-6g** (1.00 g, 6.02 mmol) in anhydrous CH_2Cl_2 (9.0 mL) at 0 °C under argon was treated portionwise with 1,1′-carbonyldiimidazole (1.27 g, 7.83 mmol). The reaction mixture was stirred for 40 min at room temperature, treated with triethylamine (1.2 mL, 8.6 mmol) and *N,O*-dimethylhydroxylamine hydrochloride (826 mg, 8.43 mmol) at 0 °C, and stirred overnight at room temperature under argon. A sample of 1 M HCl (10 mL) was added. The organic extract was washed with water, dried (Na_2SO_4) and concentrated to give a transparent oil. Chromatography [silica, hexanes/ EtOAc (1:1)] afforded a transparent oil (735 mg, 58%): ^{1}H NMR δ 3.17 (s, 3H), 3.39 (s, 3H), 3.42 (br, 3H), 5.12 (s, 1H), 7.32–7.39 (m, 3H), 7.44–7.46 (m, 2H); ^{13}C NMR δ 32.6, 57.4, 61.2, 81.0, 127.5, 128.4, 128.9, 136.7, 172.0. HRMS (ESI). Calcd for $C_{11}H_{15}NO_3Na$ $(M + Na)^+$: 232.0944. Found: 232.0952. IR (neat) 3504, 2938, 2823, 1675, 1455, 1385, 1197, 1176, 1111 $cm^{-1.}$

***N*-Methoxy-*N*-methyl-1,3-dithiolane-2-carboxamide (V-7h).** Following a general procedure with modifications,[36] a vigorously stirred slurry of **V-6h** (1.50 mL, 10.5 mmol) and *N,O*-dimethylhydroxylamine hydrochloride (2.57 g, 26.2 mmol) in THF (21 mL) at –78 °C under argon was treated dropwise with isopropylmagnesium bromide (52.5 mmol, 26.3 mL, 2 M in THF) over 40 min. The reaction mixture was stirred for 1 h at –78 °C under argon. Saturated aqueous NH_4Cl/H_2O (1:1) was added. The aqueous phase was extracted with ether (3 x 100 mL). The combined organic extract was washed (water, brine), dried (Na_2SO_4), concentrated and chromatographed [silica, EtOAc/hexanes (2:1)] to afford a yellow oil that solidified upon storage at 1 °C (985 mg, 49%). The characterization values

[^{1}H NMR, ^{13}C NMR, HRMS (ESI)] were consistent with those for the title compound prepared via a different synthetic route.[43]

8,8,18,18-Tetramethyl-2,12-di-*p*-tolyl-5-[2-(trimethylsilyloxy)ethoxy]bacteriochlorin (BC-3). Following a general procedure,[44] a solution of **V-3c** (255 mg, 0.758 mmol) and 2,6-DTBP (1.36 mL, 6.06 mmol) in CH_2Cl_2 (42 mL) was treated with TMSOTf (0.55 mL, 3.0 mmol) at room temperature. The reaction mixture was stirred for 22 h at room temperature. The reaction mixture was diluted with CH_2Cl_2 and saturated aqueous $NaHCO_3$. The organic phase was washed (water, brine), dried (Na_2SO_4) and concentrated. Column chromatography [silica, CH_2Cl_2/hexanes (1:1)] afforded a green solid (77 mg, 30%): mp 230–232 °C (dec.); ^{1}H NMR δ –1.92 (br, 1H), –1.80 (br, 1H), 0.34 (s, 9H), 1.89 (s, 6H), 1.91 (s, 6H), 2.61 (s, 6H), 4.32 (t, *J* = 4.4 Hz, 2H), 4.38 (s, 2H), 4.43 (s, 2H), 4.66 (t, *J* = 4.4 Hz, 2H), 7.56–7.58 (m, 4H), 8.08–8.15 (m, 4H), 8.68 (s, 2H), 8.78 (s, 1H), 8.81 (s, 1H), 9.07–9.08 (m, 1H); ^{13}C NMR δ 0.22, 21.6, 31.10, 31.16, 45.94, 46.18, 47.9, 51.9, 62.6, 76.8, 79.3, 95.7, 95.8, 97.8, 116.8, 121.0, 129.9, 130.0, 130.3, 131.1, 131.3, 133.2, 133.8, 134.1, 134.2, 134.4, 134.8, 135.6, 137.0, 137.2, 137.5, 153.4, 159.6, 169.6, 170.0; LD-MS obsd 681.8. HRMS (ESI). Calcd for $C_{43}H_{51}N_4O_2Si$ $(M + H)^+$: 683.3776. Found: 683.3762. λ_{abs} 355, 374, 512, 732 nm.

5-(2-Hydroxyethoxy)-8,8,18,18-tetramethyl-2,12-di-*p*-tolylbacteriochlorin (BC-4). A solution of **BC-3** (20 mg, 0.029 mmol) in THF (3.0 mL) was treated with TBAF (44 μL, 0.044 mmol, 1 M in THF) under argon at room temperature for 45 min. Water and CH_2Cl_2 were added. The organic extract was washed (brine), dried (Na_2SO_4), concentrated and chromatographed (silica, CH_2Cl_2) to afford a green solid (15 mg, 83%): mp 208–210 °C

(dec.); ^{1}H NMR δ –1.85 (br, 1H), –1.75 (br, 1H), 1.90 (s, 6H), 1.91 (s, 6H), 2.60 (s, 3H), 2.61 (s, 3H), 2.62–2.68 (m, 1H), 4.31–4.37 (m, 2H), 4.40 (s, 4H), 4.70 (t, *J* = 4.0 Hz, 2H), 7.55–7.59 (m, 4H), 8.08–8.12 (m, 4H), 8.67 (s, 2H), 8.77 (s, 1H), 8.80 (s, 1H), 8.94 (s, 1H); ^{13}C NMR δ 21.61, 21.64, 31.05, 31.20, 46.0, 46.3, 47.8, 52.1, 63.1, 78.9, 95.8, 96.0, 98.0, 116.0, 121.4, 129.8, 129.97, 130.03, 131.1, 131.3, 133.0, 133.6, 133.7, 134.2, 134.3, 135.3, 136.0, 137.1, 137.6, 137.7, 152.6, 160.1, 169.6, 170.3; LD-MS 610.0. HRMS (ESI). Calcd for $C_{40}H_{43}N_4O_2$ $(M + H)^+$: 611.3381. Found: 611.3365. λ_{abs} 355, 374, 511, 731 nm.

15-Bromo-5-(2-hydroxyethoxy)-8,8,18,18-tetramethyl-2,12-di-*p*-tolylbacteriochlorin (BC-5). A sample of **BC-4** (14 mg, 0.023 mmol) in THF (11.5 mL) was treated with NBS (0.23 mL, 0.023 mmol, 100 mM in THF) at room temperature. After stirring for 1 h, water and CH_2Cl_2 were added. The organic extract was washed (brine), dried (Na_2SO_4) and concentrated. Chromatography (silica, CH_2Cl_2) afforded a green solid (10 mg, 64%): mp 205–207 °C (dec.); ^{1}H NMR (400 MHz, THF-d_8) δ –2.01 (br, 1H), –1.82 (br, 1H), 1.90 (s, 12 H), 2.47 (s, 6H), 4.17–4.22 (m, 2H), 4.47 (s, 2H), 4.47–4.50 (m, 1H), 4.51 (s, 2H), 4.67 (t, *J* = 4.4 Hz, 2H), 7.55–7.59 (m, 4H), 8.06–8.11 (m, 4H), 8.77 (s, 1H), 8.82 (s, 1H), 8.98–8.99 (m, 1H), 9.04–9.05 (m, 1H); ^{13}C NMR (THF-d_8) δ 21.6, 31.3, 31.5, 46.4, 46.9, 49.0, 55.0, 62.9, 81.3, 96.4, 98.4, 119.5, 121.6, 129.1, 129.8, 130.67, 130.70, 132.0, 132.1, 133.1, 133.9, 134.0, 134.6, 134.8, 135.4, 135.8, 137.0, 137.6, 138.1, 138.3, 158.0, 158.7, 169.1, 172.9; LD-MS, 688.4. HRMS (ESI). Calcd for $C_{40}H_{41}BrN_4O_2Na$ $(M + Na)^+$: 711.2305. Found: 711.2297. λ_{abs} 362, 378, 524, 734 nm.

Conversion of BC-3 to BC-5. A sample of **BC-3** (73 mg, 0.11 mmol) in THF (53.5 mL) was treated with NBS (19 mg, 0.11 mmol) at room temperature. After stirring for 1 h at room temperature, water and CH_2Cl_2 were added. The organic phase was washed (brine), dried (Na_2SO_4) and concentrated. Chromatography (silica, CH_2Cl_2) afforded a green solid (48 mg, 65%). The characterization values (^{1}H NMR, LD-MS) were consistent with those reported above.

The content of this chapter was published.[46]

V.5. References

(1) Lindsey, J. S. *Acc. Chem. Res*. **2010**, *43*, 300–311.

(2) Senge, M. O. *Chem. Commun.* **2011**, *47*, 1943–1960.

(3) Ptaszek, M.; Lahaye, D.; Krayer, M.; Muthiah, C.; Lindsey, J. S. *J. Org. Chem*. **2010**, *75*, 1659–1673.

(4) Galezowski, M.; Gryko, D. T. *Curr. Org. Chem*. **2007**, *11*, 1310–1338.

(5) Taniguchi, M.; Cramer, D. L.; Bhise, A. D.; Kee, H. L.; Bocian, D. F.; Holten, D.; Lindsey, J. S. *New J. Chem.* **2008**, *32*, 947–958.

(6) Yang, E.; Kirmaier, C.; Krayer, M.; Taniguchi, M.; Kim, H.-J.; Diers, J. R.; Bocian, D. F.; Lindsey, J. S.; Holten, D. *J. Phys. Chem. B* **2011**, *115*, 10801–10816.

(7) Lindsey, J. S.; Mass, O.; Chen, C.-Y. *New J. Chem*. **2011**, *35,* 511–516.

(8) Wasielewski, M. R.; Svec, W. A. *J. Org. Chem.* **1980**, *45*, 1969–1974.

(9) Osuka, A.; Wada, Y.; Maruyama, K.; Tamiaki, H. *Heterocycles* **1997**, *44*, 165−168.

(10) Fukuzumi, S.; Ohkubo, K.; Chen, Y.; Pandey, R. K.; Zhan, R.; Shao, J.; Kadish, K. M. *J. Phys. Chem. A* **2002**, *106*, 5105–5113.

(11) Mironov, A. F.; Grin, M. A.; Tsiprovskiy, A. G.; Kachala, V. V.; Karmakova, T. A.; Plyutinskaya, A. D.; Yakubovskaya, R. I. *J. Porphyrins Phthalocyanines* **2003**, *7*, 725–730.

(12) Sasaki, S.-i.; Tamiaki, H. *J. Org. Chem.* **2006**, *71*, 2648–2654.

(13) Grin, M. A.; Mironov, A. F.; Shtil, A. A. *Anti-Cancer Agents Med. Chem.* **2008**, *8*, 683–697.

(14) Tamiaki, H.; Kunieda, M. In *Handbook of Porphyrin Science;* Kadish, K. M., Smith, K. M., Guilard, R., Eds.; World Scientific Publishing Co.: Singapore, Vol. 11, 2011, pp 223–290.

(15) Dorough, G. D.; Miller, J. R. *J. Am. Chem. Soc.* **1952**, *74*, 6106–6108.

(16) Whitlock, H. W., Jr.; Hanauer, R.; Oester, M. Y.; Bower, B. K. *J. Am. Chem. Soc.* **1969**, *91*, 7485–7489.

(17) Shea, K. M.; Jaquinod, L.; Khoury, R. G.; Smith, K. M. *Tetrahedron* **2000**, *56*, 3139–3144.

(18) Chen, Y.; Li, G.; Pandey, R. K. *Curr. Org. Chem*. **2004**, *8*, 1105–1134.

(19) Pereira, N. A. M.; Serra, A. C.; Pinho e Melo, T. M. V. D. *Eur. J. Org. Chem.* **2010**, 6539–6543.

(20) Samankumara, L. P.; Zeller, M.; Krause, J. A.; Brückner, C. *Org. Biomol. Chem*. **2010**, *8*, 1951–1965.

(21) Singh, S.; Aggarwal, A.; Thompson, S.; Tomé, J. P. C.; Zhu, X.; Samaroo, D.; Vinodu, M.; Gao, R.; Drain, C. M. *Bioconjugate Chem*. **2010**, *21*, 2136–2146.

(22) Pereira, N. A. M.; Fonseca, S. M.; Serra, A. C.; Pinho e Melo, T. M. V. D.; Burrows, H. D. *Eur. J. Org. Chem.* **2011**, 3970–3979.

(23) Minehan, T. G.; Cook-Blumberg, L.; Kishi, Y.; Prinsep, M. R.; Moore, R. E. *Angew. Chem. Int. Ed.* **1999**, *38*, 926–928.

(24) Wang, W.; Kishi, Y. *Org. Lett.* **1999**, *1*, 1129–1132.

(25) Kim, H.-J.; Lindsey, J. S. *J. Org. Chem.* **2005**, *70*, 5475–5486.

(26) Ruzié, C.; Krayer, M.; Balasubramanian, T.; Lindsey, J. S. *J. Org. Chem*. **2008**, *73*, 5806–5820.

(27) Krayer, M.; Balasubramanian, T.; Ruzié, C.; Ptaszek, M.; Cramer, D. L.; Taniguchi, M.; Lindsey, J. S. *J. Porphyrins Phthalocyanines* **2009**, *13*, 1098–1110.

(28) Krayer, M.; Ptaszek, M.; Kim, H.-J.; Meneely, K. R.; Fan, D.; Secor, K.; Lindsey, J. S. *J. Org. Chem*. **2010**, *75*, 1016–1039.

(29) Krayer, M.; Yang, E.; Diers, J. R.; Bocian, D. F.; Holten, D.; Lindsey, J. S. *New J. Chem*. **2011**, *35*, 587–601.

(30) Ogikubo, J.; Brückner, C. *Org. Lett.* **2011**, *13*, 2380–2383.

(31) Sutton, J. M.; Clarke, O. J.; Fernandez, N.; Boyle, R. W. *Bioconjugate Chem.* **2002**, *13*, 249–263.

(32) Kobayashi, M.; Akiyama, M.; Kano, H.; Kise, H. In *Chlorophylls and Bacteriochlorophylls: Biochemistry, Biophysics, Functions and Applications;* Grimm, B.; Porra, R. J.; Rüdiger, W.; Scheer, H., Eds.; Springer: Dordrecht, The Netherlands, 2006, pp 79–94.

(33) Fan, D.; Taniguchi, M.; Lindsey, J. S. *J. Org. Chem.* **2007**, *72*, 5350–5357.

(34) Tiecco, M.; Testaferri, L.; Tingoli, M.; Bartoli, D. *J. Org. Chem*. **1990**, *55*, 4523–4528.

(35) Mentzel, M.; Hoffmann, H. M. R. *J. Prakt. Chem.* **1997**, *339*, 517–524.

(36) Williams, J. M.; Jobson, R. B.; Yasuda, N.; Marchesini, G.; Dolling, U.-H.; Grabowski, E. J. J. *Tetrahedron Lett.* **1995**, *36*, 5461–5464.

(37) Pereira, C. L.; Chen, Y.-H.; McDonald, F. E. *J. Am. Chem. Soc*. **2009**, *131*, 6066–6067.

(38) Utimoto, K.; Wakabayashi, Y.; Shishiyama, Y.; Inoue, M.; Nozaki, H. *Tetrahedron Lett.* **1981**, *22*, 4279–4280.

(39) Kirchmeyer, S.; Mertens, A.; Arvanaghi, M.; Olah, G. A. *Synthesis* **1983**, 498–500.

(40) Suzuki, H.; Sakai, N.; Iwahara, R.; Fujiwaka, T.; Satoh, M.; Kakehi, A.; Konakahara, T. *J. Org. Chem.* **2007**, *72*, 5878–5881.

(41) Beutner, G. L.; Kuethe, J. T.; Kim, M. M; Yasuda, N. *J. Org. Chem.* **2009**, *74*, 789–794.

(42) Kawabata, T.; Yahiro, K.; Fuji, K. *J. Am. Chem. Soc.* **1991**, *113*, 9694–9696.

(43) Balasubramaniam, S.; Aidhen, I. S. *Synlett* **2007**, 959–963.

(44) Krayer, M.; Yang, E.; Kim, H.-J.; Kee, H. L.; Deans, R. M.; Sluder, C. E.; Diers, J. R.; Kirmaier, C.; Bocian, D. F.; Holten, D.; Lindsey, J. S. *Inorg. Chem.* **2011**, *50*, 4607–4618.

(45) Aravindu, K.; Krayer, M.; Kim, H.-J.; Lindsey, J. S. *New J. Chem*. **2011**, *35*, 1376–1384.

(46) Mass, O.; Lindsey, J. S. *J. Org. Chem*. **2011**, *76*, 9478–9487.